YU ISSN 0042-8450

ВОЈНОСАНИТЕТСКИ ПРЕГЛЕД

Часопис лекара и фармацеута Војске Србије

Military Medical and Pharmaceutical Journal of Serbia

Vojnosanitetski pregled

Vojnosanit Pregl 2019; May Vol. 76 (No. 5): p. 461–566.

Vojnosanitetski Pregled 2019 May Vol. 76 (No. 5): p. 461–566.

vol. 76, br. 5, 2019

VOJNOSANITETSKI PREGLED

Prvi broj *Vojnosanitetskog pregleda* izašao je septembra meseca 1944. godine

Časopis nastavlja tradiciju *Vojno-sanitetskog glasnika*, koji je izlazio od 1930. do 1941. godine

IZDAVAČ
Univerzitet odbrane, MO Republike Srbije

ISSN 0042-8450
eISSN 2406-0720
Open Access
(CC BY-SA)

Adresa redakcije: Univerzitet odbrane, Institut za naučne informacije, Crnotravska 17, 11 040 Beograd, Srbija.
Informacije o pretplati: Tel.: +381 11 3608 997. E-mail (redakcija): **vsp@vma.mod.gov.rs**

Radove objavljene u „Vojnosanitetskom pregledu“ indeksiraju: Science Citation Index Expanded (SCIE), Journal Citation Reports/Science Edition, SCOPUS, Excerpta Medica (EMBASE), Google Scholar, EBSCO, Biomedicina Serbica. Sadržaje objavljuju Giornale di Medicine Militare i Revista de Medicina Militara. Prikaze originalnih radova i izvoda iz sadržaja objavljuje International Review of the Armed Forces Medical Services.

Časopis izlazi dvanaest puta godišnje. Pretplate: Žiro račun br. 840-19540845-28, poziv na broj 122742313338117. Za pretplatu iz inostranstva obratiti se službi pretplate na tel. +381 11 3608 997. Godišnja pretplata: 5 000 dinara za građane Srbije, 10 000 dinara za ustanove iz Srbije i 150 € za pretplatnike iz inostranstva. Kopiju uplatnice dostaviti na gornju adresu.

Štampa Vojna štamparija, Beograd, Resavska 40b

vol. 76, No. 5, 2019

VOJNOSANITETSKI PREGLED

The first issue of *Vojnosanitetski pregled* was published in September 1944
The Journal continues the tradition of *Vojno-sanitetski glasnik* which was published between 1930 and 1941

PUBLISHER
University of Defence, Ministry of Defence of the Republic of Serbia, Belgrade, Serbia

ISSN 0042-8450
eISSN 2406-0720
Open Access
(CC BY-SA)

Editorial Office: University of Defence, Institute for Scientific Information, Crnotravska 17, 11 040 Belgrade, Serbia.
E-mail: **vsp@vma.mod.gov.rs**

Papers published in the Vojnosanitetski pregled are indexed in: Science Citation Index Expanded (SCIE), Journal Citation Reports/Science Edition, SCOPUS, Excerpta Medica (EMBASE), Google Scholar, EBSCO, Biomedicina Serbica. Contents are published in Giornale di Medicine Militare and Revista de Medicina Militara. Reviews of original papers and abstracts of contents are published in International Review of the Armed Forces Medical Services.

The Journal is published monthly. Subscription: Giro Account No. 840-19540845-28, refer to number 122742313338117. To subscribe from abroad phone to +381 11 3608 997. Subscription prices per year: individuals 5,000.00 RSD, institutions 10,000.00 RSD, and foreign subscribers 150 €.

Printed by: Vojna štamparija, Beograd, Resavska 40b

CONTENTS / SADRŽAJ

Every year about 250,000 women around the world are diagnosed with ovarian cancer and 140,000 women die of it, making this cancer the one with the lowest survival rate in women (in Serbia, every day, three women suffer from the ovarian cancer, and one dies from this disease). Due to a widespread lack of awareness and the absence of early screening tests, many cases of ovarian cancer are diagnosed late which leads to "poor outcomes".

World Ovarian Cancer Day (WOCD) that is marked on May 8 every year beginning from 2013, aims to unite those living with the ovarian cancer, survivors, their families and friends as well as medical professionals in sharing their experiences and helping the education of the public about this deadly disease.
The Editorial Board of Vojnosanitetski Pregled invites all its associates to assist in the realization of these goals.

Svake godine kod oko 250 000 žena širom sveta dijagnostikuje se karcinom jajnika od koga umire njih 140 000, što ga čini karcinomom žena sa najnižom stopom preživljavanja (u Srbiji, svakog dana tri žene obole, a jedna umre od ove bolesti). Zbog rasprostranjenog nedostatka svesti o tome i nepostojanja testova za rano otkrivanje bolesti, mnogi slučajevi karcinoma jajnika se kasno dijagnostikuju što dovodi do "loših ishoda".
Svetski dan borbe protiv karcinoma jajnika, koji se obeležava 8. maja svake godine, počevši od 2013, ima za cilj da objedini obolele od karcinomom jajnika, preživele, njihove porodice i prijatelje, kao i zdravstvene radnike u razmeni iskustava i pomoći u edukaciji javnosti o ovoj smrtonosnoj bolesti. Urednistvo "Vojnosanitetskog pregleda" poziva sve svoje saradnike da pomognu u realizaciji ovih ciljeva.

ORIGINAL ARTICLES

UDC: 616.831-006:612.118
https://doi.org/10.2298/VSP161230104A

ABO blood group and risk of glioma: a case control study from Serbia

ABO krvne grupe i rizik od nastanka glioma: studija slučaj-kontrola iz Srbije

Ana Azanjac Arsić*, Svetlana Miletić Drakulić*†, Katarina Vesić*, Gordana Tončev*†

University of Kragujevac, Faculty of Medical Sciences, *Department of Neurology, Kragujevac, Serbia; Clinical Center Kragujevac, †Clinic of Neurology, Kragujevac, Serbia

Abstract

Backgraund/Aim. Gliomas are the most common primary brain tumors and the etiology is unknown. The aim of this study was to investigate possible association between incidence in relation to glioma and certain blood groups. **Methods.** The case-control study included 100 pathologically confirmed cases of glioma at the Clinical centar of Kragujevac, Serbia, between 2014 and 2015, and 200 age- and sex-matched controls without malignant diseases in personal and family history at the same institution. After signing the informed consent, all patients filled out an epidemiological questionnaire. **Results.** In the analysis comparing the glioma patients with the control group, a significant association ($p < 0.0005$) was observed in relation to the blood group AB. Furthermore, it was not observed a significant association in relation to the blood group A ($p = 0.070$), blood group B ($p = 0.256$), blood group O ($p = 0.768$) among the compared groups. Also, in the analysis comparing glioma patients with the control group, a significant association was observed in relation to the years spent in hometown ($p = 0.035$), changing the place of residence ($p = 0.007$), the body weight ($p = 0.002$) and the body mass index ($p < 0.0005$). Univariate binary logistic regression showed that higher number of years spent in the hometown [odds ratio (OR) 1.011 95% confidence interval (Cl) 1.000–1.023; $p = 0.043$], increased body weight (OR 0.976 95% Cl 0.959–0.993, $p = 0.006$) and increased body mass index (OR 0.898 95% Cl 0.839–0.961; $p = 0.002$) increase the risk of glioma. However, a change of the residence decreases the risk of glioma (OR 0.327 95% Cl 0.147–0.727; $p = 0.006$). Univariate binary logistic regression analysis revealed that the individuals with group AB were at 3.5-fold increased risk of developing glioma compared to the individuals with other ABO blood groups (OR 3,429 95% Cl 1,83–6,41; $p < 0.0005$). Also, there was more male patients with glioma with the blood group AB ($p = 0.001$). **Conclusion.** In a present study, we demonstrate that individuals with the group AB have an increased risk of developing glioma.

Key words:
glioma; blood group system; risk factors.

Apstrakt

Uvod/Cilj. Gliomi su najčešći primarni tumori mozga čija je etiologija nepoznata. Cilj ove studije bio je da ispita da li je učestalost glioma povezana sa određenom krvnom grupom. **Metode.** Studija slučaj-kontrola uključila je 100 bolesnika sa patohistološki potvrđenim gliomom u Kliničkom centru Kragujevac, u Srbiji, između 2014. i 2015. godine i 200 ispitanika kontrolne grupe ukrštenih po polu i godinama koji nisu imali istoriju malignih bolesti u ličnoj i porodičnoj anamnezi. Nakon potpisivanja pristanka svi bolesnici popunjavali su epidemiološki upitnik. **Rezultati.** U analizi, u kojoj su upoređivani bolesnici sa gliomom i ispitanici kontrolne grupe, značajna veza ($p < 0,005$) ustanovljena je za krvnu grupu AB. Nije zapažena statistički značajna veza za krvnu grupu A ($p = 0,070$), B ($p = 0,256$) i O ($p = 0,768$) između poređenih grupa. Poređenjem bolesnika sa gliomom i bolesnika kontrolne grupe, nađena je statistički značajna veza sa godinama života provedenih u mestu rođenja ($p = 0,035$), promenom mesta boravka ($p = 0,007$), telesnom masom ($p = 0,002$) i indeksom telesne mase ($p < 0,0005$). Primenom univarijantne binarne logističke regresije pokazano je da veći broj godina života provedenih u mestu rođenja [*odds ratio* (OR) 1,011 95% *confidence itnerval* (Cl) 1,000–1,023; $p = 0,043$], povećana telesna masa (OR 0,976 95% Cl 0,959– 0,993; $p = 0,006$) i povećan indeks telesne mase (OR 0.898 95% Cl 0,839–0,961) povećavaju rizik od nastanka glioma. Međutim, promena mesta boravka smanjuje rizik od nastanka glioma (OR 0,327 95% Cl 0,147–0,727; $p = 0,006$). Primenom univarijantne binarne logističke regresije otkriva se da kod osoba sa krvnom grupom AB postoji 3,5 puta veći rizik za nastanak glioma u poređenju sa osobama sa drugim krvnim grupama (OR 3,429 95% Cl 1,83–6,41, $p < 0,0005$). Takođe, bilo je više bolesnika muškog pola sa

Correspondence to: Ana Azanjac Arsić, 34 000 Kragujevac, Serbia. E-mail: ana.azanjac@yahoo.com

gliomom koji su imali krvnu grupu AB (p = 0,001). **Zaključak.** Ova studija pokazuje da kod osoba sa krvnom grupom AB postoji povećan rizik od nastanka glioma.

Ključne reči:
gliom; krvne grupe; faktori rizika.

Introduction

Gliomas are the most common primary brain tumors [1]. They accounts for approximately 27% of all brain and central nervous system tumors and about 80% of malignant brain tumors. Gliomas are tumors arising from glial or precursor cells and include astrocytoma, glioblastoma, oligodendroglioma, ependymoma, mixed glioma, malignant glioma, not otherwise specified (NOS) and few rare histologies [2].

The etiology of glioma is unknown. Several possible risk factors for glioma were suggested in the past, but with the exception of ionizing radiation, none was consistently confirmed [3, 4]. Several studies investigated the relationship between the blood groups ABO and glioma risk and demonstrated conflicting results [5–10]. The scientist Landsteiner found the blood group ABO system in 1901 at the University of Vienna. Locus ABO is localized on chromosome 9 and gene ABO is inherited in an autosomal dominant [11]. The A and B antigens are complex carbohydrate molecule and they represent extracellular domains on the surface membrane of red blood cells. The A and B alleles of the ABO locus encode different enzyme glycosyltransferases, adding N-acetylgalactosamine and D-galactose on a common precursor of the side chain, the H determinant, which is then converted into the A or B antigen. The group O individuals lack such functional enzymes, and express unchanged H determinant. In addition to the surface of red blood cells, A and B antigens are found on a variety of human cells and tissues, including epithelial cells, neurons, platelets and vascular endothelium [12, 13].

Distribution of the four different blood groups varies between countries. Generally, blood group O has highest prevalence, while blood group AB has the lowest [14]. In Serbia, the proportion of ABO blood groups is 41.5% for A, 37.5% for O, 16% for B and about 5.5% for AB [15].

The aim of this study was to examine incidence of glioma in the patients with different blood groups ABO.

Methods

The study group included a series of 100 consecutive patients (59 males, mean age 59.76 ± 10.76 years, and 41 females, mean age 58.36 ± 8.95 years) with histopathologically verified diagnosis of glioma according to the WHO criteria (ICD-O-3). Of these 100 patients, the blood groups were available in 96 patients. The study was realized according to the Declaration of Helsinki and performed in accordance with the Ethics Committee of Clinical Center Kragujevac. The criteria for inclusion into the study were the patients who had a consultative decision evaluated on the basis of stages of the disease and the general condition of the patient. Also, the criteria for inclusion into the study were primary, previously untreated glioma. The criteria for exclusion from the study were previously diagnosed and treated glioma and glioma recidivans. The patients were treated surgically, followed by radio and chemotherapy at the Center for Oncology, Clinical Center Kragujevac. Data were collected between April 2015 and May 2016. The control group included 200 patients matched by sex and age (109 males, mean age 59.32 ± 10.71 years, and 91 females, mean age 58.09 ± 9.12 years), who were hospitalized in the Clinical Centre Kragujevac, without malignant diseases in personal and family history. Of these 200 patients, the blood group were available in 172 patients. After obtaining the patient consent, a questionnaire based on the reviewed literature data and personal considerations was to collect detailed information. It included questions about different factors supposed to be a possible risk or protective factors.

The first part of the questionnaire referred to demographic features of the patients [sex, age, birth and residency places, blood type, Rh (D) antigen, school education, occupation, number of family members, the size of the home space]. The second part of the questionnaire included the family history of chronic diseases, including brain tumors and other malignant tumors. The third part of the questionnaire referred to the personal history of the disease including reproductive risk factors. The fourth part deals with information on the risks of exposure to external factors, the fifth included data on habits (smoking, drinking coffee, tea, alcohol) and the sixth part referred to information about nutrition.

Statistical analysis

Statistical analysis was performed using the SPSS software version 19.0. The chi-square (χ^2) test was used for the comparison of qualitative variables between the patients with glioma and the control group. The categorical variables were presented as frequencies and percentages. The univariate analysis using the logistic regression techniques, including the odds ratio (OR), was performed to determine the effects of blood groups on the dependent variable (glioma). The P value of less than 0.05 was considered statistically significant.

Results

Table 1 shows the demographic and personal characteristic of patients and controls. Difference in years spent in hometown between the study and the control group was statistically significant (p = 0.035). The control group patients were more frequently changing the residence than patients with glioma (p = 0.007). Also, the statistically significant difference was found between the compared groups in relation to the body weight (p = 0.002) and to the body mass index (p < 0.0005). The patients with glioma had a higher body weight and higher body mass index in comparison to the patients of the control group.

In comparing the patients with glioma with the control group patients, a significant association ($p < 0.005$) was observed in relation to the blood group AB. Furthermore, no significant association was observed in relation to the blood group A ($p = 0.070$), blood group B ($p = 0.256$), blood group O ($p = 0.768$) among the patients with glioma and the control group (Table 2).

In the group of patients with glioma, 32.3% of patients had the blood type AB, 25.0% of patients had the blood group A, 10.4% the blood group B and 32.3% the blood group O. The ratios of blood groups AB, A, B and O were 12.2% v.s. 32.6% v.s. 18.5% v.s. 34.9% in the control group, respectively (Table 2).

Comparing the male patients with glioma and the control group as the blood groups ABO, a significant association was observed in relation to the blood group AB ($p = 0.001$). There was no significant difference regarding the blood group A ($p = 0.726$), blood group B ($p = 0.668$) and the blood group O ($p = 0.726$), (Table 3).

Comparing the female patients with glioma and the control group as the blood group AB, differences did not reach significance there ($p = 0.057$). Also, there was no significant difference regarding the blood group A ($p = 0.288$), blood group B ($p = 0.549$) and the blood group O ($p = 0.522$) (Table 4).

Table 1

Demographic and personal characteristic of patients and controls

Variable	Patients with glioma (n = 100)	Control group (n = 200)	*p*
Age (years), mean ± SD			
male	59.76 ± 10.76	59.32 ± 10.71	0.779
female	58.36 ± 8.95	58.09 ± 9.12	0.876
Sex, n (%)			
male	59 (59)	109 (54.5)	0.537
female	41 (41)	91 (45.5)	0.537
Years spent in hometown, mean ± SD	47.39 ± 20.94	41.69 ± 23.45	0.035
Change of the place residence, n (%)	8 (8)	42 (21)	0.007
Birth weight (kg), mean ± SD	3.14 ± 0.57	3.63 ± 3.01	0.108
Body weight (kg), mean ± SD	82.88 ± 12.64	77.23 ± 17.04	0.002
Body height (cm), mean ± SD	172.84 ± 7.62	173.09 ± 9.65	0.813
BMI (kg/m^2), mean ± SD	27.57 ± 5.01	25.72 ± 3.30	< 0.0005
Rh factor (-), n (%)	8 (8)	25 (12.5)	0.921

BMI – body mass index; SD – standard deviation.

Table 2

Comparison of blood groups between the patients with glioma and the control group

Groups	Patients with glioma n (%)	Control group n (%)	*p*
AB	31 (32.3)	21 (12.2)	< 0.0005
A	24 (25.0)	63 (36.6)	0.070
B	10 (10.4)	28 (16.3)	0.256
O	31 (32.3)	60 (34.9)	0.768
Total	96 (100)	172 (100)	

Table 3

Distribution of blood groups in the male patients with glioma and the control group (male)

Groups	Patients with glioma n (%)	Control group n (%)	*p*
AB	18 (31.6)	8 (8.7)	0.001
A	14 (24.6)	30 (32.6)	0.726
B	7 (12.2)	17 (18.5)	0.668
O	18 (31.6)	37 (40.2)	0.726
Total	57 (100)	92 (100)	

Table 4

Distribution of blood groups in the female patients with glioma and the control group (female)

Groups	Patients with glioma n (%)	Control group n (%)	*p*
AB	13 (33.3)	13 (16.2)	0.057
A	10 (25.7)	33 (41.2)	0.288
B	3 (7.7)	11 (13.8)	0.549
O	13 (33.3)	23 (28.8)	0.522
Total	39 (100)	80 (100)	

Univariate binary logistic regression showed that higher number of years spent in the hometown (OR 1.011 95% confidence interval (Cl) 1.000–1.023; $p = 0.043$) increased the body weight (0.976 95% Cl 0.959–0.993) and increased the body mass index (OR 0.898 95% Cl 0.839–0.961) increased the risk of glioma. However, a change of the residence decreased the risk of glioma about three times (OR 0.327 95% Cl 0.147 – 0.727; $p = 0.006$) (Table 5).

The univariate binary logistic regression analysis revealed that the individuals with the group AB were at 3.5-fold increased risk of developing glioma compared to the individuals with other blood groups (OR 3.429 95% Cl 1.834–6.411; $p < 0.0005$). The blood groups A (OR 0.696 95% Cl 0.402–1.204; $p = 0.195$), B (OR 0.690 95% Cl 0.321–1.485; $p = 0.343$) and O (OR 1.064 95% Cl 0.632–1.792; $p = 0.816$) were not significantly associated with a glioma risk (Table 5).

Table 5

Univariate regression analysis of the relationship between the demographic features, ABO blood group and glioma

Variable	Odds ratio [95% confidence interval (CI)]	*p*
Age	1.004 (0.980 – 1.029)	0.728
Sex	0.832 (0.512 – 1.353)	0.495
Years spent in hometown	1.011 (1.000 – 1.023)	0.043
Change of the place residence	0.327 (0.147 – 0.727)	0.006
Birth weight	0.590 (0.317 – 1.101)	0.097
Body weight	0.976 (0.959 – 0.993)	0.006
Body height	0.997 (0.970 – 1.025)	0.826
BMI	0.898 (0.839 – 0.961)	0.002
Rh factor (-)	1.104 (0.857 – 1.423)	0.442
Blood group AB	3.429 (1.834 – 6.411)	< 0.0005
Blood group A	0.696 (0.402–1.204)	0.195
Blood group B	0.690 (0.321–1.485)	0.343
Blood group O	1.064 (0.632–1.792)	0.816

BMI – body mass index.

Discussion

In our study, we demonstrated that the distribution of blood groups in the patients with glioma differ significantly than in the control group, with a higher incidence of glioma reported in the individuals with the blood group AB. Previous studies showed different results about the ratios of blood groups in the patients with glioma**.** The study of Yates and Pearce [5], which was conducted on 473 cases with astrocytoma excluding glioblastoma multiforme, showed that in 164 patients, who were diagnosed before 1945, a distribution of the blood groups was normal. In 305 patients analyzed after that year, a statistically significantly lower number of glioma in the patients with the blood group O was noticed. Selvestrone and Cooper [6] also examined the relationship between the blood groups and astrocytic brain tumors, including glioblastoma multiforme, and they found a statistically significantly lower number of patients with the B and O blood types. The study of Jates [7] recruited 160 patients with glioma and the same number of controls and observed no significant difference in the distribution of blood groups between the glioma patients and controls from the Oxford region in the United Kingdom. Strang et al. [8] did not detect significant difference in the distribution of blood group between 900 astrocytoma patients and the control population. However, once adjusted for sex, there was significantly more male cerebral astrocytoma patients with group A ($p < 0.05$). In the meta-analysis by Zhang et al. [11] which examined the relationship between the blood groups and cancer risk were included 89 studies (82 case control studies and 7 cohort studies). The study by Akhtar et al. [9] analyzed 1674 patients with glioma and results suggested that the blood groups were not significantly associated with a glioma risk. In a recent study, Allouh et al. [12] reported a significant association between the distribution of blood group ABO antigens and glioblastoma multiforme in Jordanians, with a higher incidence reported in the persons with the blood group A.

In the last five decades, relationship between the blood groups ABO and carcinoma has been extensively investigated.

Mechanisms that explain the relationship between the blood groups ABO and a cancer risk are unclear. Several hypotheses have been proposed, including a modulatory role of blood group ABO antigens. The blood group antigens (A, B) are expressed on the surface of red blood cells and numerous other tissues. For a variety of tumor types, the blood group antigens expressed on the surface of malignant cells was found to be different from the antigens expressed on normal cells [15–17]. Modified expression of blood group antigens on the surface of cancer cells may alter cell motility, sensitivity to apoptosis and immune escape, and thus influence the initiation and spread of cancer [18]. Also, the blood group ABO system regulate the level of circulating proinflammatory and adhesion molecules (such as E-selectin, P-selectin and intracellular adhesion molecule-1), which are important for tumourigenesis. Chronic inflammation was extensively linked with a cancer development and provides a potential mechanisms by which the ABO antigens may influence a risk of cancer. One of the possible explanations about the role of the blood group ABO in the tumourigenesis process is the recent discovery of vWF that is an important modulator of angiogenesis and apoptosis. Individuals with other blood groups have significantly higher levels of plasma concentrations of vWF compared to individuals with blood group O. On the other hand, vWF may not have a significant role in cancer progression, and the elevated vWF levels can simply be an indication of the extent of endothelial dysfunction caused by tumor growth [19]. Some research have shown that the structure of certain tumor antigens is similar to the structure of antigens of the ABO blood group system. For example, Prieto and Smith [20] presented the Forssman antigen. This antigen is synthesized predominantly in stomach and colon cancer and structurally it is identical to the A antigen determinant. One study found neoexpression of ABO blood group antigens in hepatocellular carcinoma tissues. These mechanisms are biologically plausible to explain the association between the ABO blood group and a risk of cancer; the underlying mechanisms for the discrepancy among different cancer sites still remains a challenge [19].

Morever, our results suggest that a change of place of living decreases a risk of glioma and that higher number of years spent in hometown increases the risk of glioma. Until now, there have been no studies that have examined the relationship between the change of residence and a number of years spent in hometown and a risk of glioma. In this case control study, increased body weight and increased body mass index increase a risk of glioma.

Conclusion

To our knowledge, this is the first study that examined the frequency of blood group in patients with glioma among the Serbian population. Also, for the first time our study results suggest that blood group AB increases the risk of glioma.

The results of our study suggest that the blood group AB can be the one of hereditary factors which have an influence on the occurrence of glioma. The further research on a much larger sample is needed to confirm these findings as well as potential mechanisms by which the blood group ABO system affects the occurrence of glioma.

Conflict of interest

The authors report no conflict of interest.

R E F E R E N C E S

1. *Ostrom QT, Bauchet L, Davis FG, Deltour I, Fisher JL, Langer CE*, et al. The epidemiology of glioma in adults: A "state of the science" review. Neuro Oncol 2014; 16(7): 896–913.
2. *Ostrom QT, Gittleman H, Fulop J, Liu M, Blanda R, Kromer C,* et al. CBTRUS Statistical Report: Primary Brain and Central Nervous System Tumors Diagnosed in the United States in 2008-2012. Neuro Oncol 2015; 17 Suppl 4: iv1–iv62.
3. *Malmer B, Adatto P, Armstrong G, Barnholtz-Sloan J, Bernstein JL, Claus E*, et al. GLIOGENE an International Consortium to Understand Familial Glioma. Cancer Epidemiol Biomarkers Prev 2007; 16(9): 1730–4.
4. *Bondy ML, Scheurer ME, Malmer B, Barnholtz-Sloan JS, Davis FG, Il'yasova D,* et al. Brain tumor epidemiology: consensus from the Brain Tumor Epidemiology Consortium. Cancer 2008; 113(7 Suppl): 1953–68.
5. *Yates PO, Pearce KM*. Recent change in blood-group distribution of astrocytomas. Lancet 1960; 1(7117): 194–5.
6. *Selvestrone B, Cooper DR*. ABO blood group and astrocytomas. J Neurosurg 1961; 18: 602–4.
7. *Yates PO*. Malgnant glioma and ABO blood group. Br Med J 1964; 1(5378): 310.
8. *Strang RR, Tovi D, Lopez J*. Astrocytomas and the ABO blood groups. J Med Genet 1966; 3: 274–5.
9. *Akhtar K, Mehdi G, Sherwani R, Sofi L*. Relationship between various cancers and ABO blood groups: A Northern India experience. Int J Pathol 2010; 13(1): 1–4.
10. *Akca Z, Mutlu H, Erden A, Buyukcelik A, Sezer Y, Inal A*. The relationship between ABO blood group and glioblastoma multiforme. Med Sci 2014; 3(4): 1639–47.
11. *Zhang B, He N, Huang Y, Song F, Chen K*. ABO blood groups and risk of cancer: A systematic review and meta-analysis. Asian Pac J Cancer Prev 2014; 15(11): 4643–50.
12. *Allouh MZ, Barbarawi AM, Hiasat MY, Al-Qaralleh MA, Ababneh EI*. Glioblastoma and ABO blood groups: Further evidence of an association between the distribution of blood group antigens and brain tumours. Blood Transfus 2017; 15(6): 543–7.
13. *Landsteiner K*. Über Agglutinationserscheinungen normalen menschlichen Blutes. In: *Harper PS,* editor. Landmarks in Medical Genetics. Oxford: Oxford University Press; 1901. p. 112–4.
14. *Franchini M, Liumbruno GM*. ABO blood group: Old dogma, new perspectives. Clin Chem Lab Med 2013; 51(8): 1545–53.
15. *Liumbruno GM, Franchini M*. Beyond immunohaematology: The role of the ABO blood group in human diseases. Blood Transfus 2013; 11(4): 491–9.
16. *Hsiao L, Liu N, You S, Hwang L*. ABO blood group and the risk of cancer among middle-aged people in Taiwan. Asia Pac J Clin Oncol 2015; 11(4): e31–6.
17. *Jovanović SS, Veljković DK*. Immunobiological and clinical significance of blood groups. Beograd: Intra Net Communication; 2009. (Serbian)
18. *Louis DN, Perry A, Reifenberger G, Deimling A, Figarella-Branger D, Cavenee WK,* et al. The 2016 World Health Organization Classification of Tumors of the Central Nervous System: A summary. Acta Neuropathol 2016; 131(6): 803–20.
19. *Franchini M, Lippi G*. The intriguing relationship between the ABO blood group, cardiovascular disease, and cancer. BMC Med 2015; 13: 7.
20. *Prieto PA, Smith DF*. A new ganglioside in human meconium defected by antiserum against the human milk sialylohigosaccharide 2S-tetrasaccharide b. Archives of Biochemistry and Biophysics 1985; 241(1): 281–9.

Received on December 30, 2016.
Revised on March 24, 2017.
Accepted on July 06, 2017.
Online First September, 2017.

ORIGINAL ARTICLE

UDC: 616.936
https://doi.org/10.2298/VSP170509124P

Severe imported malaria in a Serbian referral center

Teška importovana malarija u tercijarnoj zravstvenoj ustanovi u Srbiji

Jasmina Poluga*†, Uroš Karić*, Zorica Dakić‡, Nataša Katanić*§, Lidija Lavadinović*, Branko Milošević*†, Nataša Nikolić*, Aleksandar Urošević*†, Boris Jegorović*, Milorad Pavlović†

Clinical Centre of Serbia, *Infectious and Tropical Diseases University Hospital, Department of Microbiology, ‡Parasitological Laboratory, Belgrade, Serbia; University of Belgrade, †Faculty of Medicine, Belgrade, Serbia; University of Priština/Kosovska Mitrovica, §Faculty of Medicine, Kosovska Mitrovica, Serbia

Abstract

Background/Aim. The World Health Organization estimates that 3.2 billion people are at a risk of being infected with malaria. Thus, the adequate diagnostic protocols for malaria, especially those aimed at determining disease severity, are paramount both in endemic and non-endemic setting. The aim of this study was to identify the demographic, parositological, clinical and laboratory characteristics associated with severe malaria in a non-endemic settings. **Methods.** We analyzed 22 patients with severe malaria and compared their clinical and laboratory findings with those of the patients with non-severe malaria in a search of predictors of disease severity. All patients were treated at the Infectious and Tropical Diseases University Hospital, Clinical Centre of Serbia in Belgrade, Serbia from 2000 to 2010. **Results.** The average age of patients with with severe malaria was 44.86 ± 12.33 years and men predominated (95.45%). The patients with severe malaria were infected *Plasmodium falciparum* (*P. falciparum*) significantly more frequently compared with those with non-severe disease (p =0.047). Jaundice was the most commonly observed feature of severe malaria, followed by anemia and renal failure. The multifactor analysis of variance showed that thrombocytopenia (p = 0.05) and high serum tumor necrosis factor-alpha levels (p = 0.02) were significantly associated with the disease severity. **Conclusion.** A high index of suspicion for malaria should be maintained when evaluating febrile patients returning from the malaria endemic regions. The elevated serum tumor necrosis factor-alpha levels and thrombocytopenia are associated with severe malaria in non-endemic settings.

Key words:
malaria; tumor necrosis factor-alpha; thrombocytopenia; severity of illness index; serbia.

Apstrakt

Uvod/Cilj. Svetska zdravstvena organizacija procenjuje da je oko 3,2 milijarde ljudi u riziku od inficiranja malarijom. Dakle, adekvatni dijagnostički protokoli za ovu bolest, naročito oni koji su namenjeni za utvrđivanje težine bolesti, od presudnog su značaja u enedemskim i neendemskim regijama. Cilj rada bio je identifikacija demografskih, parazitoloških kliničkih i laboratorijskih obeležja udruženih sa teškim oblikom malarije u neendemskim regijama. **Metode.** Analizirali smo 22 bolesnika sa teškom malarijom i uporedili njihove kliničke slike i laboratorijske analize sa nalazima kod bolesnika koji su imali manje teške forme malarije, a sve u cilju identifikovanja prediktora težine bolesti. Svi bolesnici bili su lečeni u Klinici za infektivne i tropske bolesti Kliničkog centra Srbije u Beogradu u periodu od 2000. do 2010. godine. **Rezultati.** Oboleli od teške malarije su bili prosečne starosti od 44,86 ± 12,33 godina i to pretežno muškarci (95,45%). *Plasmodium falciparum* (*P. falciparum*) je bio značajno češći izolat kod bolesnika sa teškom malarijom u odnosu na bolesnike sa lakšim formama malarije (p = 0,047). Oboleli sa teškom formom malarije najčešće su imali žuticu, a zatim anemiju i akutnu bubrežnu slabost. Multifaktorska analiza varijanse pokazala je da su trombocitopenija (p = 0,05) i visoke koncentracije faktora alfa nekroze tumora (p = 0,02) bile značajno povezane sa teškom malarijom. **Zaključak.** Pri evaluaciji febrilnih bolesnika koji se vraćaju iz područja koja su endemska za malariju potrebno je posumnjati na ovu bolest. Visoke koncentracije faktora nekroze tumora-alfa i trombocitopenija povezane su sa teškom malarijom u neendemskim područjima.

Ključne reči:
malarija; faktor nekroze tumora-alfa; trombocitopenija; bolesti, indeks težine; srbija.

Correspondence to: Uroš Karić, Clinical Centre of Serbia, Infectious and Tropical Diseases University Hospital, 11 000 Belgrade, Serbia. E-mail: uroskaric@gmail.com

Introduction

The World Health Organization (WHO) estimates that some 3.2 billion people (about 44% of the world population) are at a risk of being infected with malaria and developing the disease [1]. Some 214 million cases of malaria were reported in 2015 and resulted in 438,000 deaths [2]. The WHO African region carries a disproportionately high share of the global malaria burden, considering it was home to 88% of malaria cases and 90% of malaria deaths in 2015 [2].

Severe malaria is defined by clinical or laboratory evidence of vital organ dysfunction [3]. In 1990, the WHO established the criteria for severe malaria in order to facilitate future clinical and epidemiological studies [4]. In the year 2000, these criteria were revised to include other clinical and laboratory abnormalities that portend a poor prognosis based on the clinical experience in the semi-immune patients [5]. *Plasmodium falciparum* (*P. falciparum*) is the most common cause of severe malaria, but *P. vivax and P. knowlesi* can also cause severe disease [6]. Although rare, *Plasmodium ovale* (*P. ovale*) were also reported in the patients with severe malaria [7].

The circulating level of tumor necrosis factor-alpha (TNF-alpha) was shown to be a marker of organ failure and, as such, was correlated to malaria severity [8–10]. Low thrombocyte counts were also proven to be related to the severity both of vivax and falciparum malaria, although some authors questioned their usefulness for triage and prognostication [11–13]. Most studies correlating the platelet counts and TNF-alpha levels to disease severity were conducted in endemic settings [9–13].

In 1975, the WHO announced that malaria was eradicated from Europe, with what was then the Socialist Federal Republic of Yugoslavia designated as malaria free since 1964. This meant that malaria was also eradicated from Serbia which was one of the six republics constituting the federation [14]. However, imported malaria remained a concern in the years that follow [15].

The aim of this study was to identify the demographic, parasitological, clinical and laboratory characteristics associated with severe malaria in a non-endemic setting.

Methods

We conducted a case control study in order to analyze the clinical, laboratory and parasitological characteristics of severe malaria in the Republic of Serbia. The researchers browsed through the archived paper-based medical records and identified all patients who were treated for malaria at the Infectious and Tropical Diseases University Hospital, Clinical Centre of Serbia in Belgrade, Serbia in the 11-year period (2000–2010).

The Infectious and Tropical Diseases University Hospital is a tertiary health care facility that treats the patients with infectious and/or tropical diseases that cannot be diagnosed and/or treated in other hospitals in Serbia and the patients who reside in the capital city of Belgrade and present directly to the Clinic.

The researchers then analyzed the selected medical records and determined which subset of malaria patients met the criteria for severe disease. Severe malaria was defined according to the WHO criteria as the presence of one of the following: hyperparasitemia (more than 5% parasitized erythrocytes), shock, abnormal bleeding, pulmonary edema/acute respiratory distress syndrome (ARDS), jaundice (a bilirubin concentration higher than 50 μmol/L), renal failure (a urine output < 400 mL per 24 hours and a serum creatinine concentration higher than 265 μmol/L), severe anemia (a hemoglobin concentration less than 7 g/dL or a hematocrit less than 20%), hemoglobinuria, impaired consciousness (a Glasgow coma score less than 11), prostration, multiple convulsions (at least two convulsions in 24 hours), acidosis (a bicarbonate concentration less than 15 mmol/L or arterial/capillary pH lower than 7.25), hyperlactatemia (an arterial lactate concentration >5 mmol/L) hypoglycemia (a plasma glucose concentration lower than 2.2 mmol/L) [5]. The patients with non-severe malaria were used as controls.

The findings on physical examination, parasitological and immunological investigation and blood chemistry panel and complete blood count results were entered into a Microsoft Excel 2010 document. We determined the TNF-alpha concentration in the patients' serum using the ELISA-based standardized kit called the Quantikine ELISA Kit (R&D Systems, 614 McKinley Place NE, Minneapolis) and examined thick and thin peripheral blood stained with Giemsa. Parasitemia was expressed as a percentage of parasitized erythrocytes.

Statistical analysis was preformed using the IMB's SPSS Statistics v14 utilizing descriptive statistics, the χ^2 test, Fisher's exact test (where assumptions for the χ^2 test were not met) and multivariate analysis of variance (MANOVA). We analyzed an average age of the patients, malaria chemoprophylaxis compliance, immunity to malaria, the presence of comorbidities, symptoms duration before admission to hospital, severe thrombocytopenia (platelet count < 50,000 x 10^9/L) and the TNF-α level as possible predictors of severe malaria using MANOVA.

The authors obtained ethical approval from the Ethics Committee of the School of Medicine, University of Belgrade.

Results

We identified 103 patients treated for malaria at the Infectious and Tropical Diseases University Hospital, Clinical Centre of Serbia from 2000 to 2010. A subgroup of 22 (21.35%) patients met the criteria for severe malaria at presentation. Men (95.45%) predominated and the average age of the patients was 44.86 ± 12.33 years (ranging from 21 to 61 years). The age distribution of the patients with severe malaria is represented in Table 1. It was not statistically significantly different than the age distribution of patients with non-severe malaria (Fisher's exact test, $p = 0.759$).

All 3 patients who suffered a fatal outcome had severe malaria making the overall lethality of malaria 2.91% and the lethality of severe malaria 13.64%.

Table 1

Age distribution of patients with malaria

Age (years)	Number (%) of patients	
	non-severe malaria	severe malaria
0–10	1 (1.23)	0 (0)
11–20	1 (1.23)	0 (0)
21–30	6 (7.41)	3 (13.64)
31–40	14 (17.28)	4 (18.18)
41–50	22 (27.16)	6 (27.27)
51–60	24 (29.63)	8 (36.36)
61–70	13 (16.05)	1 (4.55)
Total	81 (100)	22 (100)

A majority of patients with severe malaria were infected with *P. falciparum* (90.9%) which was a statistically significant difference compared with the patients with non-severe forms of the disease (Fisher's exact test, $p = 0.047$). We identified *P. vivax* in the blood of 2 patients with severe malaria, whereas one patient had malaria caused by *P. ovale*. No patients with severe malaria were infected with *P. malariae*. A vast majority of patients with severe malaria (95.45%) had a single *Plasmodium* species as the causative agent. One patient had a mixed *P. falciparum* and *P. vivax* infection (Table 2).

Table 2

Patient distribution by *Plasmodium* species

Plasmodium species	Number (%) of patients	
	severe malaria	non-severe malaria
Plasmodium falciparum	19 (86.38)	56 (69.13)
Plasmodium falciparum + *vivax*	1 (4.54)	4 (4.94)
Plasmodium vivax	1 (4.54)	19 (23.46)
Plasmodium ovale	1 (4.54)	0 (0)
Plasmodium malariae	0 (0)	2 (2.47)
Total	22 (100)	81 (100)

Thirteen patients (59.10%) fulfilled only one criteria for severe malaria at presentation, while 9 (40.90%) had two or more criteria. A single patient fulfilled five criteria for severe malaria and suffered a lethal outcome (Table 3). No patient met more than five criteria. We did not analyze the correlation between the number of fulfilled criteria and disease outcome due to the sparsity of data.

Table 3

Distribution of patients with severe malaria according to the number of fulfilled the World Health Organisation (WHO) criteria

Number of fulfilled criteria	Number (%) of patients
1	13 (59.10)
2	4 (18.19)
3	3 (13.63)
4	1 (4.54)
5	1 (4.54)
Total	22 (100)

The distribution of patients according to the features of severe malaria is represented in Table 4. Jaundice was present in 28.21% of patients making it the most commonly fulfilled criterion for severe malaria in our cohort ($\chi^2 = 22.744$, $p = 0.05$). No criteria of disease severity aside from those represented in Table 4 were fulfilled by the patients in the study cohort.

Table 4

Distribution of patients according to the features of severe malaria

Features of severe malaria (WHO criteria)	Number (%) of patients
Cerebral malaria	3 (7.69)
Pulmonary edema/ARDS	2 (5.12)
Renal failure	4 (10.26)
Disseminated intravascular coagulation	1 (2.56)
Jaundice	11 (28.21)
Anemia	7 (17.95)
Haemoglobinuria	1 (2.56)
Hyperparasitemia	10 (25.65)

WHO – World Health Organization; ARDS – acute respiratory distress syndrome

Two patients with severe malaria had arterial hypertension, while one had diabetes mellitus. The rest had no comorbidities.

The average TNF-alpha serum level was 31.91 pg/mL. Fourteen patients (63.63%) had severe thrombocytopenia (less than $50{,}000 \times 10^9$ thrombocytes/L). MANOVA revealed that the patients with severe malaria had statistically significantly higher levels of TNF-α ($p = 0.02$) and a statistically significantly higher frequency of severe thrombocytopenia ($p = 0.05$) compared with the patients with non-severe malaria (Table 5).

Table 5

Multivariate analysis of variance (MANOVA)

Variables	Non-severe malaria	Severe malaria	F	*p*
Avarage age (years)	47.47	43.68	0.48	0.49
Lack of Chemoprophylaxis (% of patients)	75.31	77.28	1.69	0.20
Absence of Immunity (% of patients)	46.92	50.00	0.84	0.36
Comorbidities (% of patients)	23.45	13.63	0.15	0.70
Duration of symptoms (days)	6.47	7.23	0.03	0.85
Serum TNF-α level (pg/mL)	17.12	31.91	5.79	0.02*
Number of platelets < $50{,}000 \times 10^9$/L (% of patients)	18.52	63.63	4.10	0.05*

***statistically significant result**

Discussion

In the timespan analyzed in our study, 103 patients with malaria were treated in our Clinic. According to data provided by the Institute of Public Health of Serbia "Dr Milan Jovanović Batut", the total number of malaria cases reported in Serbia in that same period was 121 [16]. The patients not treated in our Clinic were treated in other hospitals, mostly in the Military Medical Academy in Belgrade which treated a number of patients with severe malaria, especially if an interdisciplinary approach was necessary [17].

There is a lack of data when it comes to the severe forms of malaria in countries where the disease is not endemic because most studies can include only a small number of patients [18]. The results of our study showed that 21.35% of patients had severe malaria according to the WHO criteria. Other authors found that the proportion of patients with severe disease varies from 1% to 38% of the total number of patients with malaria [19]. Variations in the percentage of patients with the severe form of malaria are best illustrated by the following: the disease was severe in 7.5% of patients with malaria in Canada, 15.9% in the US and 16% in the UK [20–22]. In Germany, 27.9% of patients with malaria caused by *P. falciparum* had severe disease [23].

The vast majority of patients in our study (approximately 91%) had malaria caused by *P. falciparum*, which is in concordance with data from other studies. Both this and other studies indicated that severe malaria can be caused by *P. vivax*, the so called "falciparum like" syndrome [24–27]. No cases of severe *P. knowlesi* malaria were reported in Serbia in the analyzed time span. In our study, *P. falciparum* was significantly over-represented in the subgroup of patients with severe malaria compared with those with non-severe malaria.

This study shows that the most common features of severe malaria are the following (listed by decreasing frequency): jaundice, hyprparasitemia, anemia, renal failure, cerebral malaria, pulmonary edema/ARDS. Haemoglobinuria (also called blackwater fever) and disseminated intravascular coagulation (DIC) occurred leach in one patient. According to the research by authors from Germany and Spain, hyperbilirubinemia and hyperparasitemia were most commonly associated with severe malaria [23, 28]. A multicentric study from Thailand showed that jaundice was present in 529 (50.4%) of 1,050 patients with severe malaria and hyperparasitemia was present in 33.3% [29].

Cerebral malaria, renal failure, ARDS, anemia and DIC were most commonly associated with a fatal outcome in the US [30]. In this study, the fatal outcomes occurred in 3 (2.91%) patients; the immediate causes of death being cerebral malaria, renal failure and pulmonary edema/ARDS.

Many studies have shown that increasing age is a risk factor for severe malaria although some authors questioned this view [31–35]. The average age of patients with severe malaria in this study was approximately 44 years and the statistical analysis led us to the conclusion that an old age was not a risk factor for severe malaria. The lack of chemoprophylaxis is the second most commonly cited risk factor for severe malaria [31, 36, 37]. Extensive research that had been conducted in France from 1996 to 2003 and included the results from 120 reference laboratories analyzed at the National Center for imported and autochthonous malaria, showed an association between the severe malaria and increasing age, lack of chemoprophylaxis and duration of symptoms before diagnosis [36]. No such associations were proven in this study. The absence of acquired immunity to malaria was not a risk factor for the development of severe disease; a finding was similar to those of French authors [38]. Moreover, previous research suggests that congenital immunity is of a greater importance, and that the acquired immunity depends on the long-term exposure to malaria parasites making it generally limited to areas of high endemicity [39].

According to the results of our study, the patients with severe malaria had significantly higher TNF-α levels and a significantly higher frequency of severe thrombocytopenia compared with the patients with non-severe disease. A retrospective study that had been conducted at the University Hospital of Heidelberg, Germany and included 122 patients with falciparum malaria, showed that thrombocytopenia was a significant predictor of severe malaria [23]. These findings were corroborated by other authors [22, 40]. In severe malaria, the concentrations of proinflammatory cytokines such as TNF-α, interleukin-1 (IL-1), interleukin-6 (IL-6), and interleukin-12 (IL-12) are elevated [41]. The high level of TNF-α in the patients with falciparum malaria correlates with disease severity, hypoglycemia, hyperparasitemia, jaundice, renal failure, cardiovascular complications and death [42]. Many studies showed a statistically significant correlation between the severe malaria and TNF-α levels, the presence of hyperparasitemia, jaundice and acute renal failure [43–44].

Conclusion

Even though it is a rare cause of morbidity in a non-endemic setting, a high index of suspicion for malaria should be maintained when evaluating febrile patients returning from malaria endemic regions. TNF-alpha is significantly higher and thrombocytes are significantly lower in the patients with severe malaria both in endemic and non-endemic settings and Serbia is no exception. Other proinflammatory cytokines may also represent a viable early diagnostic test for predicting malaria severity and presents us with an avenue of future research. Since *P. falciparum* causes a large proportion of imported malaria cases in Serbia and is most strongly associated with severe disease (lethal in one in eight patients), the identification of *Plasmodium spp.* in a patient's blood or even a febrile illness in a patient returning from a *P. falciparum* endemic region, should prompt the clinician to request a determination of the TNF-alpha levels and platelet counts in order to take measures to prevent and/or more effectively treat possible organ failure. Whether this approach is cost-effective remains to be elucidated.

R E F E R E N C E S

1. *World Health Organization*. Malaria. 2015. [cited 2015 Dec 16]. Available from: http://www.who.int/mediacentre/factsheets/fs094/en/
2. *World Health Organization*. World Malaria Report. Geneva: WHO Document Production Services; 2015.
3. *World Health Organization*. Management of severe malaria: A practical handbook. 3rd ed. Geneva: WHO Press; 2012.
4. *World Health Organization*. Division of Control of Tropical Diseases. Severe and complicated malaria. Trans R Soc Trop Med Hyg 1990; 84(Suppl 2): 1–65.
5. World Health Organization. Communicable Diseases Cluster. Severe falciparum malaria. Trans R Soc Trop Med Hyg 2000;94(Suppl 1): S1-90.
6. *World Health Organization*. Guidelines for the treatment of malaria, third ed. Geneva: WHO Press; 2015.
7. *Strydom KA, Ismail F, Frean J*. Plasmodium ovale: a case of not-so-benign tertian malaria. Malar J 2014; 13: 85.
8. *Kern P, Hemmer CJ, van Damme J, Gruss HJ, Dietrich M*. Elevated tumor necrosis factor alpha and interleukin-6 serum levels as markers for complicated Plasmodium falciparum malaria. Am J Med 1989; 87(2): 139–43.
9. *Scuderi P, Sterling KE, Lam KS, Finley PR, Ryan KJ, Ray CG*, et al. Raised serum levels of tumour necrosis factor in parasitic infections. Lancet 1986; 2(8520): 1364–5.
10. *Day NP, Hien TT, Schollaardt T, Loc PP, Chuong LV, Chau TT*, et al. The prognostic and pathophysiologic role of pro- and anti-inflammatory cytokines in severe malaria. J Infect Dis 1999; 180(4): 1288–97.
11. *Hanson J, Phu NH, Hasan MU, Charunwatthana P, Plewes K, Maude RJ*, et al. The clinical implications of thrombocytopenia in adults with severe falciparum malaria: a retrospective analysis. BMC Med 2015; 13: 97.
12. *Leowattana W, Tangpukdee N, Thar SK, Nakasiri S, Srivilairit S, Kano S,* et al. Changes in platelet count in uncomplicated and severe falciparum malaria. Southeast Asian J Trop Med Public Health 2010; 41(5): 1035–41.
13. *Saravu K, Docherla M, Vasudev A, Shastry BA*. Thrombocytopenia in vivax and falciparum malaria: an observational study of 131 patients in Karnataka, India. Ann Trop Med Parasitol 2011; 105(8): 593–8.
14. *Popovic B, Mikic D, Zeljkovic J, Čekanac R, Vidanović M*. Malarija u srpskoj vojsci na Solunskom frontu sa posebnim osvrtom na pocetak epidemije polovinom 1916. godine. Opšta medicina 2008; 14(1–2): 37–44. (Serbian)
15. *Dakić Z, Pelemiš M, Djurković-Djaković O, Lavadinović L, Nikolić A, Stevanović G*, et al. Imported malaria in Belgrade, Serbia, between 2001 and 2009. Wien Klin Wochenschr 2011; 123 Suppl 1: 15–9
16. Institute of Public Health of Serbia "Dr Milan Jovanović Batut". Godišnji Izveštaji O Zaraznim Bolestima Na Teritoriji Republike Srbije. 2011. Sept. 2011. Web.. [cited 2017 Jul 15]. Available from: http://www.batut.org.rs/index.php?content
17. *Mikic D, Djokic M, Bojic I, Pavlovic M, Balint B, Vucinic Z,* et al. A severe form of falciparum malaria associated with staphylococcal endocarditis. Vojnosanit Pregl 2001; 58(6): 689–94. (Serbian)
18. *Seringe E, Thellier M, Fontanet A, Legros F, Bouchaud O, Ancelle T*, et al. French National Reference Center for Imported Malaria Study Group. Severe imported Plasmodium falciparum malaria, France, 1996-2003. Emerg Infect Dis 2011; 17: 807–13.
19. *Trampuz A, Jereb M, Muzlovic I, Prabhu RM*. Clinical review: Severe malaria. Crit Care 2003; 7(4): 315–23.
20. *Kain KC, Harrington MA, Tennyson S, Keystone JS*. Imported malaria: prospective analysis of problems in diagnosis and management. Clin Infect Dis 1998; 27(1): 142–9.
21. *Mali S, Kachur SP, Arguin PM*. Division of Parasitic Diseases and Malaria, Center for Global Health; Centers for Disease Control and Prevention (CDC), Malaria surveillance - United States, 2010. MMWR Surveill Summ 2012; 61(2): 1–17.
22. *Phillips A, Bassett P, Zeki S, Newman S, Pasvol G*. Risk factors for severe disease in adults with falciparum malaria. Clin Infect Dis 2009; 48(7): 871–8.
23. *Schwake L, Streit JP, Edler L, Encke J, Stremmel W, Junghanss T*. Early treatment of imported falciparum malaria in the intermediate and intensive care unit setting: an 8-year single-center retrospective study. Crit Care 2008; 12(1): R22.
24. *Mueller I, Galinski MR, Baird KJ, Carlton JM, Kochar DK, Alonso PL*, et al. Key gaps in the knowledge of Plasmodium vivax, a neglected human malaria parasite. Lancet Infect Dis 2009; 9(9): 555–66.
25. *Baird KJ*. Neglect of Plasmodium vivax malaria. Trends Parasitol 2007; 23(11): 533–9.
26. *Sharma A, Khanduri U*. How benign is benign tertian malaria? J Vector Borne Dis 2009; 46(2): 141–4.
27. *Singh H, Parakh A, Basu S, Rath B*. Plasmodium vivax malaria: is it actually benign? J Infect Public Health 2011; 4(2): 91–5.
28. *González A, Nicolás JM, Muñoz J, Castro P, Mas J, Valls ME,* et al. Severe imported malaria in adults: retrospective study of 20 cases. Am J Trop Med Hyg 2009; 81(4): 595–9.
29. *Dondorp AM, Lee SJ, Faiz MA, Mishra S, Price R, Tjitra E,* et al. The relationship between age and the manifestations of and mortality associated with severe malaria. Clin Infect Dis 2008; 47(2): 151–7.
30. *Newman RD, Parise ME, Barber AM, Steketee RW*. Malaria-related deaths among U.S. travelers, 1963-2001. Ann Intern Med 2004; 141(7): 547–55.
31. *Rabe C, Paar WD, Knopp A, Münch J, Musch A, Rockstroh J,* et al. Malaria in the emergency room. Results of the emergency treatment of 137 patients with symptomatic malaria. Dtsch Med Wochenschr 2005; 130(4): 145–9.
32. *Muhlberger N, Jelinek T, Behrens RH, Gjorup I, Coulaud JP, Clerinx J*. Surveillance importierter Infektionen in Deutschland Surveillance Networks . Age as a Risk Factor for Severe Manifestations and Fatal Outcome of Falciparum Malaria in European Patients: Observations from TropNetEurop and SIMPID Surveillance Data. Clin Infect Dis 2003; 36(8): 990–5.
33. *Schwartz E, Sadetzki S, Murad H, Raveh D*. Age as a risk factor for severe Plasmodium falciparum malaria in nonimmune patients. Clin Infect Dis 2001; 33(10): 1774–7.
34. *Gjørup IE, Rønn A*. Malaria in elderly nonimmune travelers. J Travel Med 2002; 9(2): 91–3.
35. *Koh KH, Chew PH, Kiyu A*. A retrospective study of malaria infections in an intensive care unit of a general hospital in Malaysia. Singapore Med J 2004; 45(1): 28–36.
36. *Legros F, Bouchaud O, Ancelle T, Arnaud A, Cojean S, le Bras J*, et al. The French National Reference Centers for Imported and Autochthonous Malaria Epidemiology and Chemosensitivity Network. Risk factors for imported fatal Plasmodium falciparum malaria, France, 1996-2003. Emerg Infect Dis 2007; 13(6) :883–8.
37. *Krause G, Schöneberg I, Altmann D, Stark K*. Chemoprophylaxis and malaria death rates. Emerging Infect Dis 2006; 12(3): 447–51.
38. *Bruneel F, Hocqueloux L, Alberti C, Wolff M, Chevret S, Bédos J,* et al. The clinical spectrum of severe imported falciparum malaria

in the intensive care unit: report of 188 cases in adults. Am J Respir Crit Care Med 2003; 167(5): 684–9.

39. Oliveira-Ferreira J, Lacerda MV, Brasil P, Ladislau JL, Tauil PL, Daniel-Ribeiro CT. Malaria in Brazil: an overview. Malar J 2010; 9(1): 115.
40. *Matteelli A, Colombini P, Gulletta M, Castelli F, Carosi G.* Epidemiological features and case management practices of imported malaria in northern Italy 1991-1995. Trop Med Int Health 1999; 4(10): 653–7.
41. *Lyke KE, Burges R, Cissoko Y, Sangare L, Dao M, Diarra I,* et al. Serum levels of the proinflammatory cytokines interleukin-1 beta (IL-1beta), IL-6, IL-8, IL-10, tumor necrosis factor alpha, and IL-12(p70) in Malian children with severe Plasmodium falciparum malaria and matched uncomplicated malaria or healthy controls. Infect Immun 2004; 72(10): 5630–7.
42. *Jennings RM, de Souza BJ, Todd JE, Armstrong M, Flanagan KL, Riley EM,* et al. Imported Plasmodium falciparum malaria: are patients originating from disease-endemic areas less likely to develop severe disease? A prospective, observational study. Am J Trop Med Hyg 2006; 75(6): 1195–9.
43. *Akanmori BD, Kurtzhals JA, Goka BQ, Adabayeri V, Ofori MF, Nkrumah FK,* et al. Distinct patterns of cytokine regulation in discrete clinical forms of Plasmodium falciparum malaria. Eur Cytokine Netw 2000; 11(1): 113–8.
44. *Idro R, Jenkins NE, Newton CR.* Pathogenesis, clinical features, and neurological outcome of cerebral malaria. Lancet Neurol 2005; 4(12): 827–40.

Received on May 9, 2017.
Revised on July 15, 2017.
Accepted on August 2, 2017.
Online First September, 2017.

ORIGINAL ARTICLE

UDC: 616-006:618.19-006-037
https://doi.org/10.2298/VSP170313118C

The concentration of matrix metalloproteinase 9 in the tumor and peritumoral tissue as a prognostic marker in the breast cancer patients

Koncentracija matriks metaloproteinaze 9 u tumoru i peritumorskom tkivu kao prognostički marker kod bolesnica sa karcinomom dojke

[1]Danijela M. Cvetković*, [1]Bojan Z. Milošević[†‡], Aleksandar M. Cvetković[†‡], Srdjan M. Ninković[†‡], Jovana V. Jovankić*, Dalibor V. Jovanović[§], Snežana D. Marković*

[1] equal value

University of Kragujevac, Faculty of Science, *Institute of Biology and Ecology, Kragujevac, Serbia; University of Kragujevac, Faculty of Medical Sciences, [†]Department of Surgery, [§]Department of Pathology, Kragujevac, Serbia; Clinical Center Kragujevac, [‡]General and Thoracic Surgery Department, Kragujevac, Serbia

Abstract

Background/Aim. Breast cancer is one of the most common malignancies among women all over the world. Tumor microenvironment represents one of the main regulators of tumorigenesis. We investigated the role of matrix metalloproteinases 9 (MMP-9) concentration in peritumoral tissue as a prognostic marker in the breast cancer patients. **Methods.** The ELISA test was used to determine a total MMP-9 concentration in carcinoma and peritumoral tissue sample in the patients with breast cancer. Comparison of MMP-9 protein expression with the clinicopathological parameters was evaluated. **Results.** Peritumoral tissue at 3 cm distance from the tumor produces more MMP-9 than the tumor itself. The ratio of concentrations of MMP-9 in the tumor and peritumoral tissue considerably changes in favor of peritumoral tissue with the increase of tumor size and the involvement of axillary lymph nodes. In N0 stage, the concentration ratio of MMP-9 in the tumor and peritumoral tissues was 1 : 1.44, but in the N2 stage, the ratio was 1 : 26.5. **Conclusion.** In patients with breast cancer even in an early stadium there is a change in MMP-9 concentration in peritumoral tissue. We can extract the group of patients at increased risk for the development of lymph node metastasis. A statistically significant difference between the concentrations of MMP-9 in the peritumoral tissue and cancer tissue exists only in case of metastatic disease not in MO stadium implying need for early detection of still unknown metastases in such patients.

Key words:
breast neoplasms; disease progression; matrix metalloproteinase 9; risk assessment; tissues.

Apstrakt

Uvod/Cilj. Karcinom dojke je jedna od najčešćih malignih bolesti žena širom sveta. Tumorsko mikrookruženje predstavlja jedan od glavnih regulatora tumorogeneze. Istraživali smo ulogu koncentracije matriks metaloproteinaze 9 (MMP-9) u peritumorskom tkivu kao prognostičkog markera kod bolesnica sa karcinomom dojke. **Metode.** ELISA test je korišćen za određivanje koncentracije ukupne MMP-9 u uzorcima karcinomskog i peritumorskog tkiva kod bolesnica sa karcinomom dojke. Vršeno je poređenje proteinske ekspresije MMP-9 sa kliničko-patološkim parametrima. **Rezultati.** Peritumorsko tkivo na distanci od 3 cm od tumora produkovalo je više MMP-9 nego sam tumor. Odnos koncentracija MMP-9 u tumorskom i peritumorskom tkivu se znatno menjalo u korist peritumorskog tkiva sa porastom veličine tumora i obimom zahvaćenosti aksilarnih limfnih nodusa. U N0 stadijumu odnos koncentracija MMP-9 u tumorskom i peritumorskom tkivu bio je 1 : 1,44, dok je u N2 stadijumu bolesti taj odnos bio čak 1 : 26,5. **Zaključak.** Kod bolesnica sa karcinomom dojke čak i u ranom stadijumu postoje promene u koncentraciji MMP-9 u peritumorskom tkivu koje mogu poslužiti kao prognostički parametar u proceni agresivnosti bolesti. Analizom odnosa MMP-9 u

Correspondence to: Danijela Cvetković, University of Kragujevac, Faculty of Science, Laboratory for Cell and Molecular Biology, Institute of Biology and Ecology, Radoja Domanovića 12, 34 000 Kragujevac, Serbia. E-mail address: c_danijela@yahoo.com

tumorskom i peritumorskom tkivu možemo izdvojiti grupu bolesnica koja je pod povećanim rizikom od razvoja limfonodalnih metastaza. Statistički značajna razlika između koncentracija MMP-9 u peritumorskom tkivu i tkivu karcinoma postoji samo u slučaju metastatske bolesti, ali ne u M0 stadijumu, ukazujući na potrebu za ranom detekcijom još uvek nedijagnostikovanih metastaza kod takvih bolesnica.

Ključne reči:
dojka, neoplazme; bolest, progresija; matriks, metaloproteinaze 9; rizik, procena; tkiva.

Introduction

Breast cancer is one of the most common malignancies among women all over the world. Breast cancer mortality in the European Union is 58,000 women a year with an estimation of 135,000 new patients diagnosed every year [1]. According to the data from 2012, breast cancer morbidity in Central Serbia was 26% of all malignant diseases [2]. Although breast tumors can appear at early age, the incidence is much higher after the 5th decade and is connected with hormonal changes [3].

Tumor environment (microenvironment, or peritumoral tissue) represents one of the main regulators of tumorigenesis containing cancer-associated fibroblasts having the role in the synthesis of proteins that can remodel extracellular matrix [4, 5]. It is well-known that matrix metalloproteinase-9 (MMP-9) can be secreted from the cancer stromal fibroblasts and endothelial cells [6, 7]. The metastasis of primary tumors depends not only on cancer cells themselves, but the microenvironment as well [8]. Peritumoral tissue must not be considered as a static organ for energy storage, but as an active factor in the communication between the tumor itself and its microenvironment, producing many cytokines, growth factors and hormones that can affect the tumor growth and development [9]. Matrix metalloproteinases (MMPs) is also known as a gelatinase B and is involved in the degradation of extracellular matrix and type IV collagen, the main component of basement membrane [10–13]. It promotes cancer progression by increasing the cancer cell proliferation, migration, invasion, metastasis and angiogenesis [14]. Numerous papers suggest that MMP-9 could be used as a good prognostic marker [15]. MMP-9 protein is located in the tumor cell cytoplasm, but in the stromal fibroblast cells as well, representing one of the tumor microenvironment components [16]. Although the tumor cells are the ones breaking several tissue barriers with the aim of proliferation and spreading, there is some evidence suggesting that the tumor microenvironment cells, such as stromal cells, support the processes of tumor progression [17–19]. The findings suggested that MMPs overexpression might be associated with poor prognosis in breast cancer and its expression is increased with the increase of tumor stage [20–23]. Appropriate resection of cancer considers macroscopically and microscopically clean margins of specimen. We hypothesized that despite the absence of malignant cells, there are some parameters in peritumoral tissue, which can, on a molecular level, indicate a biologically aggressive tumor with poor outcome. Therefore, we performed the study to explore the concentration of MMP-9 in the invasive breast cancer and peritumoral tissue and its value as a prognostic marker. The novelty in our work was the analysis of ratio of MMP-9 concentration between the tumor and peritumoral tissues as a prognostic parameter in the patients with the breast cancer.

Methods

Tissue collection and processing

This work was performed in compliance with the Helsinki Declaration. Both carcinoma and surrounding peritumoral tissue were analyzed. After the decision made by the medical specialists on the combined meeting of surgeons, oncologists and radiologists, an indication for surgery was achieved. All patients who were eligible for surgery were included in the study. After approval of the Ethics Committee of Clinical Centre in Kragujevac (CC Kragujevac No. 01-4990) and written patients' informed consent, the samples were collected from 50 patients. During the surgery regularly performed at the General and Thoracic Surgery Department in Kragujevac, the samples of breast cancer tissue and peritumoral tissue were collected from each patient. The samples of carcinoma tissue were different in size, depending on the size of the tumor itself, whereas the samples of peritumoral, macroscopic unchanged tissue were taken at 3 cm distance from the macroscopic tumor margin. All the samples were histopathological verified by the Department for Pathological and Anatomical Diagnostics in Kragujevac. Weight of samples was measured and they were stored at the temperature of -196ºC until using. All samples were frozen after the initial histopathologic and immunohistochemical analysis after the surgery and all at once thawed and analyzed. The cases were evaluated for the histological type, tumor grade, histological grade (according to the Nottingham histological scores), patient age, lymph node metastasis and estrogen (ER), progesterone (PR), and human epidermal growth factor receptor 2 (HER2/neu) status, according to the American Joint Committee on Cancer (AJCC, 7th ed., 2010) [24, 25].

The study excluded the patients with preoperatively conducted neoadjuvant therapy. The study excluded the patients with previous breast cancer history. Metastatic tumors from other tissue origins were excluded.

Tissue sample preparation

The sample preparation was performed on ice. Homogenization was conducted by adding 500 µl lysis buffer for 0.01 g sample. The IKA Homogenizers IKA®-Werke GmbH & Co. KG, Germany and Ultrasonic homogenizers Sonopuls, BANDELIN electronic GmbH & Co, Germany were used for the automatic sample homogenization. Lysis buffer contained the following components: 31.25 mM Tris-HCl pH 6.8, 2% SDS, 10% glycerol and filled with up to 100 mL dH2O. After 10-min centrifugation at 10,000 rpm at 4°C, supernatant, representing the total cell lysis, was isolated. In this manner, total proteins

from the carcinoma and peritumoral tissue were isolated and the total protein concentration in supernatant was determined. Supernatants were aliquoted and preserved at -80°C until used.

Protein concentration determination

Concentrations of protein in supernatant (samples of carcinoma and peritumoral tissue) were determined using the Lowry method [26].

Determination of metalloproteinases 9 concentration (MMP-9)

Concentration of total MMP-9 (human MMP-9 assay measures the 92 kDa Pro-MMP-9 and the 82 kDa active MMP-9) was detected by the immune/sandwich ELISA method according to the kit procedure (Human MMP-9, R&D Systems). The method is based on the measurement of total MMP-9 amount, the enzyme included in degradation of extracellular matrix which could be in active form or preform [27]. After determination, the total protein concentration, supernatants of peritumoral and carcinoma tissue were used as the samples for the total MMP-9 concentration. The MMP-9 concentration in ng/mL (*per* mg proteins) was calculated according to the known concentrations of MMP-9 from a standard curve.

Statistics

The data were analyzed by using the SPSS (ver. 13.0, Chicago, IL, USA). The data were expressed as mean (four biological replicates) and the standard error of mean (SEM). The unpaired Student's t-test, ANOVA, abnormal χ^2 test, Mann–Whitney *U* tests, Kruskal-Wallis H tests were used. The correlations between two variables were assessed using the Spearman's rho test. All statistical tests were two-sided and the *p* values of 0.05 were considered as statistically significant.

Results

The clinical and pathological parameters of patients with the breast cancer such as margin purity, histological type, histological grade, tumor size, lymph node infiltration, presence of distant metastases (M), receptor status for ER, PR and HER, patient age are given in Table 1.

Figure 1 represents the values of the total MMP-9 concentrations in peritumoral and carcinoma tissue individually for each patient. After comparing the total MMP-9 concentrations, it was indicated that the microenvironment of carcinoma tissue in most samples (72%) produced higher concentrations of MMP-9 than carcinoma tissue (28%).

The mean concentration value of total MMP-9 in peritumoral tissue was significantly higher compared to the concentration in carcinoma breast tissue (Table 2). The correlation between production of total MMP-9 in the carcinoma and peritumoral tissue in the breast cancer patients was statistically significant indicating that the increase of MMP-9 production in carcinoma tissue was associated with the increase of MMP-9 production in peritumoral tissue (Spearman's correlation coefficient, $r = 0.612$, $^{**}p < 0.01$).

The concentration of total MMP-9 in peritumoral and carcinoma tissue of breast cancer was analyzed and compared to margin "cleanness" (Figure 2). The study showed that the highest percentage of samples had clean margins on macroscopic and microscopic examination or R0 resection without the residual carcinoma cells (96% of the total number of samples).

Table 1

Clinical and pathological characteristics of breast cancer patients

Characteristics	Patients, number (%)
Samples	
peritumoral tissue	50 (50)
cancerous tissue	50 (50)
Resection (R) margin	
R0 – no residual tumor	48 (96)
R1 – microscopic residual tumor	2 (4)
R2 – macroscopic residual tumor	0
Histological type of tumor	
invasive ductal carcinoma	43 (86)
invasive lobular carcinoma	7 (14)
Histological grade (G)	
G1 – well differentiated (low grade)	6 (12)
G2 – moderately differentiated (intermediate grade)	28 (56)
G3 – poorly differentiated (high grade)	16 (32)
G4 – undifferentiated (high grade)	0
Tumor (T) size	
T1 (≤ 2)	21 (42)
T2 (2–5)	27 (54)
T3 (> 5)	2 (4)
T4 (tumor extends to skin or chest wall)	0
Age (years)	
< 40	2 (4)
> 40	48 (96)

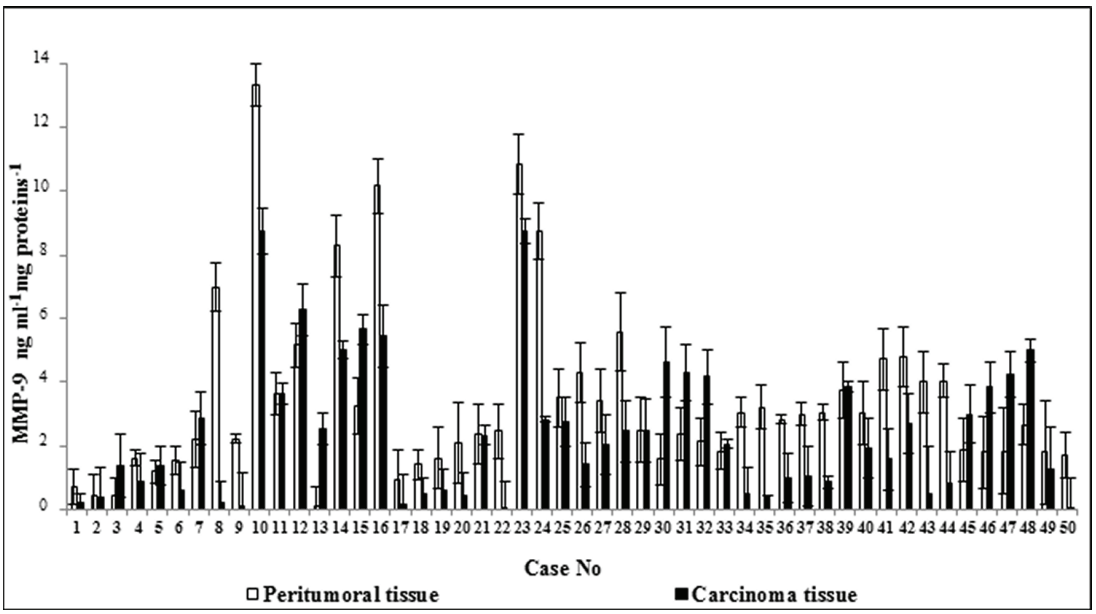

Fig. 1 – Concentrations of total matrix metalloproteinase 9 in carcinoma and peritumoral tissue in the breast cancer patients.
The data were expressed as mean ± standard error (SE) for four independent measurements of each sample.

Table 2

Concentrations of total matrix metalloproteinase 9 (MMP-9) *vs* clinical and pathological characteristics of breast cancer patients

Concentrations of total MMP-9	Peritumoral tissue (mean ± SD)	Carcinoma tissue (mean ± SD)
Mean	3.41 ± 0.27	2.40 ± 0.42*
Invasive ductal carcinoma	3.39 ± 0.31	2.40 ± 0.24*
Invasive lobular carcinoma	3.42 ± 0.27	2.45 ± 0.21*
Age (years)		
< 40	4.61 ± 0.33	3.95 ± 0.58
> 40	3.37 ± 0.28	2.95 ± 0.21

***p < 0.05 statistically significant difference carcinoma *vs* peritumoral tissue.**

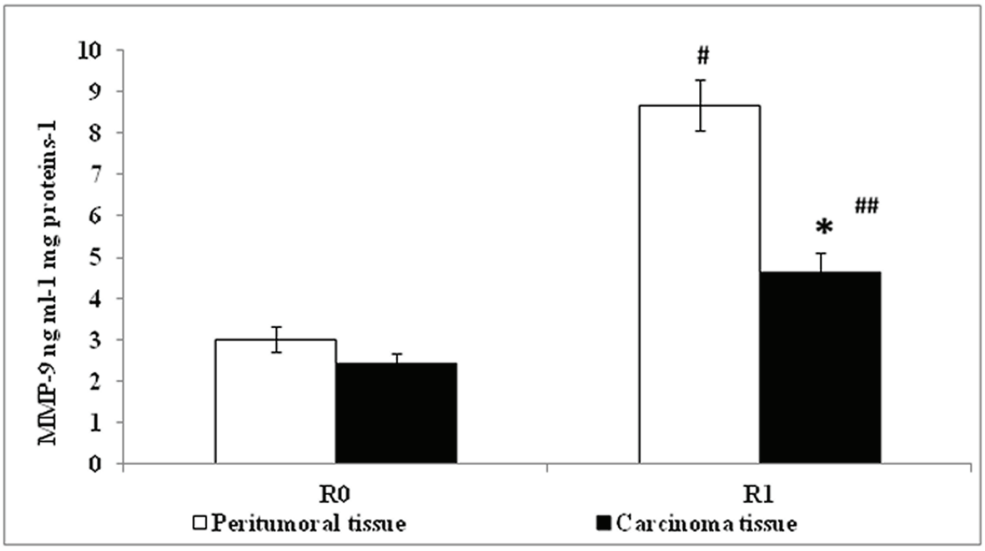

Fig. 2 – Concentration of total matrix metalloproteinase 9 (MMP-9) in peritumoral and carcinoma tissue in the breast cancer in relation to clean margins (R0) and tumor cell affected margins (R1).
The data were expressed as mean ± standard error (SE); n = the number of samples with R0 and R1; *p < 0.05 statistically significant difference carcinoma *vs* peritumoral tissue; #p < 0.05 statistically significant difference R1 *vs* R0 in peritumoral tissue; ##p < 0.05 statistically significant difference R1 *vs* R0 in carcinoma tissue.

Peritumoral tissue around ductal and lobular carcinoma type produced statistically significant higher concentrations of MMP-9 compared to carcinoma tissue (Table 2). The difference in production of MMP-9 in the carcinoma and peritumoral tissue was statistically significant in the ductal and lobular carcinoma type.

It was found that peritumoral tissue around the tumor with the histological grade G3 produced statistically higher concentration of total MMP-9 compared to carcinoma tissue (Figure 3). Amount of MMP-9 was proportionally growing in peritumoral tissue with the increase of histological grade. Peritumoral tissue around the cancer with the high grade (G3) produced statistically higher MMP-9 concentrations compared to other groups.

Figure 4 represents the concentration and distribution of MMP-9 in relation to the TNM classification (Figure 4). The results showed that the MMP-9 concentration was statistically higher in peritumoral tissue around the tumor of the largest dimensions (T3). At the same time, the tumor T3 produced statistically considerably smaller amounts of MMP-9 compared to the small dimension tumors.

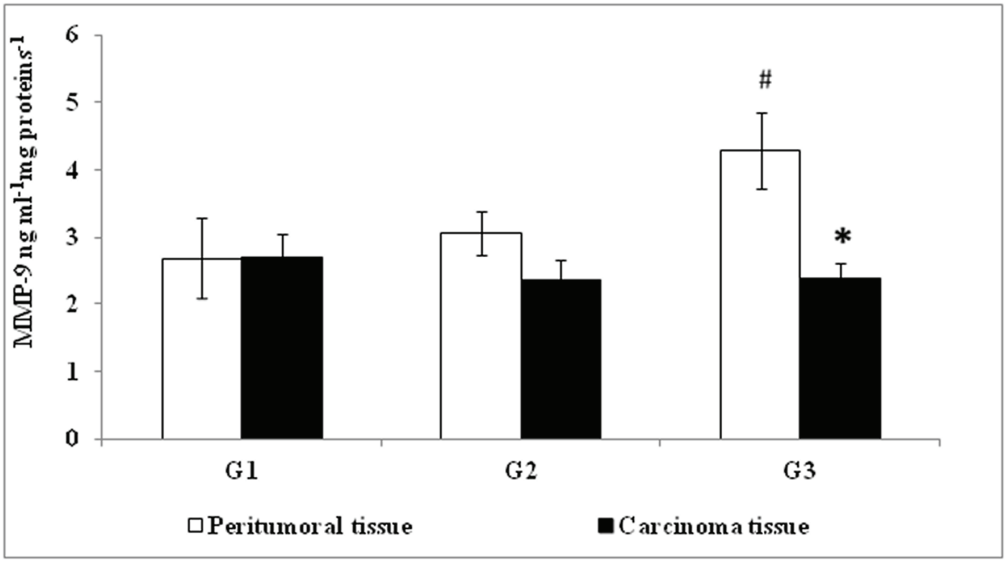

Fig. 3 – Concentration of total matrix metalloproteinase 9 (MMP-9) in peritumoral and carcinoma tissue in the breast cancer in relation to histological grade (G1 – low grade; G2 – intermediate grade; G3 – high grade).
The data were expressed as mean ± standard error (SE); n = the number of samples with G1, G2 and G3; *$p < 0.05$ statistically significant difference carcinoma *vs* peritumoral tissue; #$p < 0.05$ statistically significant difference G3 *vs* G1, G2 in peritumoral tissue.

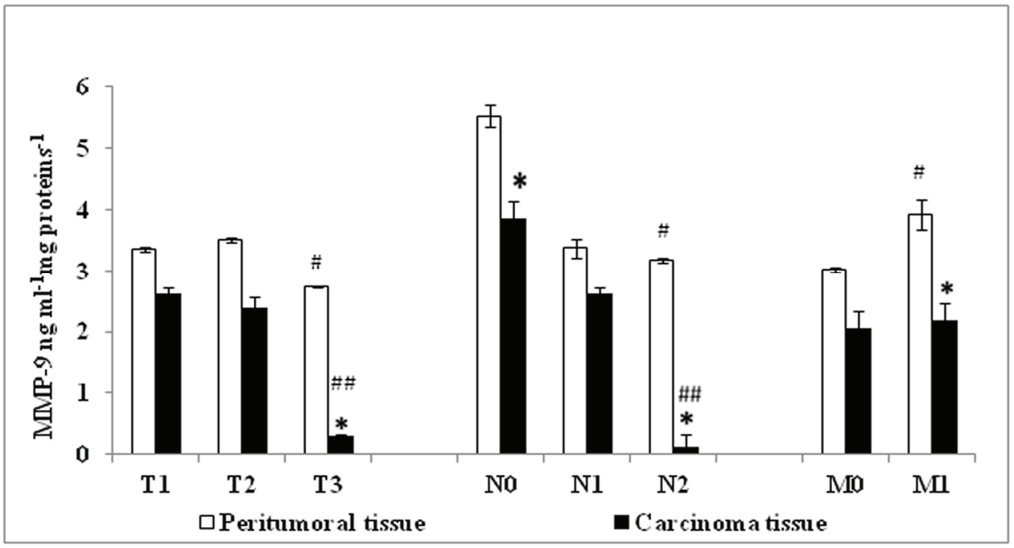

Fig. 4 – Concentration of matrix metalloproteinase 9 (MMP-9) in peritumoral and carcinoma tissue in the breast cancer in relation to tumor mode metastasis (TNM) classification.
The data were expressed as mean ± standard error (SE); n = the number of samples with T1, T2, T3, N0, N1, N2, M0 and M1; *$p < 0.05$ statistically significant difference carcinoma *vs* peritumoral tissue; #$p < 0.05$ statistically significant difference T3 *vs* T1, T2; N2 *vs* N0, N1 and M1 *vs* M0 in peritumoral tissue; ##$p < 0.05$ statistically significant difference T3 *vs* T1, T2; N2 *vs* N0, N1 and M1 *vs* M0 in carcinoma tissue.

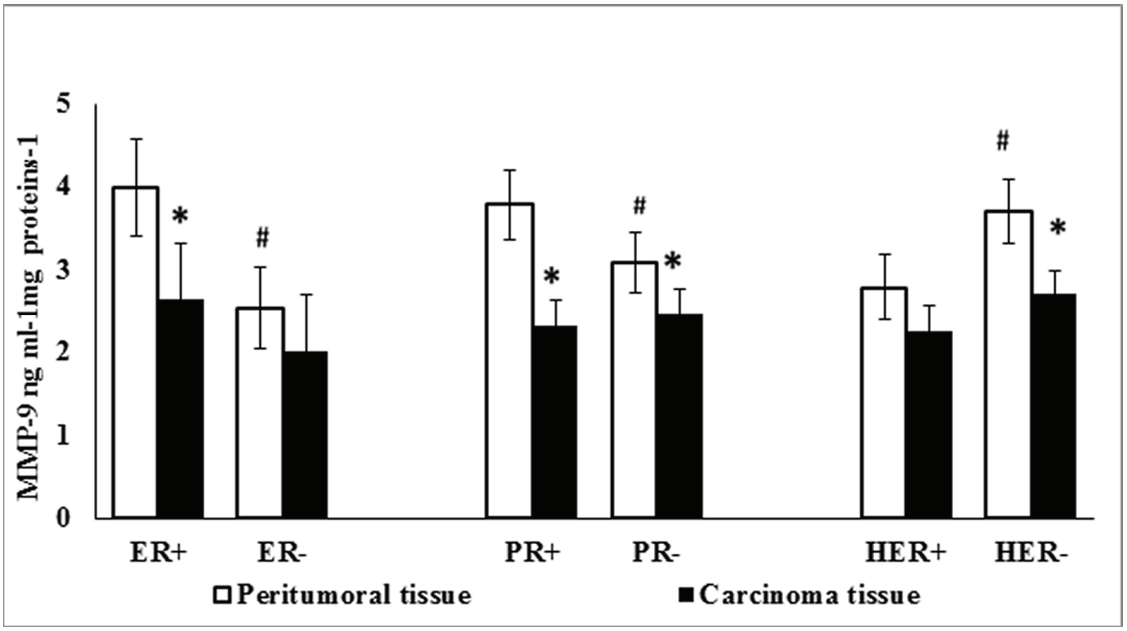

Fig. 5 – Concentration of total matrix metalloproteinase 9 (MMP-9) in peritumoral and carcinoma tissue in the breast cancer with positive (+) or negative (-) receptor expression for estrogen (ER), progesterone (PR) and human epidermal growth factor receptor (HER) [28].
The data were expressed as mean ± standard error (SE); n = the number of samples with ER +, ER-, PR +, PR-, HER + and HER-; *$p < 0.05$ statistically significant difference carcinoma *vs* peritumoral tissue; #$p < 0.05$ statistically significant difference ER + *vs* ER-; PR + *vs* PR- and HER + *vs* HER- in peritumoral tissue.

The concentration of MMP-9 was statistically higher in peritumoral tissue in the N0 and N2 groups compared to carcinoma tissue. Peritumoral tissue around the tumor with "clean" lymph nodes (N0) produced the highest concentrations of MMP-9.

There was one group of patients without confirmation of metastatic disease (Mx group). It included 12% of patients representing a limiting factor of the study. Therefore, this group was excluded from the research. When we compared the MMP-9 production in the patients with determined presence or absence of distant metastasis, we came to the conclusion that peritumoral tissue around the cancer with distant metastasis (M1) produced statistically higher concentrations of total MMP-9 compared to all other groups.

When peritumoral tissue was analyzed, it was noticed that the patient groups marked as T2, N0 and M1 produced the highest concentrations of total MMP-9, whereas the lowest concentrations were noticed in the patient groups marked as T3 (tumor size > 5 cm), N2 (metastases present in the ipsilateral axillary nodes) and M0. In carcinoma tissue, the groups T1, N0 and M1 produced the highest concentrations of MMP-9, whereas the lowest values were produced in the groups T3, N2 and M0. When the MMP-9 production ratio in peritumoral and carcinoma tissue was analyzed, it was concluded that the patients with the biggest cancer dimension (T3) had the biggest ratio 1 : 9.41. Also, there was a drastically big difference in the MMP-9 production in the N2 patient group where the ratio was 1 : 26.5, whereas in the group M1, the MMP-9 production difference between carcinoma and peritumoral tissue was 1 :1.8.

Considering that the status of receptor for estrogen, progesterone and HER2 has a significant role in the breast cancer therapy, concentrations of total MMP-9 in peritumoral and carcinoma tissue were analyzed in relation to expression of these receptors. It was proved that peritumoral tissue in all the examined patient groups produced bigger amounts of total MMP-9 compared to carcinoma tissue (Figure 5). Peritumoral tissue around cancer with the expressed steroid receptors (ER+, PR+) produced a statistically higher amount of MMP-9 compared to the environment around the cancer without these receptors. To the contrary, the concentration of total MMP-9 was higher in peritumoral tissue around the cancer with no expressed receptor for human growth factor (HER-).

In relation to the concentrations of total MMP-9 in peritumoral and carcinoma tissue in relation to patient age with diagnosed breast cancer, it can be said that the microenvironment around the tumor, in the patients younger than 40, produced statistically higher concentrations of MMP-9 compared to the same tissue in older patients.

Discussion

Since the breast cancer represents a systemic disease, surgical treatment is insufficient in treatment of these patients, so the researches on molecular and genetic level are in their full expansion. Surgical intervention is considered as properly oncologically conducted if R0 resection was performed. It means that preparation margins are "clean" both macroscopically and microscopically, without the residual

malignant cells in peritumoral tissue. The R1 resection indicates "macroscopically clean" preparation of margins, yet, the histopathological analysis indicates the presence of tumor on preparation margins. The R2 resection indicates that preparation margins are neither macroscopically nor microscopically "clean" [16, 28–31]. Our assumption is that pathohistological analysis of tumor and peritumoral tissue is insufficient and an examination on the molecular level is required for better prediction of tumor progression. Even if there are no malignant cells in peritumoral tissue, there are some changes on the level of molecular markers indicating a further course of disease. Peritumoral tissue does not represent a passive factor in pathogenesis and tumor development, so we tried to find which parameters or markers in peritumoral tissue could help us predict the progression of malignant disease. According to the literature data, considering its role in the degradation of extracellular matrix, it would be logical to expect that MMP-9 could have a significant role in these processes [32]. We consider that the determination of MMP-9 concentration is significant in prediction of biological tumor behavior in terms of disease aggressiveness not only in carcinoma but in peritumoral tissue as well. To our knowledge, there is just one study described in literature that analysed the MMP-9 concentration in peritumoral breast tissue. There was an isolated group of patients with higher risk of disease metastases and/or recidivism despite correctly conducted radical surgical R0 resection, which was indicated by the elevated level of MMP-9 in peritumoral tissue. Numerous literature data suggest that there is a correlation between MMP-9 and certain clinical and pathological parameters [21]. This study compared both MMP-9 concentration in the tumor and its environment and correlation with the clinical and pathological parameters in the patients with the breast cancer. We proved that the production of total MMP-9 was higher in peritumoral tissue than in tumor itself with a statistically significant difference. There are only a few papers with studies on the MMP-9 level in peritumoral tissue [12]. We found statistically higher concentrations of MMP-9 in peritumoral than in cancer tissue in the ductal as well as the lobular breast cancer. Results showed that the MMP-9 content in the tumor microenvironment increased with the increase of histological grade. Peritumoral tissue at G3 grade produced significantly higher concentrations of MMP-9 compared to G1 and G2 grades. The results correspond to the literature, indicating that the higher MMP-9 concentrations correlate with the less differentiated high grade cancer phenotype [32]. According to our study, there was no correlation between the MMP-9 production and the histological carcinoma type. However, both ductal and lobular types were ascertained with significantly higher concentrations in peritumoral than in carcinoma tissue. These data are in accordance with the literature data [12]. Some papers presented often contradictory attitudes about the correlation of MMP-9 serum concentration and certain clinical and pathological features, but they mostly agreed on absence of correlation between the MMP-9 level and tumor size and/or distant metastases, as well as on presence of correlation between the MMP-9 concentration and metastases in the axillar lymph nodes [33]. The results revealed that the high MMP-9 expression was associated with the small tumor size (T1) as well as with the poor differentiation (G3) which is in accordance with the literature [33]. An interesting fact is that the increase of tumor size considerably changes the concentration ratio in the tumor and peritumoral tissue. In case of T1 tumor, the ratio was 1 : 1.27 in advantage of peritumoral tissue, whereas in the tumor size T3, the ratio was even 1 : 9.41. The increase of tumor size causes the production of smaller amount of MMP-9 but peritumoral tissue continues to produce MMP-9 in unreduced amount. We consider that it is very important to analyze the MMP-9 concentrations both in peritumoral tissue and tumor since the altered ratio proves peritumoral tissue to be an active factor in tumorigenesis. Heo et al. [33] demonstrated a positive correlation between the serum and MMP-9 levels in lymph node metastasis in the breast cancer patients. In this respect, our results are consistent with the literature data. It was noticed that peritumoral tissue produced significantly more MMP-9 than carcinoma tissue in advanced disease stadium (T3, N2, M1). Such a tumor environment in developed disease takes over the role and becomes a dominant source of MMP-9, e.g., MMP-9 concentration ratio in carcinoma and peritumoral tissue was 1 : 1.44 in the N0 stadium, whereas in the N2 stadium, the ratio was 1 : 26.5. Therefore, we conclude that the MMP-9 concentration in peritumoral tissue is directly proportional to involvement degree of axillar lymph nodes. A bigger difference in favor of peritumoral tissue indicates poor prognosis. It could be concluded that even though the primary tumor is removed, MMP-9 activity will not be reduced due to the increased production in peritumoral tissue. A statistically significant difference between the concentrations of MMP-9 in peritumoral tissue and cancer tissue (in favor of the peritumoral tissue) existed only in case of metastatic disease, but not in the M0 stage. This is a very important conclusion because it highlights the importance of seeking and diagnosing still unknown metastases. The results revealed that the increased production of MMP-9 in peritumoral tissue in the breast cancer appeared in the patients with the positive ER and PR receptors [34]. Literature contains data indicating that there is no statistically significant correlation between the serum MMP-9 level on the one, and the ER, PR and HER-2 status on the other hand [35]. It was confirmed that in breast cancer estrogen could promote pathological tumor-stromal interactions through degradation and remodeling of extracellular matrix. Members of the MMP family and their inhibitors play the key role in these processes. There are evidence that ER and related compounds could participate in regulation of these processes [36–38]. We found a statistically significant difference between MMP-9 in peritumoral tissue of the PR+ patients in regard to the PR- patients, but did not demonstrate such difference in cancer tissue, respectively. The results confirmed that a higher concentration of MMP-9 was produced in the patients with unexpressed receptors for HER-2 in carcinoma and peritumoral tissue. According to the MMP-9 expression, it could be concluded which distant organs the breast cancer metastases would appear in. Therefore, in experiment with cells with the expressed HER-2 receptors and higher MMP-9

level, metastases commonly appear in the brain, whereas in the group without expressed HER-2, metastases could be expected in other organs such as bones and pleura. This suggests that analyzing MMP-9 could influence a further treatment course in these patients [39, 40]. The results showed that, in the whole group of patients, a significantly higher level of MMP-9 in peritumoral tissue was associated with the HER-2 negative breast cancer. Literary data claim that the MMP-9 overexpression in the carcinoma cells was associated with the HER-2 overexpression, but only in the subgroup of node-negative patients. Also, the stromal MMP-9 overexpression was associated with the HER-2 overexpression only in the ER+ tumors. It suggests that the relation among the MMP-9 levels and different clinical and pathological features is very complicated and further investigations are needed [32]. In all age categories, the MMP-9 concentration is higher in peritumoral tissue than in carcinoma tissue. Additionally, the MMP-9 concentration in peritumoral tissue was a statistically significantly higher in the group of patients younger than 40 years compared to those older than 40 years. This result agreed with that of Rashad et al. [41].

Conclusion

Our research confirms that breast cancer even in early stage without regional lymph or distant metastases leads to changes in peritumoral tissue detectable on the molecular but not on histopathological level. The analysis of the total MMP-9 concentration indicates that peritumoral tissue does not represent a passive factor in the process of development and dissemination of malignant disease. Tumor environment in the developed disease takes over the role becoming a dominant source of MMP-9. Peritumoral tissue at distance of 3 cm from the tumor produces more MMP-9 than the tumor itself. The increase of tumor size and involvement of axillar lymph nodes changes the ratio of MMP-9 concentration in the tumor and peritumoral tissue in favor of peritumoral tissue. In N0 stage, the concentration ratio of MMP-9 in the tumor and peritumoral tissues is 1 : 1.44, but in N2 stage ratio is 1 : 26.5. A statistically significant difference between the concentrations of MMP-9 in the peritumoral tissue and cancer tissue (in favor of peritumoral tissue) exists only in case of metastatic disease, but not in M0 stage. This is a very important conclusion because it highlights the importance of early detecting of still unknown metastases in such cases.

Conflict of interest

The authors have declared that no competing interests exist.

Acknowledgements

The authors are grateful to the Ministry of Education, Science and Technological Development of the Republic of Serbia for financial support (Grants No. III41010, III41007). The authors are thankful to Prof. Nataša Rakić for proofreading. This work is dedicated in memory of the late Prof. Dr Ljubiša D. Aćimović.

R E F E R E N C E S

1. *Ferlay J, Steliarova-Foucher E, Lortet-Tieulent J, Rosso S, Coebergh JW, Comber H,* et al. Bray Cancer incidence and mortality patterns in Europe: Estimates for 40 countries in 2012., Eur J Cancer 2013; 49: 1374–403.
2. *Miljus D, Zivkovic S, Bozic Z.* Cancer registry of central Serbia. Cancer incidence and mortality in Central Serbia 2012 Report 14. Belgrade: Institute of Public Health of Serbia "Dr Milan Jovanović Batut"; 2014.
3. *Ławicki S, Głażewska EK, Sobolewska M, Będkowska GE, Szmitkowski M.* Plasma Levels and Diagnostic Utility of Macrophage Colony-Stimulating Factor, Matrix Metalloproteinase-9, and Tissue Inhibitor of Metalloproteinases-1 as New Biomarkers of Breast Cancer. Ann Lab Med 2016; 36(3): 223–9.
4. *Franco OE, Shaw AK, Strand DW, Hayward SW.* Cancer associated fibroblasts in cancer pathogenesis. Semin Cell Dev Biol 2010; 21(1): 33–9.
5. *Lorusso G, Ruegg C.*The tumor microenvironment and its contribution to tumor evolution toward metastasis. Histochem Cell Biol 2008; 130(6): 1091–103.
6. *Taguchi A, Kawana K, Tomio K, Yamashita A, Isobe Y, Nagasaka K,* et al. Matrix metalloproteinase (MMP)-9 in cancer-associated fibroblasts (CAFs) is suppressed by omega-3 polyunsaturated fatty acids in vitro and in vivo. PLoS One 2014; 9(2): e89605.
7. *Stuelten CH, Byfield SD, Arany PR, Karpova TS, Stetler-Stevenson W.* Breast cancer cells induce stromal fibroblasts to express MMP-9 via secretion of TNF-α and TGF-β. 2005, J Cell Sc 2005; 118(Pt 10): 2143–53.
8. *Psaila B, Lyden D.* The metastatic niche: adapting the foreign soil. Nat Rev Cancer 2009; 9(4): 285–93.
9. *Nieman KM, Romero IL., Van Houten B, Lengyel E.* Adipose tissue and adipocytes support tumorigenesis and metastasis. Biochim Biophys Acta 2013; 1831(10): 1533–41.
10. *Tabouret E, Bertucci F, Pierga JY, Petit T, Levy C, Ferrero JM*, et al. MMP2 and MMP9 serum levels are associated with favorable outcome in patients with inflammatory breast cancer treated with bevacizumab-based neoadjuvant chemotherapy in the BEVERLY-2 study. Oncotarget 2016; 7(14): 18531–40.
11. *Giganti MG, Tresoldi I, Sorge R, Melchiorri G, Triossi T, Masuelli L,* et al. Physical exercise modulates the level of serum MMP-2 and MMP-9 in patients with breast cancer. Oncol Lett 2016; 12(3): 2119–26.
12. *Wu QW, Yang QM, Huang YF, She HQ, Liang J, Yang QL,* et al. Expression and clinical significance of matrix metalloproteinase-9 in lymphatic invasiveness and metastasis of breast cancer. PLoS One 2014; 9(5): e97804.
13. *Li Y, Jia Q, Wang Y, Li F, Jia Z, Wan Y.* Rab40b upregulation correlates with the prognosis of gastric cancer by promoting migration, invasion, and metastasis. Med Oncol 2015; 32(4): 126.
14. *Bjorklund M, Koivunen E.* Gelatinase-mediated migration and invasion of cancer cells. Biochim Biophys Acta 2005; 1755(1): 37–69.
15. *Yousef EM, Tahir MR, St-Pierre Y, Gaboury LA.* MMP-9 expression varies according to molecular subtypes of breast cancer. BMC Cancer 2014; 14: 609.
16. *Pellikainen JM, Ropponen KM, Kataja VV, Kellokoski JK, Eskelinen MJ, Kosma VM.* Expression of matrix metalloproteinase (MMP)-2 and MMP-9 in breast cancer with a special reference

to activator protein-2, HER2, and prognosis. Clin Cancer Res 2004; 10(22): 7621–8.
17. *O-Charoenrat P, Rhys-Evans PH, Eccles SA*. Expression of matrix metalloproteinases and their inhibitors correlates with invasion and metastasis in squamous cell carcinoma of the head and neck. Arch Otolaryngol Head Neck Surg 2001; 127(7): 813–20.
18. *Charous SJ, Stricklin GP, Nanney LB, Netterville JL, Burkey BB*. Expression of matrix metalloproteinases and tissue inhibitor of metalloproteinases in head and neck squamous cell carcinoma. Ann Otol Rhinol Laryngol 1997; 106(4): 271–8.
19. *Zhang B, Cao X, Liu Y, Cao W, Zhang F, Zhang S,* et al. Tumor-derived matrix metalloproteinase-13 (MMP-13) correlates with poor prognoses of invasive breast cancer. BMC Cancer 2008; 8: 83.
20. *Murawski M, Woźniak M, Duś-Szachniewicz K, Kołodziej P, Rzeszutko M, Ziółkowski P*. Significance of Matrix Metalloproteinase 9 Expression as Supporting Marker to Cytokeratin 19 mRNA in Sentinel Lymph Nodes in Breast Cancer Patients. Int J Mol Sci 2016; 17(4): pii: E571.
21. *Song ZB, Ni JS, Wu P, Bao YL, Liu T, Li M*, et al. Testes-specific protease 50 promotes cell invasion and metastasis by increasing NF-kappaB-dependent matrix metalloproteinase-9 expression. Cell Death Dis 201; 6(3): e1703.
22. *Zeng Y, Liu C, Dong B, Li Y, Jiang B, Xu Y,* et al. Inverse correlation between Naa10p and MMP-9 expression and the combined prognostic value in breast cancer patients. Med Oncol 2013; 30(2): 562.
23. *Zhao S, Ma W, Zhang M, Tang D, Shi Q, Xu S,* et al. High expression of CD147 and MMP-9 is correlated with poor prognosis of triple-negative breast cancer (TNBC) patients. Med Oncol 2013; 30(1): 335.
24. *Elston CW, Ellis IO*. Pathological prognostic factors in breast cancer. I. The value of histological grade in breast cancer: experience from a large study with long-term follow-up. Histopathology 1991; 19(5): 403–10.
25. *Edge SB, Compton CC*. The American Joint Committee on Cancer: the 7th edition of the AJCC cancer staging manual and the future of TNM. Ann Surg Oncol 2010; 17(6): 1471–4.
26. *Lowry OH, Rosebrough NJ, Farr AL, Randall RJ*. Protein measurement with the Folin phenol reagent. J Biol Chem 1951; 193(1): 265–75.
27. *Koepke J, Dresel M, Schmid S, Greulich T, Beutel B, Schmeck B,* et al. Therapy with plasma purified alpha1-antitrypsin (Prolastin®) induces time-dependent changes in plasma levels of MMP-9 and MPO. PLoS One 2015; 10(1): e0117497.
28. *Margonis GA, Buettner S, Sasaki K, Kim Y, Ratti F, Russolillo N*, et al. The role of liver-directed surgery in patients with hepatic metastasis from primary breast cancer: a multi-institutional analysis. HPB (Oxford) 2016; 18(8): 700–5.
29. *Khan SA, Amnekar R, Khade B, Barreto SG, Ramadwar M, Shrikhande SV*, et al. p38-MAPK/MSK1-mediated overexpression of histone H3 serine 10 phosphorylation defines distance-dependent prognostic value of negative resection margin in gastric cancer. Clin Epigenetics 2016; 8: 88.
30. *Uggeri F, Ronchi PA, Goffredo P, Garancini M, Degrate L, Nespoli L,* et al. Metastatic liver disease from non-colorectal, non-neuroendocrine, non-sarcoma cancers: a systematic review. World J Surg Oncol 2015; 13: 191.
31. *Seinen JM, Styring E, Verstappen V, Vult von Steyern F, Rydholm A, Suurmeijer AJ,* et al. Radiation-associated angiosarcoma after breast cancer: high recurrence rate and poor survival despite surgical treatment with R0 resection. Ann Surg Oncol 2012; 19(8): 2700–6.
32. *Köhrmann A, Kammerer U, Kapp M, Dietl J, Anacker J*. Expression of matrix metalloproteinases (MMPs) in primary human breast cancer and breast cancer cell lines: New findings and review of the literature. BMC Cancer 2009; 9: 188.
33. *Heo DS, Choi H, Yeom MY, Song BJ, Oh SJ*. Serum levels of matrix metalloproteinase-9 predict lymph node metastasis in breast cancer patients. Oncol Rep 2014; 31(4): 1567–72.
34. *Kousidou OC, Berdiaki A, Kletsas D, Zafiropoulos A, Theocharis AD, Tzanakakis GN,* et al. Estradiol-estrogen receptor: a key interplay of the expression of syndecan-2 and metalloproteinase-9 in breast cancer cells. Mol Oncol 2008; 2(3): 223–32.
35. *Momeny M, Saunus JM, Marturana F, McCart Reed AE, Black D, Sala G*, et al. Heregulin-HER3-HER2 signaling promotes matrix metalloproteinase-dependent blood-brain-barrier transendothelial migration of human breast cancer cell lines. Oncotarget 2015; 6(6): 3932–46.
36. *Stark AM, Anuszkiewicz B, Mentlein R, Yoneda T, Mehdorn HM, Held-Feindt J*. Differential expression of matrix metalloproteinases in brain- and bone-seeking clones of metastatic MDA-MB-231 breast cancer cells. J Neurooncol 2007; 81(1): 39–48.
37. *Daniele A, Zito AF, Giannelli G, Divella R, Asselti M, Mazzocca A,* et al. Expression of metalloproteinases MMP-2 and MMP-9 in sentinel lymph node and serum of patients with metastatic and non-metastatic breast cancer. Anticancer Res 2010; 30(9): 3521–7.
38. *Elkin M, Cohen I, Zcharia E, Orgel A, Guatta-Rangini Z, Peretz T,* et al. Regulation of heparanase gene expression by estrogen in breast cancer. Cancer Res 2003; 63(24): 8821–6.
39. *Nilsson UW, Garvin S, Dabrosin C*. MMP-2 and MMP-9 activity is regulated by estradiol and tamoxifen in cultured human breast cancer cells. Breast Cancer Res Treat 2007; 102(3): 253–61.
40. *Losordo DW, Isner JM*. Estrogen and angiogenesis: A review. Arterioscler Thromb Vasc Biol 2001; 21(1): 6–12.
41. *Rashad YA, Elkhodary TR, El-Gayar AM, Eissa LA*. Evaluation of Serum Levels of HER2, MMP-9, Nitric Oxide, and Total Antioxidant Capacity in Egyptian Breast Cancer Patients: Correlation with Clinico-Pathological Parameters. Sci Pharm 2013; 82(1): 129–45.

Received on March 13, 2017.
Revised on June 23, 2017.
Accepted on July 04, 2017.
Online First September, 2017.

ORIGINAL ARTICLE

UDC: 616.8-009.1-053.2:[616-053.2-071+616.71
https://doi.org/10.2298/VSP170508125Z

Bone mineral density in comparison to the anthropometric parameters and level of gross motor function in children with cerebral palsy

Mineralna koštana gustina u poređenju sa antropometrijskim parametrima i stepenom oštećenja grube motoričke funkcije kod dece sa cerebralnom paralizom

Jelena Zvekić-Svorcan*†, Mirjana Stojšić*‡, Rastislava Krasnik*‡, Nataša Nenadov*§, Čila Demeši Drljan*‡, Aleksandra Mikov*‡, Maja Radovanov‖

University of Novi Sad, *Faculty of Medicine, Novi Sad, Serbia; †Special Hospital for Rheumatic Diseases, Novi Sad, Serbia; ‡Institute of Child and Youth Health Care of Vojvodina, Novi Sad, Serbia; §Home „Veternik“, Veternik, Serbia; ‖Health Center „Novi Sad“, Novi Sad, Serbia

Abstract

Background/Aim. Children with cerebral palsy (CP) grow at a slower rate relative to their peers. Their body height, body weight and bone mineral density are significantly below those measured for healthy children of corresponding age. The aim of this work was to estimate bone mineral density in relation to the anthropometric parameters and the level of gross motor function in the children with cerebral palsy. **Methods.** This cross-sectional pilot study included 23 children with CP, aged 6 to 17 years, in whom the gross motor function level was estimated according to the Gross motor function classification system- expanded and revised (GMFCS-E&R), while the anthropometric parameters were established in relation to the developmental charts for healthy children as well as those pertaining to children with CP. Bone mineral density was measured by dual energy X-ray absorptiometry and the findings were interpreted in accordance with the International Society for Clinical Densitometry Official Positions of Adults & Pediatrics. Mean values with interquartile deviations, along with frequencies and percentages were the descriptive statistical measures employed in the analyses. Differences between groups were ascertained through the Kruskal-Wallis test. **Results.** Our sample of 23 children comprised of 56.5% boys and 43.5% girls, aged 13.00 ± 3.56 years, of whom 3/4 had a severe form of gross motor dysfunction (GMFCS-E&R levels IV and V). All subjects had lower bone density in both regions of interest [spinal Z-score -1.60 ± 1.40 standard devation (SD); hip Z-score -2.00 ± 3.00 SD], as well as lower anthropometric parameters [height Z-score -2.74 ± 4.28; body weight Z-score -3.22 ± 6.96; body mass index (BMI) Z-score -2.64 ± 6.03]. In the observed sample, bone mineral density in the spine ($p < 0.01$) and the hip ($p < 0.05$) was reduced in all subjects, and all children had a lower body weight ($p < 0.01$) and the BMI ($p < 0.01$), but not body height, in relation to the existing developmental charts for the CP children adopted from the US. Children with the CP Level IV on the GMFCS-E&R had a significantly lower bone density (spinal Z-score -1.90 SD; hip Z-score -3.40 SD), with the reduction even more pronounced at level V (spinal Z-score -3.80 SD; hip Z-score -2.30 SD). **Conclusion.** A significantly lower bone mineral density as well as the decreased values of all observed anthropometric parameters, were noted in the children with CP. In the observed sample, bone mineral density in both spine and hip was reduced in all subjects, all of whom also had lower body weight and the BMI, but not body height compared to the existing developmental charts for the children with CP adopted from the US. The children with severe forms of CP (GMFCS-E&R levels IV and V) had significantly lower bone mineral density.

Key words:
cerebral palsy; child; anthropometry; bone density; muscle tonus.

Apstrakt

Uvod/Cilj. Deca sa cerebralnom paralizom (CP) rastu sporije u odnosu na svoje vršnjake. Njihova telesna visina, telesna težina i mineralna koštana gustina značajno su niže u odnosu na opštu populaciju zdrave dece. Cilj ovog rada bio je procena mineralne koštane gustine u odnosu na antropometrijske parametre i nivo grube motoričke funkcije

Correspondence to: Jelena Zvekic-Svorcan, Special Hospital for Rheumatic Diseases, Futoška 68, 21 000 Novi Sad, Serbia.
E-mail: jelena.zvekic-svorcan@mf.uns.ac.rs

kod dece sa CP. **Metode.** Pilot sudija preseka obuhvatila je 23 dece sa CP, uzrasta od 6 do 17 godina, motoričkog nivoa procenjenog prema sistemu klasifikacije grubih motornih funkcija (*The gross motor function classification system-expanded and revised* – GMFCS-E&R) i antropometrijskih parametara prema kartama razvoja za zdravu decu, kao i prema kartama razvoja za decu sa cerebralnom paralizom. Mineralna koštana gustina merena je dvostrukom X-zračnom apsorpciometrijom, a za očitavanje nalaza korišćene su preporuke Internacionalnog udruženja kliničke denzitometrije – *The International Society for Clinical Densitometry Official Positions of Adults & Pediatrics*. Od deskriptivnih statističkih mera korišćena je srednja vrednost sa interkvartilnim odstupanjima, frekvencije i procenti. Razlike između grupa procenjivane su Kruskal-Wallis-ovim testom. **Rezultati.** U uzorku od 23 dece, bilo je 56,5% dečaka i 43,5% devojčica, starosne dobi 13,00 ± 3,56 godina. Njih 4/5 je imalo teži oblik motoričke onesposobljenosti (GMFCS-E&R, nivoi IV i V). Naši ispitanici imali su nižu koštanu gustinu na obe posmatrane regije [Z-skor kičme -1,60 ± 1,40 standardne devijacije (SD); Z-skor kuka -2,00 ± 3,00 SD], kao i niže antropometrijske parametre [Z-skor telesne visine –2,74 ± 4,28; Z-skor telesne mase -3,22 ± 6,96, Z-skor indeksa telesne mase (BMI) -2,64 ± 6,03]. U posmatranom uzorku kod svih ispitanika bila je snižena mineralna koštana gustina na kičmi ($p < 0,01$) i na kuku ($p < 0,05$), a svi su imali nižu telesnu masu ($p < 0,01$) i BMI ($p < 0,01$), ali ne i telesnu visinu u odnosu na postojeće karte razvoja dece sa CP (SAD). Deca sa CP nivo IV GMFCS-E&R imala su značajno manju koštanu gustinu (Z-skor kičme -1,90 SD, Z-skor kuka -3,40 SD), dok kod nivoa V sniženje je bilo još izraženije (Z-skor kičme -3,80 SD, Z-skor kuka -2,30 SD). **Zaključak.** Deca sa CP imala su značajno manju vrednost mineralne koštane gustine kao i svih posmatranih antropometrijskih parametara. U posmatranom uzorku kod svih ispitanika bila je snižena mineralna koštana gustina na kičmi i na kuku, a svi su imali nižu telesnu masu i BMI, ali ne i telesnu visinu u odnosu na postojeće karte razvoja dece sa CP (SAD). Deca sa težim oblicima CP (GMFCS-E&R, nivoi IV i V stepen) imala su značajno manju vrednost mineralne koštane gustine.

Ključne reči:
paraliza, cerebralna; deca; antropometrija; kost, gustina; mišići, tonus.

Introduction

Cerebral palsy (CP) encompasses a group of disorders that, while not progressive, are subjected to frequent change due to the damage to a developing brain [1, 2]. In addition to issues with fine and gross motor functions, communication, and perception and numerous muscle and skeletal difficulties, growth and development of children with cerebral palsy is also compromised [3, 4]. The CP children grow at a slower rate relative to their peers [4]. Their body mass and length as well as bone mineral density are considerably lower than those pertaining to healthy children of comparable age [5–8]. The poorer nutritional status of these children is typically attributed to numerous difficulties in feeding, inadequate calorie intake and variable, often increased, energy requirements [9–11]. The oromotor dysfunction, inadequate chewing and difficulties in swallowing solid, pulpy and/or liquid food are among factors contributing to the stagnation in body weight and length in these children [8, 11]. Growth and development of children with moderate and severe form of cerebral palsy differs from that of their healthy peers. For example, they enter puberty earlier and reach sexual maturity later than healthy children [4, 12]. The assessment of growth and development is facilitated by developmental charts defined by the World Health Organization (WHO) as well as by the Centers for Disease Control and Prevention (CDC). The CDC provides 16 developmental charts (8 per gender) for assessing boys and girls aged 2 to 20. The parameters in these charts are expressed as a percentile and refer to the body height (BH), body weight (BW) and body mass index (BMI) for the children of the same age group [13]. The body mass index is defined as a ratio of body mass and the square of body height expressed in meters (kg/m^2) [14, 15]. Due to the different clinical manifestations of this entity, these charts are not sufficiently precise for use in the assessment and monitoring of children with CP. In recent years, intense efforts have been dedicated to the systematization of the data pertaining to growth and development of CP children in order to formulate nomograms for growth and development of this cohort. BH and BW of children with CP does not meet the reference standards and can therefore not be assessed using the existing developmental charts for healthy children [6, 13–15]. The developmental pattern for children aged under 10 years with the quadriplegic type of CP was developed by Krick et al. [13] based on a sample of 360 children with this condition. The 10th, 50th and 90th percentile for body length (for age group), body weight (for age group) and body weight (for body length) was graphically represented. Day et al. [6] investigated the development of children and adolescents with CP by studying a sample of 24,920 patients, taking into consideration their disability level, gross motor function and the ability to independently eat or be fed via the gastrostomy tube. The authors supplemented their findings by a graphic representation of the development of both genders according to the age [16]. For the assessment of gross motor function in the CP children aged ≤ 18 years, the revised and extended Gross Motor Function Classification System − Expanded & Revised (GMFCS-E&R) is typically used, whereby children are scored on a scale comprising of five levels [17, 18]. The first level on the gross motor function scale is designated for patients who are capable of moving independently, while level V pertains to those that are not able to move independently [18]. For measurements of bone mineral density (BMD), dual energy X-ray absorptiometry (DEXA) is used [19]. When performing the scans, the posterior-anterior (PA) L1-L4 (femoral neck and total hip) are defined as regions of interest (ROI). “Low bone mineral density” is the preferred term for pediatric DXA reports when BMD Z-scores are ≤ 2 standard deviation (SD) [20]. Non-ambulatory children with neurological disorders such as

CP whose muscle tone in all four limbs is increased often have low bone mineral density and are therefore at a greater risk of experiencing fractures [21]. The aim of this research was to evaluate BMD in relation to the anthropometric parameters and the level of gross motor function in the children with CP.

Methods

The sample employed in this pilot prospective study consisted of 23 children with CP aged 6 to 17 years, residing in the "Veternik" Home residential care facility, and the Clinic for Children's Habilitation and Rehabilitation at the Institute for Child and Youth Health Care of Vojvodina, Novi Sad, Serbia. The pilot study was conducted between January 1st and December 31st, 2014. The patients' BMI was calculated based on their body weight (BW) in kg and body height (BH) in m. Using these values, the following parameters were analyzed: BW Z-score (derived from the body weight nomogram, expressed as the Z-score in comparison to the age-equivalent healthy children). The Z-scores for BW, BH and BMI were calculated from nomograms represented as a percentile. TT-p was obtained from the body weight nomograms, expressed as a percentile in comparison to the age-equivalent healthy cohort. The BH Z-score was deduced from the body height nomograms expressed as the Z-score in comparison to the age-equivalent healthy children, BW-p was derived from the body weight nomograms expressed as a percentile in comparison to the age-equivalent healthy cohort. The BMI Z-score was obtained from the BMI nomogram, expressed as the Z-score in comparison to the age-equivalent healthy children, and the BMI-p was obtained from the BMI nomogram expressed as a percentile in comparison to the age-equivalent healthy children. BMI-p was interpreted as follows: below the 5th percentile – malnutrition; from the 5th to the 84th percentile – normal weight; from the 85th to the 94th percentile – excessive body weight; and the 95th percentile and above – obesity [22]. Height for a specific age group, expressed as a percentile, was interpreted as follows: below the 5th percentile – short stature; from the 5th to the 94th percentile – normal height; the 95th percentile and above – tall stature. Weight in relation to that of the peer group, expressed in percentiles, was interpreted as follows: below the 5th percentile – malnutrition; from the 5th to the 84th percentile – normal weight; from the 85th to the 94th percentile – risk of obesity; and the 95th percentile and above – obesity [14, 23]. The body weight and height data was analyzed according to the developmental charts for healthy children issued by the CDC [23] as well as those for children with CP (Growth Charts − Life Expectancy for CP) [24]. Gross motor function for the patients of both genders were classified according to the GMFCS-E&R [18]. All patients were referred for osteodensitometry at the Special Hospital for Rheumatic Diseases, Novi Sad, Serbia. Osteodensitometry was performed using the Lunar device, with the L1-L4 segment and/or the hip serving as ROI. In three of the examined children, DXA failed to provide the adequate spinal data due to the presence of neuromuscular scoliosis, while hips could not be assessed in 12 children owing to flexion contractures associated with the more severe form of CP. The obtained results for BMD (g/cm^2) were interpreted as standard deviations, expressed as the Z-score. In interpreting the BMD results, recommendations from the International Society for Clinical Densitometry, Official Positions Adults & Pediatrics (ISCD) were used [25]. The following parameters were monitored for all patients: gross motor function level according to the GMFCS-E&R scale, BW, BH, and BMI. These values were compared to those pertaining to the age-matched healthy cohort and children with CP and were examined in relation to their BMD presented as the Z-score. The research was carried out with the approval of the Ethics Committee. The clinical data was subjected to the descriptive statistical analyses, whereby the median with interquartile deviations was used, along with frequencies and percentiles. The Kolmogorov-Smirnov and Shapiro-Wilk test results confirmed that the distributions of spine and hip Z-scores were not statistically significantly different from the normal distribution. The between-group differences were determined using the Kruskal-Wallis test. A statistical significance was defined at the zero hypothesis probability level ranging from $p \leq 0.05$ to $p < 0.01$. The statistical processing and analysis was performed using the SPSS (Statistical Package for the Social Sciences) v.20 software.

Results

The pilot study sample comprised 13 boys and 10 girls (56.5% v.s. 43.5%), aged 13.00 ± 3.565 years. According to the CP type, 74% of the patients had quadriparesis and the most severe motor impairment – level V according to the GMFCS-E&R was noted in 69.6% of the sample. The analysis of nomograms for BH, BW and BMI, expressed as the Z-score, revealed that the values pertaining to the study sample were lower than those expected for a healthy cohort. All patients had lower bone mineral density in at least one region of interest. The spine and hip Z-score distributions did not statistically significantly differ from the normal distribution, as indicated by the Kolmogorov-Smirnov test findings and confirmed by the more rigorous Shapiro-Wilk test (Table 1). When assessed using the nomograms for healthy children, more than a half of the children included in our pilot study had short stature (52.2%) and were malnourished relative to their BW (60.9%) and BMI (56.5%). On the other hand, according to the nomograms for the children with CP, 95.7% of our sample had normal BH and normal nutritional status based on the BW (56.5%) and BMI (78.3%) (Table 2). The findings yielded by the Kruskal-Wallis analysis revealed absence of statistically significant differences in the Z-score for hip between the patients with different BH measured in relation to their peers. As all patients for whom the Z-score was measured with the hip serving as ROI were of regular height, it was not possible to calculate the p value. Statistically significant differences ($p < 0.01$) were also noted in the Z-scores measured with the spine used as ROI between the subjects with different BH

and the healthy age-matched cohort. In addition, the Z-score at the spine for the patients with different BW was statistically significantly different at the 0.01 level from that for the age-matched healthy cohort ($\chi^2 = 10.40$; $p = 0.00$) as well as for children with CP ($\chi^2 = 12.27$; $p = 0.00$). A statistically significant difference at the 0.05 level was also noted in the Z-score at the spine between the patients with different BMI in comparison to a healthy age-matched cohort ($\chi^2 = 5.97$; $p = 0.015$) as well as relative to the children with cerebral palsy ($\chi^2 = 9.65$; $p = 0.00$) at the 0.01 level. The Kruskal-Wallis analysis revealed a statistically significant difference at the 0.01 level in the Z-score at the spine ($\chi^2 = 11.33$; $p = 0.00$) and at the 0.05 level in the Z-score at the hip ($\chi^2 = 7.15$; $p = 0.03$) between the patients with different GMFCS (Table 3).

Table 1

Sample characteristics of the study group compared to the healthy cohort

Variables	n	%	Min	Max	Median	IR	Statistic	df	*p*
Gender (total)	23	100.0							
boy	13	56.5							
girl	10	43.5							
Age (years)	23	100.0	6.00	17.00	13.00	3.565			
CP subtypes									
quadriplegia	17	74							
diplegia	3	13							
hemiplegia	3	13							
GMFCS-E&R levels	23	100.0							
I	4	17.391							
IV	3	13.043							
V	16	69.565							
Height Z-score	23	100.0	-6.07	1.66	-2.74	4.28			
Weight Z-score	23	100.0	-20.03	1.47	-3.22	6.96			
BMI Z-score	23	100.0	-22.90	1.83	-2.64	6.03			
BMD spine (g/cm^2)	20	86.956	0.32	1.12	0.558	0.42			
BMD hip (g/cm^2)	11	47.826	0	1	0.6	0			
Z-score spine (SD)	20	86.956	-3.80	1.00	-1.60	1.40			
Kol.-Smir.							0.207	11	0.200
Shap.-Wilk							0.943	11	0.561
Z-score hip (SD)	11	47.826	-4.00	0.00	-2.00	3.00			
Kol.-Smir.							0.154	11	0.200
Shap.-Wilk							0.943	11	0.560

CP – cerebral palsy; GMFCS-E&R – Gross Motor Function Classification System- Expanded & Revised; BMI – body mass index; BMD – bone mineral density; SD – standard deviaton; IR – interquartile range; Kol.-Smir. – Kolmogorov-Smirnov test; Sharp.-Wilk – Shapiro-Wilk test.

Table 2

The body height, body weight and body mass index (BMI) of patients in comparison to the nomograms of healthy children and children with cerebral palsy

Parameters	Nh n (%)	Ncp n (%)
Height Z-score		
short	12 (52.20)	1 (4.30)
normal	10 (43.50)	22 (95.70)
tall	1 (4.30)	
Weight Z-score		
undernourished	14 (60.90)	10 (43.50)
normal	7 (30.40)	13 (56.50)
the risk for obesity	2 (8.70)	
BMI Z-score		
undernourished	13 (56.50)	5 (21.70)
normal	7 (30.40)	18 (78.30)
overweight	2 (8.70)	
obesity	1 (4.30)	
Total	23 (100.00)	23 (100.00)

Nh – characteristics of the sample in relation to the nomograms of healthy children; Ncp – characteristics of the sample in relation to the nomograms of children with cerebral palsy; BMI – body mass index.

Table 3

Bone mineral density in comparison to the anthropometric parameters and the level of gross motor function in the patients with cerebral palsy according to the nomograms of healthy children and children with cerebral palsy

Parameters	Z-score lumbar spine		Z-score hip	
	Nh	Ncp	Nh	Ncp
Height				
short	-3.80	-4.20	-2.60	/
normal	-1.70	-1.90	-1.70	-2.00
tall	-0.70	/	-0.50	/
χ^2	9.99	1.70	2.05	/
p value	0.01†	0.19	0.36	/
Weight				
underweight	-3.80	-4.10	-3.00	-3.40
healthy weight	-1.60	-1.60	-2.00	-1.85
at risk of overweight	-0.40	/	-0.20	/
χ^2	10.40	13.27	1.08	1.24
p value	0.00†	0.00†	0.30	0.27
BMI				
underweight	-3.95	-4.20	-3.40	-3.40
healthy weight	-1.80	-1.90	-2.00	-1.85
overweight	-0.40	/	-0.20	/
obesity	-1.90	/	-2.00	/
χ^2	5.97	9.65	0.36	1.24
p value	0.01†	0.00†	0.54	0.27
GMFCS-E&R levels				
I		0.30		-0.40
IV		-1.90		-3.40
V		-3.80		-2.30
χ^2		11.33		7.15
p value		0.00†		0.03*

Nh – characteristics of the sample in relation to the nomograms of healthy children; Ncp – characteristics of the sample in relation to nomograms of children with cerebral palsy; BMI – body mass index; GMFCS-E&R – Gross Motor Function Classification System Expanded & Revised.
***p* < 0.05; †*p* < 0.01.**

Discussion

The children with CP, especially those with the most frequent spastic type, are less physically active than their healthy peers. Along with the mobility difficulties, deviations in growth and development are often noted in this cohort. Monitoring the growth and development is of the utmost importance in ensuring optimal child health. The assessment of these parameters is simplified by the use of nomograms developed by the WHO and other institutions. As the growth and nutritional status assessments aimed at the children with cerebral palsy are not standardized, this represents a real challenge for medical practitioners [26]. The children with CP living both in developed and undeveloped countries have lower BH and BW in comparison to their healthy peers, as indicated by numerous studies and observed in this research [5, 24]. In our pilot study, 19 of 23 subjects had the most severe type of gross motor disability (GMFCS-E & R levels IV and V), while the most frequent type of CP was quadriparesis (the bilateral spastic type). All subjects had lower BH, nutritional status and BMD relative to that measured in their healthy peers. In our pilot study, the DXA scanning could not be performed at lumbar spine in three patients due to the presence of neuromuscular scoliosis, while DXA of either hip was unfeasible for 12 patients because of flexion contracture of the hip. Indeed, the difficulties associated with performing the DXA scans were some of the obstacles, in terms of technical feasibility in assessing the bone health of children with CP. Conditions such as hip contractures and hip dysplasia, scoliosis and metal implants often prohibit the DXA measurements at the desired region of interest (lumbar spine or proximal femur) [26, 27]. "Low bone mineral density" is the preferred term for the pediatric DXA reports when the BMD Z-scores are ≤ 2 SD [20]. As mineral density is often low in the children with CP, they are at a risk of fractures at a minimal trauma, which additionally compromises their quality of life [28]. Our results showed that more than a half of the subjects included in our sample had shorter stature and were malnourished according to the body weight and BMI nomograms pertaining to their healthy peers. In comparison to the age-equivalent cohort with cerebral palsy, a majority of the subjects had normal body height and were well nourished according to the BMI, while approximately the same number of children were in the malnourished and well-nourished group. Malnutrition is a frequent problem in the CP children, resulting in the lower muscle strength and poor immunological status [29]. In the study conducted by Karagiozoglou-Lampoudi et al. [15], the anthropometric data for 42 CP patients aged 8.0 ± 4.0 years was analyzed using the Z-scores given by the WHO. Subjects were divided into three groups (comprising 10, 8 and 24 children, respectively), based on

the level of gross motor function according to the GMFCS-E&R: mild (GMFCS-E&R levels I and II), moderate (GMFCS-E&R levels III) and severe (GMFCS-E&R Level IV and V). Thus, a majority of the subjects had either poor mobility or were immobile. When the nutritional status of the sample was assessed in terms of the Z-score according to the WHO, 38.1% of the patients were malnourished while 7.1% were over-nourished. In this study, the Z-scores provided by the WHO was a useful instrument for monitoring the level of nourishment in the CP children [15]. In the study conducted by Dahlseng et al. [9], data from a Norwegian registry of cerebral palsy was analyzed. According to the results reported by the authors, 21% of the children whose data was included in the evaluation were completely dependent on others for help with feeding, while 14% of the sample was fed using the gastrostomy tube. Even though prolonged gastrostomy feeding is connected to the higher body mass and BMI, but not to increased BH, one in four children included in the aforementioned study was malnourished. In our pilot study, our aim was to ascertain whether there were statistically significant differences in the Z-scores pertaining to the hip and spine among subjects with the different body height, body weight and BMI. Extant literature indicates that children of short stature do have lower BMD measured at the lumbar spine in comparison to the CDC nomograms for healthy children [14]. When BW was analyzed in relation to the BMI, the group of underweight children was found to have lower BMI at the lumbar spine in comparison to the CDC nomograms for the healthy age-equivalent cohort, as well as relative to the developmental charts for the children with CP. Children with more severe motor impairment had lower bone mineral density both at the lumbar spine and the hip. Wren et al. [30] used quantitative computed tomography to assess bone density in 37 children with CP and compared their findings with those pertaining to their healthy peers. The children with CP had lower bone density measured at the tibia, while volumetric bone density decreased with the rise of the GMFCS level [30]. Nevertheless, the clinical importance of abnormal DXA findings and its correlation to an increased risk of fracture is still unclear. A careful assessment is necessary, with a close monitoring of patients at a greater bone demineralization risk [31]. Due to the significantly decreased bone mineral density, the children with CP often suffer from the painful fractures following even minimal trauma, and this fragility considerably affects their day-to-day functioning and quality of life. If a child is at a risk, it is necessary to repeat the osteodensitometric measurements at 1−2 year intervals, depending on the clinical findings and existing risk factors specific to the child [28]. Our investigation revealed a highly statistically significant difference in the Z-score for the spine ($p < 0.01$) and the hip ($p < 0.05$) between subjects classified at different GMFCS-E&R levels. More specifically, children with more severe motor disability (GMFCS-E&R level V) had a considerably lower Z-score measured at the spine in comparison to children who were ambulatory without limitations (GMFCS-E&R level I). The ambulatory children with CP classified at GMFCS-E&R Level I had a higher BMD at the hip in comparison to the CP children with more severe motor disability (GMFCS-E&R levels IV and V). By analyzing the nutritional status of the children included in our study sample, and comparing the findings with the growth charts for the children with CP in the US [16], we obtained similar results. Since, in Serbia, no developmental charts for the CP children presently exist, we utilized the Growth Charts-Life Expectancy for the CP chart 24 in our analyses. The growth patterns for the children with CP differ significantly from those observed in the general population and exhibit a considerable deviation according to the severity of functional damage based on GMFCS [32]. The study conducted in Turkey by Şimşek and Tuç [33] marked the first attempt to investigate the connection among the BMI, functional independence and quality of life in children with cerebral palsy. The authors concluded that lower BMD may decrease the everyday activity level as well as compromise quality of life of the children with CP. In an earlier study, Henderson et al. [34] analyzed the data pertaining to 117 children aged 2 to 19 years, all of whom had a moderate or severe CP type according to the GMFCS. The BMD value expressed as the Z-score was lower at the distal femur relative to that measured at the lumbar spine. The lower BMI values were found in children with more severe CP types in comparison to those with the moderate type.

The key limitations in our pilot study stem from the small, heterogenic sample investigated, which did not include the children with levels II and III gross motor function abilities, as well as a small number of children rated at level I (according to the GMFCS-E&R scale). Moreover, other possible risk factors, such as the type and number of anti-epileptic drugs and long-term effects of these medications, a lack of exposure to sunlight (which can cause vitamin D deficiency), nutritive limitations, etc., were not considered in the analyses.

Conclusion

In our pilot study, a much lower bone mineral density, as well as the values of other assessed anthropometric parameters, were recorded for children with CP. In all subjects included in the study sample, the spine and hip BMD was reduced, as was their BW and BMI, but not BH, relative to the available development scales for the CP children used in the US. Inadequate nutritional support for children with CP (especially those with more severe CP forms) was likely to contribute to the lower body weight and BMI values recorded in this study when compared to the utilized nomograms. The children with the more severe CP forms (GMFCS-E&R levels IV and V) had a statistically significantly lower BMD.

The findings yielded by our study indicate regular evaluation of children with CP, their BW, BH, BMI and BMD. We further suggest to invest greater efforts into the understanding and application of various preventive measures aimed at maintaining BMD (nutritive support, vitamin supplementation, kinesitherapy, etc.).

A multidisciplinary approach to the evaluation of children with CP, as well as a set of recommendations and good clinical practice for those populations are clearly needed.

R E F E R E N C E S

1. *Bax M, Goldstein M, Rosenbaum P, Leviton A, Paneth N, Dan B*, et al. Proposed definition and classification of cerebral palsy, April 2005. Dev Med Child Neurol 2005; 47(8): 571–6.
2. *Mejaški-Bošnjak V*. Neurological syndromes in infancy and cerebral palsy. Paediatr Croat 2007;
3. *Rosenbaum P, Paneth N, Leviton A, Goldstein M, Bax M, Damiano D*, et al. A report: the definition and classification of cerebral palsy April 2006. Dev Med Child Neurol Suppl 2007; 109: 8–14.
4. *Kuperminc MN, Stevenson RD*. Growth and nutrition disorders in children with cerebral palsy. Dev Disabil Res Rev 2008; 14(2): 137–46.
5. *Aggarwal S, Chadha R, Pathak R*. Nutritional status and growth in children with cerebral palsy: a review. Int J Med Sci Public Health 2015; 4(6): 737–44.
6. *Day S, Strauss D, Vachon P, Rosenbloom L, Shavelle R, Wu Y*. Growth patterns in a population of children and adolescents with cerebral palsy. Dev Med Child Neurol 2007; 49: 67–71.
7. *Stevenson RD, Conaway M, Chumlea WC, Rosenbaum P, Fung EB, Henderson RC,* et al. Growth and Health in Children With Moderate-to-Severe Cerebral Palsy. Pediatrics 2006; 118(3): 1010–8.
8. *Fung EB, Samson-Fang L, Stallings VA, Conaway M, Liptak G, Henderson RC,* et al. Feeding dysfunction is associated with poor growth and health status in children with cerebral palsy. J Am Diet Assoc 2002; 102(3): 361–73.
9. *Dahlseng MO, Finbråten A, Júlíusson PB, Skranes J, Andersen G, Vik T*. Feeding problems, growth and nutritional status in children with cerebral palsy. Acta Paediatr 2012; 101(1): 92–8.
10. *Marchand V*. Nutrition in neurologically impaired children. Paediatr Child Health 2009; 14(6): 395–401.
11. *Bell KL, Davies PS*. Energy expenditure and physical activity of ambulatory children with cerebral palsy and of typically developing children 1-3. Am J Clin Nutr 2010; 92(2): 313–9.
12. *Worley G, Houlihan CM, Herman-Giddens ME, Donnell MO, Conaway M, Stallings VA,* Calvert RE. Secondary sexual characteristics in children with cerebral palsy and moderate to severe motor impairment: a cross-sectional survey. Pediatrics 2002; 110(5): 897–902.
13. *Krick J, Murphy-Miller P, Zeger S, Wright E*. Pattern of growth in children with cerebral palsy. J Am Diet Assoc 1996; 96(7): 680–5.
14. *Centers for Disease Control and* Prevention (CDC). Growth charts. 2000. Available from: www.cdc.gov/growthcharts/.
15. *Karagiozoglou-Lampoudi T, Daskalou E, Vargiami E, Zafeiriou D*. Identification of feeding risk factors for impaired nutrition status in paediatric patients with cerebral palsy. Acta Paediatr 2012; 101(6): 649–54.
16. New Growth Charts-Life Expectancy for CP, VS, TBI and SCI. Available from: www.lifeexpectancy.org/articles/NewGrowthCharts.shtml
17. *Palisano R, Rosenbaum P, Walter S, Russell D, Wood E, Galuppi B*. Development and reliability of a system to classify gross motor function in children with cerebral palsy. Dev Med Child Neurol 1997; 39(4): 214–23.
18. *Palisano R, Rosenbaum P, Bartlett D, Livingston M*. Gross Motor Function Classification System-Expanded & Revised (GMFCS-E & R). Available from: www.canchild.ca.
19. *Jelić D, Stefanović D, Petronijević M, Jelić MA*. Why dual X-ray absorptiometry is the gold standard in diagnosing osteoporosis. Vojnosanit Pregl 2008; 65(12): 919–22. (Serbian)
20. International Society For Clinical Densitometry (ISCD). Available from: www.iscd.org.
21. *Bowden S, Jessup A, Akusoba C, Mahan D*. Zoledronic acid in non-ambulatory children and young adults with fragility fractures and low bone mass associated with spastic quadriplegic cerebral palsy and other neuromuscular disorders. J Endocrinol Diabetes Mellit 2015; 3(2): 35–41.
22. *Barlow SE*. Expert Committee Recommendations Regarding the Prevention, Assessment, and Treatment of Child and Adolescent Overweight and Obesity: Summary Report. Pediatrics 2007; 120(Suppl): 164–92.
23. *Kuczmarski RJ, Ogden CL, Grummer-Strawn LM, Flegal KM, Guo SS, Wei R*, et al. CDC growth charts: United States. Adv Data 2000; (314): 1–27.
24. *Brooks J, Day S, Shavelle R, Strauss D*. Low weight, morbidity and mortality in children with cerebral palsy: new clinical growth charts. Pediatrics 2011; 128(2): e299–307.
25. *Gordon CM, Bachrach LK, Carpenter TO, Crabtree N, El-Hall Fuleihan G, Kutilek S*, et al. Dual energy X-ray absorptiometry interpretation and reporting in children and adolescents: the 2007 ISCD Pediatric Official Positions. J Clin Densitom 2008; 11(1): 43–58.
26. *Zemel BS, Stallings VA, Leonard MB, Paulhamus DR, Kecskemethy HH, Harcke HT*, et al. Revised pediatric reference data for the lateral distal femur measured by Hologic Discovery/Delphi dual energy X-ray absorptiometry. J Clin Densitom 2009; 12(2): 207–18.
27. *Henderson RC, Berglund LM, May R, Zemel BS, Grossberg RI, Johnson J,* et al. The relationship between fractures and DXA measures of BMD in the distal femur of children and adolescents with cerebral palsy or muscular dystrophy. J Bone Miner Res 2010; 25(3): 520–6.
28. *Houlihan CM, Stevenson RD*. Bone density in cerebral palsy. Phys Med Rehabil Clin N Am 2009; 20(3): 493–508.
29. *Feeley BT, Gollapudi K, Otsuka NY*. Body mass index in ambulatory cerebral palsy patients. J Pediatr Orthop B 2007; 16(3): 165–9.
30. *Wren T, Lee DC, Kay RM, Dorey FJ, Gilsanz V*. Bone density and size in ambulatory children with cerebral palsy. Dev Med Child Neurol 2011; 53(2): 137–41.
31. *Coppola G, Fortunato D, Auricchio G, Mainolfi C, Operto FF, Signoriello G*, et al. Bone mineral density in children, adolescents, and young adults with epilepsy. Epilepsia 2009; 50(9): 2140–6.
32. *Day SM*. Improving growth charts for children and adolescents with cerebral palsy through evidence-based clinical practice. Dev Med Child Neurol 2010; 52(9): 793.
33. *Şimşek TT, Tuç G*. Examination of the relation between body mass index, functional level and health-related quality of life in children with cerebral palsy. Turk Pediatri Ars 2014; 49(2): 130–7.
34. *Henderson RC, Lark RK, Gurka MJ, Worley G, Fung EB, Conaway M*, et al. Bone density and metabolism in children and adolescents with moderate to severe cerebral palsy. Pediatrics 2002; 110(1 Pt 1): e5.

Received on May 8, 2017.
Revised on August 6, 2017.
Accepted on August 8, 2017.
Online First September, 2017.

ORIGINAL ARTICLE

UDC: 616.314-089.843:615.46
https://doi.org/10.2298/VSP170809097M

Cytotoxicity of a titanium alloy coated with hydroxyapatite by plasma jet deposition

Citotoksičnost legure titana obložene hidroksiapatitom pomoću mlaza plazme

Marko Magić*, Božana Čolović[†], Vukoman Jokanović[†], Saša Vasilijić[‡§], Milan Marković[‡], Dragana Vučević[‡§], Rebeka Rudolf[‖], Snježana Čolić*, Miodrag Čolić[‡§¶]

University of Belgrade, *School of Dentistry, Department of Oral Surgery, [†]Vinča Institute of Nuclear Sciences, [¶]Institute for the Application of Nuclear Energy, Belgrade, Serbia; Military Medical Academy, [‡]Institute for Medical Research, Belgrade, Serbia; University of Defence, [§]Faculty of Medicine of the Military Medical Academy, Belgrade, Serbia; University of Maribor, [‖]Faculty of Mechanical Engineering, Maribor, Slovenia

Abstract

Background/Aim. The deposition of hydroxyapatite (HAP) on the surface of titanium (Ti) alloys enhances bioactivity and osseointegration of the alloys which are widely used as implant materials in dentistry and orthopaedic surgery. However, the stability of HAP and subsequent biocompatibility of such alloys depends on the coating technique. The aim of this work was to test the cytotoxicity of a Ti alloy (Ti6Al4V), coated with HAP by a new plasma deposition method. **Methods.** The Ti6Al4V samples prepared as discs, 10 mm in diameter and 2 mm in thickness, were coated with HAP (one or both sides of the alloy) by an innovative atmospheric plasma jet method. The cytotoxicity of uncoated and HAP coated Ti6Al4V samples was evaluated by examining the morphological changes and viability of L929 fibroblasts in direct contact with the test materials. Adequate negative (polystyrene) and positive (nickel) control discs of the same size were used. The indirect cytotoxicity was determined by cultivating L929 cells with conditioning medium (CM), prepared as extract of the test samples incubated in the complete Roswell Park Memorial Institute (RPMI) 1640 medium for cell cultures. The cytotoxic effect was evaluated based on the degree of metabolic activity, necrosis, apoptosis and proliferation of L929 cells, using the appropriate assays. **Results.** Uncoated and one side HAP coated Ti6Al4V alloys were classified as non-cytotoxic according to the current ISO 10993-5 criteria, whereas two sides HAP coated Ti6Al4V alloy samples were slightly-moderate cytotoxic. The cytotoxicity manifested as the inhibition of metabolic activity and proliferation of L929 cells as well as the induction of their apoptosis and necrosis was significantly reduced by conditioning of HAP/Ti6Al4V alloys for 24 hours. The cytotoxic effect of HAP/Ti6Al4V CM only partly decreased in the presence of nifelate, a calcium (Ca) channel blocker, suggesting that Ca ions were not the only responsible cytotoxic agent. **Conclusion.** The original HAP coating procedure by atmospheric plasma spraying with high energy input enables the production of the stable adhesive coatings on Ti6Al4V alloys. Their cytotoxicity, which depends on the quantity of HAP coating layer, could be significantly reduced up to the non-cytotoxic level by prior conditioning of the alloys in culture medium. Such a procedure, which removes leachable toxic components, could be useful before implantation of HAP coated alloys *in vivo*.

Key words:
dental alloys; titanium; materials testing; hydroxyapatites.

Apstrakt

Uvod/Cilj. Oblaganje površine legura titana (Ti) hidroksiapatitom (HAP) poboljšava bioaktivnost i oseointegraciju Ti legura, koje se široko koriste kao implantacioni materijali u stomatologiji i ortopediji. Međutim, stabilnost HAP prevlake i biokompatibilnost takvih legura zavise od primenjene tehnike oblaganja. Cilj ovog rada je bio da se ispita citotoksičnost Ti6Al4V legure obložene sa HAP pomoću plazme korišćenjem originalne metode. **Metode.** Uzorci Ti6Al4V legure u obliku diska, prečnika 10 mm, debljine 2 mm su presvučeni sa HAP (jednostrano ili obostrano) mlazom atmosferske plazme. Citotoksičnost neobložene i HAP-om obloženih Ti6Al4V legura je ispitivana na osnovu morfoloških karakteristika i vijabilnosti L929 fibroblasta u direktnom kontaktu ćelija sa test materijalima. Odgovarajuća

Correspondence to: Marko Magić, University of Belgrade, School of Dentistry, Department of Oral Surgery, Dr Subotića 4, 11 000 Belgrade, Serbia. E-mail: markomagic@ymail.com

negativna kontrola (polistirenski diskovi) i pozitivna kontrola (diskovi od nikla) istih veličina kao i diskovi Ti6Al4V legura su takođe uključeni u eksperimente. Indirektna citotoksičnost je procenjivana nakon kultivisanja L929 ćelija sa kondicioniranim medijumom (CM), koji je predstavljao ekstrakt testiranih uzoraka inkubiranih u kompletnom Roswel Park Memorial Institute (RPMI) 1640 medijumu za ćelijske kulture. Citotoksični efekat CM je procenjivan na osnovu stepena metaboličke aktivnosti, nekroze, apoptoze i proliferacije L929 ćelija, korišćenjem adekvatnih testova. **Rezultati.** Neobložena Ti6Al4V legura i Ti6Al4V legura obložena jednostrano sa HAP su okarakterisane kao necitotoksične na osnovu ISO 10993-5 kriterijuma, dok je Ti6Al4V legura obložena sa HAP obostrano pokazivala blagu do umerenu citotoksičnost. Citotoksičnost, koja se manifestovala smanjenjem metaboličke aktivnosti i proliferacije L929 ćelija kao i indukcijom njihove apoptoze i nekroze, je bila značajno smanjena ako su uzorci HAP-om presvučenih legura kondicionirani u medijumu u toku 24 časa. Citotoksičnost CM pripremljenih od Ti6Al4V legura obloženih sa HAP je bila samo delimično smanjena u prisustvu nifelata, blokatora kalcijumovih (Ca) kanala, što ukazuje da Ca joni nisu jedini citotoksični faktor. **Zaključak.** Originalna metoda oblaganja Ti6Al4V legure sa HAP pomoću atmosferske plazme u obliku spreja visoke energije omogućava stabilnu adheziju prevlake. Citotoksičnost ovako obrađene legure, koja zavisi od količine nanetog HAP, se može znatno smanjiti do necitotoksičnog nivoa prethodnim kondicioniranjem u medijumu. Ova procedura, kojom se uklanjaju rastvorljive toksične komponente, može biti korisna pre *in vivo* implantacije legura obloženih sa HAP.

Ključne reči:
legure, stomatološke; titan; materijali, testiranje; hidroksiapatiti.

Introduction

Due to their good physical and mechanical properties and biocompatibility [1, 2] , titanium (Ti) and its alloys are widely used as implant materials, predominantly in orthopaedic and dental implant surgery. However, their corrosion properties in acid or alkaline solutions and biological fluids are not satisfactory. Such biomaterials show high friction coefficient, poor wear properties and low abrasion resistance *in vivo* [3, 4]. These disadvantages can be overcome by modification of Ti or Ti alloy surface by different methods, which can lead to favourable bone regeneration and integrity between the bone tissue and implant surface. At the same time, these procedures can improve the clinical performance of implants, without affecting their original biocompatibility. Ideally, surface modifications should enhance osseointegration and fasten the healing phase after implantation. Biofunctionality of coating depends on the coating technique and factors that influence the process of osseointegration such as surface microroughness, coating thickness and nanotopography [5].

Deposition of hydroxyapatite (HAP) coatings on the surface of Ti alloys, due to its similarity to the biological apatite, enhances implant bioactivity and bonding with bone [3–5]. Besides, HAP coatings with corresponding roughness improve the primary stability of implants and can also induce osteogenic differentiation of human mesenchymal stem cells [6–8] and promotion of the ingrowth of new bone tissue [9]. The nanoscale features of HAP coatings increase the rate of the bone formation around the implant surface, diminishing particularly the friction in contact of the implants with natural bone and reducing significantly wearing of bone tissue in direct contact with implant [10]. Plasma-sprayed HAP coatings frequently show a large variation in coating thickness and density, insufficient coating-metal adhesion strength as well as changes in structural and chemical properties during the coating process, especially transformation of the crystalline structure of HAP to the amorphous phase [11, 12].

In our previous paper we described the microstructure and sintering mechanism of HAP coatings on pure Ti obtained by an innovative atmospheric plasma jet method with a high electric energy input [13]. The coating was stable because its adhesion was unusually high, around 60 MPa. Due to such a high adhesion, the coating was stable. On the other hand, the phase composition was appropriate because the crystalline phase of HAP predominates over the amorphous one. In this work, a similar procedure was applied for coating of the Ti6Al4V alloy. The principal goal of the study was to investigate cytotoxicity of uncoated, one side and two sides HAP coated TiV4Al6 test samples using L929 as a target cell line, recommended for the biocompatibility testing of medical devices [14], in different *in vitro* models.

Methods

HAP coatings of Ti6Al4V by plasma jet deposition

The rods of DC Ti6Al4V alloy (Bien-Air Medical Technologies, Switzerland) were cut into discs, diameter 10 mm and height 2 mm, by means of electro-erosion. The discs were firstly polished on one or both sides using fine aluminium oxide (Al_2O_3) powders with granulation of 5 –0.05 mm. The specimens were then immersed in 5 M NaOH aqueous solution for 24 h at 60°C after which they were removed from the solution and washed with distilled water. Afterwards, they were immersed in 1 M $Ca(NO_3)_2$ aqueous solution for 24 h at 60°C, rinsed with distilled water after removing from the solution, and dried at room temperature. Finally, the specimens were heated at 600°C for 4 h in the electrical furnace in an air atmosphere, and cooled to room temperature in the furnace.

Prepared titanium alloy (Ti6Al4V) specimens were further used as a substrate for plasma jet deposition of HAP. The plasma installation PJ-100 (Plasma Jet, Serbia) was used for the plasma spray process. The basic parameters of installation used for the coating deposition were: Plasma power 52.0 ± 1.5 kW, voltage 120 ± 2 V, current 430 ± 5 A, argon flow 38.5 ± 1.2 L/min, powder carrier gas (air) 8 L/min and powder feed rate 2.0 ± 0.1 g/s. The diameter of aperture of

the anode nozzle was 8 mm, while the length of plasma jet was between 60 and 70 mm. The spraying process was controlled fully by a computer-driven device which enabled the nozzle to be moved at chosen speed and direction. Commercially available HAP powder (Captal® 90, Plasma Biotal Limited, UK), with an average grain size of 90 μm was used for the plasma deposition.

Test samples and conditioning

Test samples included: uncoated Ti6Al4V; one side and two sides HAP coated Ti6Al4V discs; polystyrene discs (negative control) and nickel (Ni) discs (positive control). All discs had the same dimensions, diameter of 10 mm and height of 2 mm. The polystyrene discs were prepared by cutting a polystyrene plate (Sarstedt, Germany). The nickel discs were prepared from a Ni road using the same procedure as used for cutting of the Ti6Al4V alloy. Before use in the cell culture experiments, the samples were sonicated in distilled water in an ultrasonic bath for 10 minutes, washed again with distilled water, sterilized in 70% alcohol for 30 minutes and transferred into the sterile Petri dishes to dry on ambient temperature.

The extracts of test samples in culture medium, named as conditioned medium (CM), were prepared by incubating the test samples in complete culture medium consisting of Roswell Park Memorial Institute (RPMI) 1640 medium (Sigma, Munich, Germany) with addition of 10% foetal calf serum (Sigma), 2 mM of L-glutamine (Sigma) and antibiotics (penicillin, streptomycin and gentamicin) (all from Galenika, Belgrade), in an incubator with carbon dioxide (CO_2) at 37°C. The surface area of test samples/volume of complete medium was 1cm^2/mL. Conditioning lasted either 24 hours or 7 days. A similar procedure was applied for the preparation of medium extract from already conditioned samples. After the incubation, CM were collected, centrifuged at 3000 rpm/ 10 min and then frozen at -20°C until use in the cell culture experiments. HAP and $Ca(OH)_2$ (Merck), both at the concentrations of 40 mg/mL were also extracted in the cell culture medium. The control CM was complete RPMI medium without the test samples.

Cytotoxicity assays

The cytotoxicity tests were performed *in vitro* by using a direct contact method of the discs samples with the subconfluent monolayer of L929 cells or indirectly by examining the metabolic activity of L929 cells in the presence of different dilutions of CM according to the ISO-10993-5 guideline [14]. The L929 cells are a mouse fibroblast cell line (ADCC collection, Rockville, MA, USA).

In the direct assay, L929 cells were cultivated in complete RPMI medium in 6-well plates (Sarstedt, Germany) until reaching about 80% confluency. The Ti6Al4V alloys, coated or uncoated as well as positive and negative control samples were placed into the centre of the wells and cultivated for 24 hours in an incubator with 5% CO_2. The surface of the test samples/volume of medium was 1 cm^2/mL. The cells without the test samples served as the negative control. All cultures were done in triplicates. After cultivation, the cultures were examined under the invert microscope (IX51 Inverted Microscope, Olympus) at 10 and 20x magnifications. The quality of cell monolayer was analysed in the proximity and at the distance from the samples. Confluences of cell growth indicated the absence of cytotoxicity while the rounding, vacuolization and detachment of cells indicated the existence of cytopathic effects of the samples. After the microscopic examination, the samples were removed and detached from the plastic surface by using 0.25% of trypsin dissolved in the serum free RPMI medium with addition of 0.02% ethylenediamine tetracetic acid (EDTA). The viability of L929 cells was determined by using 1% Trypan blue. The viability was calculated by subtracting the percent of dead (Trypan blue$^+$ cells) from 100%.

In the experiments with CM, the L929 cells were cultivated in 96-well plates in complete RPMI medium (1 x 10^4/well; volume 200 μL) overnight in sixplicates. After that, the medium was carefully removed and replaced with different dilutions of CM and the cells were cultivated for another 24 hours as described for direct assay. In the experiments where the effect of Ca in CM was investigated, the cultures were treated with nifelate (10 μg/mL), prior to placing CM in the cell cultures. The triplicates of cultures were used for the MTT test, whereas other triplicates were used for the detection of necrosis and apoptosis, respectively.

MTT assay

Metabolic activity was assessed by performing the assay based on mitochondrial succinate dehydrogenase ability to reduce 3- [4,5 dimethyl-thiazol-2-lyl]-2.5 diphenyl tetrazolium bromide (MTT) into the water-insoluble blue Formazan product. This reaction is directly proportional to the cell survival *in vitro* [15]. The L929 cells (1 x 10^4) were cultivated in presence of CM as described above. After cultivation, the medium was carefully removed and filled with new complete culture medium without phenol red (100 μL) in which 0.1mg/ml of MTT was dissolved. The cells were then cultivated for 4 h. After that, 100 μL of 10% sodium dodecyl sulphate (SDS) in hydrochloric acid solution 0.01 mol/L (0.01M HCl) (Serva) was added and cells were cultivated additionally for 18 h.

Formation of formazan was detected in cultures by reading the optical density (OD) of samples at 570 nm (Behring ELISA Processor II, Heidelberg, Germany). The test results were presented as the percentage of the metabolic activity of cells in the culture with the analysed samples in comparison with the metabolic activity of control, non-treated cells. Metabolic activity was calculated as follows: Metabolic activity (%) = [(OD of cells cultivated with test samples – OD of test samples cultivated without cells) / (OD of cells cultivated alone - OD of control medium)] x 100.

Apoptosis and necrosis assays

After 24 hours of cultivation in CM, apoptosis of L929 cells was determined by a morphological method. The cells

were detached from the plastic substrate by trypsine and stained with the Turk solution, as we have already originally described [16]. The apoptotic cells were identified on the basis of their homogeneously stained, condensed nuclei. The number of totally calculated cells/sample was 500. The results were expressed as percentages of apoptotic cells.

Necrosis was detected after staining of the L929 cells with propidium iodide (PI) (Sigma) and the subsequent analysis of cells by the flow cytometry using the Partec Cube 6 flow cytometer. For this purpose, the L929 cells were collected from the wells after trypsinization, washed with phosphate buffered saline (PBS) and incubated with 500 μLof PI (10 μg/mL) dissolved in PBS. The labeled (necrotic) cells were analyzed immediately after staining. The results were expressed as percentages of necrotic cells by analysing 10.000 cells/sample.

Proliferation assay

The proliferative activity of the cells was studied by using a [^{3}H]-thymidine incorporation assay. The L929 cells (1 x 10^4) were plated in 96-well plates in triplicates and incubated overnight. After that, the medium was carefully removed and replaced with different dilutions of CM and the cells were cultivated for 24 hours, followed by a pulse with [^{3}H]-thymidine (1 μCi/well, Amersham, Books, UK) for another 8 hours. After that, the labelling fluids were removed and the cells were detached with 0.25% trypsine. The released radioactivity was measured in the β- liquid scintillation counter (LKB-1219 Rackbeta, Finland). The results are expressed as count per minute (cpm). The relative proliferation was determined by comparing cpm of CM cultures with cpm of cultures with the control medium used as 100%.

Statistical analysis

All experiments were carried out at least three times. The values were expressed as the mean ± standard deviation (SD). The differences between the samples were tested using one-way ANOVA with the Bonferoni post-test. The differences at $p < 0.05$ were considered as statistically significant.

Results

Cytotoxicity of HAP coated Ti6Al4V alloy samples

The first aim of this study was to examine the cytotoxicity of HAP coated Ti6Al4V alloy samples by using a direct assay on the L929 cells according to the ISO 10993-5 guideline. Three Ti6Al4V samples were tested: uncoated Ti6Al4V, one side, and two sides HAP coated Ti6Al4V disc samples. Cytotoxic Ni discs were used as the positive control. Negative controls were polystyrene disks and the L929 cells without any test materials. As presented in Figure 1, no significant changes in the cell morphology and morphological signs of cytotoxicity were observed around the Ti6Al4V samples and negative control samples compared to the control cells. The cells in culture with the positive control samples showed clear signs of cytotoxicity manifested as rounding, deadherence, necrosis and completely inhibited growth of L929 cells. No significant signs of cytotoxicity, except slight inhibition of growth, were observed around the one side coated Ti6Al4V samples. However, the morphological signs of cytotoxicity were visible around the two sides HAP coated Ti6Al4V discs, whereas the distant cells appeared healthy. When the test discs were removed, the cytotoxicity signs were noticed under all test samples, except under the negative, polystyrene controls.

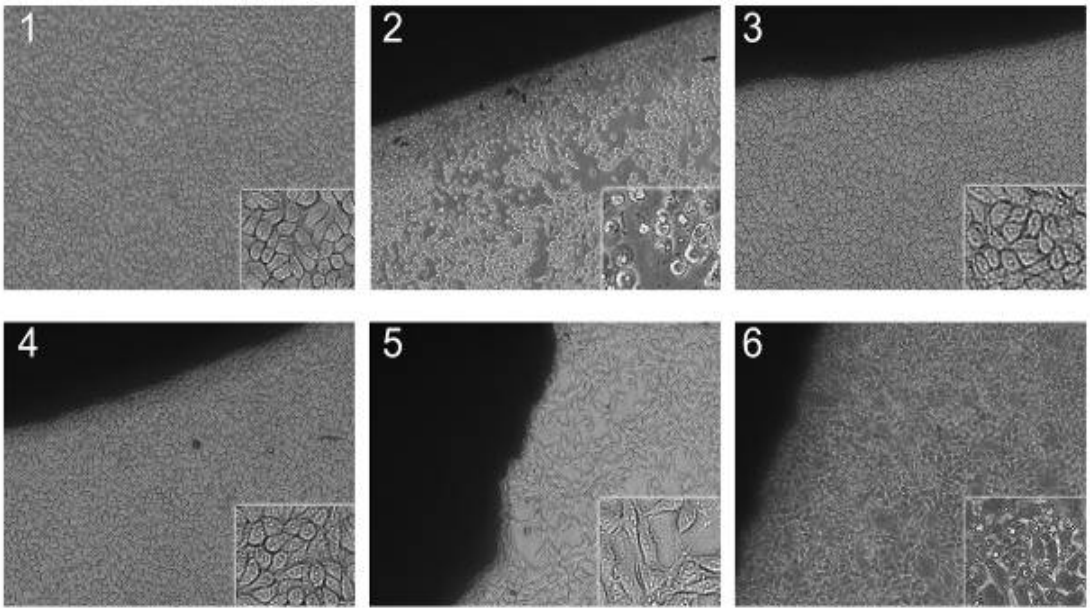

Fig. 1 – Morphological appearance of L929 cells monolayers in culture with different test samples. 1) Negative control (cells alone); 2) Positive control (nickel disc); 3) Negative control (polystyrene disc); 4) Ti6Al4V uncoated disc; 5) One side hydroxyapatite (HAP) coated Ti6Al4V disc; 6) Two sides HAP coated Ti6Al4V disc. (Magnification: x100; Inserts x 300).

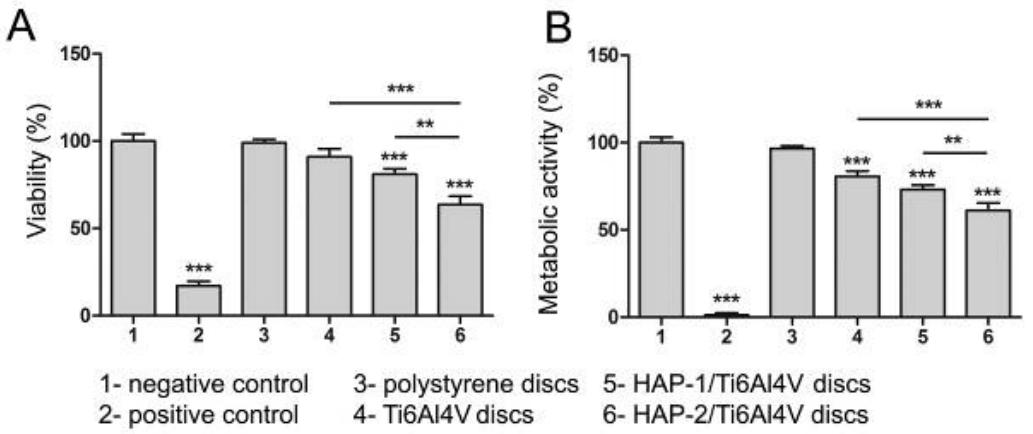

Fig. 2 – The effect of uncoated and HAP coated Ti6Al4V alloys and control samples on viability (A) and metabolic activity (B) of L929 cells.
The test samples were incubated with the L929 cells for 24 hours as described in methods. Viability was determined after removal of the samples. Metabolic activity was determined after the treatment of L929 cells with the conditioning medium (CM) of test samples by using the cell viability (MTT) assay. The results are presented as relative values (mean ± standard deviation (SD) of triplicates) compared to the negative control (cells cultivated alone) values used as 100%.
****-$p < 0.01$; *****-$p < 0.005$ compared to the negative control or to the corresponding samples, as indicated by bars**
HAP-1/HAP-2: hydroxyapatite coated on one or two sides of Ti6Al4V alloy, respectively.

These morphological observations were confirmed by using the quantitative viability assay, based on the calculation of Trypan blue positive (dead) cells (Figure 2A). The differences between the two sides HAP/Ti6Al4V and one side HAP/Ti6Al4V samples as well as between the two sides HAP/Ti6Al4V and uncoated Ti6Al4V samples, respectively, were statistically significant ($p < 0.005$). To examine whether the observed cytotoxicity was due to the released toxic products from the HAP/ Ti6Al4V alloys, CM prepared after a 24-hour conditioning of the samples in the culture medium were used. The results presented in Figure 2B showed the same pattern of cytotoxicity, except that the level of cytotoxicity was slightly higher compared to the viability assay. Based on the ISO 10993-5 criteria, the uncoated Ti6Al4V alloy and one – side HAP/Ti6Al4V alloy were classified as non–cytotoxic (reduction of viability less than 30%), whereas the two sides HAP/Ti6Al4V alloy was classified as slight–moderate cytotoxic (reduction of viability by 30%–55%).

Both apoptosis and necrosis are involved in cell death induced by CM of the HAP/Ti6Al4V alloy

The additional tests were performed to evaluate the mode of cytotoxicity: PI staining to evaluate necrosis; Türk staining to evaluate apoptosis and [^{3}H]-thymidine incorporation assay as an indicator of cell proliferation. Figure 3A showed that undiluted CM of Ti6Al4V alloys (uncoated, one side – and two sides HAP coated) induced necrosis of L929 cells. Necrosis was the highest using CM prepared from the two sides HAP/Ti6Al4V alloys and was dilution dependent. It is interesting that the lower concentrations of HAP/Ti6Al4V CM induced higher degree of apoptosis that the higher ones (Figure 3B). The observed necrosis/apoptosis results were in agreement with the results obtained in the proliferation assay. As expected, the inhibition of [^{3}H] - thymidine incorporation by the L929 cells was the highest using CM of two sides HAP/Ti6Al4V samples. All three tested Ti6Al4V CM samples showed the higher degree of inhibition of cellular proliferation compared to the level of cytotoxicity obtained by using the necrosis/apoptosis assays (Figure 3C).

Conditioning decreases the cytotoxicity of HAP/Ti6Al4V samples

Next, we examined whether the conditioning modified the cytotoxicity of HAP/Ti6Al4V alloys. In this context, the two sides coated HAP/Ti6Al4V discs were conditioned for 24 hours and then tested in the direct cytotoxicity assay. At the same time the 24 hour CM, prepared from already conditioned HAP/Ti6Al4V alloys, was tested by the MTT. The same procedures were applied for the uncoated Ti6Al4V and control samples. As presented in Figures 4A and 4B, both the direct and indirect assays clearly showed that conditioning significantly decreased the cytotoxic effect of HAP/Ti6Al4V alloys. The cytotoxicity of two sides HAP/Ti6Al4V alloys determined by the MTT assays (initial 48.2 ± 4.73) was decreased after conditioning (23.5 ± 3.0) to the level of accepted cytotoxicity according to the ISO 10993-5 criteria ($p < 0.005$). In contrast, the cytotoxicity of uncoated Ti6Al4V as well as Ni discs and their CM were not significantly modified. No further reduction of cytotoxicity was observed after the additional conditioning of samples for 7 days (Figures 4C and 4D).

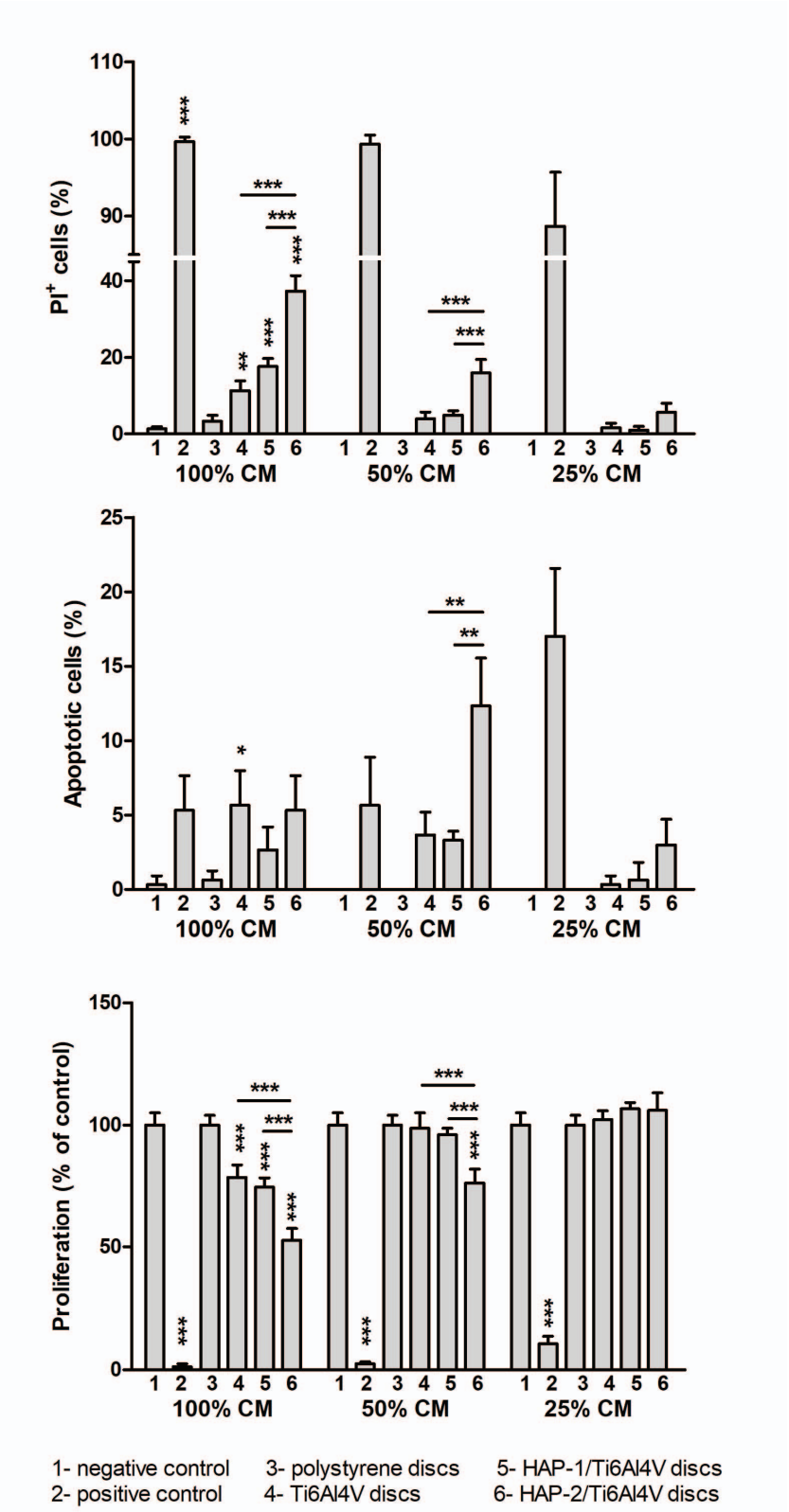

Fig. 3 – The effect of conditioned medium (CM) of Ti6Al4V alloys and control samples on necrosis (A), apoptosis (B) and proliferation (C) of L929 cells.

The L929 cells were cultivated with undiluted (100%), 50% and 25% conditioning medium (CM) for 24 hours. After that necrosis, apoptosis and proliferation were determined as described in methods. Results are presented as percentages of necrotic (propidium iodide – PI+ cells), percentage of apoptotic cells or as relative proliferation compared to the negative control used as 100% [all as mean ± standard deviation (SD) of triplicates].

***-$p < 0.05$; **-$p < 0.01$; ***-$p < 0.005$ compared to the negative control or to corresponding samples, as indicated by bars. HAP-1/HAP-2: hydroxyapatite coated on one or two sides of Ti6Al4V alloy, respectively.**

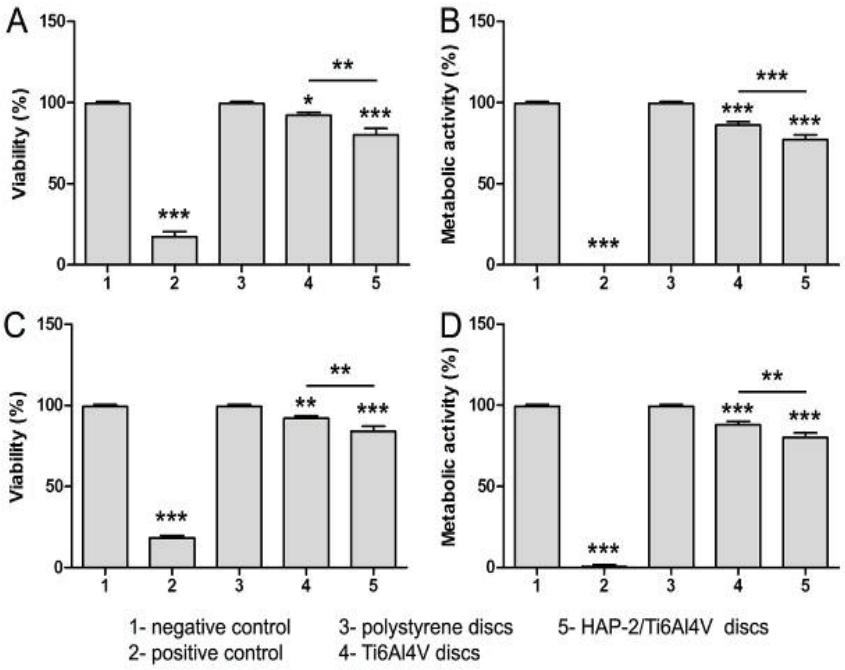

Fig. 4 – The effect of conditioned Ti6Al4V alloys and CM of the conditioned Ti6Al4V alloys on viability (A, C) and metabolic activity (B, D) of L929 cells.

The test samples were conditioned in RPMI culture medium for 24 hours (A, B) or 7 days (C, D) as described, and used in the direct assays with the L929 cells to assess the viability. CM were prepared by incubating the conditioned samples for 24 hours. Such CM were cultivated with L929 cells for 24 hours and then the metabolic activity of the cells was examined.
-$p < 0.05$; ****$p < 0.01$; **-$p < 0.005$ compared to the negative control or to corresponding samples, as indicated by bars**
HAP-1/HAP-2: hydroxyapatite coated on one or two sides of Ti6Al4V alloy, respectively.

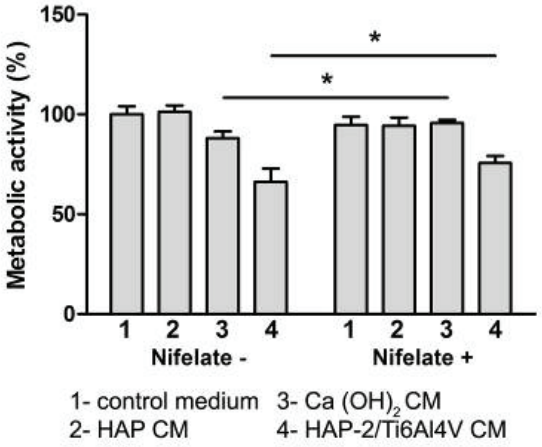

Fig. 5 – The effect of nifelate on the metabolic activity of L929 cells treated with different conditioned media.

The L929 cells were treated with CM prepared from the HAP, $Ca(OH)_2$ or two sides HAP-coated Ti6Al4V alloy in presence or absence of nifelate (10 μg/mL) for 24 hours and after that the metabolic activity of the cells was determined by cell viability (MTT) assay as described in methods.
The results are presented as relative metabolic activity [mean ± standard deviation (SD); n = 3] compared to the values of control cells.
***-$p < 0.05$ compared to corresponding samples as indicated by bars.**

The role of Ca in cytotoxicity of the HAP coated Ti6Al4V alloy

The final aim of this work was to examine the possible role of Ca ions in the HAP/Ti6Al4V cytotoxicity, based on the previous results which showed that this process depended on the amount of HAP used for coating. The estimated amount of HAP on the two sides coated Ti6Al4V alloy was 40 mg. Therefore, this amount of HAP was conditioned in the same volume of complete RPMI medium as used for the Ti alloy conditioning. As shown in Figure 5, CM from HAP was not cytotoxic, indicating that released HAP from the alloy was probably not a cause of cytotoxicity. Since HAP is hardly soluble in water solutions, we tested CM prepared

from Ca(OH)2 which is more soluble under the same conditions. We showed that CM from $Ca(OH)_2$ was slightly cytotoxic, but much lower than CM of HAP/ Ti6Al4V samples.

Finally, we used nifelate (Ca channel blocker) in the assay with CM. Nifelate abrogated completely the cytotoxic effect of $Ca(OH)_2$ CM, but only slightly reduced the cytotoxicity of HAP/Ti6Al4V CM.

Discussion

Modification of surface of the Ti alloys, which are used as implants in dentistry and orthopaedic surgery, can lead to favourable bone regeneration and integrity between the bone tissue and implant surface [17]. In this context, HAP has been widely used due to its good biocompatibility. However, the bioactivity of HAP coatings *in vivo* largely depends on the applied method [18]. The plasma-sprayed HAP coatings frequently show a large variation in the quality of the HAP layer including poor coating – metal adhesion strength, non-uniformity in coating thickness and density, as well as changes in the structural properties during the coating process [18]. The process of plasma spraying can also influence the change from crystal to amorphous form in the HAP phase composition [19].

To improve most of these parameters, our research group used an innovative plasma jet method, with high electric energy input, for the HAP coating on high purity Ti substrate [13]. The procedure enabled extraordinarily high adhesion strengths of the obtained coatings, showing a very rough surface with micro and nano patterns. Therefore, the same method was applied in this study for the HAP coating of Ti6Al4V alloy. Although there was no detailed microstructural analysis of the Ti6Al4V coating, during cytotoxicity investigation we found that HAP layer was quite stable, thus demonstrating the paramount importance for oseointegration.

The biocompatibility studies start from the cytotoxicity assay *in vitro* [14] and this was the principal goal of this work. Our results showed that all examined Ti6Al4V samples exerted a certain degree of cytotoxicity. The cytotoxicity of uncoated and one side coated Ti6Al4V samples was acceptable according to the current ISO 10993-5 criteria [14], since the degree of cytotoxicity did not exceed 30%. The cytotoxicity of two sides HAP coated Ti6Al4V samples was in the range of 30%–55% and because of that they were classified as slight-moderate cytotoxic. The cytotoxicity was verified according to the reduction of cell viability (MTT and morphological assays), decrease of cellular proliferation and induction both of necrosis and apoptosis of L929 cells.

It is interesting that we observed a lower level of apoptosis when CM, prepared from the two sides HAP Ti6Al4V alloys, was tested in higher concentrations. In contrast, necrosis of L929 cells was concentration dependent. This phenomenon could be explained by the fact that cells triggered to undergo apoptosis will die by necrosis when the intracellular energy level is low, such as adenosine triphosphate (ATP) depletion [20]. Based on this concept, it can be postulated that the higher concentrations of toxic compounds in the medium extract blocked the mitochondrial or glycolytic ATP generation and caused necrosis. When their concentrations are lower the threshold ATP concentrations are sufficient to execute the apoptotic programme.

What could be the mechanisms involved in cytotoxicity? It is obvious that they are different depending on the used samples. A slight cytotoxicity of uncoated Ti6Al4V alloy, which was already described in literature [21] could be due to the release of cytotoxic Ti, aluminium (Al) and vanadium (V) ions [21, 22]. The release of these ions is usually bellow cytotoxic concentrations, due to the formation of a Ti-oxide protective layer [21–23], but they could act synergistically at the subtoxic concentrations. These ions could be also released from the HAP coated Ti6Al4V discs.

However, a certain degree of cytotoxicity might be caused by the HAP coatings. Crystalline HAP is not cytotoxic because it is hardly soluble in water solutions. We also confirmed in this study that CM prepared from HAP did not modify the metabolic activity of L929 cells. The nanostructure forms of HAP show some degree of cytotoxicity as demonstrated on HepG2 cells [24] due to the induction of oxidative stress and subsequent cytopathic effects through both necrotic and apoptotic mechanisms.

We hypothesize that the most pronounced cytotoxic effect on the L929 cells observed in this study by the two sides HAP coated Ti6Al4V was induced by the amorphous forms of the coating layer, including calcium oxide (CaO), three- and tetracalcium phosphate. These phases, which were developed during the applied plasma spraying procedure [13, 25] are soluble in water solutions [26]. Of them, CaO is the most soluble and non-biocompatible compound [26–28]. CaO forms $Ca(OH)_2$ in water. Therefore, we tested whether CM prepared from $Ca(OH)_2$ suspension was cytotoxic. The answer was yes, similarly as described for the $Ca(OH)_2$ nanoparticles [29] , but the degree of cytotoxicity was lower compared to CM from the HAP/Ti6Al4V alloys.

The hypothesis that soluble components of HAP coating could be responsible for the obtained results is in line with the observations that conditioning of the two sides HAP/Ti6Al4V alloy significantly reduced its cytotoxic effect up to the non-cytotoxic level according to the ISO 10993-5. Based on this original finding, we can suggest using a kind of conditioning procedure for the HAP coated metal alloys before their implantation *in vivo*, as a helpful method to reduce the cytotoxicity. However, to make this presumption more relevant, it is necessary to determine the concentrations of Ca released in the culture media during conditioning simultaneously with the characterization of HAP coating by Auger microscopy, as well as to test other water solutions instead of culture medium.

To check the possible effect of soluble Ca for the observed cytotoxicity of CM prepared from the HAP-Ti6Al4V alloys, we blocked the Ca channels by nifelate. We showed that the cytotoxicity under such experimental conditions was only slightly diminished, indicating that Ca ions could not be a key factor influencing the cytotoxicity. Other mechanisms could be related to the ingestions of micro or nano HAP particles which might be released in CM. Such particles were visible around disc samples in the direct cytotoxicity assay. Recent studies showed that nano-HAP was cytotoxic due to

the interference of ingested particles with different signalling mechanisms including those related to cell proliferation/death [30]. It is also possible that cytotoxicity of HAP/Ti6Al4V CM could be due to the synergism between released metal ions and the component of amorphous HAP phases, either in their soluble or particulate forms. To make this conclusion more relevant, elemental analysis of these components will be necessary and this investigation is in progress.

Conclusion

This study shows that the HAP coatings obtained by an innovative plasma jet deposition on the Ti6Al4V alloy enables good adhesion stability of the coated layer. However, when both sides of disc samples of the Ti6Al4V alloy are coated, the cytotoxicity of target L929 cells was enhanced. The cytotoxicity was reduced to the non-cytotoxic level by conditioning of the HAP/Ti6Al4V alloy in culture medium for 24 hours, most probably due to the removal of the amorphous phase of HAP. Therefore, a conditioning procedure could be helpful if applied before the implantation of HAP coated metal alloys *in vivo*.

Acknowledgements

This study was supported by following grants: Ministry of Education, Science and Technological Development of the Republic of Serbia (Projects ON 175102 and 172026) and Faculty of Medicine of the Military Medical Academy, University of Defence in Belgrade (project MFVMA 07/17-19).

R E F E R E N C E S

1. *Okazaki Y, Rao S, Ito Y, Tateishi T*. Corrosion resistance, mechanical properties, corrosion fatigue strength and cytocompatibility of new Ti alloys without Al and V. Biomaterials 1998; 19(13): 1197–215.
2. Fojt J, Joska L, Malek J. Corrosion behaviour of porous Ti–39Nb alloy for biomedical applications. Corr Sci 2013; 71: 78–83.
3. *Geetha M, Singh AK, Asokamani R, Gogia AK*. Ti based biomaterials, the ultimate choice for orthopaedic implants – A review. Prog Mater Sci 2009; 54(3): 397–425.
4. *Upadhyay D, Panchal MA, Dubey RS, Srivastava VK*. Corrosion of alloys used in dentistry: A review. Mater Sci Eng A 2006; 432: 1–11.
5. *Bral A, Mommaerts MY*. In vivo biofunctionalization of titanium patient-specific implants with nano hydroxyapatite and other nano calcium phosphate coatings: A systematic review. J Craniomaxillofacial Surg 2016; 44(4): 400–12.
6. *Palanivelu R, Kalainathan S, Kumar AR*. Characterization studies on plasma sprayed (AT/HA) bi-layered nano ceramics coating on biomedical commercially pure titanium dental implant. Ceram Int 2014; 40: 7745–51.
7. *Drevet R, Viteaux A, Maurin JC, Benhayoune H*. Human osteoblast-like cells response to pulsed electrodeposited calcium phosphate coatings. RSC Advances 2013; 3(28): 11148–54.
8. *Urquia Edreira ER, Wolke JG, Al Farraj Aldosari A, Al-Johany SS, Anil S, Jansen JA,* et al. Effects of calcium phosphate composition in sputter coatings on in vitro and in vivo performance. J Biomed Mater Res A 2015; 103(1): 300–10.
9. *Goodman SB, Yao Z, Keeney M, Yang MF*. The future of biologic coatings for orthopaedic implants. Biomaterials 2013; 34(13): 3174–83.
10. *Zhang BG, Myers DE, Wallace GG, Brandt M, Choong PF*. Bioactive coatings for orthopaedic implants - Recent trends in development of implant coatings. Int J Mol Sci 2014; 15(7): 11878–921.
11. *Mohseni E, Zalnezhad E, Bushroa AR*. Comparative investigation on the adhesion of hydroxyapatite coating on Ti–6Al–4V implant: A review paper. Int. J Adhes Adhes 2014, 48: 238–57.
12. *Maxian SH, Zawadsk JP, Dunn MG*. Mechanical and histological evaluation of amorphous calcium phosphate and poorly crystallized hydroxyapatite coatings on titanium implants. J Biomed Mater Res 1993; 27(6): 17–28.
13. *Jokanović V, Vilotijević M, Čolović B, Jenko M, Anžel I, Rudolf R*. Enhanced adhesion properties, structure and sintering mechanism of hydroxyapatite coatings obtained by plasma jet deposition. Plasma Chem Plasma Process 2015; 35: 1–19.
14. International Standards Organization. ISO10993-5: Biological evaluation of medical devices, part 5. Geneva: ISO; 2009.
15. *Sieuwerts AM, Klijn JG, Peters HA, Foekens JA*. The MTT tetrazolium salt assay scrutinized: how to use this assay reliably to measure metabolic activity of cell cultures in vitro for the assessment of growth characteristics, IC50-values and cell survival. Eur J Clin Chem Clin Biochem 1995; 33(11): 813–23.
16. *Čolić M, Gasić S, Vucević D, Pavicić L, Popović P, Jandrić D* et al. Modulatory effect of 7-thia-8-oxoguanosine on proliferation of rat thymocytes in vitro stimulated with concanavalin A. Int J Immunopharmacol. 2000; 22(3): 203–12.
17. *Hannon P*. A brief review of current orthopedic implant device issues: biomechanics and biocompatibility. Biol End Med 2016; 1(1): 1–2.
18. *Mohseni E, Zalnezhad E, Bushroa AR*. Comparative investigation on the adhesion of hydroxyapatite coating on Ti–6Al–4V implant: A review paper. Int J Adhes 2014; 48: 238–57.
19. *Maxian SH, Zawadsk JP, Dunn MG*. Mechanical and histological evaluation of amorphous calcium phosphate and poorly crystallized hydroxyapatite coatings on titanium implants. J Biomed Mater Res 1993; 27(6): 717–28.
20. *Leist M, Single B, Castoldi AF, Kuhnle S, Nicotera P*. Intracellular adenosine triphosphate (ATP) concentration: a switch in the decision between apoptosis and necrosis. J Exp Med 1997; 185(8): 1481–6.
21. *Li Y, Wong C, Xiong J, Hodgson P, Wen C*. Cytotoxicity of titanium and titanium alloying elements. J Dent Res 2010; 89(5): 493–7.
22. *Sidambe AT*. Biocompatibility of Advanced Manufactured Titanium Implants—A Review. Materials 2014; 7(12): 8168–88.
23. *Chandar S, Kotian R, Madhyastha P, Kabekkodu SP, Rao P*. In vitro evaluation of cytotoxicity and corrosion behavior of commercially pure titanium and Ti-6Al-4V alloy for dental implants. J Indian Prosthodont Soc 2017; 17(1): 35–40.
24. *Yuan Y, Liu C, Qian J, Wang J, Zhang Y*. Size-mediated cytotoxicity and apoptosis of hydroxyapatite nanoparticles in human hepatoma HepG2 cells. Biomaterials 2010; 31(4): 730–40.
25. *Rahman ZU, Shabib I, Haider W*. Rahman ZU, Shabib I, Haider W. Surface characterization and cytotoxicity analysis of plasma sprayed coatings on titanium alloys. Mater Sci Eng C Mater Biol Appl 2016; 67: 675–83.
26. *Radin SR, Ducheyne P*. The effect of calcium phosphate ceramic composition and structure on in vitro behaviour. II. Precipitation. J Biomed Mater Res 1993; 27(1): 35–45.

27. *Sun L, Berndt CC, Gross KA, Kucuk A*. Material fundamentals and clinical performance of plasma-sprayed hydroxyapatite coatings: a review. J Biomed Mater Res 2001; 58(5): 570–92.
28. *Mozayeni MA, Milani AS, Marvasti LA, Asgary S*. Cytotoxicity of calcium enriched mixture cement compared with mineral trioxide aggregate and intermediate restorative material. Aust Endod J 2012; 38(2): 70–5.
29. *Dianat O, Azadnia S, Mozayeni MA*. Toxicity of calcium hydroxide nanoparticles on murine fibroblast cell line. Iran Endod J 2015; 10(1): 49–54.
30. *Zhao X, Ng S, Heng BC, Guo J, Ma L, Tan TT* et al. Cytotoxicity of hydroxyapatite nanoparticles is shape and cell dependent. Arch Toxicol 2013; 87(6): 1037–52.

Received on August 9, 2017.
Accepted on August 14, 2017.
Online First September, 2017.

ORIGINAL ARTICLE

UDC: 616.31-085.46
https://doi.org/10.2298/VSP170721127P

In vitro cytotoxicity assessment of the 3D printed polymer based epoxy resin intended for use in dentistry

In vitro procena citotoksičnosti 3D štampanog polimera na bazi epoksi smole namenjenog za upotrebu u stomatologiji

Tatjana Puškar*, Branka Trifković†, Daniela Djurović Koprivica*, Vesna Kojić‡, Ana Jevremović§, Siniša Mirković*, Dominic Eggbeer‖

University of Novi Sad, Faculty of Medicine, *Department of Dentistry, Novi Sad, Serbia; University of Belgrade, Faculty of Dentistry, †Clinic for Prosthodontics, Belgrade, Serbia; University of Novi Sad, Faculty of Medicine, ‡Oncology Institute of Vojvodina, Sremska Kamenica, Serbia; University Business Academy in Novi Sad, §Faculty of Dentistry, Pančevo, Serbia; Cardiff Metropolitan University, ‖National Centre for Product Design and Development Research, Cardiff, United Kingdom

Abstract

Background/Aim. There is limited published evidence on the cytotoxicity of 3D printed polymer materials for dentistry applications, despite that they are now widely used in medicine. Stereolithography (SLA) is one of the foremost 3D processes used in 3D printing, yet there are only a small number of resin materials reported to be suitable for medical applications. The aim of this study was to investigate, *in vitro*, the cytotoxic effect of the 3D printed resin in order to establish the suitability for its usage in dentistry and related medical applications such as surgical dental guides, occlusal splits and orthodontic devices. **Methods**. To examine the cytotoxicity of the 3D printed polymer-based epoxy resin, Accura® ClearVue™ (3D-Systems, USA), two cell cultures were used: mouse fibroblasts L929, and human lung fibroblasts MRC-5. The cell viability was determined by the Mosmann's colorimetric (MTT) test and the agar diffusion test (ADT). **Results.** Direct contact of the tested material with the ADT test showed nontoxic effects of tested material in any cell culture. The tested material showed no cytotoxic effect after 3 days of extraction of the eluate by the MTT, but mild cytotoxic effect after 5, 7 and 21 days on both cell lines. The cytotoxicity increased with increasing the time of the eluate extraction. **Conclusion.** The 3D printed polymer-based epoxy resin, Accura® ClearVue™ (3D-Systems, USA) is considered appropriate for making surgical dental implant guides according to the cytotoxic behavior. According to the mild level of cytotoxicity after the longer extraction periods, there is a need for further evaluation of biocompatibility for its application for the occlusal splints and orthodontic devices.

Key words:
cell culture techniques; dental materials; epoxy resin; material testing; printing, three-dimensional.

Apstrakt

Uvod/Cilj. Malo je objavljenih dokaza o citotoksičnosti 3D štampanih polimernih materijala za upotrebu u stomatologiji, bez obzira na njihovu sve širu primenu u medicini. Stereolitografija (SLA) jedan je od najvažnijih 3D procesa koji se primenjuje za 3D štampu, ali postoji samo mali broj materijala na bazi smola za koje je dokazano da su pogodni za medicinsku primenu. Cilj ove studije je bio da se ispita, *in vitro*, citotoksični efekat 3D štampanog polimera kako bi se utvrdila mogućnost za njegovu upotrebu u stomatologiji i srodnim medicinskim oblastima, kao što su hirurške dentalne vođice, okluzalni splintovi i ortodontski aparati. **Metode.** Da bi se ispitala citotoksičnost 3D štampanog polimera na bazi epoksi smole, Accura® ClearVue ™ (3D-Sistems, USA), korišćene su dve ćelijske kulture: fibroblasti miša L929 i humani fibroplasti pluća MRC-5. Vijabilnost ćelija utvrđena je Mosmannovim kolorimetrijskim testom (MTT) i testom difuzije agara (ADT). **Rezultati.** Direktan kontakt testiranog materijala ispitan pomoću ADT pokazao je da materijal nije imao citotoksičan efekat ni na jednu ćelijsku kulturu. Testitrani materijal je imao blag citotoksični efekat posle 5, 7 i 21 dana ekstrakcije eluata primenom MTT na obe ćelijske linije. Citotoksičnost je rasla sa produženjem vremena ekstrakcije eluata. **Zaključak.** 3D štampani polimer na bazi epoksi smole, Accura® ClearVue ™ (3D-Sistems, USA) se može smatrati pogodnim za izradu hirurških dentalnih implantnih vođica sa tačke

Correspondence to: Branka Trifković, University of Belgrade, Facutly of Dentistry, Clinic for Prosthodontics, 4 Rankeova Street, 11 000 Belgrade, Serbia. E-mail: branka.trifkovic@stomf.bg.ac.rs

gledišta njegovog citotoksičnog uticaja. Zbog pokazanih blagih citotoksičnih efekata nakon dužih ekstrakcionih perioda eluata potrebna su dalja istraživanja u oblasti biokompatibilnosti materijala da bi se taj polimer mogao koristiti za izradu okluzalnih splintova i ortodontskih aparata.

Ključne reči:
ćelije, kultura; stomatološki materijali; smole, sintetičke; materijali, testiranje; štampanje, trodimenzionalno.

Introduction

Manufacturing processes that create physical three-dimensional (3D) objects by successive deposition or adding layers of material are commonly known as the Additive Manufacturing (AM) or 3D printing. There is a wide range of 3D printing processes capable of fabricating in polymer and metal materials, some of which are used in dental applications [1]. The various types of additive manufacturing include the stereolithography (SLA), fused deposition modeling (FDM), selective laser sintering (SLS), laminated object manufacturing (LOM), polymer jetting (polyjet) technology, Electron Beam Melting (EBM) and laser melting (LM) [2–5]. All 3D printing processes start with the 3D Computer Aided Design (CAD) geometry as an input. The CAD data is typically translated into the STL file format. Then it is sliced into a discrete number of layers, which are rebuilt using the 3D printing process. This enables the construction of parts with complex geometries and features, such as undercuts, cavities, complex internal geometry, etc., without the necessity for using molds or tools [5]. The 3D printing is widely used in medicine and related fields including: orthopedic surgery, maxillofacial and dental reconstructions, bioprinting tissues, and organs, and also for educational tools [4, 6]. Accuracy in planning and performing surgical procedures in dentistry is extremely important to achieve the desired clinical results and avoid iatrogenic damage of the surrounding tissue. Patient-specific, transient use surgical guides produced using the 3D printing allow a precise, safe and minimally invasive surgical procedure. The guides produced on the basis of 3D data obtained using cone beam computed tomography (CBCT) are specifically indicated for high-risk patients with severe orofacial anatomy such as expanded maxillary sinus or alveolar bone loss [7–10]. Data obtained from the CBCT images are transformed by the software into a format compatible with the 3D printers [8]. The surgical guides are used to place implants into the correct position and at the planned angulations [8, 9]. The 3D computer systems allow a detailed preoperative diagnosis and setting up a detailed treatment plan as well as the creation of surgical guides [10].

In recent years, implantology has become a very important field of dentistry, since patients' demand for such restorative procedures continuously grows. Consequently, the need for the surgical guides that transfer planned implant position directly into operative field is also increasing [11]. Furthermore, the development of computerized procedures led to dramatic changes and intervention options in implantology [12]. Comparing to a standard surgical procedure, a guided surgery offers high accuracy, preservation of anatomical structures as well as examination of vital structures, followed by the reduced surgical time, less invasiveness in the operation procedure and predictable prosthetic outcomes [13–15]. It was also proven that the surgical guides, produced on bases of the CBCT imaging, lead to a more accurate implant placement, comparing to conventionally fabricated guides [16]. The 3D printers appear as a logical fabrication technology for the surgical guides, since they can produce required models quickly and efficiently, revolutionizing dental and medical practice in general.

Due to the increasing requirements for treating patients with dental implants there is a need for the development of new materials for the fabrication of surgical guides by the 3D printing. Since guides come into direct contact with the open surgical wound and must stay in place during the surgical procedure, the material must be biocompatible and remain dimensionally stable during the sterilization process. To ensure a successful clinical use of materials in dentistry, it is necessary to have information about their physical, chemical, mechanical and biological properties. These properties depend not only on the chemical structure of the material and production technology but also on the behavior of materials in changeable conditions prevailing in the oral cavity [17, 18]. Dental materials and implants have special requirements such as nontoxic, non-allergic and noncancerous effects, all of which involve chemically and physically stable material [17, 19].

In vitro tests are the most appropriate strategies for determining the biological response to material and are used as the initial tests when examining biocompatibility [20, 21]. *In vitro* tests are faster, easier, cheaper, lighter and easier to repeat in comparison to other types of tests [19]. It is important that *in vitro* tests simulate the conditions *in vivo* and the conditions prevailing in the oral cavity in order to obtain significant results that can be properly interpreted [22]. In the oral environment, human gingiva cells come into contact with the components of the material directly (e.g., oral mucosa and the denture base, oral mucosa and the periosteum and surgical guides) and indirectly (oral mucosa comes into contact with the substances released in saliva). To imitate *in vivo* conditions in the presented research, the cytotoxic effects of the tested material was investigated both by the direct contact between the samples and the cells [agar diffusion test (ADT)] and by the contact of the cells with eluates of the tested material 3-(4,5-dimethylthiazol-2-yl)-2,5-diphenyltetrazolium bromidefor (MTT test).

This research investigates used *in vitro* methods to evaluate the biological response of the SLA material Accura® ClearVue™. This material is reported by the manufacturer to be capable of meeting the United States Pharmacopeia (UPS) Class VI. The USP Class VI compounds must be made from ingredients with clear histories of biocompatibility that meet

tight requirements for leachates. The SLA process also creates 100% dense, highly cross-linked, humidity-resistant polymer parts in the Accura® ClearVue™ clear material, making it one of the most suitable for implant dentistry and related surgical applications from the aspect of their physical properties [23]. Available information on this material that originates from the manufacturer indicates its good perquisite biocompatibility and mechanical properties, but there is little scientific data on its possible citotoxicity and behavior in oral cavity.

The aim of this research was to investigate *in vitro* cytotoxic effects of the 3D printed polymer based epoxy resin Accura® ClearVue™ (3D-Systems, USA) on two different cell lines, murine L929, and human MRC-5 cell line with ADT and the MTT test, to test the increase or decrease of cytotoxicity in time and to give the answer whether the tested material can be used as material for fabrication of the 3D printed surgical dental guides, occlusal splints or orthodontic devices from the aspect of cytotoxicity.

Methods

Test material

The chemical composition of the Accura® ClearVue ™ in unpolymerised state is given in Table 1 [23].

The CAD (Magics v19, Materialise, Belgium) was used to create disk with a diameter of 5.5 mm and thickness of 3 mm (Figure 1). Thirty-six samples were analyzed. The samples were supported using the standard preparation software (Magics v19) and fabricated by the SLA-6000HD machine (3D-Systems, USA) using a 0.1 mm layer thickness. Once complete, the samples were removed from the build platform, soaked in isopropyl alcohol for 10 minutes, moved to a second isopropyl alcohol bath for 30 min, air dried before being subjected to ultraviolet light in a post-curing apparatus for 30 min to ensure full polymerization of the material. All samples were handled with gloves and were sealed in polythene back for delivery. These processes were discussed previously and the effectiveness of cleaning was established [24].The samples were cleaned and disinfected by ultrasound in an alcoholic aqueous solution, for a period of 5 min. Afterwards, they were washed in distilled water and again sonicated for a 5 min in isopropyl alcohol. The eluates (extracts) were obtained by incubation of samples in 4 mL of modified Dulbecco's solution (DMEM, Sigma) without serum, in a sealed tube at a temperature of 37 ± 1°C and in a water bath (GFL, Germany) [25, 26].

The length of the extraction period was 3, 5, 7 and 21 days. After each period of extraction, the extracts were removed and the tubes were again filled with fresh solution. All extracts were filtered off before working for sterilization purposes. During the ADT, the contact between cell lines and material samples was conducted direct, while during the MTT test it was done through eluates (extracts).

Fig. 1 – Analyzed samples.

The cytotoxicity effect was determined 24 hours after incubation of cells with the solid test samples and with the eluates from the 3rd day up to 21 days.

Cell lines

For *in vitro* biocompatibility testing, two different fibroblast cell lines (L929 and MRC-5) were used. The L929 (ATCCCRL-636) cell line was of mouse origin, whereas the MRC-5 line (ATCC CCL-171) was a human fibroblast line. The cells were cultivated in DMEM medium (Sigma, Munich, Germany) supplemented with 10% fetal calf serum (FCS) (Sigma, Munich, Germany), 2 mM L-glutamine (Sigma, Munich, Germany) and antibiotics antimycotic solution (Sigma, Munich, Germany). The cells were subcultured twice a week and a single cell suspension was obtained using 0.1% trypsin in EDTA (Serva, Heidelberg, Germany).

Mosmann's colorimetric test with tetrazolium salt

The test is based on the reduction of 3-(4,5-dimethylthiazol-2-yl)-2,5-diphenyltetrazolium bromide to the products of formazan and it was used for the estimation of cell attachment and proliferation [27]. The cells were collected in the logarithmic growth phase, tripsinized, resuspended and counted in 0.1% trypan blue. The viable cells were seeded in Petri dishes (50 mm Center well, Falcon) with the tested substance/discs, in concentration of 2×10^5/mL. The control samples did not contain tested substance.

Table 1

Chemical composition of Accura® ClearVue ™ [23]

Component	%
4.4' isopropyliden 2-cycloheksanol, the oligomeric products of reaction with 1-chloro-2.3-epoxypropane	40–65
mixture of triarylsulfonium salt (50% of propylene carbonate and 50% of a triarylsulfonium hexafluoroantimonate salt)	1–10
3-ethyl-3-hydroxymethyl-oxetane	10–20

The Petri dishes with the seeded cells were left in thermostat at 37°C and 5% CO_2 for 48 h. After incubation, the cells were seeded in fresh medium. The viable cells were seeded (5×10^3/100 µL) in quadruplicates in a micro titer plate with 96 holes. The plates with the seeded cells were left at the thermostat at 37°C, 5% CO_2 for 24, 48 and 72 h [27]. Immediately prepared MTT solution was added into all holes in the plate in a volume of 10 µL per hatch and incubation was continued for the next 3 h (in the incubator at 37°C, 5% CO_2). At the end of the 3rd h, 10 µL 0.04 mol/L HCl in isopropanol was added in every hole. The absorbance was read immediately after the incubation on the micro titer plate reader (Multiscan, MCC/340) at a wave length of 540 nm and referent wave length of 690 nm. The holes on the panel that contained only medium and MTT, but no cells, were used as blanks ("blank").

Cytotoxicity was expressed in percentage according to following equation: CI(%) = 1−Ns/Nk × 100, where Nk is the number of cells in the samples and the Ns is the number of cells with tested substance.

The results are presented as percentages of viable cells (% cell viability = [total viable cells / total cells (viable + dead)] × 100). Quantitative changes in cell viability were presented descriptively: cell viability > 90% control – material is noncytotoxic; cell viability = 60–90% control – material is mildly cytotoxic; cell viability = 30–59% control – material is moderately cytotoxic; cell viability of < 30% control – material is serious cytotoxic [25].

Agar diffusion test

The agar diffusion test is carried out according to the international standard ISO 10993 and ISO 7405 [20, 21].

Eagle's Basal Medium which contained 2.2 g/L sodium bicarbonate, 3.0 g/L HEPES and 50 ml/L of serum was used in this test. Double concentration of medium was prepared without HEPES, and Na_2CO_3 1 g/L was reduced. Agar medium was sterilized by autoclaving and filtration. Neural-red solution was kept protected from light. The Petri dishes were used in diameter 100 mm suitable for the cell culture. The cells were harvested in the logarithmic growth phase.

The samples of test material in the form of discs were placed on the top layer of agar in each dish and were incubated under controlled conditions (37° C, 5% CO_2) for 24 h. After hardening of the agar nutritive medium at room temperature (about 30 min), the cells were stained with neutral red (10 mL) and left in the dark for 15 min. Staining of the cells was achieved by adding neutral red (10 mL, a solution of 0.01% neutral red in phosphate buffer) that diffuses through the agar and makes living cells intensively red. Excess of a neutral red solution was aspirated [28, 29].

The decolorization zone around the test materials and controls was assessed using an inverted microscope with a calibrated screen, and the Decolorization Index and Lysis Index were determined for each specimen in accordance with the criteria presented in Table 2.

Table 2

Decolorization index and lysis index for agar diffusion test (ADT)

Decolorization index	Decolorization	Lysis Index
0	No decolorization detectable	no cell lysis detectable
1	Decolorization only under the test substance	less than 20% cell lysis
2	Decolorization zone not greater than 5.0 mm from the test substance	20–40% cell lysis
3	Decolorization zone not greater than 10.0 mm from the test substance	40–60% cell lysis
4	Decolorization zone greater than 10.0 mm from the test substance	60–80% cell lysis
5	The total culture is decolorized	more than 80% cell lysis

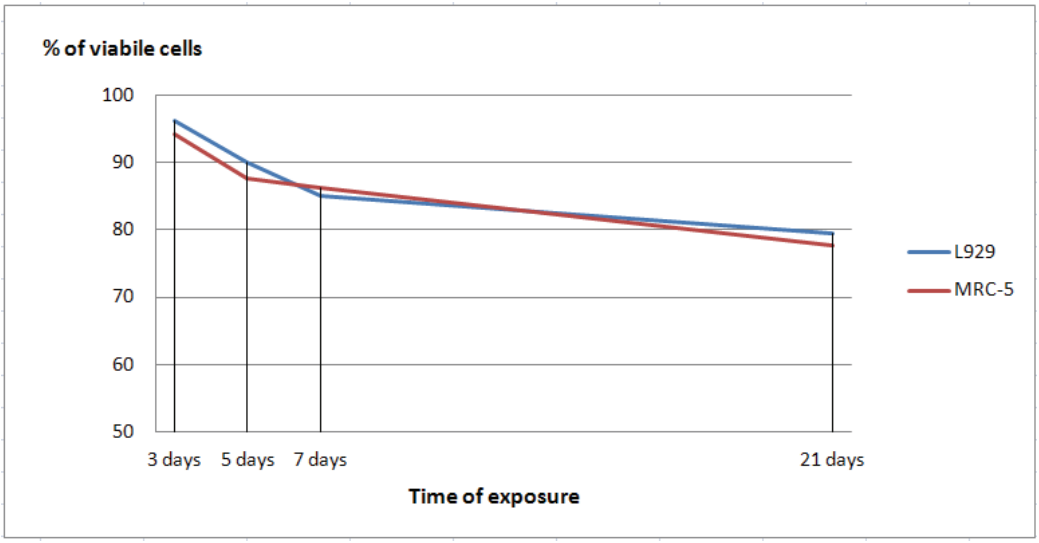

Fig. 2 – Viability of L929 and MRC-5 cell line presented as the percentage of the control found by the Mosmann's colorimetric (MTT) assay.

The results were statistically analyzed using the SPSS. The results obtained by the MTT assay and ADT are expressed as the mean (M) with a standard deviation (SD) and standard error (SE). The mean value, standard deviation and coefficient of variation (CV) were calculated for the replicates (at least triplicate) samples in each experiment. Cytotoxicity was expressed as a percentage. Comparison of the response of two cultures at different extraction period was performed using the *t* test with a significance level of $p = 0.05$.

Results

MTT test

The results of the MTT test are presented in Figure 2 and Table 2.

The results are presented as the percentage of viable cells compared to the control group without tested material.

After the incubation of murine fibroblast L929 cell line with the extracts of experimental material in DMEM, it was observed that the tested material was found noncytotoxic after the first tested period of 3 days and mildly cytotoxic after all other tested periods. After 3 days of exposition, the percentage of viable cells was 96.26%, after 5 days 89.96%, after 7 days 85.10% and after 21 days 79.40% (Figure 2 and Table 3). After the incubation of human fibroblast MRC-5 cell line with extracts of experimental material in DMEM, it was observed that the tested material was also found noncytotoxic after the first tested period of 3 days and mildly cytotoxic after all other tested periods. After 3 days of exposition, the percentage of viable cells was 94.10%, after 5 days 87.61%, after 7 days 86.21% and after 21 days 77.60% (Figure 2 and Table 3). The cytotoxic effect depends on the period of extraction and tends to rise with the period length. The highest cytotoxicity was expressed by the eluate from the 21 days, and a minimal from the 3rd day. The tests on both cell lines with the eluate of the first extraction period of 3 days showed that the material had noncytotoxic effect, as opposed to cells that were in contact with the eluate of the 5th, the 7th and the 21st day of the extraction, which showed mild cytotoxicity of tested material (Figure 2 and Table 3).

By comparing the responses of two different cell cultures, it was found that the viability of L929 murine fibroblasts was slightly higher compared to the viability of the MRC-5 human fibroblasts, for all periods of extraction except for the extraction of eluent from the 7th day of extraction, when the viability of human fibroblasts was slightly higher (Figure 2).

Agar diffusion test

The results of the agar diffusion test were obtained according to the 4 replicate tests. Cytotoxic effect of 3D printed samples from Accura® ClearVue ™ was not recorded neither on L929 cell line nor on MRC-5 cell line. There was no discoloration around the specimen in any cell culture and the lysis index was 0 (Table 3).

Table 3

The results of the Mosmann's colorimetric (MTT) assay on the L929 and MRC-5 cell line

Cell line		Days			
	C	3	5	7	21
L929	1.008	0.855	0.689	0.824	0.742
	0.962	0.915	0.457	0.769	0.781
	0.951	0.824	0.650	0.725	0.743
	0.985	0.822	0.695	0.773	0.784
	0.968	0.971	0.839	0.745	0.738
	0.860	0.895	0.760	0.798	0.764
	0.943	0.856	0.920	0.812	0.719
	0.963	0.872	0.840	0.821	0.743
Blank: 0.012					
mean ± SD	0.934 ± 0.050	0.899 ± 0.051	0.840 ± 0.065	0.794 ± 0.034	0.741 ± 0.018
Cv	5.375	5.667	7.779	4.283	2.490
Ci %	0.000	3.749	10.043	14.944	20.624
C %		96.251	89.957	85.056	79.376
MRC-5	0.539	0.525	0.475	0.572	0.442
	0.575	0.555	0.496	0.611	0.436
	0.458	0.522	0.407	0.588	0.458
	0.457	0.519	0.499	0.602	0.441
	0.599	0.477	0.409	0.540	0.412
	0.616	0.566	0.411	0.464	0.410
	0.543	0.556	0.548	0.419	0.423
	0.461	0.489	0.576	0.490	0.422
Blank: 0.034					
mean ± SD	0.555 ± 0.070	0.522 ± 0.045	0.486 ± 0.089	0.478 ± 0.051	0.431 ± 0.007
Cv	12.591	8.713	18.210	10.569	1.557
Ci %	0.000	5.904	12.393	13.790	22.397
C %		94.096	87.607	86.210	77.603

***C – control; Ci –cytotoxicity.**
SD – standard deviation; CV – coefficient of variation.

To grade the test material, the scale that takes into account the decolorization index and cell lysis index was used. The cell response was calculated by Decolorization Index divided by Lysis Index. Cell response was 0, so obtained results are considered noncytotoxic.

Discussion

The present research was made by the MTT assay in which the material was in contact with the cells by means of the eluate and the agar diffusion test in which the samples were in direct contact with the cells, as the monomers and other components diffuse through a thin layer of agar. Cytotoxicity tests are considered to be primary, *in vitro* tests, for the research of biocompatibility of materials that are to be used for medical purposes. They provide information about the cytotoxicity of the material and cytotoxicity of eventual leaking agents from the material on the cell culture [30]. They are standardized and the results can be easily compared with required levels of safety [21, 22]. According to ISO 7405 standard, both the direct contact test and the contact of the cells with eluates, are recommended [21]. With the direct contact tests, *in vivo* conditions are better imitated, but they involve a certain risk of mechanical damage of the cells and also increase the risk of bacterial contamination of the cell culture [22].

Agar diffusion method, which is less sensitive compared to the MTT test, showed a completely negative result. The MTT test showed a drop-in cell number with an increase of the length of extraction in relation to the control group. The difference in results is caused mainly due to different sensitivity of the two tests.

By comparing the cell viability of two different cell cultures in the present research, it can be noted that the higher rate of survival showed the mission in relation to human fibroblasts. The exception is the 7th day, where the MRC-5 culture cells were more viable. These differences may be related to the differences in cell lines (human and murine fibroblasts) as well as to the differences in their doubling period, but the final ranking of the results of cytotoxicity did not differ for the L929 and MRC-5 cell line. Murine fibroblasts belonging to the permanent cell cultures (L929) as well as human fibroblasts (MRC-5) can be regarded as analogues of cells of oral mucosa [31]. Murine fibroblasts are often used in various studies of dental materials [32]. Permanent cell lines are simpler systems without specific metabolic potential as target cells (target cells *in vivo*). However, some research suggests that these cells are more sensitive to a variety of tests in relation to the primary culture [32]. Fibroblast cell line MRC-5 in the present research was used to obtain the results of the human cell line and check whether there is a difference between the mouse and human fibroblasts in terms of cellular response. Thus, the obtained results may be interpreted in a clinically relevant manner.

The MTT test carried out on the cell culture MRC-5 showed that the material had a satisfactory degree of biocompatibility, which was not less than 77.60% and more than 94.10% cell viability. The lowest recorded viability was 77.60% and this value represents the viability of MRC-5 culture in contact with eluates from the 21st day. The fibroblasts viability of both cell lines measured by the MTT assay was the lowest in the most concentrated eluate.

The tested material showed no cytotoxic effect in direct contact with the cells and after 3 days of the extraction period. This finding indicates that the 3D printed polymer-based epoxy resin, Accura® ClearVue™ (3D-Systems, USA) can be used for the production of surgical dental guides that are to be in the contact with the wound or mucosa for a short period of time (up to a couple of hours). Findings of the mild cytotoxic effect after 5, 7 and 21 days of extraction and increasing cytotoxic effect with increasing the time of extraction indicate that the tested material could be used even for production of occlusal splints and orthodontic devices, but the additional tests of biocompatibility are necessary, because of the long term contact of those dental devices with oral mucosa.

Similar tests conducted on the acrylic materials, denture base materials used for decades, showed mild to moderate cytotoxicity [28, 29]. The release of toxic substances from the acrylate is most intense in the first 24 hours after polymerization. Research show that greatest cytotoxicity of composite resin can be expected in the first 24 hours after polymerization, in contrast to the presented study where the cytotoxicity was the lowest in the first 3 days, but increased with the period of extraction.

In addition to the chemical composition of materials, the method of polymerization is one of the decisive factors as far as the cytotoxicity of acrylic resin is concerned [33]. An extension of the polymerization time can reduce the toxicity of the resin. The Accura® ClearVue ™ material is continuously polymerized during the SLA process, then further post-cured after being cleaned [3]. It can be assumed that this method of polymerization contributes to reduction of the amount of residual monomer and consequently better biocompatibility of epoxy resin.

Although the epoxy-based material evaluated in this research met prerequisite material and processing standards for medical applications, similar cross-linking acrylic materials were proven to be potentially toxic, mutagenic or allergenic [34]. Some studies showed that the 3D printed objects can be toxic [35, 36], allergenic [15, 36] , or cause inflammatory response combined with infections [31]. Besides adverse reaction to the generated product, some hazardous particles can be found in the air during specimen production [31, 37]. It is, therefore notable that very few research articles discussing the biocompatibility issue of the 3D printed materials can be found in the available literature [37, 38]. A recent study, where toxicity of the 3D printed parts was assessed on zebra fish embryos, concluded that both FDM and SLA samples were measurably toxic [37]. Furthermore, the SLA specimens showed greater toxic potential, that could, however, be greatly reduced by post-processing of samples by means of the UV light exposure. Though direct comparison is not implementable since different resin was used opposed to present research, safety data sheets indicate that it is likely the both materials contain the acrylic and/or metacrylic groups. Another study [38] on the same culture also revealed a potential health risk that can be reduced by a post-printing treatment of the specimens. Ho-

wever, it has to be noted that human application differs from aquatic animals; therefore implication of further tests is necessary.

With a growing field of 3D printers, their size reduction to a desktop variant would certainly make the surgical guides more reachable for everyday clinical use. Those guides are in a limited contact with live tissues (< 24 h), yet clinical situation might demand bone or blood communication, which might require sensitization, irritation or systemic toxicity tests, according to ISO 10993. Despite many advantages of its application, biocompatibility of printed parts still remains a field for further investigation.

Conclusion

Within the limitations of this study it was concluded that the 3D printed Accura® ClearVue™ material had non-cytotoxic effect on the cell cultures L929 and MRC-5 in direct contact with the cell culture tested by the ADT. MTT assay showed no cytotoxic effect after 3 days of extraction of eluates and mild cytotoxic effect after 5, 7 and 21 days of extraction on both cell cultures. Cytotoxicity increases with the longer extraction patterns. Human cell line was somewhat more sensitive to the action of the material, but it is not clinically relevant. The 3D printed polymer-based epoxy resin, Accura® ClearVue™ (3D-Systems, USA) is considered appropriate for making surgical dental implant guides according to the cytotoxic behavior. According to the mild level of cytotoxicity after the longer extraction periods, there is a need for further evaluation of biocompatibility for its application for occlusal splints and orthodontic devices.

Further research shall be focused on *in vivo* testing to reach comprehensive data about biocompatibility and potential use of the 3D printed epoxy resin in different fields of dentistry.

Acknowledgement

The results presented in this paper are obtained in the framework of the projects: “Research and development of modeling methods and approaches in manufacturing of dental recoveries with the application of modern technologies and computer aided systems” (TR 35020), funded by the Ministry of Education, Science and Technological Development of the Republic of Serbia, and the project No. 114-451-2723/2016-03 “Improving the treatment of diseases of dental system through the development of modern diagnostic methods for the detection of occlusal loading”, which is funded by the Provincial Secretariat for Science and Technological Development of AP Vojvodina, through the program “Projects of importance for science and technological development of AP Vojvodina for the project cycle 2016 to 2019”.

REFERENCES

1. *Mahamood S, Khader MA, Ali H.* Applications of 3D Printing in Orthodontics: A Review. Int J Sci Stud 2016; 3(11): 267-70.
2. *Van Noort R.* The future of dental devices is digital. Dent Mater 2012; 28(1): 3–12.
3. *Bens TA, Tille C, Bermes G, Emons M, Seitz H.* Novel, biocompatible polyether(meth)acrylate-based formulations for stereolithography. e-Polymers 2005; 5(1): 377–86.
4. *Shie MY, Chang WC, Wei LJ, Huang YH, Chen CH, Shih CT*, et al. 3D Printing of Cytocompatible Water-Based Light-Cured Polyurethane with Hyaluronic Acid for Cartilage Tissue Engineering Applications. Materials (Basel) 2017; 10(2): pii: E136.
5. *Wang X, Jiang M, Zhou Z, Gou J, Hui D.* 3D printing of polymer matrix composites: A review and prospective. Composites Part B Eng 2017; 110: 442–58.
6. *Puskar T, Jevremovic D, Williams RJ, Eggbeer D, Vukelic Dj, Budak I.* A Comparative Analysis of the Corrosive Effect of Artificial Saliva of Variable pH on DMLS and Cast Co-Cr-Mo Dental Alloy. Materials 2014; 7(9): 6486–501.
7. *Kim SH, Kang SM, Choi YS, Kook YA, Chung KR, Huang JC.* Cone-beam computed tomography evaluation of mini-implants after placement: Is root proximity a major risk factor for failure? Am J Orthod Dentofacial Orthop 2010; 138(3): 264–76.
8. *Bornstein MM, Scarfe WC, Vaughn VM, Jacobs R.* Cone beam computed tomography in implant dentistry: a systematic review focusing on guidelines, indications, and radiation dose risks. Int J Oral Maxillofac Implants 2014; 29 Suppl: 55–77.
9. *Bae MJ, Kim JY, Park JT, Cha JY, Kim HJ, Yu HS*, et al. Accuracy of miniscrew surgical guides assessed from cone-beam computed tomography and digital models. Am J Orthod Dentofacial Orthop 2013; 143(6): 893–901.
10. *Ramasamy M, Giri, Raja R, Subramonian, Karthik, Narendrakumar R.* Implant surgical guides: From the past to the present. J Pharm Bioallied Sci 2013; 5(Suppl 1): S98–S102.
11. *Widmann G, Bale RJ.* Accuracy in computer-aided implant surgery-a review. Int J Oral Maxillofac Implants 2006; 21(2): 305–13.
12. *Avrampou M, Mericske-Stern R, Blatz MB, Katsoulis J.* Virtual implant planning in the edentulous maxilla: criteria for decision making of prosthesis design. Clin Oral Implants Res 2013; 24 Suppl A100: 152–9.
13. *Stumpel LJ.* Flexible thermoplastic resin to add retention to tooth-supported stereolithographic surgical guides. J Prosthet Dent 2015; 114(4): 479–81.
14. *Nickenig HJ, Eitner S, Rothamel D, Wichmann M, Zöller JE.* Possibilities and limitations of implant placement by virtual planning data and surgical guide templates. Int J Comput Dent 2012; 15(1): 9–21. (English, German)
15. *Pozzi A, Polizzi G, Moy PK.* Guided surgery with tooth-supported templates for single missing teeth: A critical review. Eur J Oral Implantol 2016; 9 Suppl 1: S135–53.
16. Sarment DP, Sukovic P, Clinthorne N. Accuracy of implant placement with a stereolithographic surgical guide. Int J Oral Maxillofac Implants 2003; 18(4): 571–7.
17. *Kwon JS, Piao YZ, Cho SA, Yang SY, Kim JH, An S,* et al. Biocompatibility Evaluation of Dental Luting Cements Using Cytokine Released from Human Oral Fibroblasts and Keratinocytes. Materials (Basel) 2015; 8(11): 7269–77.
18. *Bettencourt AF, Neves CB, de Almeida MS, Pinheiro LM, Oliveira SA, Lopes LP,* et al. Biodegradation of acrylic based resins: A review. Dent Mater 2010; 26(5): e171–80.
19. *Schmalz G, Arenholt-Bindslev D.* Biocompatibility of dental materials. 1st ed. Heidelberg, Germany: Springer-Verlag GmbH; 2009.
20. International Standard ISO 10993 - Part 5 and Part 12: 2009: Biological Evaluation of Medical Devices and Tests for in vitro Cytotoxicity. International Organization For Standardization; 2009.
21. International Standard ISO 7405: 2008. Dentistry - Preclinical evaluation of biocompatibility of medical devices used in den-

tistry - Test methods for dental materials. International Organization for Standardization; 2008.
22. *Weijia LI, Zhou J, Yuyin XU*. Study of the in vitro cytotoxicity testing of medical devices. Biomed Rep 2015; 3(5): 617–20.
23. www.3Dsystems.com. Available online: https://www.3Dsystems.com/materials/accurar-clearvue [accessed on 2016 September 12].
24. *O'Malley FL, Millward H, Eggbeer D, Williams R, Cooper R*. The use of adenosine triphosphate bioluminescence for assessing the cleanliness of additive-manufacturing materials used in medical applications. Additive Manufacturing 2016; 9: 25–9.
25. *Vojdani M, Sattari M, Khajehoseini Sh, Farzin M*. Cytotoxicity of Resin-Based Cleansers: An In Vitro Study. Iran Red Crescent Med J 2010; 12(2): 152–62.
26. *Kostoryz LE, Tong YP, Chappelow CC, Eick DJ, Glaros GA, Yourtee MD*. In vitro cytotoxicity of solid epoxy-based dental resins and their components. Dent Mater 1999; 15(5): 363–73.
27. *Mosmann T*. Rapid colorimetric assay for cellular growth and survival: application to proliferation and cytotoxicity assays. J Immunol Methods 1983; 65(1–2): 55–63.
28. *Mendes AP, Barceleiro MO, dos Reis RS, Bonato LL, Dias KR*. Changes in surface roughness and color stability of two composites caused by different bleaching agents. Braz Dent J 2012; 23(6): 659–66.
29. *Brackett MG, Lockwood PE, Messer RL, Lewis JB, Bouillaguet S, Wataha JC*. In vitro cytotoxic response to lithium disilicate dental ceramics. Dent Mater 2008; 24(4): 450–6.
30. *Michelsen V, Moe G, Strøm M, Jensen E, Lygre H*. Quantitative analysis of TEGDMA and HEMA eluted into saliva from two dental composites by use of GC/MS and tailor-made internal standards. Dent Mater 2008; 24(6): 724–31.
31. *Stephens B, Azimi P, El Orch Z, Ramos T*. Ultrafine particle emissions from desktop 3D printers. Atmos Environ 2013; 79: 334−9.
32. *Wadajkar A, Chul A, Nguyen K, Qiang Z, Takashi K*. In Vitro Cytotoxicity Evaluation of Four Vital Pulp Therapy Materials on L929 Fibroblasts. ISRN Dentistry 2014; (2014): ID 191068.
33. *Salehi S, Gwinner F, Mitchell JC, Pfeifer C, Ferracane JL*. Cytotoxicity of resin composites containing bioactive glass fillers. Dent Mater 2015; 31(2): 195–203.
34. *Graber TM, Vanarsdall RL, Vig KW*. Orthodontics: Current principles and techniques. 4th ed. St Louis: Elsevier; 2005.
35. *Inoue Y, Ikuta, K*. Detoxification of the Photocurable Polymer by Heat Treatment for Microstereolithography. Procedia CIRP 2013; 5: 115−8.
36. *Popov V, Evseev A, Ivanov A, Roginski V, Volozhin A, Howdle S*. Laser stereolithography and supercritical fluid processing for custom-designed implant fabrication. J Mater Sci Mater Med 2004; 15: 123−8.
37. *Oskui SM, Diamante G, Liao Ch, Shi W, Gan J, Schlenk D*, et al. Assessing and Reducing the Toxicity of 3D-Printed Parts. Environ Sci Technol Lett 2016; 3(1): 1–6.
38. *MacDonald NP, Zhu F, Hall CJ, Reboud J, Crosier PS, Patton EE*, et al. Assessment of biocompatibility of 3D printed photopolymers using zebrafish embryo toxicity assays. Lab Chip 2016; 16(2): 291–7.

Received on July 21, 2017.
Revised on August 10, 2017.
Accepted on August 11, 2017.
Online First September, 2017.

ORIGINAL ARTICLE

UDC: 616.831-006-08-036-073.75
https://doi.org/10.2298/VSP170114108M

Advanced magnetic resonance techniques in early differentiation of pseudoprogression versus progression in the patients with glioblastoma multiforme

Napredne tehnike magnetne rezonance u ranom razdvajanju pseudoprogresije od progresije kod bolesnika sa glioblastomom multiforme

Jelena Mihailović*, Marko Daković†

Institute for Oncology and Radiology of Serbia, *Department for Diagnostic Radiology, Belgrade, Serbia; University of Belgrade, †Faculty for Physical Chemistry, Belgrade, Serbia

Abstract

Background/Aim. The diagnosis of glioblastoma multiforme progression may be confounded by a phenomena termed pseudoprogression (PSP) and pseudoresponse (RCT) which has become more common with the adoption of radiation therapy with concurrent and adjuvant application of temozolomide (CRT). Distinguishing of these phenomena is based on the follow-up scans since no single imaging method or technique is yet capable of performing their discrimination. In this study, we evaluated the dynamic susceptibility contrast (DSC perfusion) imaging and magnetic resonance (MR) spectroscopy to predict the prognosis and time to progression in the patients with glioblastoma multiforme. **Methods.** Fourty patients with primary glioblastoma multiforme were included in the analysis. The patients were examined in 3rd week after surgery and 10th week after the beginning of CRT. The MR exams were performed using the 1.5 T MR scanner (Avanto; Siemens, Erlangen, Germany). The maps of perfusion parameters and time-to-peak (TTP) parameter were calculated using the DPTools v3.79 software. The 3D CSI PRESS MR spectroscopy was performed in the area corresponding to the contrast enhancement on the T1W images. **Results.** Thirty-two of the 40 patients had progressive disease and 8 had pseudoprogression. Progressive disease showed the mean time of the peak values of 33 ± 7 s in 3rd and 30 ± 5 s in 10th week with no statistical significance between these two periods ($p > 0.05$). The patients with pseudoprogression showed the mean time of the peak values of 32 ± 8 s in 3rd week and 43 ± 9 s in 10th week; it was statistically significant difference ($p < 0.05$) was which favors better response to therapy. The spectroscopy results showed presence of glycine peak at 3.56 ppm in 6 patients with progressive disease which was not seen on spectra with pseudoprogression. **Conclusion.** The observed significant differences in the TTP values for PSP and RCT can provide basis for distinguishing two entities. The presence of glycine peak in the MR spectra could be a marker of RCT.

Key words:
glioblastoma; disease progression; drug therapy; radiotherapy; surgical procedures, operative; magnetic resonance imaging; spectrum analysis; diagnosis, differential.

Apstrakt

Uvod/Cilj. Uvođenje tretmana glioblastoma zračnom terapijom uz konkurentnu i adjuvantnu primenu temozolomida (CRT) dovelo je do pojave nove dijagnostičke dileme – potrebe za razlikovanjem pseudo-progresije i presudoodgovora. Razlikovanje snimaka magnetne resonance (MR) ova dva fenomena za sada je moguće samo evaluacijom u više vremenskih tačaka u toku terapije, dok nove tehnike koje bi pomogle u njihovom razlikovanju nisu još uvedene. U radu je analizirana mogućnost primene *time-to-peak* (TTP) mapa dinamičkog perfuzionog imidžinga i magnetno rezonantne spektroskopije u utvrđivanju odgovora tumora na terapiju. **Metode.** Analizirano je 40 bolesnika sa primarnim glioblastomom multiforme. Bolesnici su snimani u trećoj nedelji nakon operacije i desetoj nedelji od početka CRT. Pregledi na aparatu za MR rađeni su na aparatu 1.5 T Avanto Siemens, Erlangen Nemačka. Mape perfuzionih parametara generisane su i analizirane korišćenjem programa DPtools v3.79. 3D CSI PRESS spektroskopija sa dugim i kratkim vremenom eha rađena je kod svih bolesnika. **Rezultati.** Kod 32 od 40 bolesnika dijagnostikovana je progresija bolesti, a kod osam je dijagnostikovana pseudo-progresija. Kod bolesnika sa progresijom bolesti dobijene *time-to-peak* vrednosti su bile 33 ± 7 s u trećoj nedelji i 30 ± 5 s u desetoj nedelji, što ne predstavlja statistički značajnu razliku. Vredno-

Correspondence to: Jelena Mihailović, Institute for Oncology and Radiology of Serbia, Department for Diagnostic Radiology, Pasterova 14, 11 000 Belgrade, Serbia. E-mail: j.m.mihailovic@gmail.com

sti ovog parametra za pseudoprogresiju bile su 32 ± 8 s u trećoj i 43 ± 9 s u desetoj nedelji što je statistički značajna razlika ($p < 0.05$). Rezultati spektroskopije ukazali su na prisustvo glicinskog pika kod šest bolesnika sa progresijom bolesti, dok kod pseudoprogresije ovaj metabolit nije bio prisutan. **Zaključak.** Analizirani MR snimci pokazali su da je MR veoma uspešna tehniku za postavljanje dijagnoze progresije bolesti tokom terapije kod bolesnika sa glioblastomom.

Ključne reči:
glioblastom; bolest, progresija; lečenje lekovima; radioterapija; hirurgija, operativne procedure; magnetna rezonanca, snimanje; spektar, analize; dijagnoza, diferencijalna.

Introduction

Glioblastoma multiforme (GBM) is the most common brain tumor characterized by high aggressiveness and poor outcome. The current standard of treatment is surgical resection, followed by concomitant chemotherapy (CM) and radiotherapy (RT) [1, 2]. The evaluation of GBM response to therapy is guided by several criteria which consider findings in the post-treatment radiological and clinical evaluation. According to Macdonald et al. [3], the tumor recurrence (RCT) can be established by presence of 25% increase in the post-contrast T1W magnetic resonance images (MRI) and clinical deterioration. Recently adopted RANO (Response Assessment in Neuro-Oncology) [4] criterion states that, within period of 12 weeks upon completion of RT, a true progression can only be established if a majority of new post-contrast enhancement in the T1W images appears in region outside the area treated by the RT. However, the introduction of the new first-line chemotherapeutic temozolomide (TMZ) led to observation of a relatively new phenomenon in the follow-up of GBM treatment – pseudoprogression (PSP). PSP is a phenomenon of subacute changes observed in the glioma imaging, subsequent to radiochemotherapy, suggestive of progression, with or without associated clinical sequelae, which resolve spontaneously without further therapy [5]. In contrast to radiation necrosis which appears months to several years after RT [6], PSP usually can be observed several weeks after RT [7]. Beside the similar appearance of PSP and RCT on the post-contrast T1W images, the first could be also followed by clinical deterioration. The correct distinguishing of PSP and RCT has a large impact on decision whether TMZ application should be continued or ceased and changed with an agent specific for recurrent tumor (e.g., Avastin, etc.).

The advanced MRI methods, such as diffusion weighted imaging (DWI), perfusion imaging and magnetic resonance spectroscopy (MRS) showed variable success in distinguishing two entities. The principal obstacle in the evaluation of GBM response to therapy using DWI lies in inherently high heterogeneity of tumors appearance on the DWI and maps of the apparent diffusion coefficient (ADC), a feature which is often further increased by treatment. Chu et al. [8] reported that DWI obtained at the very high *b*-values (3000 $s \cdot mm^{-2}$), hardly obtainable in clinical MRI setups, can be used in distinguishing PS and RCT.

Since neoangiogenesis and increased vascular density are prominent features of recurrent tumors, the techniques which enable their tracing have a large potential in differentiation of RCT from radiation necrosis. So far, there is a single report dealing with the use of dynamic contrast enhanced (DCE) imaging in distinguishing RCT from PSP. Suh et al. [9] used ratios of areas under initial and, somewhat arbitrarily, selected final part of DCE curve to successfully distinguish these entities.

The perfusion parameters derived from the dynamic susceptibility weighted imaging (DSC) such as relative cerebral blood flow (rCBF), mean transition time (MTT) and particularly relative cerebral blood volume (rCBV) have been successfully used to distinguish residual/recurrent neoplasm from treatment-related radiation necrosis [10, 11]. Few studies reported the use of the DSC parameters in differentiation of RCT and PSP, although with variable success. Song et al. [12] reported that mean rCBV cannot be used for differentiation of RCT and PSP. Kong et al. [13] reported that PSP showed significantly lower rCBV values compared with RCT, so they could be distinguished with cut-off value 1.45 (81.5 % sensitivity, 77.8 % specificity). There are reports that PSP and RCT can be distinguished with somewhat higher sensitivity and specificity when cut-off value 1.8 for rCBV is used [5, 14] Mangla et al. [15] evaluated the rCBV values in the patients with GBM before and 1 month after RT-TMZ treatment and observed 41% decrease in rCBV in the PSP patients, in contrast to 12% increase in rCBV for the RCT patients. However, the studies dealing with classical analysis of perfusion maps suffer from several limitations. First, different modalities were used for correction of contrast leakage which is usually achieved by use of the pre-bolus application of small dose of a contrast agent or by use of a software; in some studies this correction was not used et all [14]. Second, the regions of observed the increase of rCBV values may contain tissue which responded to treatment as well as viable tumor in different fractions – even a minute presence of GBM (abundant less than 5 % in total) is considered as RCT [16]. There are several studies involving detailed analysis of the rCBV maps in tumor region. Baek et al. [17] used the histogram analysis of perfusion maps in two time points after completition of RT and CM and found that percentage change in the histogram parameters can be used for distingushing PSP and RCT. Cha et al. [18] implemented complex approach by combining the histograms of ADC and rCBV maps and traced changes in their parameters between two follow-up time points. They found that difference histograms with high sensitivity and accuracy can be used for distinguishing RCT and PSP. Tsien et al. [19] used the voxel-based analysis of rCBV maps before and after received therapy and significantly lower values of this parameter in PSP when compared to the RCT patients. Hu et al. [16] used interesting approach for differentiation of PSP and RCT as well as for obtaining tumor burden in enhancing lesion. In their study a

combination of histological analysis of tumor tissue and evaluation of perfusion maps was used in obtaining the rCBV cut-off values which resulted in complete differentiation of PSP from RCT.

The time-to-peak (TTP) parameter can be determined by measuring the interval from the contrast agent administration to appearance of minimum in time course of DSC signal change. The maps of this parameter are usually generated automatically using the standard software packages built in the MRI console. However, due to a variation between the time of contrast injection and the arrival of the bolus in the cerebral arteries the comparison of absolute TTP values is difficult to compare. Therefore, in order to enable comparisons between TTP for different individuals or the examinations, the standardized TTP maps should be used [20]. This parameter was extensively used in computed tomography (CT) for differentiation of pathologies outside the central nervous system (CNS) and in characterization of strokes, and in differentiation of GBM from solitary metastasis. However, to our knowledge, TTP derived from the DSC images has been used only for the evaluation of the stroke-affected tissue [21], but not for the assessment of tumor response to therapy.

MRS is frequently applied as a tool for differentiation various brain pathologies. However, the discrimination power of MRS in follow-up of tumor response to therapy is limited by considerable overlapping of spectroscopic profiles of RCT and radiation/chemo therapy. This is particularly pronounced in differentiation of RCT and TMZ/RT treatment-induced PSP since both could have the same spectroscopic features including reduction of N-acetyl aspartate (NAA), elevation of choline (Cho) and a large increase in lactate/lipid concentrations [22, 23].

Several studies showed that the GBM cells release excitoxic levels of glutamate in extracellular space [24, 25]. This may lead to the increased levels of this excitatory neurotransmitter which is followed by elevation of levels of inhibitory transmitters particularly glycine (Gly). Although there is a number of biochemical studies which dealt with transport and accumulation of glycine in the GBM cells, the reasons for this remain unclear [26]. Increased levels of Gly were also observed in some metabolic diseases, meduloblastoma and in the low grade tumor central neurocytoma.

In this study we evaluated a possibility of TTP application, as minimally subjective parameter, in distinguishing of PSP from RCT. Sensitivity and specificity of differentiation were compared to that of the routinely reported DSC parameter rCBV. The level of glycine, obtained from the analysis of MRI spectra of tumor tissue was tested as a marker for establishing presence of PSP.

Methods

Patients

This study included 40 patients with primary GBM, confirmed by histopathological analysis, (27 males and 13 females, mean age 51 years) who underwent a surgical resection followed by concomitant TMZ and RT. The treatment protocol included RT plus continuous daily TMZ (75 mg/m^2/day) followed by 6 cycles of adjuvant TMZ (150 mg/m^2 for 5 days every 28 days). The treatment started one week after the surgery.

Magnetic resonance imaging examination

All MRI examinations were performed using the 1.5T MR scanner (Avanto; Siemens, Erlangen, Germany) in the 3rd and 10th week upon the surgery (2nd and 9th week after starting the CMT+RT therapy). The first part of protocol included the T1W (TR/TE 550/9.4 ms), T2W (TR/TE 3808/89ms) and FLAIR imaging (TR/TE/TI 9900/126/2500). The MR examinations were repeated in the 6th month after the surgery in order to establish definitive diagnosis of PSP and RCT: a decrease of postcontrast enhancement on the T1w images was indicative to presence of PSP, otherwise RCT was diagnosed. The obtained images were reviewed by a neuroradiologist with 18 years of experience.

Dynamic susceptibility contrast

The DSC MRI was performed using a dynamic T2*-weighted echo-planar MR sequence**.** The multisection image data were acquired for a total of 90 s, with the bolus contrast injection occurring after 13 seconds to get a sufficient number of baseline images. The images were acquired in the axial plane with the mid-slice position at the level of the basal ganglia. A contrast medium bolus (dose, 0.1 mmoL/kg Gadovist, Bayer Schering Pharma, Berlin, Germany) was administered using an MRI injector (Ulrich Medical; Mississippi™ (MRI), Germany) with a 5 mL/s flow rate.

The data from the DSC MRI were transferred to a PC workstation and analyzed using the software package DPTools (Version 3.79). Time courses of the DSC signal were obtained from four ROIs (20–30 pixels in size) placed in regions of the row DSC images corresponding to contrast enhancement in the T1W images. Arterial input function was selected by placing single ROI over the middle cerebral artery located in the hemisphere contralateral to lesion. After obtaining the rCBV maps, four ROIs (20–30 pixels) were placed within regions of the map which correspond to the contrast enhancement in the T1W images or perifocaly to surgical cavity if no post-contrast enhancement was observed. rCBV associated with each positioned ROI was obtained and normalized (nCBV) by division by rCBV obtained for contralateral white matter. The DSC curves were obtained from ROIs identically positioned as previously described and averaged. The TTP parameter was determined as a time period from the application of contrast agent to appearance of minimum of curve.

1H magnetic resonance spectroscopy

1H MRS was performed using 3D CSI PRESS with long echo time (TE = 135 ms). The Voxel matrices were placed in the area of the high signal intensities on the T2W/FLAIR images which corresponded to edema and the contrast enhancement on T1W. The

spectra evaluation was performed using the commercial Syngo v15 workstation (Siemens, Erlangen, Germany), metabolites as choline, chromium, (Cho, Cr), N-acetylaspartate (NAA) and a single peak at 3.56 ppm in long echo time defined as Gly were taken into account. The area under the curve of a metabolite Cho, NAA was considered as relative concentration and was measured in terms of ratios in relation to Cr (Cho/Cr, NAA/Cr).

Statistical analysis

Statistical calculation was performed in the IBM SPSS Statistics17. Comparisons between the obtained mean TTP values between the patient with pseudoprogression and true progression were performed using ANOVA with Bonfferoni correction. Statistical significance was set at $p = 0.05$.

Results

In the 3rd week from the beginning of concomitant RT and CMT areas of high signal were observed in FLAIR images both in patients with PSP and RCT. However, no post-contrast enhancement was detected in the T1W images.

In the 10th week from starting the therapy, the MRI examinations demonstrated a new enhancement in the post-contrast T1W images patients, both in patients with PSP and RCT (Figures 1b and 1d). In addition, hyperintensities were observed in the regions of the FLAIR images that correspond to the non-enhancing portion of the lesion in both entities (Figures 1a and 1c). The follow-up MR imaging in the 6th month upon surgery revealed presence of RCT in 32 (80%) patients, while the PSP was established in 8 (20%).

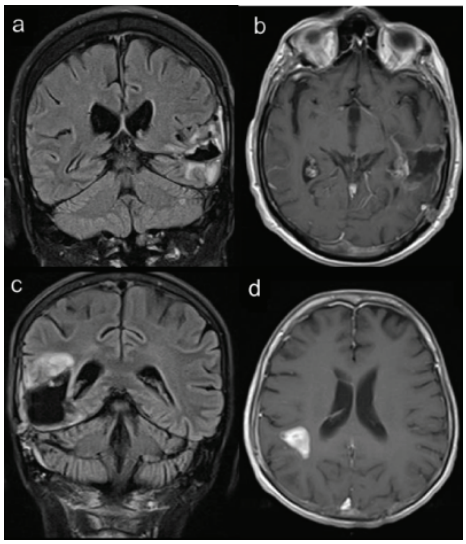

Fig. 1 – FLAIR and post-contrast T1W images obtained in the 10th week after surgery in the patients with true progression (upper row) and pseudoprogression (lower row). Although minute area of post-contrast enhancement was obeserved in b) and d) pseudoprogression (PSP) and radiation and chemotherapy (RCT). In case of pseudoprogression follow-up, the magnetic resonace imaging (MRI) demonstrated a decrease of region of post-contrast enhancement in both entities [a), c)].

Figure 2 shows the box-whiskers plot of the nCBV values for PSP and RCT in the 3rd and 10th week after surgery. No significant differences were found between the nCBV values in pseudo-progression in the 3rd week (mean 2.94 ± 0.95) and in the 10th week (mean 3.31 ± 1.32) after tumor resection. Also, no significant differences were found between the nCBV values for progressive disease in the 3rd week (mean 2.99 ± 0.97) and in the 10th week (mean 3.30 ± 1.05). Similarly, no differences were found between PSP and RCT when the nCBF values were analyzed (3rd week after surgery: nCBF(PSP) = 2.62 ± 1.10, nCBF(RCT) = 2.80 ± 1.41; 10th week: nCBF(PSP) = 2.36 ± 1.24, nCBF(RCT) = 2.74 ± 1.2).

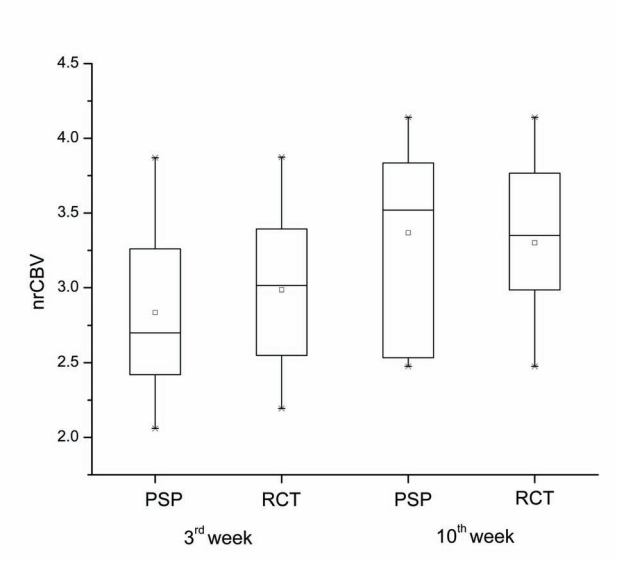

Fig. 2 – Normalized relative cerebral blood volume (arCBV) values for pseudoprogression (PSP) and recurrent tumor (RCT) in the 3rd and 10th week after surgery.

The mean DSC curves for RCT and PSP in the 3rd week and in 10th week after surgery are shown in Figures 3a and 3b.

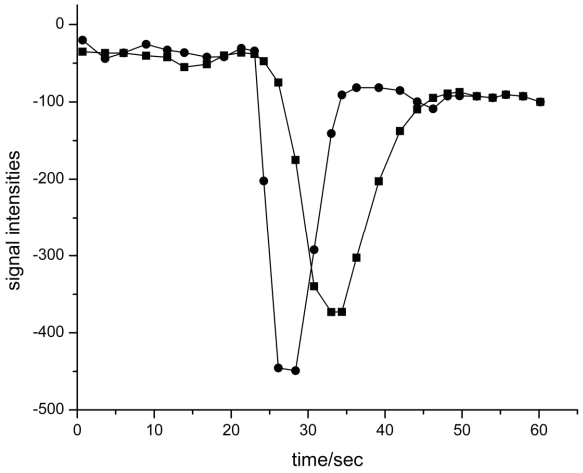

Fig. 3a – Average dynamic susceptibility contrast (DSC) curves in patients with tumor progression in the 3rd week (circles) and the 10th week (squares) after surgery.

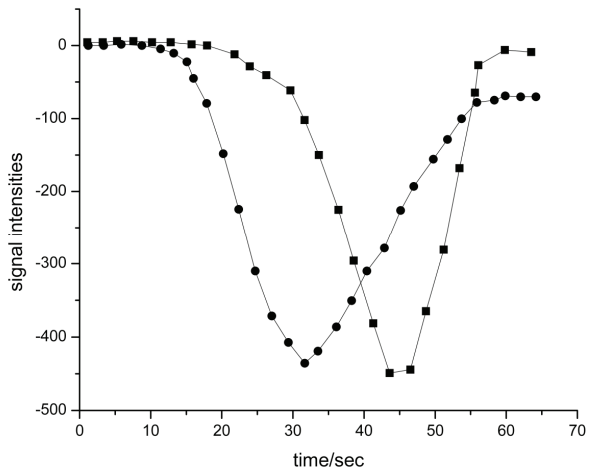

Fig. 3b – Average DSC curves in the patients with pseudoprogression in the 3rd (circles) and the 10th week (squares) after surgery.

Figure 4a shows the box-whiskers plot of TTP values for PSP and RCT in the 10th week after surgical resection. No significant differences ($p > 0.05$) were found between the TTP values in the first (mean 30 ± 5 s) and in the second time point (33 ± 7 s) in the RCT group. A significant difference ($p < 0.05$) was observed when the TTP values for PSP were compared: 32 ± 8 s in the 3rd week and 43 ± 9 s in the 10th week. Also, the TTP values for RCT and PSP differed significantly in the 10th week, but not in the 3rd after surgery.

The receiver operating characteristic (ROC) curves for differentiation RCT from PSP for the 3rd week and the 10th week after surgery are shown in Figures 5a and 5b. It can be noticed that differentiation of PSP and RCT, based on the TTP values observed in the 3rd week after surgery, is characterized by intermediate sensitivity and high specificity (64% and 94% respectively). However, in the 10th week, specificity and sensitivity for their differentiation were 78% and 99% (AUC = 0.86, $p < 0.001$), respectively.

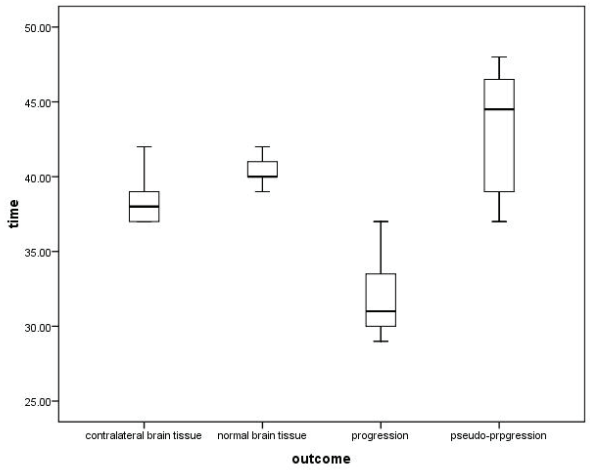

Fig. 4 – The time-to-peak (TTP) values of progression and pseudoprogression in 10th week compared with the TTP values from the normal brain tissue and contralateral brain tissue.

In 1H MR spectra for all 40 patients we observed markedly decreased the NAA/Cr ratios and prominently elevated the Cho/Cr ratio (Cho/Cr > 2) compared to the contralateral normal-appearing brain tissue (Cho/Cr = 0.8–1). The inverted lactate peak could be identified in most of the cases and usually was high in the cystic/necrotic portion of the tumor. Presence of Gly peak at 3.56 ppm was established in spectra of enhancing lesion in 6 (18%) patients with progressive disease (Figure 6b), but not in spectra of pseudoprogression (Figure 6a). The Gly was detected only in solid part of the tumor with the Gly/Cr ratio in range from 0.50 to 0.95. The observed ratio of Gly/Cho was low and range from 0.12 to 0.18.

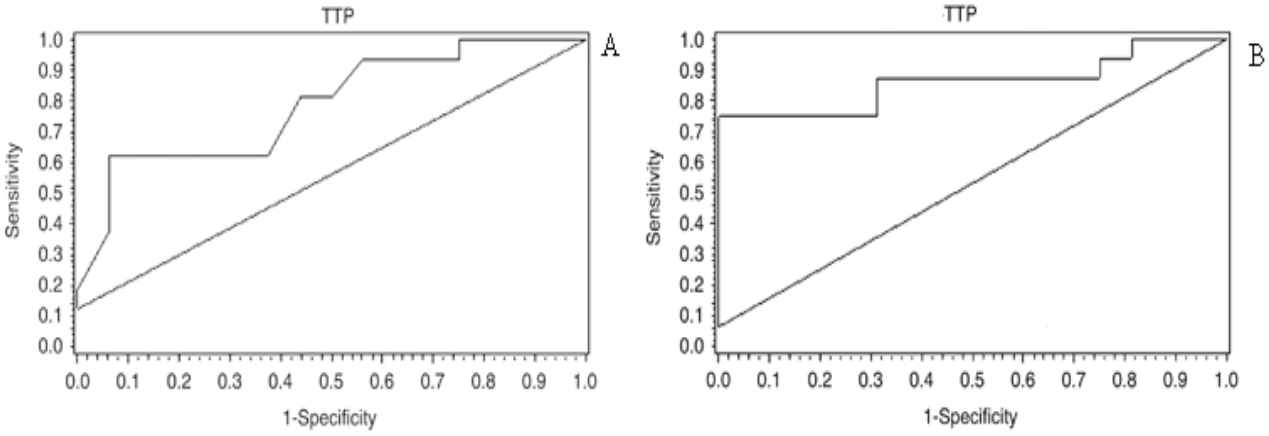

Fig. 5 – Receiver operating characteristic (ROC) curves of perfusion time-to-peak (TTP) for progression and pseudoprogression in A) 3rd and B) 10th week after surgery.

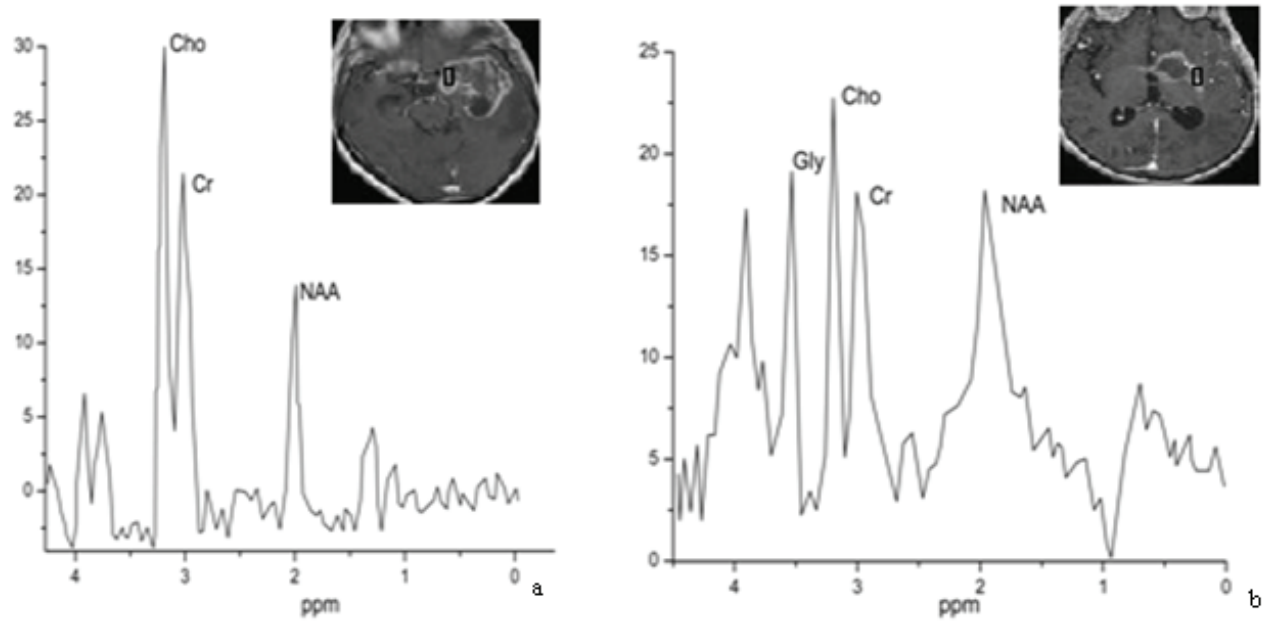

Fig. 6 – 1H magnetic resonance (MR) spectra with long echo time in the patients with a) pseudo-progression and b) progressive disease in 10th week (glycine peak is present (3.56 ppm) in the spectra of patient with diagnosed progression). The spectroscopic voxel was positioned in the solid part of the tumor.

Discussion

In this study, we used modified ("in-house") protocol for the MRI assessment of tumor response to combined RT and CMT – the first follow-up MRI was performed in the course of therapy (3rd week after surgery) while the second was performed in the first week after its finalization. The commonly reported protocols employed baseline MRI performed within 48 h after surgery and the second time point is usually within 4–12 weeks after completion of therapy.

We found no significant differences between the nCBV values for PSP and RCT regardless of time point used for comparison. The nCBV values obtained early in the course of therapy (3rd week after surgery) are in agreement with the values previously reported for non-treated GBM, which suggest that no changes in this parameter can be observed at this time point. The finding that nCBV cannot differentiate PSP and RCT in the 10th week after surgery disagrees with the findings of a majority of studies which evaluated the use of nCBV in the assessment of GBM response to therapy [5, 13, 14]. However, in those studies there were differences in cut-off values and performance of nCBV in differentiation between PSP and RCT. Song et al. [12] and Sugahara et al. [27] reported that this parameter had no value in solving this diagnostic dilemma. Leimgruber et al. [28] even claimed that nCBV could not distinguish between the RCT and effects of therapy. The absence of concordance between findings of those studies may be attributed to several causes. First, the vasodilatation and inflammation which induced by application of concomitant therapy could lead to overlap in the nCBV values for PSP and RCT. Further, different algorithms for the estimation of perfusion parameters, subjectivity in AIF selection, presence/absence of contrast leakage correction may introduce errors in nCBV determination. For example, using blood pool constrained agent and standard gadolinium based agent, Gahramanov et al. [29] demonstrated that absence of correction to leakage of contrast agent may lead to 20% increase in false negative RCTs. Last but not the least, the choice of the ROI positioning may be determining because suspected RCT/PSP may contain portions of tissue that responded to therapy as well as viable tumor [16]. Albeit, the procedures involving the advanced analysis of perfusion parameters showed a good performance in distinguishing PSP and RCT [17–19], the complexity of their algorithm made them hardly suitable for routine clinical assessment of the GBM response to treatment.

When evaluating the performance of TTP, we found that this parameter, measured in the first week after therapy, could be used in distinguishing RCT and PSP with relatively high specificity and sensitivity. The prolonged TTP in PSP compared to RCT may be explained by presence of inflammation and radiation induced damage of blood vessels and consequent decrease in tissue perfusion. This was partly supported by the lower values (but not significantly) of nCBF in PSP compared with RCT found in this study. In addition, the therapy-induced damage of vessels may result in leakage of contrast agent in interstitium which may lead to an increase in the TTP value. However, the permeability data which would confirm our assumption are available for *de novo*/recurrent GBM and normal tissue, but not for pseudo-progression [30, 31]. The use of TTP has some advantages over the standard perfusion parameters in the evaluation of GBM response to therapy. The values of rCBV and rCBF highly depend on choice of Arterial Input Function (AIF) which, in turn, relies on an operator's experience [21, 32]. Further, local AIF usually does not match that from the large arterial ves-

sels (routinely used for the definition of AIF). In turn, TTP is directly determined from the DSC signal time course and thus does not require any assumptions about AIF which makes the TTP parameter a good choice for unbiased characterization of tissue perfusion [20].

We found no significant differences between the Cho/Cr ratios in GBM and pseudoprogression. This is opposite to the reports which claim that Cho/Cr > 2 are characteristic for tumor recurrences [33]. However there are studies that compromise ability of this ratio to distinguish pseudoprogression from tumor tissue [7]. It is a well-known fact that neither reduction in the NAA/Cr ratio nor concentrations of NAA are specific in distinguishing brain pathologies [34].

Our findings suggest that excess glycine in the region of post-contrast enhancement in treated GBM might pinpoint to rest/reappearance of tumor. To our knowledge, there are no MR spectroscopic studies which dealt with the use of the Gly levels in distinguishing of recurrent tumor from pseudoprogression. However, there are both the biochemical [35] and MRI spectroscopic studies [33, 36, 37] reporting the increased gly levels of GBM. There are several assumptions about origins of increased levels of this amino acid in high grade tumors. The excess concentration of gly found in GBM may be consequence of altered metabolism of glucose in which 3-phosphoglycerate follows an alternative pathway being converted in 3-phosphoserine and further in serine and gly [38]. Recently, Chinnayian et al. [35] reported altered glucose metabolism in GBM and a severalfold increase in the levels of key metabolites glucose-6-phosphate, ribose-5-phosphate, serine and glycine. This finding could support previous assumption. In turn, the increased levels of inhibitory neurotransmitter glycine may be a response to the excitoxic levels of glutamate in extracellular space found in the GBM tissue. Although some studies suggest presence of additional gene mutations in RCT compared with primary GBM, there has not been convincing evidence, so far, for differences in their chemical constitution. This supports our speculation that the increased levels of gly may be indication of presence of RCT.

One of the major limitations of our study is difficulty of precise estimation of Gly which may be hampered by the spectral overlap with the J-coupled resonances of myo-inositol (Myo) The J evolution of resonances during the echo time can be exploited for differentiation between the Gly and Myo signals, but it cannot be excluded a contribution from Myo even in long echo times.

Other potential limitation of our study is difficulty in defining pseudoprogression. In our study, we defined pseudoprogression based on the RANO criteria. These criteria were chosen to provide the most potentially useful information to the treating neurooncologist. It is possible that some of the patients who were classified as progressive disease due to a change in treatment, however, could have had pseudoprogression and done well. On the other hand, it is possible that some patients classified as pseudoprogression had slowly progressive tumors, instead.

Our final analysis cohort was relatively small, with a low number of pseudoprogression patients. The magnitude in the differences in the TTP parameter was striking, however a statistical significance was achieved. This suggests that such differences between the two groups are real and robust enough to prompt additional, larger studies.

Conclusion

Non-invasive techniques to detect and quantify the metabolic features and hemodynamic status of human tumor tissue have outstanding clinical potential in cancer imaging. The results implies that changes in Gly levels and TTP may be related to specific signatures that favor better response on therapy and outcome for the GBM patients.

REFERENCES

1. *Easaw JC, Mason WP, Perry J, Laperriere N, Eisenstat DD, del Maestro R,* et al. Canadian recommendations for the treatment of recurrent or progressive glioblastoma multiforme. Curr. Oncol 2011; 18(3): e126–36.
2. *Carlsson SK, Brothers SP, Wahlestedt C.* Emerging treatment strategies for glioblastoma multiforme. EMBO Mol Med 2014; 6(11): 1359–70.
3. *Macdonald DR, Cascino TL, Schold SC Jr, Cairncross JG.* Response criteria for phase II studies of supratentorial malignant glioma. J Clin Oncol 1990; 8(7): 1277–80.
4. *Wen PY, Macdonald DR, Reardon DA, Cloughesy TF, Sorensen GA, Galanis E,* et al. Updated response assessment criteria for high-grade gliomas: Response assessment in neuro-oncology working group. J Clin Oncol 2010; 28(11): 1963–72.
5. *Gahramanov S, Raslan AM, Muldoon LL, Hamilton BE, Rooney WD, Varallyay CG,* et al. Potential for differentiation of pseudoprogression from true tumor progression with dynamic susceptibility-weighted contrast-enhanced magnetic resonance imaging using ferumoxytol vs. gadoteridol: a pilot study. Int J Radiat Oncol Biol Phys 2011; 79(2): 514–23.
6. *Morris JG, Grattan-Smith P, Panegyres PK, O'Neill P, Soo YS, Langlands AO.* Delayed cerebral radiation necrosis. Quarterly J Med 1994; 87(2): 119–29.
7. *Hygino da Cruz LC Jr, Rodriguez I, Domingues RC, Gasparetto EL, Sorensen AG.* Pseudoprogression and pseudoresponse: imaging challenges in the assessment of posttreatment glioma. AJNR Am J Neuroradiol 2011; 32(11): 1978–85.
8. *Chu HH, Choi SH, Ryoo I, Kim SC, Yeom JA, Shin H,* et al. Differentiation of true progression from pseudoprogression in glioblastoma treated with radiation therapy and concomitant temozolomide: comparison study of standard and high-b-value diffusion-weighted imaging. Radiology 2013; 269(3): 831–40.
9. *Suh CH, Kim HS, Choi YJ, Kim N, Kim SJ.* Prediction of pseudoprogression in patients with glioblastomas using the initial and final area under the curves ratio derived from dynamic contrast-enhanced T1-weighted perfusion MR imaging. AJNR Am J Neuroradiol 2013; 34(12): 2278–86.
10. *Barajas RF Jr, Chang JS, Segal MR, Parsa AT, McDermott MW, Berger MS,* et al. Differentiation of recurrent glioblastoma multiforme from radiation necrosis after external beam radiation therapy with dynamic susceptibility-weighted contrast-

enhanced perfusion MR imaging. Radiology 2009; 253(2): 486–96.
11. *Verma N, Cowperthwaite MC, Burnett MG, Markey MK.* Differentiating tumor recurrence from treatment necrosis: a review of neuro-oncologic imaging strategies. Neuro Oncol 2013; 15(5): 515–34.
12. *Song YS, Choi SH, Park CK, Yi KS, Lee WJ, Yun TJ,* et al. True progression versus pseudoprogression in the treatment of glioblastomas: a comparison study of normalized cerebral blood volume and apparent diffusion coefficient by histogram analysis. Korean J Radiol 2013; 14(4): 662–72.
13. *Kong DS, Kim ST, Kim EH, Lim DH, Kim WS, Suh YL,* et al. Diagnostic dilemma of pseudoprogression in the treatment of newly diagnosed glioblastomas: the role of assessing relative cerebral blood flow volume and oxygen-6-methylguanine-DNA methyltransferase promoter methylation status. AJNR Am J Neuroradiol 2011; 32(2): 382–7.
14. *Young RJ, Gupta A, Shah AD, Graber JJ, Chan TA, Zhang Z,* et al. MRI perfusion in determining pseudoprogression in patients with glioblastoma. Clin Imaging 2013; 37(1): 41–9.
15. *Mangla R, Singh G, Ziegelitz D, Milano MT, Korones DN, Zhong J,* et al. Changes in relative cerebral blood volume 1 month after radiation-temozolomide therapy can help predict overall survival in patients with glioblastoma. Radiology 2010; 256(2): 575–84.
16. *Hu LS, Eschbacher JM, Heiserman JE, Dueck AC, Shapiro WR, Liu S,* et al. Reevaluating the imaging definition of tumor progression: Perfusion MRI quantifies recurrent glioblastoma tumor fraction, pseudoprogression, and radiation necrosis to predict survival. Neuro Ooncol 2012; 14(7): 919–30.
17. *Baek HJ, Kim HS, Kim N, Choi YJ, Kim YJ.* Percent change of perfusion skewness and kurtosis: A potential imaging biomarker for early treatment response in patients with newly diagnosed glioblastomas. Radiology 2012; 264(3): 834–43.
18. *Cha J, Kim ST, Kim HJ, Kim B, Kim JK, Lee JY*, et al. Differentiation of Tumor Progression from Pseudoprogression in Patients with Posttreatment Glioblastoma Using Multiparametric Histogram Analysis. Am J Neuroradiol 2014; 35(7): 1309–17.
19. *Tsien C, Galbán CJ, Chenevert TL, Johnson TD, Hamstra DA, Sundgren PC,* et al. Parametric response map as an imaging biomarker to distinguish progression from pseudoprogression in high-grade glioma. J Clin Oncol 2010; 28(13): 2293–920.
20. *Nasel C, Azizi A, Veintimilla A, Mallek R, Schindler E.* A standardized method of generating time-to-peak perfusion maps in dynamic-susceptibility contrast-enhanced MR imaging. AJNR Am J Neuroradiol 2000; 21(7): 1195–8.
21. *Neumann-Haefelin T, Wittsack HJ, Wenserski F, Siebler M, Seitz RJ, Mödder U*, et al. Diffusion- and perfusion-weighted MRI. The DWI/PWI mismatch region in acute stroke. Stroke 1999; 30(8): 1591–7.
22. *Brandes AA, Tosoni A, Spagnolli F, Frezza G, Leonardi M, Calbucci F,* et al. Disease progression or pseudoprogression after concomitant radiochemotherapy treatment: Pitfalls in neurooncology. Neuro Oncol 2008; 10(3): 361–7.
23. *Sundgren PC.* MR Spectroscopy in Radiation Injury. Am J Neuroradiol 2009; 30(8): 1469–76.
24. *Ye ZC, Sontheimer H.* Glioma cells release excitotoxic concentrations of glutamate. Cancer Res 1999; 59(17): 4383–91.
25. *Ye ZC, Rothstein JD, Sontheimer H.* Compromised glutamate transport in human glioma cells: Reduction-mislocalization of sodium-dependent glutamate transporters and enhanced activity of cystine-glutamate exchange. J Neurosci 1999; 19(24): 10767–77.
26. *Righi V, Andronesi OC, Mintzopoulos D, Black PM, Tzika AA.* High-resolution magic angle spinning magnetic resonance spectroscopy detects glycine as a biomarker in brain tumors. Int J Oncol 2010; 36(2): 301–6.
27. *Sugahara T, Korogi Y, Tomiguchi S, Shigematsu Y, Ikushima I, Kira T,* et al Posttherapeutic intraaxial brain tumor: the value of perfusion-sensitive contrast-enhanced MR imaging for differentiating tumor recurrence from nonneoplastic contrast-enhancing tissue. AJNR Am J Neuroradiol 2000; 21(5): 901–9.
28. *Leimgruber A, Ostermann S, Yeon EJ, Buff E, Maeder PP, Stupp R,* et al. Perfusion and diffusion MRI of glioblastoma progression in a four-year prospective temozolomide clinical trial. Int J Radiat Oncol Biol Phys 2006; 64: 869–75.
29. *Gahramanov S, Muldoon LL, Varallyay CG, Li X, Kraemer DF, Fu R,* et al. Pseudoprogression of glioblastoma after chemo- and radiation therapy: Diagnosis by using dynamic susceptibility-weighted contrast-enhanced perfusion MR imaging with ferumoxytol versus gadoteridol and correlation with survival. Radiology 2013; 266(3): 842–52.
30. *Cha S, Yang L, Johnson G, Lai A, Chen MH, Tihan T*, et al. Comparison of Microvascular Permeability Measurements, Ktrans, Determined with Conventional Steady-State T1-Weighted and First-Pass T2*-Weighted MR Imaging Methods in Gliomas and Meningiomas. Am J Neuroradiol 2006; 27(2): 409–17.
31. *Law M, Yang S, Babb JS, Knopp EA, Golfinos JG, Zagzag D*, et al. Comparison of Cerebral Blood Volume and Vascular Permeability from Dynamic Susceptibility Contrast-Enhanced Perfusion MR Imaging with Glioma Grade. AJNR Am J Neuroradiol 2004; 25(5): 746–55.
32. *Rempp KA, Brix G, Wenz F, Becker CR, Gückel F, Lorenz WJ.* Quantification of regional cerebral blood flow and volume with dynamic susceptibility contrast-enhanced MR imaging. Radiology 1994; 193(3): 637–41.
33. *Lehnhardt F, Bock C, Röhn G, Ernestus R, Hoehn M.* Metabolic differences between primary and recurrent human brain tumors: A 1H NMR spectroscopic investigation. NMR Biomed 2005; 18(6): 371–82.
34. *Ken S, Vieillevigne L, Franceries X, Simon L, Supper C, Lotterie JA*, et al. Integration method of 3D MR spectroscopy into treatment planning system for glioblastoma IMRT dose painting with integrated simultaneous boost. Radiat Oncol 2013;8: 1.
35. *Chinnaiyan P, Kensicki E, Bloom G, Prabhu A, Sarcar B, Kahali S,* et al. The metabolomic signature of malignant glioma reflects accelerated anabolic metabolism. Cancer Res 2012; 72(22): 5878–88.
36. *Hattingen E, Lanfermann H, Quick J, Franz K, Zanella FE, Pilatus U.* 1H MR spectroscopic imaging with short and long echo time to discriminate glycine in glial tumours. MAGMA 2009; 22(1): 33–41.
37. *Tugnoli V, Tosi MR, Barbarella G, Bertoluzza A, Ricci R, Trevisan C.* In vivo 1H MRS and in vitro multinuclear MR study of human brain tumors. Anticancer Res. 1996; 16(5A): 2891–9.
38. *Jain M, Nilsson R, Sharma S, Madhusudhan N, Kitami T, Souza AL,* et al. Metabolite profiling identifies a key role for glycine in rapid cancer cell proliferation. Science 2012; 336(6084): 1040–4.

Received on January 14, 2017.
Revised on July 4, 2017.
Accepted on July 10, 2017.
Online First September, 2017.

ORIGINAL ARTICLE

UDC: 617.5-089.844:618.19-007-089
https://doi.org/10.2298/VSP170410101P

The impact of breast augmentation on the skin temperature of the breast

Uticaj augmentacione mamaplastike na temperaturu kože dojke

Branislav Piščević*, Zorica Brdareski[†‡], Nenad Stepić*[‡], Boban Djordjević*[‡], Dejan Vulović[§], Marko Jovanović[‖], Dejan Vulović[§]

Military Medical Academy, *Clinic for Plastic Surgery and Burns, [†]Clinic for Physical Medicine and Rehabilitation, Belgrade, Serbia; Clinical Center "Kragujevac", [‖]Center for Plastic Surgery, Kragujevac, Serbia; University of Kragujevac, [§]Faculty of Medical Sciences, Kragujevac, Serbia; University of Defence, [‡]Faculty of Medicine of the Military Medical Academy, Belgrade, Serbia

Abstract

Background/Aim. Complications of breast augmentation, as one of the most common cosmetic surgery, may be different. Besides usual early, local postoperative complicatons, the most common late complication is capsular contracture. As a specific complication of skin functions after this operation only disturbance of sensibility is described. Since the skin has other functions as well, and because there are no literature data available, the aim of this research was measuring the skin temperature before and after surgery. **Methods.** A prospective intervential study was done in 49 adult women. Bilateral augmentative mammaplasty was performed for breast hypoplasia or on the personal request of a patient with autrophic breasts. Measuring the temperature of the breast skin was done in two points, before the operation, and seven days and three months after surgery. The temperature measurement was done by the infrared thermometer (Pyrometer TROTEC BP21). Statistically significant difference was determined using the *t*-test for related samples. Differences were considered statistically significant if p was less than 0.05. Eta squared coefficient was use to determine the import size and according to the Cohen criteria everything over 10:14 signified a major impact**.** The data were analyzed by the IBP SPSS Statistics v20. **Results.** In a majority of patients the breasts were hypoplastic (69.39%). The most commonly used implants were 275–500 mL volume (46.94%), and the least common implants were over 500 mL (16.33%). In a little less than 2/3 of the patients submammary incision was used (61.22%). In a majority of patients (67.35%) the prosthesis were placed subglandularly. The average value of the temperature before the operation at the point 1 was 34.49ºC, seven days after surgery 34.81ºC, and three months after surgery 34.10ºC; and at the point 2: 34.60 ºC, 34.91ºC and 34.19ºC in the same time intervals. In relation to the size of the breasts before operation and the size of the implant manufacturer, the localization of the incision and placement of the localization of the prosthesis, no statistically significant differences in the temperature of the skin of the breast before and after surgery was observed. **Conclusion.** Our results on the change of skin temperature after the breast augmentation could be significant preoperative information for the patients.

Key words:
breast implantation; reconstructive surgical procedures; skin temperature; treatment outcome.

Apstrakt

Uvod/Cilj. Komplikacije augmentacije grudi, kao jedne od najčešćih estetskih operacija, su moguće i različite. Osim uobičajenih ranih, lokalnih postoperativnih komplikacija, najčešća kasna komplikacija je kapsularna kontraktura. Kao specifična komplikacija poremećaja funkcije kože posle ove operacije opisan je samo poremećaj senzibiliteta. S obzirom na to da koža ima i druge funkcije, kao i zbog toga što ne postoje podaci u literaturi, cilj istraživanja bio je merenje temperature kože dojke pre i posle operacije. **Metode.** Urađena je prospektivna intervencijska studija kod 49 punoletnih žena koje nisu rađale. Bilateralna augmentaciona mamoplastika je rađena zbog hipoplazije dojki ili na lični zahtev pacijenta sa eutrofičnim dojkama. Merenje temperature kože dojke je rađeno u dve tačke, pre operacije, sedam dana posle operacije i tri meseca posle operacije. Merenje temperature je učinjeno infracrvenim termometrom (Pyrometer BP21 TROTEC). Statistička značajnost razlike je određena korišćenjem *t*-testa za vezane uzorke. Razlike su smatrane statistički značajnim ukoliko je $p < 0,05$. Koeficijent eta kvadrat određivao je veličinu uticaja i prema kriterijumu

Correspondence to: Dejan Vulović, Center for Plastic Surgery, Clinical Center "Kragujevac", Zmaj Jovina 30, 34 000 Kragujevac, Serbia. E-mail: dejanavu@eunet.rs

Cohena, sve preko 0,14 označavalo je veliki uticaj. Dobijeni su analizirani programom IBM SPSS Statistics v20. **Rezultati.** Kod većine ispitanica dojke su bile hipoplastične (69,39%). Najčešće su korišćeni implantati zapremine 275–500 mL (46,94%), a najređe implantati zapremine preko 500 mL (16,33%). Kod nešto manje od 2/3 pacijenata primenjen je submamarni rez (61,22%). Kod većine pacijenata (67,35%), proteza je plasirana subglandularno. Prosečna vrednost temperature pre operacije u tački 1 bila je 34,49°C, sedam dana nakon operacije 34,81°C, a tri meseca nakon operacije 34,10°C, a u tački 2: 34,60°C, 34,91°C i 34,19°C u istim vremenskim intervalima. U odnosu na veličinu dojki pre operacije, veličinu i proizvođača implantata, lokalizaciju incizije i lokalizaciju plasiranja proteze, nisu nađene statistički značajne razlike u temperaturi kože dojke pre i posle operacije. **Zaključak.** Naši rezultati o promeni temperature kože dojke posle augmentacije mogli bi da imaju značaj u preoperativnom informisanju pacijenta.

Ključne reči:
dojka, implantati; hirurgija, rekonstruktivna, procedure; koža, temperatura; lečenje, ishod.

Introduction

Breast augmentation is one of the most frequent aesthetic surgeries and in some countries it is the leading one [1]. For example, there are more than 300,000 mammaplasties in the USA, every year. Different surgical approaches and different implants are used [2–6]. For the most plastic surgeons, this is the routine surgery, but as any placement of a foriegn material into the body, it must be taken seriosly.

Complications of mammaplasty are possible and different in type and incidence [7–14]. They are more or less frequent, minor or significant, nonspecific or specific, local or systemic, early or late. Some of the mammaplasty complications are specific to this type of operation, the capsular contracture being the most common, which was studied in detail [9]. According to literature data, the possible specific complication of mammaplasty augmentation is a sensory disturbance [10–13].

There are no available data on the skin temperature after mammaplasty augmentation. A woman with the great desire to resize and reshape the breast, very often is not interested in possible complications, and sometimes, not completely informed by a surgeon. Therefore, the aim of this paper was to research breast skin temperature after augmentation using silicon prosthesis, assuming that a change occurs on the breast skin after the operation, which could be important in providing information to the patient before surgery.

Methods

In the prospective intervention study, breast skin temperature was taken on 49 Caucasian women before and after augmentation using silicon prosthesis. The operations were performed at the Clinic for Plastic Surgery and Burns of the Military Medical Academy in Belgrade, over the period from January 1, 2012 until January 1, 2016, with the approval of the Ethics Committee of the Military Medical Academy.

The inclusion criteria for participation in the study were: women of age up to 60 years that did not give birth, bilateral mammaplasty augmentation due to hypoplasia of the breasts or at personal request of the examiners with eutrophic breasts. Furthermore, an inclusion criterion was also a signed consent to participate in the study, after the patient was first acquainted in detail by the researcher with the purpose and significance of the research. An eutrophic breast was considered a concave shaped breast, vertically stretching from 3rd or 4th rib to the 6th or 7th rib, and horizontally, from the parasternal line to the medial axillary line, with a base forming an angle of approximately 100° (Figure 1). The excluding criteria in the study were certain changes in the local status of the breast [congenital anomalies of the breast except hypoplasia, higher grade of breast ptosis (Grade 3 and 4 according to Becker), mastectomy, secondary augmentation mammaplasty, scar]; unilateral mammaplasty augmentation; ovulation and menstruation; severe forms of chronic disease (diabetes melitus, cardiovascular, respiratory, nephrological, hepatological, neurological, dermatological, autoimmune); psychiatric examinees; autoimmune nervous system disorders; use of certain drugs (estrogens, gestagens or their antagonists, sympathomimetics, adrenergic blockers, cholinergics, antimuscarinic drugs); early postoperative complications (higher degree of edema in one or both breasts, hematoma, seroma, dehiscence, necrosis, infection, implant protrusion), followed by incomplete medical documentation, and inability of adequate control testing until the end of research.

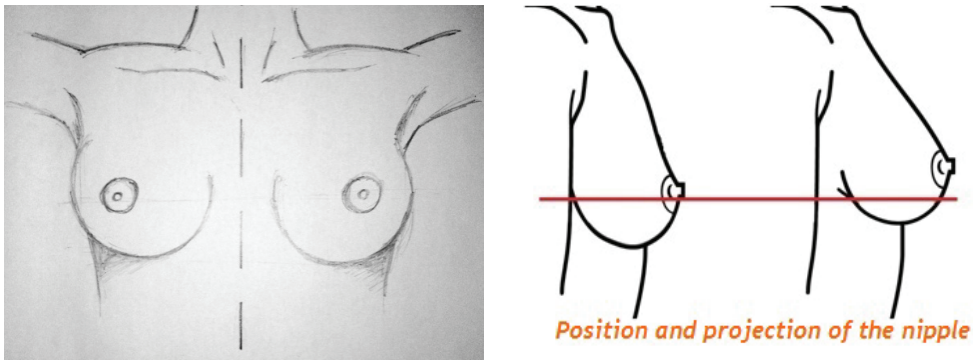

Fig. 1 – Morphology and topography of eutrophic breast.

On admission to the Clinic, the participants had the following medical documentation: specialist medical report, the breast ultrasound examination findings, mammography, hematogram, glycemy, urea and creatinine values, international normalised ratio (INR) and activated partial thromboplastin time (APTT), laboratory urine findings, X-ray of the lungs, electrocardiogram, internist's findings and breast photo. All the operations were performed under general endotracheal anesthesia. Submammary or periareoal incision was applied. Textured silicone implants of different shape, by different manufacturers were used and placed in front of (subglandular) or behind the large chest muscle (subpectoral). The implant size depended on the degree of hypoplasia, size of eutrophic breast and patient's wish. The breast temperature was taken at three-time periods: before the operation (up to 24 h), seven days and three months after the operation. The tests were performed at the Clinic for Physical Medicine and Rehabilitation of the Military Medical Academy in Belgrade. The breast temperature measurement was performed by specialists in physical medicine and rehabilitation. While doing so, during the postoperative measurement, they did not have insight into the results of preoperative measurement of the same patient. The same conditions were provided during the test: room temperature about 21ºC, relative air humidity 40%–55% and relaxed lying position of the patient. The breast skin temperature was taken by the infrared thermometer (Pyrometer BP21 TROTEC) in two points (Figure 2). The first point was the areola area, directly medially from the mamilla, and the second point was in the middle of the horizontal line that connects the center of the frontal part of the sternum and mamilla (Figure 1, drawing and photos).

Statistical processing of the data was performed applying the IBM SPSS Statistics v20 program. The results were presented descriptively, using the table and graph. The continuous variables are shown as mean values and standard deviations, and categorical variables as percentile share of certain categories. Statistical significance of temperature difference between two moments in time was determined by using the *t*-test for paired samples. The differences were considered statistically significant if $p < 0.05$. The eta squared coefficient determined the impact value and according to the Cohen criteria, everything above 0.14 indicated a large impact.

Results

The age in a 49-patient sample was in the range of 18–60 years (average 29.41 years). In most of the subjects the breasts were hypoplastic (69.39%), and in 15 subjects eutrophic (30.61%). Implants volume of 275–500 mL (46.94%) were most commonly used, in 18 (36.73%) patients while implants up to 275 mL, and implants volume of over 500 mL were rarely used (16.33%). In less than 2/3 of the participants, submammary incision was applied (61.22%), and less commonly the periareolar incision (38.78%). In most of the participants (67.35%), the placement of the prosthesis was subglandular, and in 16 (32.66%) submuscularly participants (Table 1).

Table 1
Patient's data and information about the operation

Variable	Patients, n (%)
Size of the breast	
hypoplastic	34 (69.39)
eutrophic	15 (30.61)
Size of the implant	
to 275 cc	18 (36.73)
from 276 ccm to 500 cc	23 (46.93)
over 500 cc	8 (16.32)
Type of the incision	
submammary	30 (61.22)
periareolar	19 (38.78)
Placement of the implant	
subglandularly	33 (67.35)
submuscularly	16 (32.65)

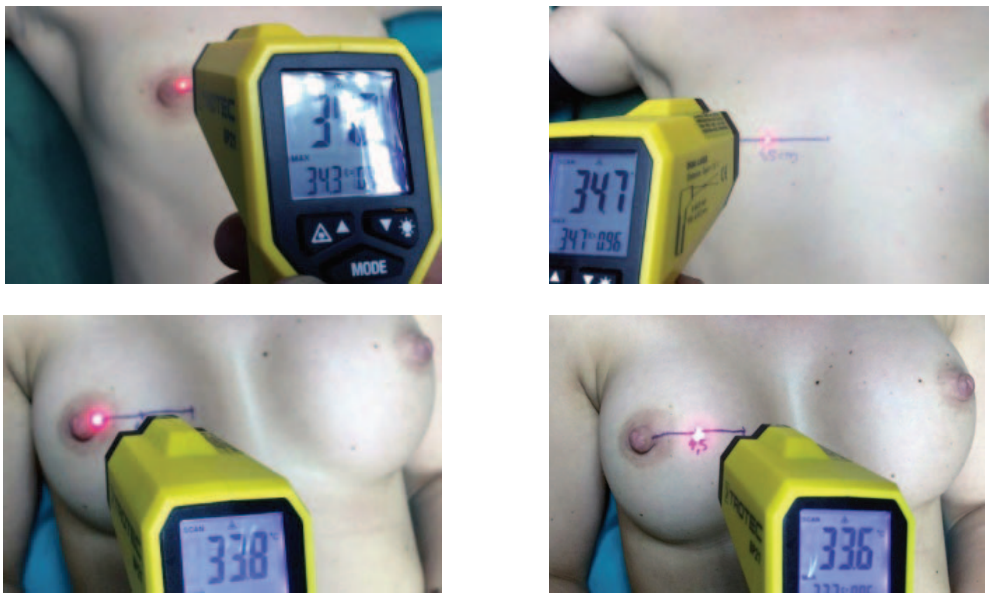

Fig. 2 – Breast skin temperature measurement by infrared thermometer at two points. Up: preoperation; down: postoperation in the same patient.

Table 2

Average values of the differences in the breast skin temperature after breast angmentation in relation to the value before operation

Time after operation	Average differences (Δ) in the breast skin temperature (ºC)	
	Point 1	Point 2
7 days	Δ = 0.32 (t = 16.248; df = 48; p = 0.000; eta^2 = 0.85)	Δ = 0.31 (t = 22.947; df = 48; p = 0.000; eta^2 = 0.92)
3 months	Δ = 0.39 (t = 31.738; df = 48; p = 0.000; eta^2 = 0.95)	Δ = 0.41 (t = 34.687; df = 48; p = 0.000; eta^2 = 0.96)

Point 1 – the areola area, directly medially from the mamilla;
Point 2 – middle of the horizontal line that connects the center of the frontal part of the sternum and mamilla.

The average temperature value before the operation at the point 1 was 34.49°C, seven days after the operation 34.81°C, and three months after the operation 34.10°C. The average temperature value before the operation at the point 2 was 34.60°C, seven days after the operation 34.91°C, and three months after the operation 34.19°C. No statistically significant differences were determined in the breast skin temperature before and after the operation in relation to the breast size before the operation, the implant size and manufacturer, incision and prosthesis placement localization.On the other hand, by applying the *t*-test for paired samples, we reached a conclusion that there was a statistically significant difference between the breast skin temperature at the point 1 before and seven days after the operation; this difference on average was 0.32°C (t = -16.25, df = 48, p = 0.000) (Table 2). The average temperature value, seven days after the operation at the point 1 was 34.81°C, and three months after the operation 34.10°C. Applying the *t*-test for paired samples we concluded that there was a statistically significant difference between the skin temperature seven days and three months after the operation (Δ = 0.72°C t = 47.33, df = 48, p = 0.000). The *t*-test for paired samples also showed a statistically significant difference between the preoperative temperature and temperature after three months. This difference was 0.39°C (t = 31.74, df = 48, p = 0.000). The eta squared coefficient determined the impact value and according to the Cohen criteria everything above 0.14 indicates a large impact. Considering that our values were significantly higher for all three previous conclusions, it means that there was a great difference between the breast skin temperature at the different intervals of time after operation in relation to the value before operation (Table 2).

Using the *t*-test for paired samples, it was found that there was a statistically significant difference between the breast skin temperature at the point 2 before the operation and three months after; the average difference was 0.41°C (t = 34.69, df = 48, p = 0.000). According to the eta squared coefficient, the obtained values were significantly higher for all three previous conclusions; therefore, the difference between the temperatures was great (Table 2).

Discussion

Human skin temperature is one of the four vital parameters. Localized, designated measurement of skin temperature of a specific body region is rarely used in medical practice. The examples of this are vascular, endocrine, rheumatic and skin diseases [15–17]. Measurement of skin temperature in surgery is used in the postoperative monitoring with the use of arterial, free tissue flaps, mostly free-microvascular [18–21] as well as after tissue expanson [22]. The measurement of breast skin temperature was taken in analysis of the periods after physical strain and in nursing mothers [22–24].

On research of references pertaining to mammaplasty, particularly the analysis of possible early and later postoperative complications, we did not find the data that directly indicate a change in the breast skin temperature after this operation. The other authors mostly analyzed the hematoma, seroma, dehiscence, infection, hypertrophic scar and Mondor's disease (superficial thromophlebitis), as well as possible early complications, asymmetry, capsular contracture, mamilla and areola sensitivity disorder, prosthesis deflation or rupture, appearance of autoimmune diseases and anaplastic large cell lymphoma (ALCL) as possible later complications [7–14]. ALCL is a rare type of non-Hodgkin's lymphoma, the appearance of which after breast augmentation was published for the first time in January 2011 according to the FDA report, and some 40 cases have been described in the world to date [14]. The relation between prosthesis implantation and the appearance of breast malignancy was not proven.

Until today, there is no reachable data about the temperature changes of the breast skin after augmentation mammaplasty. We can try to explain our results. Our measurements indicated that there was a statistically significant difference between the temperature before and seven days after the operation, whereas this difference on average was 0.31°C (p = 0.000). Also, we recorded a statistically significant difference between the temperature seven days and three months after the operation (p = 0.000). A statistically significant difference was noted between the preoperative temperature and temperature after three months.

Augmentation mammaplasty is some kind of tissue injuries. Tissue injury can be induced by: allergic reactions, autoimmunity, infection or mechanical damage often results in the disruption of normal tissue architecture, initiating a healing response [25]. Tissue healing process after the injury includes two more very important processes- inflammation and healing.

Tissue integrity is disrupted and inflammation is normal answer. Also, inflammation additionally disturbs the tissue.

All these facts, which include very strong immunity reaction, contribute to the cellular damage and the tissue destruction. Local inflammation implies synthesis of different proinflammatory cytokines: interleukin (IL)-1, IL-6, TNF-α, chemokines, etc [26]. Cytokines and chemokines by their gradients recruit the inflammatory cells on the place of tissue injuries [27]. Neutrophils, eosinophils, lymphocytes and macrophages are observed at sites of acute injury with cell debris and areas of necrosis cleared by phagocytes [28]. Vascular changes are detected like increased permeability with increased influx of the inflammatory cells at the site of injury. These cells have the role to clean the inflammation place and to make the base for the healing process. Inflammatory cells secrete the chemokines which induce the profibrotic cells to settle the injury place [29]. Fibroblasts with profibrotic conduction of cytokines activate the process of the healing. At the end of this process, the fibrin-rich scaffold formation, wound contraction, closure and re-epithelialization can be observed [30]. Augmentation mammaplasty, as some kind of the tissue injury, activates this very compound process. Ojo-Amaize et al. [31] recorded the elevated concentrations of proinflammatory cytokines IL-1b and IL-1 receptor antagonist in plasma of women with silicone breast implants [32]. Also, some data indicated that physiatric procedures (electromagnetic pulse field) decreased pain and IL-1b level after the augmentation mammoplasty [32]. Including all these facts, we can explain the temperature changes of the skin after augmentation mammaplasty. Increased temperature seven days after the surgery, noticed in our results, can be explained by the inflammation process. Inflammation is the answer to the local tissue injury (surgery, foreign body-silicone implants). As the process is continued by activating the healing cascade, we propose the explanation for the decreased skin temperature three months after the surgery. The healing process, including the fibrotic tissue production for modeling the tissue after the inflammation with decreased local blood flow at the site of the inflammation, is the possible answer for this phenomenon.

Conclusion

According to the existing literature and results of our research, we concluded that the implantation of silicon prosthesis can affect the change in breast skin temperature in the postoperative period. Skin temperature changes can be explained by the inflammation and healing process, as the consequence of the augmentation mammaplasty. The obtained data can have a significant impact on the patient's decision concerning this operation. In addition to this, this paper can also be an incentive to test other functions of the breast skin in mammaplasty augmentation.

REFERENCES

1. *American Society of Plastic Surgeons*. National Clearinghouse of Plastic Surgery Procedural Statistics. 2013 Plastic Surgery Statistics Report. American Society of Plastic Surgeons; 2014.
2. *Codner MA, Mejia JD, Locke MB, Mahoney A, Thiels C, Nahai FR*, et al. A 15-year experience with primary breast augmentation. Plast Reconstr Surg 2011; 127(3): 1300–10.
3. *Swanson E*. Prospective outcome study of 225 cases of breast augmentation. Plast Reconstr Surg 2013; 131(5): 1158–66.
4. *Hidalgo DA, Sinno S*. Current Trends and Controversies in Breast Augmentation. Plast Reconstr Surg 2016; 137(4): 1142–50.
5. *Namnoum JD, Largent J, Kaplan HM, Oefelein MG, Brown MH*. Primary breast augmentation clinical trial outcomes stratified by surgical incision, anatomical placement and implant device type. J Plast Reconstr Aesthet Surg 2013; 66(9): 1165–72.
6. *Adams WP, Small KH*. The Process of Breast Augmentation with Special Focus on Patient Education, Patient Selection and Implant Selection. Clin Plast Surg 2015; 42(4): 413–26.
7. *Vitug A, Newman L*. Complications in Breast Suregry. Surg Clin N Am 2007; 87(4): 431–51.
8. *Shi H, Cao C, Li X, Chen L, Li S*. A retrospective study of primary breast augmentation: Recovery period, complications and patient satisfaction. Int J Clin Exp Med 2015; 8(10): 18737–43.
9. *Headon H, Kasem A, Mokbel K*. Capsular Contracture after Breast Augmentation: An Update for Clinical Practice. Arch Plast Surg 2015; 42(5): 532–43.
10. *Okwueze MI, Spear ME, Znyghuizen AM, Braün SA, Ajmal N, Nanney LB*, et al. Effect of augmentation mammaplasty on breast sensation. Plast Reconstr Surg 2006; 117(1): 73–83; discussion 84–5.
11. *Mofid M, Klatsky SA, Singh NK, Nahabedian MY*. Nipple-areola complex sensitivity after primary breast augmentation: A comparison of periareolar and inframammary incision approaches. Plast Reconstr Surg 2006; 117(6): 1694–8.
12. *Araco A, Araco F, Sorge R, Gravante G*. Sensitivity of the nipple-areola complex and areolar pain following aesthetic breast augmentation in a retrospective series of 1200 patients: Periareolar versus submammary incision. Plast Reconstr Surg 2011; 128(4): 984–9.
13. *Lund HG, Turkle J, Jewell ML, Murphy DK*. Low Risk of Skin and Nipple Sensitivity and Lactation Issues After Primary Breast Augmentation with Form-Stable Silicone Implants: Follow-Up in 4927 Subjects. Aesthet Surg J 2016; 36(6): 672–80.
14. *Xu J, Wei S*. Breast implant-associated anaplastic large cell lymphoma: Review of a distinct clinicopathologic entity. Arch Pathol Lab Med 2014; 138(6): 842–6.
15. *Staffa E, Bernard V, Kubíček L, Vlachovský R, Vlk D, Mornstein V*, et al. Using Noncontact Infrared Thermography for Long-term Monitoring of Foot Temperatures in a Patient with Diabetes Mellitus. Ostomy Wound Manage 2016; 62(4): 54–61.
16. *Greenwald M, Ball J, Guerrettaz K, Paulus H*. Using dermal Temperature to identify rheumatoid arthritis examiners with radiologic progressive disease in less than one minute. Arthritis Care Res 2016; 68(8): 1201–5.
17. *Engebretsen KA, Johansen JD, Kezic S, Linneberg A, Thyssen JP*. The effect of environmental humidity and temperature on skin barrier function and dermatitis. J Eur Acad Dermatol Venereol 2016; 30(2): 223–49.
18. *Jones NF*. Postoperative monitoring of microsurgical free tissue transfers for head and neck reconstruction. Microsurgery 1988; 9(2): 159–64.
19. *Furnas H, Rosen JM*. Monitoring in microvascular surgery. Ann Plast Surg 1991; 26(3): 265–72.
20. *Kozarski J, Pantelić Lj, Novaković M, Pavlica M, Panajotović Lj*. Temperature of the skin in microvascular flaps. Vojnosanit Pregl 1999; 56(5): 483–9. (Serbian)
21. *Kraemer R, Lorenzen J, Knobloch K, Papst S, Kabbani M, Koennecker S*, et al. Free flap microcirculatory monitoring correlates to

free flap temperature assessment. J Plast Reconstr Aesthet Surg 2011; 64(10): 1353–8.
22. *Gazzola R, Cavallini M, Parodi PC, Benanti E, Vaienti L.* Radiometric infrared temperature detection in skin expansion. Plast Reconstr Surg 2012; 130(5): 762e–4e.
23. *Kimura C, Matsuoka M.* Changes in breast skin temperature during the course of breastfeeding. J Hum Lact 2007; 23(1): 60–9.
24. *Ayres B, White J, Hedger W, Scurr J.* Female upper body and breast skin temperature and thermal comfort following exercise. Ergonomics 2013; 56(7): 1194–202.
25. *Wynn TA.* Common and unique mechanisms regulate fibrosis in various fibroproliferative diseases. J Clin Invest 2007; 117(3): 524–9.
26. *Gauldie J.* Pro: inflammatory mechanisms are a minor component of the pathogenesis of idiopathic pulmonary fibrosis. Am J Resp Crit Care Med 2002; 165(9): 1205–6.
27. *Erjefalt JS, Sundler F, Persson CG.* Eosinophils, neutrophils, and venular gaps in the airway mucosa at epithelial removal: Restitution. Am J Resp Crit Care Med 1996; 153(5): 1666–74.
28. *Bringardner BD, Baran CP, Eubank TD, Marsh CB.* The role of inflammation in the pathogenesis of idiopathic pulmonary fibrosis. Antioxid Redox Signal 2008; 10(2): 287–301.
29. *Agostini C, Gurrieri C.* Chemokine/cytokine cocktail in idiopathic pulmonary fibrosis. Proc Am Thorac Soc 2006; 3(4): 357–63.
30. *Iwano M, Plieth D, Danoff TM, Xue C, Okada H, Neilson EG.* Evidence that fibroblasts derive from epithelium during tissue fibrosis. J Clin Invest 2002; 110(3): 341–50.
31. *Ojo-Amaize EA, Lawless OJ, Peter JB.* Elevated concentrations of interleukin-1 beta and interleukin-1 receptor antagonist in plasma of women with silicone breast implants. Clin Diagn Lab Immunol 1996; 3(3): 257–9.
32. *Rohde CH, Taylor EM, Alonso A, Ascherman JA, Hardy KL, Pilla AA.* Pulsed Electromagnetic Fields Reduce Postoperative Interleukin-1β, Pain, and Inflammation: A Double-Blind, Placebo-Controlled Study in TRAM Flap Breast Reconstruction Patients. Plast Reconstr Surg 2015; 135(5): 808–17.

Received on April 10, 2017.
Revised on July 18, 2017.
Accepted on August 17, 2017.
Online First September, 2017.

ORIGINAL ARTICLE

UDC: 612.017:616.24-002.5-036
https://doi.org/10.2298/VSP170519098V

Pulmonary tuberculosis in the immunocompromised patients

Plućna tuberkuloza imunokompromitovanih bolesnika

Danijela Vukosav*, Kristina Tot Veres†

***Institute for Pulmonary Diseases of Vojvodina, Sremska Kamenica, Serbia;**
†Military Medical Center, Novi Sad, Serbia

Abstract

Background/Aim. During the last few decades, immunocompromising diseases led to an increase in the number of tuberculosis cases. The aim of this study was to examine the influence of immunocompromising diseases on the course of tuberculosis. **Methods**. The research included two groups, each consisting of 40 subjects with tuberculosis, who were treated at the Institute for Pulmonary Diseases of Vojvodina during 2010 and 2011. The first group had no immunocompromising diseases (the kontrol group), whereas the second group contained patients with accompanying immunocompromising diseases. The data from the patients' medical history, from the Center for Microbiology and from the Radiology Center were used. The two groups were compared according to the following characteristics: age, sex, bacteriological status, radiological presence of the disease, presence of adverse effects of drugs, presence of resistance to drugs, duration of the therapy regimen and the duration of hospitalization. **Results**. The group of immunocompromised patients was older in average than the control group and included a higher percentage of males. The immunocompromised group had statistically important longer average time required for the sputum smear conversion ($p = 0.000$) and for the conversion of sputum cultures to *M. tuberculosis* ($p = 0.010$), more frequent presence of cavity ($p = 0.030$), longer average therapy regimen duration ($p = 0.000$) and higher average number of hospital days ($p = 0.000$) compared to the control group. The most frequent localization of changes in the immunocompromised patients was in all lobes of both lungs (32.5%) whereas the changes in the control group were mostly localized in the upper lung lobes (62.5%). There was no statistically important difference in the finding of sputum smear positive acid-fast bacilli on direct micoscropy, the presence of adverse effects of drugs and *M. tuberculosis* resistance to drugs between the two groups of patients. **Conclusion**. The immunocompromising diseases change the course of tuberculosis, primarily by affecting bacteriological status, radiological presentation, the length of therapy regimen and the duration of hospitalization.

Key words:
tuberculosis; immunocompromised host; prognosis.

Apstrakt

Uvod/Cilj. Imunokompromitujuće bolesti su tokom poslednjih decenija dovele do porasta broja obolelih od tuberkuloze. Cilj rada je bio da se ispita uticaj imunokompromitujućih bolesti na tok tuberkuloze. **Metode**. Ispitivanjem su obuhvaćene dve grupe od po 40 bolesnika obolelih od tuberkuloze koji su lečeni u Institutu za plućne bolesti Vojvodine tokom 2010. i 2011. godine. Prva grupa nije imala imunokompromitujuće bolesti (kontrolna grupa), dok su u drugoj grupi bili bolesnici sa pridruženim imunokompromitujućim bolestima. Korišćeni su podaci iz istorija bolesti, podaci Centra za mikrobiologiju i Centra za radiologiju. Dve grupe su poređene prema sledećim karakteristikama: starost, pol, bakteriološki status, radiološki nalaz, prisustvo neželjenih efekata lekova, prisustvo rezistencije *M. tuberculosis* na lekove, trajanje terapijskog režima i dužina hospitalizacije. **Rezultati**. Grupa imunokompromitovanih bolesnika je bila starija od kontrolne grupe i sa većom zastupljenošću muškog pola. Grupa imunokompromitovanih je imala statistički značajno duže prosečno vreme potrebno za direktnu konverziju sputuma ($p = 0,000$) i konverziju kultura sputuma na *M. tuberculosis* ($p = 0,010$), značajno češće prisustvo kaverne ($p = 0,030$), prosečno duže trajanje terapijskog režima ($p = 0,000$) i prosečno veći broj bolničkih dana ($p = 0,000$) u odnosu na kontrolnu grupu. Najčešća lokalizacija promena kod imunokompromitovanih je bila u svim režnjevima oba plućna krila (32,5%) dok su u kontrolnoj grupi promene bile najčešće lokalizovane u gornjim plućnim režnjevima (62,5%). Nije bilo statistički značajne razlike u nalazu mikobakterija u sputumu direktnom mikroskopijom, prisustvu neželjenih efekata lekova i prisustvu rezistencije na lekove između dve grupe bolesnika. **Zaključak**. Imunokompromitujuće bolesti menjaju tok tuberkuloze, prvenstveno utičući na bakteriološki status, radiološku prezentaciju, dužinu terapijskog režima i dužinu hospitalizacije.

Ključne reči:
tuberkuloza; imunokompromitovan domaćin; prognoza.

Correspondence to: Danijela Vukosav, Filipa Višnjića 1, 21 000 Novi Sad, Serbia. E-mail: duledacans@gmail.com

Introduction

After human immunodeficiency virus (HIV) infection, tuberculosis is the second most frequent cause of death among infectious diseases in the world. Annually, 8–10 million people are infected, and around 2 million people die [1]. One person with active tuberculosis infects 10–15 individuals per year. It is believed that one third of the entire human population is infected with *Mycobacterium tuberculosis* (*M. tuberculosis*) [2]. The epidemiological situation of tuberculosis has changed during recent years, primarily due to an increasing number of patients with immunocompromising diseases (the patients with transplanted organs, patients undergoing immunosuppressive therapy, people infected with HIV, people suffering from malignant diseases, diabetes mellitus, liver cirrhosis, renal insufficiency, alcoholism) that change the course of tuberculosis infection [3, 4]. An increase in the number of these patients can be expected in the future [5].

Aquired cell mediated immunodeficiency is the most common kind of immunodeficiency and it is very important in pathogenesis of tuberculous infection. The patients who have impared cell mediated immunity are predominantly susceptible to infections caused by intracellular microorganisms including *M. tuberculosis* inside alveolar macrophages [3].

Individuals suffering from immunocompromising diseases with latent tuberculosis infection (LTBI) have an increased risk of developing active tuberculosis.

LTBI is a complex clinical condition where the exact biological status of *M. tuberculosis* is not sufficiently known. It is believed that during LTBI the bacteria persist in a subclinical state with minimum replication, and, therefore, do not cause a clinically manifested disease. It is believed that 5%–10% of individuals with LTBI have a risk of developing active tuberculosis. The greatest risk of LTBI developing into active tuberculosis occurs in the first two years when a half of the infected individuals become ill. The tuberculin test and the more recent interferon-gamma release assays (IGRA) tests are used for LTBI screening. The limitation of the tuberculin test is based on the fact that the test is a mixture of different antigens that are not specific for *M. tuberculosis*. Therefore, it cannot be determined whether the positive result comes from the response to the Bacillus Calmette-Guerin (BCG) vaccine *M. bovis*, *M. tuberculosis*, or non-tuberculosis *mycobacteria*. Unlike the tuberculin test, the IGRA test detects the presence of cellular immune response to antigens specific to *M. tuberculosis* so that the results of this test do not depend on the previous BCG vaccination or non-tuberculosis *mycobacteria* infection. Therefore, the application of IGRA tests has an advantage in the BCG vaccinated population [6]. In the immunocompromised individuals, the IGRA tests do not distinguish between latent or active tuberculosis. They play a role within the entire risk assessment for LTBI which entails insight into the epidemiological data, risk factors, radiogram, and tuberculin test. Following this assessment, if a patient is determined to be in a risk of developing active tuberculosis, chemoprophylaxis is administered [1]. The aim of this study is to point out the influence of immunocompromising diseases on the course of tuberculosis.

The HIV infected patients have dominantly impared cell immunity with lower number of CD4+ lymphocites. If these patients suffer from latent tuberculosis infection, they have 20–30 times higher risk to develop active tuberculosis then the immunocompetent persons. The HIV positive patients exhibit more frequent occurrences of disseminated and extrapulmonary forms of tuberculosis, more frequent occurrence of sputum smear negative pulmonary disease, and an atypical radiological presentation of changes in the patients with CD4+ lymphocyte number lower than 200 cells/uL. The adverse effects of drugs are also more frequent. Hepatotoxicity is connected to the overlapping of adverse effects of antituberculotics, antiretroviral therapy, antibiotics and antimycotics that are used simultaneously [7, 8]. It should be noted that rifampicin affects the metabolism of protease inhibitors by inducing cytochrome P450 enzyme system in the liver [7].

The patients with liver cirrhosis have increased risk to develop tuberculous infection due to the multifactorial process, dominantly reticuloendothelial system dysfunction. These patients more frequently exhibit extrapulmonary forms of tuberculosis with predominant peritoneal localization of the disease. The tuberculosis treatment regimen must be modified in accordance with the level of damage to the liver functions. Considering that the basal function of the liver is often disturbed, the most common adverse effect during the treatment is hepatotoxicity. Three out of four of the first-line antituberculotics are potentially hepatotoxic. Pyrazinamide is considered to be the most frequent cause of hepatotoxicity, followed by isoniazid, and thirdly by rifampicin. According to the recommendation of the World Health Organization (WHO), the larger extent of damage to the liver function, the smaller number of the hepatotoxic drugs can be used [9].

The patients with chronic renal failure have 10–15 times higher incidence of tuberculosis mostly due to impaired cellular immunity [10]. In those patients, tuberculosis is usually diagnosed later on, because of unspecific clinical signs and due to 50% more frequent occurrence of extrapulmonary form of the disease, especially with peritoneal localization. Mortality rate in the patients on hemodialysis who develop tuberculosis is two times higher compared to the patients without tuberculosis. The tuberculosis treatment regimes usually last six or nine months. Duration of treatment is individual reflecting the different clinical circumstances, immunosuppression level, or the spread of disease. Usually, the standard doses of antituberculotics are used and they are administered daily or in an intermittent therapy regimen, depending on the drug metabolism and creatinine clearance. Hemodialysis eliminates most of the antituberculotics, therefore they are administered after hemodialysis. The adverse drug effects are observed in a majority of cases, the most common being neurotoxicity, hepatotoxicity, and optic neuropathy [10, 11].

Systemic diseases are connected with the increased risk of tuberculosis infection. It remains unknown whether that risk is linked only to the use of immunosuppressive therapy or to the immunologic disease itself as well. The cases of ac-

tive tuberculosis were reported in the patients who used corticosteroid therapy in doses of 15–20 mg of prednisone or equivalent for a month or longer [12]. The cases of active tuberculosis following the usage of methotrexate and cyclophosphamide were also reported [13]. Recently, a biological therapy has been successfully applied in rheumatoid arthritis which entails the use of tumor necrosis alpha (TNF-alpha) inhibitors. TNF-alpha is an important proinflammatory cytokine which plays an important role in the tuberculosis granuloma formation. There is an increasing amount of data that suggests that the use of these drugs is linked to the risk of developing active tuberculosis [14, 15].

In the patients with malignancies, the increased risk of developing tuberculosis occurs due to the drop in immunity conditioned by the local or systemic effect of the tumor mass itself, or as a consequence of chemo- and radiotherapy [16].

The patients with transplanted organs require the application of immunosuppressive therapy with the aim of preventing the rejection of organs which significantly increases the risk of active tuberculosis [3, 4, 11].

Alcohol is the most commonly abused substance throughout numerous countries [17]. The chronic alchocolics have impaired the neutrophils function and the impaired alveolar macrophage phagocytosis and superoxide production. T cells of the alchoholics show the impiared delayed type hypersensitivity responses. It has been proven that individuals who use more than 40 g of alcohol per day are three times more likely to develop active tuberculosis [17–20].

Diabetes mellitus is predisposing factor for developing tuberculous infection. The frequency of tuberculosis is four times higher in diabetics then in nondiabetics [21]. The diabetic patients show the neutrophil and macrophage disfunctions which includes: impared chemotaxis, adherence, phagocytosis and ability to kill the phagocyted microorganisms. These patients show alternations in the T lymphocyte subsets. Tuberculosis incidence among the diabetics increases proportionally with the duration of the diabetes and the increase of insulin doses required for glucoregulation [22, 23]. If diabetes is well-regulated, the course of tuberculosis and the response to the antituberculotics therapy shows no significant difference compared to the individuals without diabetes, whereas poorly-regulated diabetes has a negative impact on the course of pulmonary tuberculosis [24].

Methods

The research included two groups, each consisting of 40 subjects with recently diagnosed pulmonary tuberculosis who were treated at the Institute for Pulmonary Diseases of Vojvodina during 2010 and 2011. The first group consisted of patients with pulmonary tuberculosis without accompanying immunocompromising diseases whereas the other group contained the patients with pulmonary tuberculosis with accompanying immunocompromising diseases, including: diabetes mellitus (27 patients), use of alchohol (9 patients), liver cirrhosis (2 patients) and malignancy (2 patients). The HIV positive patients were not included in the examined sample. The patients were analyzed and the two groups were compared according to the following characteristics: age, sex, bacteriological status, radiological presentation of the disease, presence of adverse effects of drugs, presence of resistance to antituberculotics, duration of the therapy regimen in months and the duration of hospitalization. The data from the patients' medical history, from the Center for Microbiology and from the Radiology Center of the Institute for Pulmonary Diseases of Vojvodina were used.

The collected data were analyzed on the level of descriptive statistics by the measures of central tendency (arithmetic mean) and measures of variability (standard deviation), as well as on the level of percentage representation of certain variable categories. On the level of inferential statistics, the significance of the research hypotheses was tested by using the χ^2 test and the Student's *t*-test. The statistical data were processed by using the statistical program package SPSS 16.0.

Results

As seen in Table 1, the group of patients suffering from tuberculosis with accompanying immunocompromising diseases was older in average than the group of subjects suffering from tuberculosis, but without accompanying immunocompromising diseases. While the group of patients with tuberculosis without accompanying immunocompromising disease had slightly more women (52.5%), the group of tuberculosis patients with accompanying immunocompromising diseases had significantly more male patients (77.5%). In the group of patients with accompanying immunocompromising conditions, diabetes mellitus was the most common, followed by the use of alcohol. The number of patients with liver cirrhosis and malignancies was significantly smaller (Table 1).

By analyzing the frequency of presence or absence of finding sputum smear positive acid-fast bacilli on direct microscopy between the tested groups of subjects, no statistically significant difference was found (χ^2 = 0.457; p = 0.499). By using the *t*-test, a statistically significant difference was determined between the average length of time required for the sputum smear conversion (t = -7.532; p = 0.000) and the average length of time required for the sputum culture conversion (t = -6.403; p = 0.010) between the two groups of patients. In both cases, the group of patients with immunocompromising diseases had longer average time required for the sputum conversion to *M. tuberculosis* (Table 2).

By analyzing the frequency of presence or absence of cavities, a statistically significant difference could be noted between the groups, where a significantly higher number of patients with cavities was observed among the patients with tuberculosis and accompanying immunocompromising diseases (χ^2= 4.713; p = 0.030). A statistically im significant portant difference between the two groups of patients was also present in relation the affected area of the lung lobes. In the group of patients without accompanying immunocompromising diseases, only the upper lobe was affected in the majority of patients; on the other hand, in the group of patients with immunocompromising diseases, all lobes of both lungs were affected in the majority of patients (χ^2= 16.358; p = 0.006) (Table 3).

Table 1

Distribution of patients according to age, sex, and accompanying immunocompromising diseases

Sample description	Tuberculosis without accompanying diseases (n = 40)	Tuberculosis with accompanying diseases (n = 40)
Age (years), mean ± SD (range)	51.87 ± 18.83 (19–84)	61.55 ± 12.13 (25–83)
Sex, n (%)		
males	19 (47.5)	31 (77.5)
females	21 (52.5)	9 (22.5)
Immunocompromising conditions, n (%)		
diabetes mellitus		27 (67.5)
alcohol abuse		9 (22.5)
liver cirrhosis		2 (5.0)
malignancy		2 (5.0)

SD – standard deviation.

Table 2

Mycobacteriological status of the patients

Parameter	Patients without accompanying diseases (n = 40)	Patients with accompanying diseases (n = 40)
Sputum smear positive, n (%)		
no	6 (15.0)	4 (10.0)
yes	34 (85.0)	36 (90.0)
Time required for sputum smear conversion (days), mean ± SD	20.91 ± 6.70	40.64 ± 13.80
Time required for the *M. tuberculosis* culture conversion (days), mean ± SD	32.37 ± 8.12	47.67 ± 12.74

SD – standard deviation.

Table 3

Radiological presentation of pulmonary tuberculosis

Parameter	Tuberculosis without accompanying diseases (n = 40)	Tuberculosis with accompanying diseases (n = 40)
Cavity, n (%)		
no	17 (42.5)	8 (20.0)
yes	23 (57.5)	32 (80.0)
Affected lobes, n (%)		
only upper	25 (62.5)	8 (20.0)
only middle	1 (2.5)	1 (2.5)
upper and middle	6 (15.0)	12 (30.0)
lower and middle	1 (2.5)	4 (10.0)
lower and upper	0 (0.0)	2 (5.0)
all lobes of both lung	7 (17.5)	13 (32.5)

Table 4

Drug susceptibility, adverse drug reactions and length of tuberculosis treatment

Parameter	Tuberculosis without accompanying diseases (n = 40)	Tuberculosis with accompanying diseases (n = 40)
Resistance to drugs, n (%)		
no	40 (100.0)	38 (95.0)
yes	0 (0.0)	2 (5.0)
Adverse drug effects, n (%)		
no	28 (70.0)	29 (72.5)
yes	12 (30.0)	11 (27.5)
Length of hospitalization (days), mean ± SD	38.98 ± 11.44	58.00 ± 17.03
Length of treatment (month), mean ± SD	6.25 ± 0.67	6.75 ± 0.98

SD – standard deviation.

Between the examined groups, no statistically significant difference was recorded in the frequency of presence of adverse effects of drugs (χ^2= 0.061; p = 0.805) as well as in resistance to drugs (χ^2= 2.051; p = 0.152). In both groups, a significantly higher number of patients did not have the adverse effects of antituberculosis drugs, nor resistance to the drugs. In the group of patients with accompanying immunocompromising diseases, there were two patients with drug resistant tuberculosis. In the first case it was monoresistance to isoniazid, and in the second case polyresistance to isoniazid and streptomycin. By using the *t*-test, a statistically significant difference between the two groups was determined in terms of the average length of hospitalization (t = -5.864; p = 0.000) where the group of patients with accompanying

immunocompromising diseases exhibited longer hospitalization time compared to the group without accompanying immunocompromising diseases. A statistically important difference between the two groups of patients was also determined in terms of the average length of treatment expressed in months (t = -2.663; p = 0.000). In this case as well, the group of patients with accompanying immunocompromising diseases exhibited longer average length of treatment (Table 4).

Discussion

The group of tuberculosis patients with accompanying immunocompromising diseases in this study was mostly comprised of diabetics (67.5%) and a significantly lower number of patients who abuse alcohol (22.5%), the patients with liver cirrhosis and patients with malignancies (5% in both cases). A majority of published results refer to the course of tuberculosis in diabetics and the HIV positive individuals (the latter were not included in the examined sample), while considerably less data can be found on the influence of other immunocompromising conditions on the course of tuberculosis [25]. For this reason, the obtained results were mostly compared to the results of the authors who researched the influence of diabetes on the course of tuberculosis infection.

The results of this study showed that the group of patients with accompanying immunocompromising diseases was older in average and consisted of a substantially higher percentage of males than the control group. These results coincide with the results of other authors. In a study conducted by Perez-Guzman et al. [26], the group of tuberculosis patients with diabetes was older in age than the group of patients with tuberculosis in the control group. A study done by Singla et al. [27] also showed that the group of tuberculosis patients with accompanying diabetes was considerably older with a higher percentage of males. The individuals who abused alcohol were exclusively males which coincides with the results of other authors. This was probably conditioned by some social prejudices towards female alcoholics because of which women are less likely to admit that they have an alcohol abuse problem[18].

In terms of bacteriological status, the results of this study pointed to a slightly higher frequency of sputum smear findings on direct microscopy and statistically significantly longer time required for the sputum smear conversion and the conversion of sputum cultures to *M. tuberculosis* in the group of patients with immunocompromising diseases. The acquired results were probably linked to the higher frequency of cavity occurrence in this group of patients (although results of some studies are opposite, denying the role of cavities on sputum positivity). In studies that were conducted earlier, different results were reached in terms of the bacteriological status of patients. Yurteri et al. [21] proved that there was a lower number of patients with positive sputum smear among diabetics. In their study, Jabbar et al. [28] reached a different result that showed a higher number of patients with positive sputum smear among diabetics, and a longer time required for the conversion of *M. tuberculosis* sputum cultures. Singla et al. [27] also proved that diabetics require longer time for the conversion of sputum cultures to *M. tuberculosis*. In a study conducted in North Carolina, Fiske et al. [29] proved that there was a higher frequency of patients with positive sputum smear among the individuals who used alcohol excessively.

In terms of radiological presentation of pulmonary changes, this study proved that there was a statistically significant higher occurrence of cavities and atypical radiological presentation of pulmonary tuberculosis in the group of patients with immunocompromising diseases. These results were in concordance with the results of certain authors. Yurteri et al. [21], Perez-Guzman et al. [26] and Singla et al. [27] published that the occurrence of cavities was significantly higher among diabetics. On the other hand, in a study conducted by Jabbar et al. [28] a more rare occurrence of cavities among diabetics was proven. Bacakoglu et al. [30] proved that there was no difference in the frequency of cavity occurrence between the diabetics and individuals without diabetes. In their study, Kiyan et al. [25] reached results that showed no significant difference in the frequency of cavity occurrence between the immunocompromised individuals (who are not HIV positive) and immunocompetent individuals, whereas Fiske et al. [29] proved that there was a higher frequency of cavity occurrence among the alcoholics. Perez-Guzman et al. [26], Jabbar et al. [28] and Singla et al. [27] published results showing that the majority of diabetics had radiological changes in lower lobes. On the other hand Yurteri et al. [21] published that the atypical radiological presentation of tuberculosis was present only in a minor number of patients with tuberculosis and accompanying diabetes.

This study found no statistically important difference in the presence of adverse antituberculotics effects between the two groups of patients. The percentage of patients who showed the adverse effects in both groups matched the results of other authors [31]. In a study conducted by Kumar et al. [9], the patients with liver cirrhosis demonstrated hepatotoxicity in 17% of the cases, but there was no statistically important difference compared to the patients without liver cirrhosis.

This study found no statistically important difference in the presence of resistance to antituberculotics between the two groups of patients. The obtained result was in accordance with the fact that the examination included newly-diagnosed tuberculosis cases and that the therapy regimen of the majority of patients were not interrupted due to the demonstrated adverse effects of antituberculotics. Furthermore, the examination did not include the patients with multiresistant tuberculosis. According to this facts, two patients who had drug resistant tuberculosis probably were initially infected with drug-resistant strains of *M. tuberculosis* (transmitted or primary drug resistant tuberculosis) [32]. The results of other authors differ to a great extent among themselves. Bashar et al. [33] proved a significantly more frequent occurrence of multiresistant tuberculosis among diabetics. Contrary to their results, Yurteri et al. [21] found multiresistant tuberculosis in few diabetics only. Singla et al. [27] proved the resistance to antituberculotics was significantly rarer among diabetics, while there was no significant difference in the oc-

currence of multiresistant tuberculosis between the two groups of patients.

This study proved that a statistically significant longer therapy time was required in the group of immunocompromised patients which coincided with the results of certain authors [23, 24]. The result is probably a consequence of the longer time required for the sputum smear conversion and the conversion of sputum cultures to *M. tuberculosis*, and the slower radiological regression in immunocompromised patients as well. Results published by Singla et al. [27] confirmed that diabetes did not affect the duration of therapy regimen, while other authors published opposite results.

This study proved that the group of immunocompromised patients had a statistically significant higher average number of hospital days. This result is linked to more frequent cavity presence and longer time required for the sputum smear conversion and the conversion of sputum cultures to *M. tuberculosis* [26, 28].

Conclusion

Immunocompromising diseases affect the course of pulmonary tuberculosis. This primarily refers to the bacteriological status (meaning longer time required for the sputum smear conversion and the conversion of sputum cultures to *M. tuberculosis*), radiological presentation of the disease (more frequent cavity occurrence and atypical localization of changes), duration of the therapy regimen (longer duration in the immunocompromised patients), and the duration of hospitalization (the immunocompromised patients have more hospital days). There is no significant difference between the two groups in exhibiting the adverse effects of antituberculotics and exhibiting the resistance to antituberculotics.

The results of this study may be useful during diagnostics and treatment of tuberculous patients with accompanying immunocompromising diseases.

R E F E R E N C E S

1. *Hauck FR, Neese BH, Panchal AS, El-Amin W.* Identification and management of latent tuberculosis infection. Am Fam Physician 2009; 79(10): 879–86.
2. *Butt G, Altaf F, Hussain I.* Pulmonary tuberculosis in dermatological patients on high-dose, long-term steroid therapy. J Pak Assoc Derma 2015; 15(2): 119–31.
3. *Oh YW, Effmann EL, Godwin JD.* Pulmonary infections in immunocompromised hosts: The importance of correlating the conventional radiologic appearance with the clinical setting. Radiology 2000; 217(3): 647–56.
4. *Okafor UH.* Pattern of clinical presentations in immunocompromised patient. In: *Metodiev K*, Immunodeficiency. Rijeka, Croaia: In Tech; 2012.
5. *Grbac I, Smolčić S, Jurman D, Broz S.* Clinical picture of pulmonary tuberculosis at the end of the second millennium. Acta Clin Croat 2000; 39: 175–9.
6. *Euroean Centre for Disease Prevention and Control.* Use of interferon-gamma release assays in support of TB diagnosis. Stockholm: ECDC; 2011.
7. *Gooze L, Daley CL.* Tuberculosis and HIV: HIV in Site Knowledge Base Chapter. San Francisco: University of California; 2013.
8. *Kisembo HN, Boon DS, Davis JL, Okello R, Worodria W, Cattamanchi A*, et al. Chest radiographic findings of pulmonary tuberculosis in severely immunocompromised patients with the human immunodeficiency virus. Br J Radiol 2012; 85(1014): e130–9.
9. *Kumar N, Kedarisetty CK, Kumar S, Khillan V, Sarin SK.* Antitubercular therapy in patients with cirrhosis: challenges and options. World J Gastroenterol 2014; 20(19): 5760–72.
10. *Mimi N, Medregoniu D, Olteanu M, Golli A, Olteanu M, Maceseanu A,* et al. Tuberculosis and chronic renal failure; therapy patterns. Curr Health Sci J 2011; 37(2): 106–8.
11. *Malhotra KK.* Treatment of tuberculosis in chronic renal failure, maintenance dialysis and renal transplant. Indian J Nephrol 2003; 13: 69–71.
12. *Gardam M, Iverson K.* Rheumatoid arthritis and tuberculosis: time to take notice. J Rheumatol 2003; 30(7): 1397–9.
13. *Miras MD, Tenorio CH, Alonso JJ.* Tuberculosis in patients with Systemic Lupus Erythematosus: Spain's situation. Reumatol Clin 2013; 9(6): 369–72.
14. *Borekci S, Atahan E, Demir YD, Mazıcan N, Duman B, Ozguler Y*, et al. Factors affecting the tuberculosis risk in patients receiving anti-tumor necrosis factor-α treatment. Respiration 2015; 90(3): 191–8.
15. *Silva DG, Silva BD, Junqueira-Kipnis AP, Rabahi MF.* Tuberculosis in rheumatoid arthritis patients: The difficulty in making the diagnosis of latent infection. J Bras Pneumol 2010; 36(2): 243–51. (Portuguese)
16. *Karnak D, Kayacan O, Beder S.* Reactivation of pulmonary tuberculosis in malignancy. Tumori 2002; 88(3): 251–4.
17. *Happel KI, Nelson S.* Alcohol, immunosuppression, and the lung. Proc Am Thorac Soc 2005; 2(5): 428–32.
18. *Suhadev M, Thomas BE, Murugesan P, Chandrasekaran V, Charles N, Durga R,* et al. Alcohol use disorders(AUD) among tuberculosis Patients: A study from Chennai, South India. PLoS ONE 2011; 6(5): e19485.
19. *Lönorth K, Williams BG, Stadlin S, Jaramillo E, Dye C.* Alchocol use as risk factor for tuberculosis-a systematic review. BMC Public Health 2008; 8: 289.
20. *Vasantha R, Sridevi S, Sudhakar G.* Association between smoking, alcoholism and pulmonary tuberculosis. Int J Sci Res 2015; 4(6): 516–8.
21. *Yurteri G, Sarac S, Dalkilic O, Ofluoglu H, Demiröz OF.* Features of pulmonary tuberculosis in patients with diabetes mellitus: A comparative study. Ch Hop Yst Turk 2004; 1: 5–8.
22. *Golubović S, Đorđević I, Radović M, Pejović G, Stanković I.* Importance of early diagnosis of low respiratory tract infections in patients with diabetes mellitus. Acta Fac Med Naiss 2005; 22(3): 139–44.
23. *Guptan A, Shah A.* Tuberculosis and diabetes: An appraisal. Ind J Tub 2000; 47(1): 3–8.
24. *Ljubić S, Balachandran A, Pavlić-Renar I, Barda A, Metelko Ž.* Pulmonary infections in diabetes mellitus. Diabetolpgia Croat 2004; 33(4): 115–24.
25. *Kiyan E, Kilicaslan Z, Gurgan M, Tunaci A, Yildiz A.* Clinical and radiographic features of pulmonary tuberculosis in non-AIDS immunocompromised patients. Int J Tuberc Lung Dis 2003; 7(8): 764–70.
26. *Perez-Guzman C, Torres-Cruz A, Villarreal-Velarde H, Vargas MH.* Progressive age-related changes in pulmonary tuberculosis images and the effect of diabetes. Am J Respir Crit Care Med 2000; 162(5): 1738–40.

27. *Singla R, Khan N, Al-Sharif N, Ai-Sayegh MO, Shaikh MA, Osman MM.* Influence of diabetes on manifestations and treatment outcome of pulmonary TB patients. Int J Tuberc Lung Dis 2006; 10(1): 74–9.
28. *Jabbar A, Hussain SF, Khan AA.* Clinical characteristics of pulmonary tuberculosis in adult Pakistani patients with co-existing diabetes mellitus. East Mediterr Health J 2006; 12(5): 522–7.
29. *Fiske CT, Hamilton CD, Stout JE.* Alchocol use and clinical manifestations of tuberculosis. J Infect 2009; 58(5): 395–401.
30. *Bacakoğlu F, Başoğlu OK, Cok G, Sayiner A, Ateş M.* Pulmonary tuberculosis in patients with diabetes mellitus. Respiration 2001; 68(6): 595–600.
31. Arbex MA, Varella Mde C, Siqueira HR, Mello FA. Antituberculosis drugs: drug interactions, adverse effects, and use in special situations. Part 1: first-line drugs. J Bras Pneumol 2010; 36(5): 626–40. (English, Portuguese)
32. *Kanabus A*Information about Tuberculosis: TB Statistics-Global, Regional and High Burden. Global Health Education (GHE); 2016. Available from: www.tbfacts.org.
33. *Bashar M, Alcabes P, Rom WN, Condos R.* Increased incidence of multidrug-resistant tuberculosis in diabetic patients on the Bellevue Chest Service, 1987 to 1997. Chest 2001; 120(5): 1514–9.

Received on May 19, 2017.
Revised on July 12, 2017.
Accepted on September 11, 2017.
Online First September, 2017.

SHORT COMMUNICATION

UDC: 616.9:616.36-08
https://doi.org/10.2298/VSP170727186S

Real-life data on the efficacy and safety of ombitasvir/paritaprevir/ /ritonavir + dasabuvir + ribavirin in the patients with genotype 1 chronic hepatitis C virus infection in Serbia

Podaci iz realnog života o efikasnosti i bezbednosti ombitasvir/ /paritaprevir/ritonavir + dasabuvir + ribavirin režima kod bolesnika sa genop 1 hepas C virusnom infekcijom u Srbiji

Jasmina Simonović Babić*†, Ksenija Bojović*†, Milotka Fabri‡§, Tatjana Cvejić‖, Petar Svorcan¶, Darko Nožić††, Maja Jovanović‡‡§§, Ranko Škrbić‖‖, Miloš P. Stojiljković‖‖, Željko Mijailović¶*****

University of Belgrade, *Faculty of Medicine, Belgrade, Serbia; Clinical Centre of Serbia, †Clinic for Infectious and Tropical Diseases, ‖Clinic for Gastroenterology, Belgrade, Serbia; University of Novi Sad, ‡Faculty of Medicine, Novi Sad, Serbia; Clinical Centre of Vojvodina, §Clinic for Infectious Diseases, Novi Sad, Serbia; Clinical Hospital Centre "Zvezdara", ¶Department of Hepatology and Gastroenterology, Belgrade, Serbia; Military Medical Academy, **Clinic for Infectious Diseases, Belgrade, Serbia; University of Defence, ††Faculty of Medicine, Belgrade, Serbia; University of Niš, ‡‡Faculty of Medicine, Niš, Serbia; Clinical Centre of Niš, §§Clinic for Infectious Diseases, Niš, Serbia; University of Banja Luka, Faculty of Medicine, ‖‖Department of Pharmacology, Toxicology and Clinical Pharmacology, Banja Luka, Republic of Srpska, Bosnia and Herzegovina; University of Kragujevac, ¶¶Faculty of Medical Sciences, Kragujevac, Serbia; Clinical Centre of Kragujevac, ***Clinic for Infectious Diseases, Kragujevac, Serbia

Abstract

Background/Aim. The era of direct-acting antiviral (DAA) regimen in the treatment of chronic hepatitis C virus (HCV) started in 2011. The aim of this study was to assess the antiviral efficacy and safety of DAA regimen, ombitasvir (OBV)/paritaprevir (PTV)/ritonavir (r) + dasabuvir (DSV) + ribavirin (RBV), in patients with chronic HCV infection, genotype 1. **Methods.** The real-life data were collected. The study was multicentric and included seven infectious diseases and hepatology departments in Serbia. A total of 21 patients were enrolled in the OBV/PTV/r + DSV + RBV early access program, 20 of which were previously treated with pegylated interferon + RBV, while 1 was treatment-naive. All patients received the adequate doses of these antiviral drugs. RBV was not given to the patients with HCV genotype 1b infection according to the therapeutic protocol. For the majority of patient, the treatment duration lasted for 12 weeks. For the patients with liver cirrhosis, who were infected with HCV genotype 1a, the duration of treatment was 24 weeks. Viremia was assessed at four points in time: at baseline, 4 weeks after the treatment beginning (rapid viral response, RVR), 12 or 24 weeks after the treatment beginning (end of treatment response – ETR) and 12 weeks after the end of treatment (sustained viral response – SVR). SVR, as a confirmation of the absence of HCV was considered as endpoint of successful treatment. **Results.** Complete RVR, ETR and SVR were achieved in 64.71%, 85.71% and 95.24% of the patients, respectively. Only 3 patients had mild adverse effects which did not required dose reduction. **Conclusion.** The treatment of the patients with a chronic HCV infection with OBV/PTV/r + DSV + RBV resulted in excellent antiviral activity and tolerability.

Key words:
antiviral agents; drug therapy, combination; hepatitis c, chronic; ritonavir; sulfonamides.

Apstrakt

Uvod/Cilj. Era direktno delujućeg antivirusnog (DAA) režima lečenja bolesnika sa hroničnom hepatitis C virusnom (HCV) infekcijom započela je 2011. godine. Cilj rada bio je ispitivanje efikasnosti i bezbednosti DAA režima ombitasvir (OBV)/paritaprevir (PTV)/ritonavir (r) + dasabuvir (DSV) + ribavirin (RBV), kod bolesnika sa genotip 1 HCV infekci-

Correspondence to: Jasmina Simonović Babić, Clinical Center of Serbia, Clinic for Infectious and Tropical Diseases, Bul. Oslobođenja 16, 11 000 Belgrade, Serbia. E-mail: jasimba@gmail.com

jom u Srbiji. **Metode.** U multicentričnu studiju je bilo uključeno sedam centara u Srbiji. Prikupljeni su podaci iz realnog života. U rani pristupni program OBV/PTV/r + DSV + RBV bio je uključen 21 bolesnik od kojih jedan nije prethodno lečen, dok je ostalih 20 prethodno lečeno pegilovanim interferonom i RBV. Svi bolesnici su dobijali odgovarajuće doze lekova. Bolesnici sa HCV genotipom 1b nisu dobijali RBV u skladu sa terapijskim protokolom. Za većinu bolesnika trajanje terapije je iznosilo 12 nedelja. Za četvoro bolesnika sa cirozom i HCV genotipom 1a trajanje terapije je iznosilo 24 nedelje. Viremija je određivana četiri puta: pre početka terapije, 4 nedelje posle početka terapije (rapidni virusološko odgovor – RVR), 12 ili 24 nedelje nakon početka terapije (kraj terapije – ETR) i 12 nedelja nakon završetka terapije (stabilan virusološki odgovor – SVR). Postignut SVR kao potvrda odsustva virusne RNK u serumu, smatran je završnicom uspešnog lečenja. **Rezultati.** Kompletan RVR, ETR i SVR postignut je kod 64,71%, 85,71%, i 95,24% bolesnika sukcesivno. Samo 3 bolesnika imali su blage neželjene efekte koji nisu zahtevali korekciju doze lekova. **Zaključak.** Lečenje bolesnika sa hroničnom HCV infekcijom sa OBV/PTV/r + DSV + RBV pokazalo je odličnu antivirusnu aktivnost i podnošljivost.

Ključne reči:
antivirotici; lečenje, kombinovano; hepatitis c, hronični; ritonavir; sulfonamidi.

Introduction

Hepatitis C virus (HCV) was identified as one of the non-A-non-B hepatitis virus in 1989 [1]. It was estimated that it causes a chronic viral hepatitis in circa 71 million people throughout the world [2]. This disease that emulates the epidemiology of HIV/AIDS is also a risk factor in the development of hepatic cancer, since up to a third of the patients with chronic hepatitis C infection develop liver cirrhosis [3]. The prevalence of hepatitis C infection is highest in the Eastern Mediterranean basin (2.3%) and in Europe (1.5%), while in the rest of the world it amounts 0.5%–1% [4]. Some local data from the Balkans give an estimated prevalence of only 0.25% [5] and a relatively recent study in Serbia reports a seroprevalence of 0.19% among blood donors [6] and 1.13% in the general population [7]. Incidence of hepatitis C infections is 1.75 million, or 23.7 new infections per 100,000 people [4]. A total of seven HCV genotypes have been identified so far, with genotypes 1 and 3 responsible for 46.2% and 30% of all HCV infections, respectively. Genotype 4 is most prevalent in Africa and Middle East, where it can account for as much as 90% of all cases, such as in Egypt [8]. HCV genotype 1b is the most prevalent one in Serbia [6].

After the introduction of recombinant interferons (rIFN) in 1991 and pegylated interferons (PEG-IFN) in 2001, the combination of the latters with ribavirin (RBV) became a standard treatment, with the sustained viral response (SVR) of 44%–51% for genotype 1 and 70% for genotypes 2 and 3. Indeed, in a recent Serbian study this combination assured a total SVR of 70.5% [9]. Unfortunatelly, this combination is still the standard of care in Serbia. The era of direct-acting antivirals (DAAs) in the treatment of HCV started in 2011, when telaprevir (TVR) and boceprevir (BOC), as the first generation, were approved [1]. Our own study with BOC + PEG-IFN + RBV in the genotype 1-infected chronic HVC patients with advanced fibrosis assured the overall SVR of only 55% [10].

The low percentage of obtained SVRs and numerous adverse effects of the interferon-based regimens prompted the development of new therapeutic schemes, including the second generation of DAAs, such as the combination of ombitasvir/paritaprevir/ritonavir (OBV/PTV/r) + dasabuvir (SV). The results of phase 3 trials and real-world data with this type of treatment were excellent, with obtained SVRs of more than 93% [11, 12]. Moreover, this therapeutic regimen without ribavirin assured in the TURQUOISE-III phase IIIb open-label clinical study the 100% SVR in the HCV subgenotype 1b-infected cirrhotic patients [13].

The aim of this study was to evaluate the efficacy and safety of OBV/PTV/r + DSV therapeutic regimen in the patients with a chronic HCV infection in Serbia included in the early access program.

Methods

This prospective, multicentric, real-life clinical study was performed at seven infectology and hepatology departments of five Serbian university clinics in Belgrade, Novi Sad, Niš and Kragujevac.

The diagnostic and treatment approach to these patients was inspired by the Polish real-life (AMBER) study [14, 15]. A total of 21 male and female patients were included in this study. They had a chronic HCV infection, caused by genotype 1, and majority of them were previously treated (nonresponders or relapsers). The anatomical status of their livers was assessed by elastography (fibrosis scores F0-F4), while the hepatic functional status was assessed by the values of bilirubin, albumin, international normalized ratio (INR), alanine-aminotransferase (ALT), aspartate aminotransferase (AST) and presence of encephalopathy and ascites. Based on these parameters, the Child-Pugh score was calculated in order to assess the existence of liver dysfunction. Some additional parameters were also estimated: hemoglobin, red blood cell (RBC), white blood cell (WBC), platelet (PTL) counts and alpha-fetoprotein (AFP) concentrations.

All patients in this study received the dose of OBV/PTV/r 12.5 mg/75 mg/5 mg, two tablets as a morning dose and DSV 250 mg dose of 500 mg/day divided into two doses. The dose of RBV, administered in 200 mg tablets, was 1,000 mg/day for the patients weighing < 75 kg or 1,200 mg/day for the patients weighing > 75 kg divided into two doses. It was planned to reduce the dose of RBV in the patients who developed severe adverse effects, or laboratory abnormalities, such as anemia. RBV was given to all patients except to those with HCV genotype 1b. For the majority of patient the treatment duration was 12 weeks. The duration of the treatment was extended to 24 weeks in the high-risk patients, i.e., patients with liver cirrhosis who were infected with HCV genotype 1a.

Viremia was assessed at baseline, 4 weeks after beginning of treatment (rapid viral response – RVR), 12 or 24 weeks after beginning of treatment (the end of treatment response – ETR), and 12 weeks after the end of treatment (SVR). A number of replications of viral RNA was expressed in IU/mL. The HCV levels were obtained by the quantitative polymerase chain reaction (PCR) assay. The viral RNA detection limit was ≥ 12 IU/mL.

Descriptive statistics such as the calculation of mean values and their standard deviations (SD) were used.

Results

A total of 21 patients with the HCV infection were included in this study. Twenty of them were previously treated with PEG-IFN and RBV, while 1 was treatment-naive. Among previously treated patients, 18 paients were null-responders and 2 patients were relapsers (Table 1).

All 21 patients were infected with genotype 1. In 11 of them subgenotyping was not performed, 1 patient had a combined genotype 1a and 1b infection, 1 had a genotype 1a, while 8 were infected with genotype 1b. Out of 21 patients, 9 (42.85%) had fibrosis stages F3/F4, which are considered difficult to treat. Initial viremia varied over the large range of values (152×10^3–527×10^6 IU/mL) with the median of 1.17×10^6 IU/mL. The liver function in these patients was well preserved with the Child-Pugh score class A for 18 patients, with 3 patients without the Child-Pugh score. All the biochemical and hematological parameters were within the normal range of values (Table 1).

Table 1

Baseline demographic and clinical characteristics of patients with chronic hepatitis C treated with OBV/PTV/r + DSV + RBV

Parameters	Values (n = 21)
Age (years), mean ± SD	41.70 ± 11.59
Gender, n (%)	21 (100)
male	13 (61.91)
female	8 (38.09)
BMI (kg/m^2), mean ± SD	25.43 ± 3.82
Treatment history, n (%)	21 (100)
naive	1 (4.76)
relapser	2 (9.52)
null-responder	18 (85.71)
Fibrosis stage, n (%)	21 (100)
F0	6 (28.57)
F1	5 (23.81)
F3	7 (33.33)
F4	2 (9.52)
unknown	1 (4.76)
HCV genotype, n (%)	21 (100)
1a	1 (4.76)
1b	8 (38.09)
1a+1b	1 (4.76)
1 (subgenotype not available)	11 (52.38)
HCV RNA level (× 106 IU/mL), mean ± SD	55.80 ± 15.30
Child-Pugh score A, n (%)	18 (85.71)
Albumin (g/L), mean ± SD	43.03 ± 5.60
Bilirubin (μmol/L), mean ± SD	13.57 ± 5.22
INR	1.06 ± 0.12
Creatinine, (μmol/L), mean ± SD	72.19 ± 15.87
ALT (IU/L), mean ± SD	83.42 ± 58.60
AST (IU/L), mean ± SD	79.11 ± 70.46
Hemoglobin (g/L), mean ± SD	151.68 ± 19.94
RBC (× 10^6/L), mean ± SD	5.710 ± 0.47
WBC (× 10^3/L), mean ± SD	6.58 ± 2.62
PLT (× 10^3/L), mean ± SD	204.84 ± 51.32
AFP (ng/mL), mean ± SD	16.31 ± 34.40

BMI – body mass index; HCV – hepatitis C virus; RNA – ribonucleic acid; INR – international normalized ratio; ALT – alanine aminotransferase; AST – aspartate aminotransferase; RBC – red blood cells; WBC – white blood cells; PLT – platelets; AFP – alpha-fetoprotein; OBV – ombitasvir; PTV – partiaprevir; r – ritoravir; DSV – dasabuvir; RBV – ribavirin.

Note: Normal range of biochemical parameters – albumin: 34–55 g/L; bilirubin 0–20.5 μmol/L; INR: 2–3; creatinine 59–104 μmol/L; ALT 0–41 U/L; AST 0–37 U/L; RBC – 4.34–5.72 × 10^6/L; WBC 3.40–9.70 × 10^3/L; PLT 158–424 × 10^3/L; AFP < 20 ng/mL.

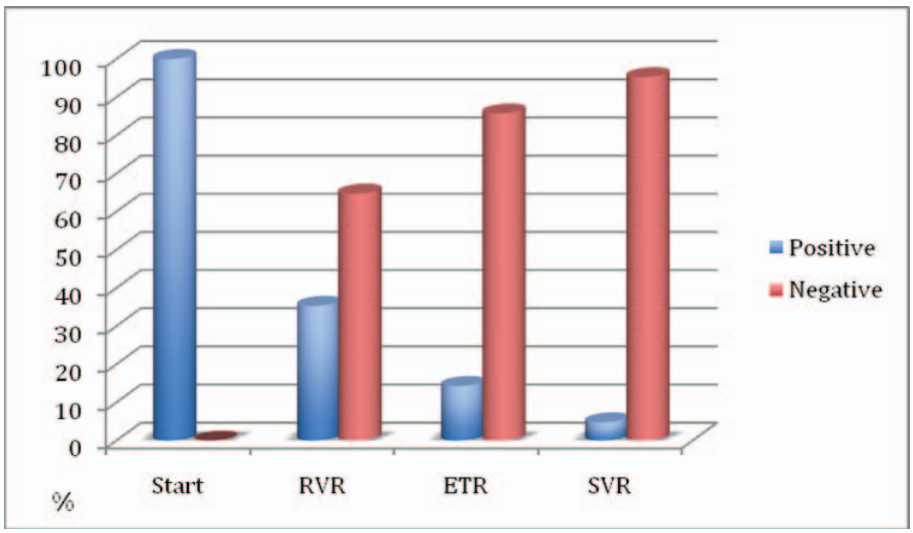

Fig. 1 – Results of the PCR testing during the treatment with OBV/PTV/r + DSV + RBV.

Start – before commencement of treatment; RVR – rapid viral response after 4 weeks of treatment; ETR – end of therapy response after 12 or 24 weeks of treatment; SVR – sustained viral response 12 weeks after the end of treatment; PCR – polymerase chain reaction; OBV – ombitasvir; PTV – paritaprevir; R – ritoravir; DSV – dasabuvir; RBV – ribavirin.

The four-week RVR data were available in 17 patients. In 11 (64%) patients, HCV could not be found, 5 patients had low viral concentration (15–623 IU/mL) and only 1 patient had a significant viral load (99.000 IU/mL). ETR was estimated after 12 weeks of therapy in 18 patients and after 24 weeks of therapy in 3 high-risk patients. Complete ETR was achieved in 18 patients, in the rest of them the viral load was 12×10^3, 192×10^3 and 1.24×10^6. Full SVR, estimated 12 weeks after the end of the treatment, was achieved in 20 patients, while only 1 had a significant viremia of 902×10^3 IU/mL (Figure 1).

The used DAAs were well-tolerated and no adverse events were recorded in 18 (85.71%) patients. The remaining 3 (14.29%) patients had adverse events. Two patients had hyperbilirubinemia and one had anemia, asthenia, fatigue, headache, insomnia and pruritus. These side effects were mild and therefore the therapy did not have to be stopped, nor the reduction of RBV dose was needed. The life-threatening treatment emergent serious adverse event (SAE) was not recorded.

Table 2

Concomitant medication in five patients

Concomitant medication	Numbers per patient
Nebivolol	1
Propylthiouracil	1
Mirtazapine, escitalopram	2
Ursodoxycholic acid, pantoprazole, iron, folic acid, vitamin B12, vitamin B6, zinc	7
Bisoprolol, levothyroxine	2
Total	13

The data on the concomitant medication were available in 19 patients. No such medication was needed in 14 patients. In 5 of them, the concomitant medication included: antihypertensives, bronchodilators, thyreosuppressant and anti-anemic drugs, antiulcers drugs, levothyroxine and anti-depressants (Table 2).

Discussion

The DAA combination OBV/PTV/r + DSV + RBV used in this study assured complete 4-week RVR in 11 out of 17 patients (64.71%). Twelve-week ETR was achieved in 18 out of 21 (85.71%) patients, while the SVR was registered in 20 out of 21 (95.24%) patients. The results obtained are in agreement with the results of other similar clinical trials [11, 13–15]. The onset of antiviral action was fast and it was similar to the one reported in a Polish clinical trial, where RVR was achieved in 69.23% [11]. In a systematic review of 19 clinical trials using the same therapeutic combination in the patients with a chronic HCV hepatitis, the average SVR of 97% was found [14]. SVR, as a confirmation of the absence of HCV was considered as an endpoint of successful treatment and as a positive predictor of the patients' lower hepatic failure and mortality rates [16].

The SVRs obtained in the present study and in the other ones with the OBV/PTV/r + DSV + RBV antiviral combination were significantly higher than in the patients treated with pegylated interferon + RBV, 95–100% versus 70.5% [9]. The 2011 registration trials for the first generation protease inhibitors BOC and TVR, each combined with PEG-IFN+RBV, assured significantly lower SVRs of 59%–66% [17] and 64%–75% [18], respectively, while the subsequent real-life SVRs were even lower, 42%–55% [10, 19]. Besides, the onset of the antiviral effect of the OBV/PTV/r + DSV + RBV was faster, with the vast majority of the patients requiring only 12 weeks of treatment, while the duration of BOC or TVR regimens was 32–48 weeks [10, 19].

All the treated patients in this study had infection with HCV genotype 1, which is in accordance with the epidemiological data obtained from Europe and the USA, where this genotype is dominant, in contrast with the data from the Middle East, where genotype 4 prevails [12, 14, 20–22]. The local epidemiological and clinical studies also confirm the predominance of genotype 1 [6, 7, 9, 10].

Adverse events were mild and rare, occurring in 3 out of 21 (14.29%) patients, all of them in those ones receiving RBV and not necessitating the decrease of the dose of RBV. Anemia is known to be associated with the RBV therapy [23]. In some other studies, considerably higher incidence of adverse events (72.20%) was noted [14]. This difference could be explained by the fact that the population of patients in the present study was younger (average age of 41.70 ± 11.59), without significant comorbidities, leaner [body mass index (BMI) 25.43 ± 3.82 kg/m^2] and with better preserved hepatic function than in the other trials [24]. The safety of the OBV/PTV/r + DSV + RBV antiviral combination in the present report was better than the one of the BOC or the TVR-based triple regimens, where the incidence of adverse effects was very high, with anemia being the most important one (in 25% of patients), followed by neutropenia and thrombocytopenia [10]. It seems that overall quality of life of patients treated with OBV/PTV/r + DSV + RBV is better than the one with BOC or TVR.

Conclusion

In this real-life multicenter clinical study, DAA combination, OBV/PTV/r + DSV + RBV, assured excellent efficacy and tolerability in the patients with genotype 1 chronic HCV infection.

REFERENCES

1. *Franciscus A.* A brief history of hepatitis C. HCSP version 4.4. 2017 Feb [cited 2017 May 19]. Available from: http://www.hcvadvocate.org/hepatitis/factsheets_pdf/Brief_History_HCV.pdf.
2. *Messina JP, Humphreys I, Flaxman A, Brown A, Cooke GS, Pybus OG,* et al. Global distribution and prevalence of hepatitis C virus genotypes. Hepatology 2015; 61: 77–87.
3. *Parkin DM.* The global health burden of infection-associated cancers in the year 2002. Int J Cancer 2006; 118(12): 3030–44.
4. World Health Organization (WHO). Hepatitis C – Fact sheet 2014 [cited 2017 Jan 15]. Available from: http://www.who.int/mediacentre/factsheets/fs164/en/.
5. *Petrović J, Salkić NN, Ahmetagić S, Stojić V, Mott-Divković S.* Prevalence of chronic hepatitis B and hepatitis C among first time blood donors in Northeast Bosnia and Herzegovina: en estimate of prevalence in general population. Hepat Mon 2011; 11(8): 629–33.
6. *Mitrović N, Delić D, Marković-Denić L, Jovičić M, Popović N, Bojović K,* et al. Seroprevalence and risk factors for hepatitis C virus infection among blood donors in Serbia: A multicentre study. Dig Liver Dis 2015; 47(7): 572–6.
7. *Mitrović N.* Epidemiological characteristics of hepatitis C viral infection in Serbia [dissertation]. Belgrade: Medical Faculty, University of Belgrade; 2015. (Serbian)
8. *Lucejko M, Parfieniuk-Kowerda A, Flisiak R.* Ombitasvir/paritaprevir/ritonavir plus dasabuvir combination in the treatment of chronic HCV infection. Expert Opin Pharmacother 2016; 17(8): 1153–64.
9. *Delić D, Mitrović N, Popović N, Urošević A, Pešić I, Simonović J.* Antiviral/immunomodulatory combination therapy: pegylated interferon alpha 2a and ribavirin in patients with chronic hepatitis C virus infection. Srp Arh Celok Lek 2012; 140(9–10): 612–8. (Serbian)
10. *Simonović Babić J, Bojović K, Fabri M, Kostić V, Jovanović M, Mijailović Ž,* et al. Boceprevir in genotype 1 chronic hepatitis C: First experiences in Serbia. Srp Arh Celok Lek 2015; 143(1–2): 35–41.
11. *Flisiak R, Janczewska E, Wawrzynowicz-Syczewska M, Wiercinska-Drapalo A, Zarebska-Michaluk D, Fleischer-Stepniewska K,* et al. Efficacy and safety of Parytaprewir/r/Ombitaswir and Dazabuwir with or without Ribavirin in real life therapy of Polish patients with chronic hepatitis C – an interim analysis of AMBER study data. Clin Exp Hepatol 2015; 1(2): 84.
12. *Flisiak R, Janczewska E, Mawrzynowicz-Syczewska M, Jaroszewicz J, Zarebska-Michaluk D, Nazzal K,* et al. Real-world effectiveness and safety of ombitasvir/paritaprevir/ritonavir + dasabuvir + ribavirin in hepatitis C: AMBER study. Aliment Pharmacol Ther 2016; 44: 946–56.
13. *Feld J, Moreno C, Trinh R, Tam E, Bourgeois S, Horsmans Y,* et al. Sustained virologic response of 100% in HCV genotype 1b patients with cirrhosis receiving ombitasvir/paritaprevir/r and dasabuvir for 12 weeks. J Hepatol 2016; 64: 301–7.
14. *Pogorzelska J, Flisiak R.* Real-world experience with ombitasvir/paritaprevir boosted with ritonavir and possibly combined with dasabuvir and ribavirin in HCV infection. Clin Exp Hepatol 2016; 2(2): 34–7.
15. *Lawitz E, Makara M, Akarca US, Thuluvath PJ, Preotescu LL, Varunok P,* et al. Efficacy and Safety of Ombitasvir, Paritaprevir, and Ritonavir in an Open-Label Study of Patients With Genotype 1b Chronic Hepatitis C Virus Infection With and Without Cirrhosis. Gastroenterology 2015; 149(4): 971–80.e1.
16. *Van der Meer AJ, Veldt BJ, Feld JJ, Wedemeyer H, Dufour JF, Lammert F,* et al. Association between sustained virological response and all-cause mortality among patients with chronic hepatitis C and advanced hepatic fibrosis. JAMA 2012; 308(24): 2584–93.
17. *Poordad F, McCone J, Bacon BR, Bruno S, Manns MP, Sulkowski MS,* et al. Boceprevir for untreated chronic HCV genotype 1 infection. N Engl J Med 2011; 364(13): 1195–206.
18. *Jacobson IM, McHutchison JG, Dusheiko G, Di Bisceglie AM, Reddy KR, Bzowej NH,* et al. Telaprevir for previously untreated chronic hepatitis C virus infection. N Engl J Med 2011; 364(25): 2405–16.
19. *Bichoupan K, Tandon N, Martel-Laferriere V, Patel NM, Sachs D, Ng M,* et al. Factors associated with success of telaprevir- and boceprevir-based triple therapy for hepatitis C virus infection. World J Hepatol 2017; 9(11): 551–61.
20. *Alswat KA, Babatin MA, Abdelrahman AA, Al-Hamoudi WK, Alghamdi AS, Abdo A,* et al. Treatment of chronic hepatitis C genotype 4-infected patients with ombitasvir /paritaprevir /ritonavir plus ribavirin: Real life data from Saudi Arabia. Hepatology 2016; 64(1 Suppl): 974A–5A.
21. *Rodriguez-Osorio I, Cid P, Morano L, Castro A, Suarez M, Delgado M,* et al. Real life experience with direct-acting antivirals agents against hepatitis C infection in elderly patients. J Clin Virol 2017; 88: 58–61.

22. *McCombs J, McGinnis J, Fox S, Tonnu-Mihara J.* Analysis of the real world effectiveness of direct acting antivirals treatments of hepatitis C in large population. J Hepatol 2016; 64(Suppl 2): S217.
23. *Lau JY, Tam RC, Liang TJ, Hong Z.* Mechanism of action of ribavirin in the combination treatment of chronic HCV infection. Hepatology 2002; 35(5): 1002–9.
24. *Backus LI, Belperio PS, Shahoumian TA, Loomis TP, Mole LA.* Comparative effectiveness of ledipasvir/sofosbuvir ± ribavirin vs. ombitasvir/paritaprevir/ritonavir + dasabuvir ± ribavirin in 6961 genotype 1 patients treated in routine medical practice. Aliment Pharmacol Ther 2016; 44(4): 400–10.

Received on July 27, 2017.
Revised on December 10, 2017.
Accepted on December 11, 2017.
Online First December, 2017.

CURRENT TOPIC

UDC: 616.43:616.37-008.64
https://doi.org/10.2298/VSP170620126C

Diabetes mellitus – factors that contribute to the occurrence, diagnosis and management of the disease

Dijabetes melitus – faktori koji doprinose nastanku, dijagnozi i terapiji bolesti

Milica Čizmić*†, Petar Ristić*, Zorana Djuran*, Jelena Karajović*, Uroš Zoranović*†, Nemanja Nenezić*

Military Medical Academy, *Department of Endocrinology, Belgrade, Serbia; University of Defence, †Faculty of Medicine of the Military Medical Academy, Belgrade, Serbia

Key words:
diabetes mellitus, type 2; vitamin d; antibodies; plasminogen activator inhibitor 1; inflammation mediators.

Ključne reči:
dijabetes melitus, insulin-nezavisni; vitamin d; antitela; plazminogen, aktivator, inhibitor 1; zapaljenje, medijatori.

Introduction

Type 2 diabetes mellitus is one of the most common endocrine disorders. Across the planet, 415 million people have diabetes (1 in 11 adults); estimates are that by the year 2040 there would be 642 million sick people. Every 6 seconds one person dies from the consequences of diabetes (5 million lethal outcome). The International Federation of Diabetes (IDF) indicated the factors that play a role in the development of the disease: genetics, lifestyle, environment and diet. The underlying mechanism in the development of type 2 diabetes is insulin resistance and insulin secretion reduced as a result of exhaustion of the beta-cells. Diabetes mellitus represents a state of chronic hyperglycemia, characterized by disturbed metabolism of carbohydrates, proteins and fats. It occurs due to the absolute or relative insulin deficiency, insulin resistance, increased glucose production and excessive action of the hormones with the opposite effect of insulin. Science has not clearly defined so far the additional contributing factors affecting the occurrence and treatment of this disease. What is the basis of the generation of diabetes is not well understood. Therefore, any contribution that leads in this direction is valuable.

Insulin antibodies and insulin receptor antibodies in the onset of diabetes mellitus

In 1950, for the first time the association between insulin resistance (IR) and insulin antibodies (IA) was described The presence of IA were then attributed to the use of non-human insulin. Hypoglycemia simultaneously with the existence of a high titre of insulin antibodies, in the patients with diabetes, was decribed as autoimmune insulin syndrome, or Harate disease [1]. The presence of postprandial hyperglycemia and hypoglycemia fasting are two of the same process in this disease and are due to binding of insulin antibodies. This insulin antibodies have a low binding affinity for insulin and never lead to IR.

Recent findings suggest that there is a need for monitoring the presence of IA in the patients with insulin resistance (IR). Anti-insulin receptor antibodies (AIRAs) are determined by a metod of radioreceptor essay. These antibodies are IgG and IgM. IgG antibodies were more frequent in the patients with autoimmune diseases such as *acanthosis nigricans*. The antibodies of the IgM class are present in type 2 diabetes [2].

AIRAs are shown in circulation in the patients with diabetes. All previous studies indicate that there is no link between insulin and receptor antibodies in type 1 diabetes. However, among the patients with type 1 diabetes receiving insulin, there is a correlation between the dose of insulin and the levels of insulin receptor antibodies, but not with anti-insulin antibodies. In any case, AIRAs are proven in the patients with diabetes but their role in the further development of diabetes is not fully understood.

In a study of 80 patients with type 1 and type 2 diabetes, along with a study of 20 patients with mixed autoimmune diseases and 20 healthy patients, AIRAs were demon-

Correspondence to: Milica Čizmić, Military Medical Academy, Department of Endocrinology, Crnotravska 17, 11 000 Belgrade, Serbia. E-mail: cizmicaleksandarmilica@hotmail.com

strated in 13 of 33 patients with type 1 diabetes and in 6 of 47 with type 2 diabetes. The antibodies were mainly IgM groups. In both groups of diabetes, there is a good correlation between the % of binding to insulin receptors and % of antibody class IgM (p <0.001), but not with class IgG. There is a correlation between the % of inhibition of insulin binding to its receptor, and daily insulin doses (p <0.001). Based on the above, it can be concluded that there is the presence of insulin receptor antibodies in patients with type 1 and type 2 diabetes [3].

The role of vitamin D in the development of diabetes

According to many authors, vitamin D plays an important role in controlling blood glucose levels, but also in alleviating chronic diabetic complications. The rationale for this is grounded on the following facts: the presence of the vitamin D receptor (VDR) in pancreatic beta-cells, the vitamin D activating 1 alpha-hydroxylase present in that cells, the presence of the VDR gene for insulin, which results in the increased synthesis of insulin under the effect of vitamin D. Furthermore, VDRs are present in skeletal muscle cells, fact that 1,25 (OH) 2D is rounding gene transcription for the insulin receptor, which stimulates this expression and suppresses the renin gene, thus reducing hyperglycemia-induced increase in the level of renin and blocks renin-angiotensin activity.

The beneficial effects of vitamin D, when it comes to diabetes may be due to its anti-inflammatory effects and the effect on the metabolism of calcium and phosphate, and gene regulation of the insulin receptor. Vitamin D increases the amount of calcium in cells, leading to increased glucose transport in muscle. The Vitamin D also regulates the nuclear PPAR (*peroxisome proliferative activated receptor*), which plays an important role in insulin sensitivity. The vitamin D deficiency is associated with the increase in inflammation. The vitamin D decreases the expression of proinflammatory cytokines involved in the development of insulin resistance, such as interleukin (IL)-1, IL-6 and tumor necrosis factor (TNF)-alpha. By such effect on this cytokine, vitamin D exerts antiapoptotic effect upon the pancreatic beta cells, the preservation of the insulin secretion from the same and increases insulin sensitivity.

In comparison to the healthy population, in type 2 diabetes, substantially lower concentrations of circulating 25(OH)D are present [4]. Common risk factors for type 2 diabetes and hypovitaminosis D are obesity, age, association with black race and reduced physical activity. The probable mechanism by which vitamin D participates in the glucose homeostasis is the effect on the beta cell dysfunction and insulin resistance in cases of the vitamin D deficiency**.** Negative correlation between the blood glucose and insulin levels to the level of 25(OH)D and the positive correlations 25(OH)D levels with insulin sensitivity was tested in several animal and human studies. In some of these studies, it was observed that vitamin D supplementation may improve insulin secretion and reduce insulin resistance in type 2 diabetes. The possible role of vitamin D in type 2 diabetes and influence on the HbA1C values is also registered. It should be noted that there are studies that do not prove the above report. It seems that there is still no general consensus on this issue.

Vitamin D deficiency has a role in type 1 and type 2 diabetes. The evidence indicates that the treatment with vitamin D reduces the insulin resistance and improves glucose tolerance. Vitamin D deficiency leads to reduced insulin secretion, and showed that vitamin D supplementation restores insulin secretion in animals. Indirect effect on insulin secretion is found through the calcium effect. In fact, vitamin D contributes to the normalization of extracellular calcium, ensuring the normal flow of calcium through the cell membrane, so that hypovitaminosis D may have the harmful effects on calcium insulin secretion. Other potential mechanisms include stimulation of insulin receptor expression, improving the insulin response to glucose transport and a decrease in systemic inflammation by direct effects on cytokine [5, 6].

In a prospective study, Jannersjö et al.[7] investigated the relationship of serum 25(OH)D and parathyroid hormone (PTH) with all-cause mortality in the patients with type 2 diabetes and found that in the men with type 2 diabetes, vitamin D levels inversely correlated with all-cause mortality independently of years, levels of PTH, HbA1c, waist circumference, 24h-monitoring of blood pressure and serum apoB. In the women with type 2 diabetes, the serum PTH was directly proportional with all causes of death. In this study, it was not proven that the substitution of vitamin D reduces the risk of mortality, but in spite of this, it was suggested that the serum level of 25(OH)D in the men and PTH in women, suffering from type 2 diabetes, could be used as the surrogate markers for prognostic information related to mortality. This is an independent risk factor in terms of blood pressure, carotid intima-medial complex (as measured in the carotid artery) and flow rate (measured in the carotid and femoral arteries). De Boer [8] in his study with the hemodialysis patients showed that vitamin D treatment improved insulin secretion and sensitivity.

There are studies which have the opposite results in comparison to the conclusions given above. Thus in Shet et al. [9] study, 912 patients (429 patients of the group with type 2 diabetes and 483 patients of non-diabetic control group) from the West Indies studied the biochemical parameters [fasting glucose, postprandial glucose, HbA1c, basal insulinemia, insulin resistance in the form of homeostatic model assessment (HOMA- IR)] and compared to the level of 25(OH)D. It was concluded that, although there was a high prevalence of vitamin D deficiency in both groups, the effect of vitamin D on these parameters could not be confirmed. The explanation for this was the increased skin pigmentation of the population in this region, but also reduced exposure to sunlight because of how they dress and the way of life [9]. Exposure to the sun takes twice as long for the people of West Indies in relation to the white race, for the same effect on the synthesis of vitamin D.

Vitamin D, according to some studies, has a role in alleviating chronic diabetic complications. Data on the effect of vitamin D deficiency in the control of diabetes and the oc-

currence of complications are modest. Ahmedieh et al. [10] in their study examined the relationship between levels of 25(OH)D and microvascular complications in the patients with type 2 diabetes. The conclusion was, that the low serum levels of 25(OH)D was independent predictor of HbA1c, diabetic neuropathy, and retinopathy. In the similar study by Zoppini et al. [11], it was found the inverse relationship between the levels of 25(OH)D and the prevalence of microvascular complications in the patients with type 2 diabetes. Whether the supplementation of vitamin D in these patients may have a benefit on the risk of microvascular complications remains to be explored. In another study, it was concluded that the vitamin D deficiency was more common in the diabetic patients with nephropathy, but not in those with retinopathy and neuropathy. Also, it was found that the level of vitamin D was lower in the patients with severe microvascular complications, and it was concluded that the vitamin D deficiency was associated with the microvascular complications in the patients with tip 2 diabetes.

Diabetic nephropathy (DN) reduces progressively the vitamin D body level due to: the loss of vitamin D-binding protein in proteinuria, compromised synthesis of vitamin D in the skin and lower activation of vitamin D in the damaged kidney. It was noted that the lack of vitamin D is higher in the diabetic chronic renal failure (CRF) than in the non diabetic patients. There are indications that the VDRs are modulators of glomerular damage. Calcitriol, endogenous VDR activator reduces the glomerulosclerosis index. In clinical terms, the patients with CRF treated with paricalcitol (selective VDR activator), exhibited a significant reduction of proteinuria after 23 weeks of the treatment, regardless of GFR, blood pressure or angiotensin converting enzyme (ACE) inhibition. However, in clinical studies, the proteinuria response in the patients treated by VDR activators was not unique. The question is whether these patients may benefit from the therapy with VDR activators. The above mentioned benefit of therapy with VDR activators refers precisely to the anti-inflammatory effect. In animal models of primary glomerulopathy, VDR activators reduced glomerular infiltration of inflammatory cells. In addition, a high serum vitamin D level in the CRF patients is associated with the reduced systemic inflammation [12]. Subantiproteinuric dose of calcitriol and paricalcitol reduces glomerular inflammation in experimental DN [13]. Clinical studies in the human population with paricalcitol in DN revealed that it has a modest and variable effect on proteinuria. Calcitriol and paricalcitol have reduced the expression of inflammatory cytokines in the kidney, reduced glomerular expression of IL-6 and monocyte chemoattractant protein-1 (MCP-1), decreased glomerular infiltration of CD43 + leukocytes, which synthesize the chemotactic factors.

Vitamin D decreases expression of renin, suppressing the transcription of renin in mesangial cell that contribute to the reduction of inflammation. Hyperglicemia suppressed calcitriol and activate renin-angiotensin system. Thus, in the study of Li et al. [14], vitamin D is recognized as a negative endocrine regulator of the renin-angiotensin system by reducing the biosynthesis of renin. The VDR deficiency resulted in the production of renin and angiotensin II, leading to arterial hypertension, and myocardial hypertrophy. In case of the vitamin D deficiency, increased renin secretion occur, while injection of 1,25(OH)2D reduces its synthesis.

Combination therapy with losartan and paricalcitol in the diabetic patients, prevents albuminuria, restores glomerular filtration membranes structure and significantly reduces glomerulosclerosis [15].

Whether VDR activators should be used to reduce the progression of CRF could still not be answered with certainty. It would take larger randomized controlled studies. The reduction of proteinuria in previous studies takes place without changes in blood pressure, which indicates that the mechanism of action is non- haemodynamic. Finally, some meta-analyzes suggest that VDR gene polymorphism may affect individual susceptibility to the development of DN in the white population.

Regarding diabetic retinopathy (DR), calcitriol inhibits angiogenesis in tumours [16]. Diabetic retinopathy is characterized by neovascularisation and angiogenesis, and high serum 1,25 (OH)2D reduces angiogenesis in ischemic retinopathy [17]. The level of 25(OH)D is significantly lower in the patients with two or three microvascular complications compared to those with no complications, and this is especially related to DR. In the study of Inuki et al. [18] , it was found the low level of 25(OH)D and higher PTH in the patients with DR and/or proteinuria in comparison with those without. In studies including 1,520 patients with type 2 diabetes it was confirmed that the vitamin D deficiency is an independent factor of risk for DR. In the another study of Jee et al. [19] of 204 patients, a statistically significant influence of vitamin D deficiency on DR was found in the males, while it was not the case in the females.

Diabetic polyneuropathy and the influence of vitamin D as a neurotropic substance on neuropathic pain is unclear. It is believed that the vitamin D deficiency can potentially stimulate the diabetic nerve damage. In the Basit et al. [20] study, a high dose vitamin D effect was investigated in the patients with painful diabetic neuropathy and it was concluded that a single intramuscular dose of 600,000 IU of vitamin D leads to a significant reduction of the symptoms of diabetic neuropathy. Its deficiency is more common in the patients with distal symmetrical polyneuropathy, and pain reduction is achieved after vitamin D deficiency correction. Three studies showed that vitamin D deficiency is independently associated with increased risk for diabetic peripheral neuropathy in the type 2 diabetes patients.

When it comes to published studies on diabetic macroangiopathy and the affecting vitamin D, Somjen et al.[21], first discovered enzymatic 1 alpha-hydroxylase activity in human vascular smooth muscle cells that may be stimulated with PTH and inhibited by the exogenous vitamin D intake. It was proven the physiological effect of vitamin D on the vascular structure. Its serum level is directly proportional to endothelial function, and vice versa to arterial calcification. Unfortunately, there are not enough valid studies regarding direct correlation of the vitamin D and diabetic macroangiopathies.

Based on the above, there appears to be serious evidence of the role of vitamin D in metabolic syndrome and type 2 diabetes mellitus. However, there are studies that have the opposite impetus. Further randomized control studies are

needed to achieve a generally accepted attitude. The role of vitamin D in type 2 diabetes and metabolic syndrome is clear when it comes to the pathophysiological mechanism of the way it performs its activity on target tissues.

Cardio-Ankle Vascular Index (CAVI), parameter in the diagnosis of occlusive blood vessel disease

This is a new parameter for determining the rigidity of the artery walls, starting from the aorta to the arteries at the lower extremity joints [22]. The determination of this index is based on the beta receptor domination, the effect of the beta 1 receptor on the rigidity of the blood vessels. There is a change in the blood artery caliber and consequently the changes in the internal pressure of the blood vessel [23]. This index is independent of the height of the pressure at that point. The parameters of blood stiffness *beta* are determined as the ratio of pulse wave velocity and diastolic blood pressure. CAVI is a constant value. Administration of alpha-blockers, which reduce contracture of smooth musculature of arterial wall decrease the CAVI value or the blood pressure value. This means that CAVI is the indicator of arteries compliance or vascular function indicator of transport blood from the heart to the peripheral arteries.

Thiazide diuretics and ACE inhibitors and beta 1 blockers, do not reduce CAVI when they reduce the blood pressure.

The parameter of constriction artery *beta*, is determined over the length of the main arteries. It is calculated by measuring the pulse wave velocity over the brachial artery and arteries of the lower leg at the level of the ankle joint. It measures systolic and diastolic blood pressure over the brachial artery. The measured values of the application are given in equation. Then it gets a new parameter called Cardio-Ankle-Vascular-Index (Figure 1).

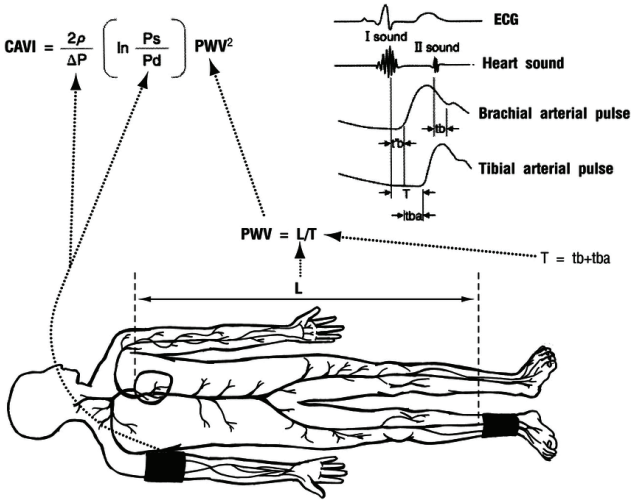

Fig. 1 – Cardio-ankle vascular index (CAVI).

PWV – pulse wave velocity; L – distance between aortic value and ankle; T – time taken for arterial pulse wave to travel from aortic value to ankle; tb – time between aortic value closing and notch of brachial pulse wave; tba – time between rise of brachial pulse wave to rise of ankle pulse wave; Ps – systolic pressure; Pd – diastolic pressure; ΔP – pulse pressure = Ps – Pd; ρ – blood density.

There is a positive correlation between the value of CAVI and the degree of arteriosclerotic disease. CAVI decreases with improving cardiovascular risk. It is a predictive factor of cardiovascular events. CAVI, at the same time, indirectly represent the contracture status of vascular smooth musculature of arterial blood vessels [24, 25].

When it comes to influence blood glucose level and the value of CAVI, high blood glucose causes contracture of smooth muscles of arteries and increases CAVI in a short period of time. Thereby, reducing HbA1C reduces CAVI, and therefore, CAVI may be a marker of glucose control. In the patients with high low density lipoprotein (LDL) cholesterol, the low CAVI values are shown. In the initial stages of hypercholesterolemia, the arteries are not rigid, but rigidity of blood vessels occurs when the process of arteriosclerosis inflammation is included. Of course, giving statins reduces CAVI. In the pathogenesis of apnea sleeping, the concentration of high and low oxygen passes through the walls of blood vessel and contrubute to rigidity [26].

It was showed that mortality decreased when the CAVI values were lower than 9 in relation to the higher CAVI. Cerebrovascular events are more common when CAVI was over these values. The results of preliminary studies indicate that preferable CAVI should be lower or equal to 9. It was proven that CAVI and diastolic ventricular heart function had linked value, and therefore CAVI is an indicator of the afterload (or CAVI was determined by compliance of the arterial blood vessel). So, the CAVI value is increased in: poorly regulated diabetes, obesity, hypertension, infection, cerebral hemorrhage, change in the structure of smooth muscles of the arteries. CAVI is an indicator of the artheriosclerosis degree and degree of contractility of blood vessels [27].

Role of concentration levels of PAI-1 in the process of angiogenesis and wound healing in diabetes type 2

Plasminogen activator inhibitor-1 (PAI-1) has an important role in the local and systemic responses to a trauma as well as in wound healing. Therefore, this points out the importance of the normal levels of PAI-1 in the treatment of tissue ischemia and necrosis of any aetiology. This fact has a bigger role in the patient with diabetes due to the already present endothelial dysfunction.

It is known that plasminogen affects the wound healing process, the process of the proteolysis of the extracellular matrix, activation of growth factors and activation of cell migration of smooth muscle blood vessel [28, 29].

As for the role of PAI-1 in the wound healing of inflamed tissue in the ischemic type 2 diabetes, it was significantly increased at the early stage of the reaction in the process of neutrophil inflammation. This directly increases the swelling and tissue necrosis. Therefore, at an early stage, PAI-1 inhibits the effects of IL-6, which decreases the concentration of proteins in the inflamed region with the delayed wound healing. This suggests that the increased concentration of PAI-1 in the acute phase protein response. It is known that PAI-1 is increased locally in the damaged tissue, under the influence of macrophages and endothelial damage. The

decrease of PAI-1 increases the impact wound in the region of neutrophil inflammation, leading to reduced tissue necrosis and edema eight hours after the tissue injury. The decrease of PAI-1 results in a decrease of IL-6, increasing the levels of protein and faster wound healing [30]. It was shown that PAI-1 at low concentration has antiapoptotic effect and increases the cell proliferation via its activity and encourages angiogenesis [31, 32].

Ischemia of lower leg represents a large problem in therapy, but these properties of the normal PAI-1 concentration can be used in the treatment of ischemia of diabetic patients. Tissue ischemia itself constitutes a stimulus for the secretion of stem cell transplantation. The angiogenic effect of inhibition of PAI-1, in terms of tissue ischemia, consists of the stimulation of secretion of neutrophilic granulocytes from bone marrow and from the tissue. The produced stimulation of secretion of vascular endothelial growth factor (VEGF), fibroblast growth factor 2 (FGF-2) and the free matrix metalloproteinase 9 (MMP-9) in tissues, increases secretion of angiogenic factors from bone marrow: VEGF, hematopoietic growth factors. Muscular infiltration with CD11h + Gr1 + neutrophils potentiates the inhibition of PAI-1 by increasing the level of FGF2 and VEGF and thus angiogenesis [33].

PAI-1 stimulate angiogenesis by increasing the FGF receptor at the endothelial level, which increases the binding of VEGF to the endothelial cells in the ischemic tissue [34, 35]. Thus, FGFs activate VEGF affecting other growth factors and cytokines, which stimulate the development of basic and collateral circulation. tPA mobilise CD11b cells and VEGFR-1 + cells from the bone marrow, accelerates healing and neovascularisation of ischemic tissue [36]. This process indicates that the normal concentrations of PAI-1 in circulation is another therapeutic approach in the treatment of ischemic tissue in the type 2 diabetic patients.

Conclusion

The determination of concentration of vitamin D levels in the obese patients, patients with metabolic syndrome and type 2 diabetes is useful, because the concentration of vitamin D in these patients is reduced. An adequate substitution of vitamin D contributes to a better quality of glycemic control. In fasting hypoglycaemia and postprandial hyperglycaemia is always overlooked the presence of insulin antibodies and insulin receptor antibody, which substantially impairs the quality of glycemic control both in type 1 and type 2 diabetes. Normal concentrations of PAI-1 is another therapeutic approach in the treatment of the ischemic tissue in the type 2 diabetic patients.

By applying new parameter CAVI, data on early and evolutionary arteriosclerosis could be obtained. Every contribution to the science pointing to all processes in the development of diabetes is valuable in order to acheieve the clear diagnosis and treatment of this disease.

R E F E R E N C E S

1. *Hao JB, Imam S, Dar P, Alfonso-Jaume M, Elnagar N, Jaume JC.* Extreme insulin resistance from insulin antibodies (not insulin receptor antibodies) successfully treated with combination immunosuppressive therapy. Diabetes Care 2017; 40(2): e19–e20.
2. *Maiza J, Caron-Debarle M, Vigouroux C, Schneebeli S.* Anti-insulin receptor antibodies related to hypoglycemia in a previously diabetic patient. Diabetes Care 2013; 36(6): e77.
3. *Cryer PE, Axelrod L, Grossman AB, Heller SR, Montori VM, Seaquist ER,* et al. Endocrine Society Evaluation and management of adult hypoglycemic disorders: an Endocrine Society Clinical Practice Guideline. J Clin Endocrinol Metab 2009; 94(3): 709–28.
4. *Talaei A, Mohamadi M, Adgi Z.* The effect of vitamin D on insulin resistance in patients with type 2 diabetes. Diabetol Metab Syndr 2013; 5(1): 8.
5. *Pittas AG, Dawson-Hughes B, Li T, Van DR, Willett WC, Manson JE*, et al. Vitamin D and calcium intake in relation to type 2 diabetes in women. Diabetes Care 2006; 29(3): 650–6.
6. *Scragg R, Sowers MF, Bell C.* Serum 25-hydroxyvitamin D, diabetes and ethnicity in the third National Health and Nutrition Examination Survey. Diabetes Care 2004; 27(12): 2813–8.
7. *Jennersjö P, Guldbrand H, Björne S, Länne T, Fredrikson M, Lindström T,* et al. A prospective observational study of all-cause mortality in relation to serum 25-OH vitamin D3 and parathyroid hormone levels in patients with type 2 diabetes. Diabetol Metab Syndr 2015; 7: 53.
8. *de Boer IH.* Vitamin D and glucose metabolism in chronic kidney disease. Curr Opin Nephrol Hypertens 2008; 17(6): 566–72.
9. *Shet JJ, Shah A, Sheth FJ, Tivedi S, Lele M, Shah N,* et al. Does vitamin D play a siglificant role in type 2 diabetes? BNC Endocr Disord 2015; 15: 5.
10. *Ahmedieh H, Azar ST, Lakkis N, Arabi A.* Hypovitaminosis D in patients with type 2 diabetes mellitus: A relation to disease control and complication. ISRN Endocrinol 2013; 2013: 641098.
11. *Zoppini G, Galletti A, Targher G, Brangani C, Pichiri I, Trombetta M*, et al. Lower levels of 25-hydroxyvitamin D3 are associated with a higher prevalence of microvascular complication in patients with type 2 diabetes. BMJ Op Diab Res Car 2015; 3: 58.
12. *Timms PM, Mannan N, Hitman GA, Noonan K, Mills PG, Syndercombe-Court D,* et al. Circulating MMP9, vitamin D and variation in the TIMP-1 response with VDR genotype: mechanisms for inflammatory damage in chronic disorders. QJM 2002; 95(12): 787–96.
13. *Sanchez-Niño MD, Bozic M, Córdoba-Lanús E, Valcheva P, Gracia O, Ibarz M,* et al. Beyond proteinuria: VDR activation reduces renal inflammation in experimental diabetic nephropathy. Am J Physiol Renal Physiol 2012; 302(6): F647–57.
14. *Li YC, Kong J, Wei M, Chen Z, Liu SQ, Cao L.* 1,25-Dihydroxyvitamin D(3) is a negative endocrine regulator of the renin-angiotensin system. J Clin Invest 2002; 110(2): 229–38.
15. *Zhang Z, Zhang Y, Ning G, Deb DK, Kong J, Li JC.* Combination therapy with AT1 blocker and vitamin D analog markedly ameliorates diabetic nephropathy. Blockade of compensatory renin increase. Proc Natl Acad Sci USA 2008; 105(41): 15886–901.
16. *Suzuki A, Kotake M, Ono Y, Kato T, Oda N, Hayakawa N*, et al. Hypovitaminosis D in type 2 diabetes mellitus: Association with microvascular complications and type of treatment. Endocr J 2006; 53(4): 503–10.
17. *Taverna MJ, Selam J, Slama G.* Association between a protein polymorphism in the start codon of the vitamin D receptor gene and severe diabetic retinopathy in C-peptide-negative type 1 diabetes. J Clin Endocrinol Metab 2005; 90(8): 4803–8.

18. *Inuki T, Fujiwara Y, Tayama K, Aso Y, Takemura Y*. Alterations in serum levels of 1alfa, 25(OH)2D and osteocalcin in patients wwith early diabetic nephropathy. Diab Res Clin Pract 2005; 38(1): 53–9.
19. *Jee D, Han K, Kim EC*. Inverse association between high blood 25-hydroxyvitamin D levels and diabetic retinopathy in a representative Korean population. PLoS One 2014; 9(12): e115199.
20. *Basit A, Basit KA, Fawward A, Shaheen F, Fatima N, Petropoulos N*, et al. Vitamin D for the treatment of painful diabetic neuropathy. BMJ Open Diabetes Res Care 2016; 4(1): e000148.
21. *Somjen D, Weisman Y, Kohen F, Gayer B, Limor R, Sharon O*, et al. 25-hydroxyvitamin D3-1alpha-hydroxylase is expressed in human vascular smooth muscle cells and is upregulated by parathyroid hormone and estrogenic compounds. Circulation 2005; 111(13): 1666–71.
22. *Shirai K, Utino J, Otsuka K, Takata M*. A novel blood pressure-independent arterial wall stiffness parameter; cardio-ankle vascular index (CAVI). J Atheroscler Thromb 2006; 13(2): 101–7.
23. *Shirai K, Song M, Suzuki J, Kurosu T, Oyama T, Nagayama D*, et al. Contradictory effects of β1- and α1- aderenergic receptor blockers on cardio-ankle vascular stiffness index (CAVI): CAVI independent of blood pressure. J Atheroscler Thromb 2011; 18(1): 49–55.
24. *Suzuki J, Sakakibara R, Tomaru T, Tateno F, Kishi M, Ogawa E, Kurosu T,* et al. Stroke and cardio-ankle vascular stiffness index. J Stroke Cerebrovasc Dis 2013; 22(2): 171–5.
25. *Miyoshi T, Doi M, Hirohata S, Sakane K, Kamikawa S, Kitawaki T*, et al. Cardio-ankle vascular index is independently associated with the severity of coronary atherosclerosis and left ventricular function in patients with ischemic heart disease. J Atheroscler Thromb 2010; 17(3): 249–58.
26. *Kumagai T, Kasai T, Kato M, Naito R, Maeno K, Kasagi S*, et al. Establishment of the cardio-ankle vascular index in patients with obstructive sleep apnea. Chest 2009; 136(3): 779–86.
27. *Shirai K, Hiruta N, Song M, Kurosu T, Suzuki J, Tomaru T*, et al. Cardio-ankle vascular index (CAVI) as a novel indicator of arterial stiffness: theory, evidence and perspectives. J Atheroscler Thromb 2011; 18(11): 924–38.
28. *Carmeliet P, Moons L, Lijnen R, Janssens S, Lupu F, Collen D*, et al. Inhibitory role of plasminogen activator inhibitor-1 in arterial wound healing and neointima formation: a gene targeting and gene transfer study in mice. Circulation 1997; 96(9): 3180–91.
29. *Carmeliet P, Moons L, Stassen JM, De Mol M, Bouché A, van den Oord JJ,* et al. Vascular wound healing and neointima formation induced by perivascular electric injury in mice. Am J Pathol 1997; 150(2): 761–76.
30. *Renckens R, Roelofs JJ, de Waard V, Florquin S, Lijnen R, Carmeliet P*. The role of plasminogen activator inhibitor type 1 in the inflammatory response to local tissue injury. J Thromb Haemost 2005; 3(5): 1018–25.
31. *Gregory AD, Capoccia BJ, Woloszynek JR, Link DC*. Systemic levels of G-CSF and interleukin-6 determine the angiogenic potential of bone marrow resident monocytes. J Leukoc Biol 2010; 88(1): 123–31.
32. *Jin DK, Shido K, Kopp H, Petit I, Shmelkov SV, Young LM,* et al. Cytokine-mediated deployment of SDF-1 induces revascularization through recruitment of CXCR4+ hemangiocytes. Nat Med 2006; 12(5): 557–67.
33. *Oh CW, Hoover-Plow J, Plow EF*. The role of plasminogen in angiogenesis in vivo. J Thromb Haemost 2003; 1(8): 1683–734.
34. *Murakami M, Simons M*. Fibroblast growth factor regulation of neovascularization. Curr Opin Hematol 2008; 15(3): 215–20.
35. *Muhs BE, Plitas G, Delgado Y, Ianus I, Shaw JP, Adelman MA*, et al. Temporal expression and activation of matrix metalloproteinases-2, -9, and membrane type 1-matrix metalloproteinase following acute hindlimb ischemia. J Surg Res 2003; 111(1): 8–15.
36. *Magnusson PU, Dimberg A, Mellberg S, Lukinius A, Claesson-Welsh L*. FGFR-1 regulates angiogenesis through cytokines interleukin-4 and pleiotrophin. Blood 2007; 110(13): 4214–22.

Received on June 20, 2017.
Accepted on August 21, 2017.
Online September, 2017.

CASE REPORTS

UDC: 616.8-053.2
https://doi.org/10.2298/VSP170406120I

GLUT1 deficiency syndrome: a case report with a novel *SLC2A1* mutation

GLUT1 sindrom deficijencije – prikaz bolesnika sa mutacijom u *SLC2A1* genu

Nikola Ivančević*, Nataša Cerovac*, Blažo Nikolić*, Goran Čuturilo†, Ana Marjanović‡, Marija Branković‡, Ivana Novaković‡

Univeristy of Belgrade, Faculty of Medicine, *Clinic of Neurology and Psychiatry for Children and Youth, †University Children's Hospital, ‡Clinic of Neurology, Belgrade, Serbia

Abstract

Introduction. GLUT1 deficiency syndrome (GLUT1 DS, *OMIM 606777*) is a metabolic brain disorder caused by mutations in *SLC2A1* gene (chromosome 1) encoding glucose transporter type 1 located on blood-brain membrane. The "classic" phenotype in children includes early onset generalized farmacoresistant epilepsy, developmental delay, complex movement disorders and acquired microcephaly. However, there are milder phenotypes without epilepsy which could be seen in older children. The ketogenic diet is a treatment of choice. **Case report.** We present a four-year-old female patient with farmacoresistant generalized epilepsy, paroxysmal dystonic posturing, ataxia, hypotonia, developmental delay (motor, attention and speech disturbances), and microcephaly. The genetic testing revealed a novel point mutation at c.156T > A (p.Y52X) in exon 3 of *SLC2A1* gene. The patient responded excellent on ketogenic diet. **Conclusion.** GLUT1 DS is treatable, and likely to be under-diagnosed neurological disorder. The ketogenic diet is resulting in good control of seizures in the patients, and it has certain benefit for the neurodevelopmental disability.

Key words:
glut1 deficiency syndrome; diagnosis; diet ketogenic; treatment outcome.

Apstrakt

Uvod. GLUT1 sindrom deficijencije (GLUT1 DS, *OMIM 606777*) je metaboličko oboljenje mozga uzrokovano mutacijom u *SLC2A1* genu (hromozom 1) koji kodira transporter glukoze tip 1 lokalizovan na krvno-moždanoj barijeri. "Klasični" fenotip kod dece uključuje ranu pojavu generalizovane farmakorezistentne epilepsije, usporen psihomotorni razvoj, poremećaje pokreta i stečenu mikrocefaliju. Međutim, blaži fenotipovi bez pojave epilepsije mogu se videti i u kasnijem uzrastu. Ketogena dijeta je terapija izbora. **Prikaz bolesnika.** U radu je prikazana devojčica, uzrasta četiri godine sa farmakorezistentnom generalizovanom epilepsijom, paroksizmalnim distonijama, ataksijom, hipotonijom, usporenim razvojem (poremećajima motorike, pažnje i govora) i mikrocefalijom. Genetsko testiranje je otkrilo novu tačkastu mutaciju u c.156T > A (p.Y52X) na egzonu 3 *SLC2A1* gena. Kod bolesnice je primećeno poboljšanje u kliničkom nalazu na primenu ketogene dijete. **Zaključak.** GLUT1 DS je lečiva neurološka bolest, koja je verovatno nedovoljno prepoznata. Ketogena dijeta dovodi do povoljne kontrole napada kod dece, a doprinosi izvesnom poboljšanju u neurološkom nalazu.

Ključne reči:
sindrom deficijencije glut1; dijagnoza; dijeta, ketogena; lečenje, ishod.

Introduction

GLUT1 deficiency syndrome (GLUT1 DS, *OMIM 606777*) is a metabolic brain disorder arising from mutations in the neuronal glucose transporter GLUT1 (now designed *SLC2A1*) at short arm of chromosome 1 (1p35–31.3)[1]. GLUT1 located at the blood brain barrier is the main vehicle for glucose transport into the brain. The disease is caused by impaired D-glucose transport across the blood brain barrier, exposing the brain to the risk of energy failure.

The syndrome was first described by De Vivo et al.[2] (1991) in two children with early-onset epilepsy, developmental delay and acquired microcephaly. They had a low cerebrospinal fluid concentration of glucose and normal plasma glucose concentration. GLUT1 DS is characterized by infantile onset refractory epilepsy, cognitive and motor develop-

Correspondence to: Nikola Ivančević, Clinic for Neurology and Psychytry for Children and Youth, Neurology Department, Dr Subotica 6a, 11 000 Belgrade, Serbia. E-mail: nikola.ivancevic.npk@gmail.com

mental delay, and mixed motor disorders including spasticity, ataxia and dystonia [1]. Affected infants have neurodevelopmental impairment of variable severity and acquired microcephaly. Some patients have milder phenotypes and others have more severe with permanent neurological deficits. The cardinal biochemical feature is a decreased ratio of cerebrospinal fluid glucose relative to the plasma glucose concentration [3].

GLUT1 DS is caused by haploinsufficiency of *SLC2A1* gene due to a *de novo* heterozygous mutation in a majority (90%) of cases. About 10% of patients have autosomal dominant inheritance and one affected parent, and only a few cases have autosomal recessive [1, 3].

GLUT1 DS is a treatable disorder and a lot of patients, especially those with a mild phenotype, are likely to be underdiagnosed [1–3]. The ketogenic diet is the mainstay of treatment, resulting in good control of seizures in most patients and it has certain benefit for the neurodevelopmental disability.

Case report

We presented a four-year-old female infant born at term by vaginal vertex delivery. There were no complications during pregnancy. Birth weight was 3 300 g and the 5-minutes Apgar score was 10. The physical examination at birth was without signs of abnormalities. Her parents were nonconsanguineous and healthy. Family history was unremarkable with no history of developmental problems, learning deficits, birth defects or genetic syndromes.

At the age of 6 months, the neurological examination revealed microcephaly, mild hypotonia, reduced motor activity, brisk deep tendon reflexes and developmental delay. The girl started to sit without support from the age of one year and to walk on a wide base, with support and with spastic-ataxic component from the age of two and a half years. She never attained the ability to walk. Speech development was also delayed. She had dysarthria with difficult understanding and very poor expressive speech. She was able to put words into phrases from the age of three years and her developmental quotient was 60. She had moderate intellectual impairment. Intensive physical and speech rehabilitation was performed.

First seizures were noticed starting from the age of 18 months with brief episodes of unresponsiveness, eye movements, head bobbing and hypotonia. The interictal electroencephalography (EEG) recording showed generalized spike and wave discharges with a frequency of 2.5–4 Hz. Antiepileptic therapy was given (valproate 30 mg/kg) and it resulted in exacerbation of seizures, so the drug was excluded. The seizures were also resistant to antiepileptic drugs clonazepam, clobasam and lamotrigine. Atypical absence seizures as the most common type of seizures were noticed at the age of three years and ethosuximide was introduced. The girl responded readily and better control of seizures was achieved. Later, levetiracetam was added with satisfactory results. The magnetic resonance imaging (MRI) of the brain done twice at the age of two and three years was normal. Metabolic investigations were within normal limits.

The genetic testing encompassed array comparative genomic hybridization (aCGH) and *SLC2A1* gene sequencing. Normal result was obtained using aCGH, showing only one polymorphic copy number variant (loss of approx. 1.3 Mb at 15q11.2). Sanger sequencing of *SLC2A1* gene disclosed variant c.156T > A (p.Y52X) in the exon 3 of the gene. This variant was not reported in the databases of The Exome Aggregation Consortium (ExAC), 1000 Genomes, and Human Gene Mutation Database (HGMD). The prediction analysis using the MutationTaster software indicated pathogenicity of the variant.

After the diagnosis of GLUT1 DS had been confirmed, the ketogenic diet (4 : 1 ratio) was introduced. Complete control of seizures was achieved. The girl is now 4 years old and shows delay in psychomotor development. She has microcephaly, abnormal gait (spastic-ataxic) and speech delay. She does not have seizures at all.

Discussion

Most patients with GLUT1 DS have perinatal history without complications, like in our reported patient [3]. The neurological findings in the "classic" GLUT1 DS include epileptic encephalopathy, complex movement disorders (ataxia, dystonia, spasticity) and developmental delay including cognitive deficits. It also includes hypotonia and acquired microcephaly. Our patient showed all these characteristic features. In the literature, the average age for confirming diagnosis is 5 years [4] and in our patient it was 4 years.

Recently, the "non-classic" clinical features of GLUT1 DS have included familiar and sporadic paroxysmal exercise-induced dyskinesia with or without epilepsy [5–7]. It could also include varying degrees of cognitive deficits, dysarthria, dysfluency and expressive language deficits. Awareness of the broad range of potential clinical phenotypes associated with GLUT1 DS facilitates diagnosis. Post et al. [8] listed the most frequent movement disorders as gait disturbances, dystonia, chorea, non-epileptic paroxysmal events, etc. Most patients have several types of movement disorders. Additionally, the syndrome of paroxysmal choreoathetosis with spasticity (DYT9), and paroxysmal exertional dyskinesia (DYT18) were also included as a part of clinical variability of GLUT1 DS [9, 10].

The onset of seizures in GLUT1 DS occurs between 4 weeks and 18 months of age and in our patient the onset was at the age of 18 months. They include all seizure types (focal, generalized, absence and myoclonic) and are resistant to antiepileptic drugs [3, 11]. In our patient, atypical absence seizures were observed to be resistant to different drugs. They showed, however, good clinical response to etosuximide and levetiracetam. The EEG findings in our patient was also typical for this syndrome (generalized 2.5–4 Hz spike and wave discharges), while the neuroimaging findings as normal [1]. In fact, the conventional anatomic neuroimaging with computed tomography (CT) or the MRI is typically normal in the patients with GLUT1 DS, whereas the metabolic imaging with ^{18}F-fluorodeoxyglucose positron emission tomography (FDG-PET) reveals a distinctive pattern of

hypometabolism in the thalami and mesial temporal regions. It suggests impaired function of thalamo-cortical network as an important factor in epileptogenesis [12].

Certain antiepileptic drugs, like valproate, have the potential to exacerbate seizures and that happened to our patient. It is confirmed that valproate can significantly inhibit the GLUT1 function and glucose transport resulting in the increased seizure activity in the patient with GLUT1 DS. Therefore, it is important to be careful with the use of valproate in the patient with compromised function of GLUT1 [1, 13].

The ketogenic diet (high-fat, carbohydrate-restricted) plays an indispensible role in the treatment of GLUT1 DS. It mimics the metabolic state of fasting, providing ketone bodies, derived from the hepatic metabolism of fatty acid, as an alternative fuel source for the brain. Therefore, the ketogenic diet is a proven therapy for the treatment of seizures and other clinical features of the syndrome. This treatment in our patient resulted in subsequent improvement in her neurological status (gait, ataxia, spasticity) as well as cessation of seizures [14–16].

Our patient fulfilled the criteria for the "classic" phenotype of GLUT1 DS: epilepsy, developmental delay, cognitive deficit, microcephalia, hypotonia, spasticity and a complex movement disorders (ataxia, dystonia). The diagnosis in our patient was confirmed by identification of pathogenic nucleotide substitution in the exon 3 of the *SLC2A1* gene.

The phenotype-genotype correlation is not well-established. The relationship between clinical and genetic characteristics is analyzed in one study [17]. Sporadic cases with *SLC2A1 de novo* mutation (direct gene sequencing revealed missense, nonsense and splice site mutation) had a more severe phenotype than familiar cases (all patients presented with missense mutation). Sporadic cases had more profound cognitive disability, more severe form of epilepsy and neurologic deficits. The milder phenotype was observed in familiar cases in the form of "benign" epilepsy and slight movement disorder. Another study presented that missense mutations more frequently showed "mild" phenotype [18], which, of course, could be observed in a variety of other genetic disorders. However, the patients with the same mutation could show phenotypic variety, suggesting that other genes or other proteins are involved in glucose transport, pathophysiology of the disease and phenotype. It raises the unsolved question on the real incidence of GLUT1 DS, treatment with ketogenic diet in milder forms of disease and concerns about genetic counseling [19, 20].

Conclusion

We presented the patient with GLUT1 DS, novel causative *SCL2A1* gene variant and effective treatment with ketogenic diet. Although presentation was rather typical, diagnosis was confirmed at the age of 4 years which is in concordance with reports from other centers. It is well-established that early initiation of the ketogenic diet results in better seizure control and improves the neurologic outcome. One solution could be an employment of massive parallel gene sequencing in an early course of infantile seizures, which could provide timely diagnosis in a substantial proportion of patients.

Acknowledgements

This work was supported by the Serbian Ministry of Education, Science and Technological Development (Grant ON175091).

R E F E R E N C E S

1. *Klepper J, Leiendecker B.* GLUT1 deficiency syndrome-2007 update. Dev Med Child Neurol 2007; 49(9): 707–16.
2. *De Vivo DC, Trifiletti RR, Jacobson RI, Ronen GM, Behmand RA, Harik SI.* Defective glucose transport across the blood-brain barrier as a cause of persistent hypoglycorrhachia, seizures, and developmental delay. N Engl J Med 1991; 325(10): 703–9.
3. *Pearson TS, Akman C, Hinton VJ, Kristin E, De Vivo DC.* Phenotypic spectrum of glucose transporter type 1 deficiency syndrome (Glut1DS). Curr Neurol Neurosci Rep 2013; 13(4): 342.
4. *Pong AW, Geary BR, Engelstad KM, Natarajan A, Yang H, De Vivo DC.* Glucose transporter type I deficiency syndrome: epilepsy phenotypes and outcomes. Epilepsia 2012; 53(9): 1503–10.
5. *Klepper J.* GLUT1 deficiency syndrome in clinica practise. Epilepsy Res 2012; 100(3): 272–7.
6. *Brockmann K.* The expanding phenotype of GLUT1-deficiency syndrome. Brain Dev 2009; 31(7): 545-52.
7. *Schneider SA, Paisan-Ruiz C, Garcia-Gorostiaga J, Quinn NP, Weber YG, Lerche H* et al. GLUT1 gene mutations cause sporadic paroxysmal exercise-induced dyskinesias. Mov Disord 2009; 24(11): 1684–8.
8. *Post R, Collins A, Rotstein M, Engelstad K, De Vivo DC.* The spectrum of movement disorders in Glut-1 deficiency. Mov Disord 2010; 25(3): 275–81.
9. *Auberger G, Ratzlaft T, Lankes A, Nelles HW, Leube B, Binkofski F,* et al. A gene for autosomal dominant paroxismal choreoathetosis/spasticity (CSE) maps to the vicinity of a potassium channel gene cluster on chromosome 1p, probably within 2cM between D1S443 and D1S197. Genomics 1996; 31(1): 90–4.
10. *Weber YG, Kamm C, Suls A, Kempfle J, Kotschet K, Schule R,* et al. Paroxysmal choreoathetosis/spasticity (DYT9) is caused by GLUT1 defect. Neurology 2011; 77(10): 959–64.
11. *Larsen J, Johannesen KM, Ek J, Tang S, Marini C, Blichfeldt S,* et al. The role of SLC2A1 mutations in myoclonic astatic epielpsy and absence epilepsy, and the estimated frequency of GLUT1 deficiency syndrome. Epilepsia 2015; 56 (12): e203–8.
12. *Akman CI, Provenzano F, Wang D, Engelstad K, Hinton V, Yu J,* et al. Topography of brain glucose hypometabolism and epileptic network in glucose transporter 1 deficiency. Epilepsy Res 2015; 110: 206–15.
13. *Wong HY, Chu TS, Lai JC, Fung KP, Fok TF, Fujii T,* et al. Sodium valproate inhibits glucose transport and exacerbates Glut1-deficiency in vitro. J Cell Biochem 2005; 96(4): 775–85.
14. *Baranano KW, Hartman AL.* The ketogenic diet: uses in epilepsy and other neurologic ilnesses. Curr Treat Options Neurol 2008; 10(6): 410–9.
15. *Strafstrom CE, Rho JM.* The ketogenic diet as a treatment paradigm for diverse neurological disorders. Front Pharmacol 2012; 3: 59.
16. *Gano LB, Patel M, Rho JM.* Ketogenic diets, mitocondria, and neurological disease. J Lipid Res 2014; 55(11): 2211–28.

17. *De Giorgis V, Teutonico F, Cereda C, Balottin U, Bianchi M, Giordano L,* et al. Sporadic and familiar glut1ds Italian patients: a wide clinical variability. Seizure 2015; 24: 28–32.
18. *Leen WG, Klepper J, Verbeek MM, Leferink M, Hofste T, van Engelen BG,* et al. Glucose transporter-1 deficiency síndrome: the expanding clinical and genetic spectrum of a treatable disorder. Brain 2010; 133(Pt 3): 655–70.
19. *De Giorgis V, Veggiotti P.* GLUT1 deficiency síndrome 2013; current state of the art. Seizure 2013; 22(10): 803–11.
20. *Melnikova AM, Korff CM.* Clinical variability of GLUT1DS. Seizure Disord 2015; 29(2): 14.

Received on April 06, 2017.
Accepted on July 07, 2017.
Online First September, 2017.

CASE REPORT

UDC: 618.11-006
https://doi.org/10.2298/VSP170424107R

Clear cell/endometrioid type ovarian carcinoma associated with endometriosis of the ipsilateral ovary

Svetloćelijski/endometrioidni karcinom jajnika udružen sa endometriozom u istom jajniku

Ivana Rudić Biljić-Erski*, Mladenko Vasiljević*†, Snežana Rakić*†, Olivera Džatić-Smiljković*†, Sladjana Mihajlović*

***Clinic of Gynecology and Obstetrics "Narodni Front", Belgrade, Serbia; University of Belgrade, †Faculty of Medicine, Belgrade, Serbia**

Abstract

Introduction. Ovarian endometriosis has been identified as a risk factor for occurrence of endometriosis-associated ovarian carcinoma. We presented a rare case of simultaneous clear cell/ endometrioid ovarian carcinoma and endometriosis of the ipsilateral ovary. **Case report.** A 47-year-old patient underwent surgery for right ovarian endometriotic cyst. A total hysterectomy with bilateral salpingo-oophorectomy, lymphadenectomy in the right psoas muscle region and omentectomy were performed as well as multiple peritoneal biopsies. Six cycles of chemotherapy were instituted postoperatively using the Taxol-CBDCA protocol. Abdominal and pelvic CT did not demonstrate recurrence of the disease postoperatively and after completed chemotherapy treatment. Six months after the completion of treatment, the patient felt well without the disease recurrence. **Conclusion.** Clear cell and endometrioid subtypes of ovarian carcinoma have good prognosis if they are diagnosed and treated at an early stage of the disease. In our patient, the carcinoma was detected in the first stage and successfully treated with combination therapy, i.e., surgical and chemotherapy.

Key words:
adenocarcinoma, clear cell; diagnosis; endometriosis; ovarian neoplasms; treatment outcome.

Apstrakt

Uvod. Endometrioza jajnika je identifikovana kao faktor rizika od nastanka karcinoma jajnika udruženog sa endometriozom. Prikazali smo bolesnicu sa istovremenom pojavom svetloćelijskog/endometrioidnog tipa karcinoma jajnika i endometrioze u istom jajniku. **Prikaz bolesnika.** Bolesnica, stara 47 godina, podvrgnuta je operativnom zahvatu zbog endometriotične ciste na desnom jajniku. Urađena je histerektomija sa obostranom adneksektomijom, limfadenektomija regije desnog slabinskog mišića, omentektomija i višestruke biopsije peritoneuma. Posle operacije primenjena je hemioterapija u toku šest ciklusa po protokolu Taxol-CBDCA. Nakon hiruškog zahvata i sprovedenog lečenja hemioterapijom urađen je kontrolni CT abdomena i male karlice i kod bolesnice nisu nađeni znakovi recidiva bolesti. Šest meseci posle završenog lečenja bolesnica se dobro osećala i nije imala recidiv bolesti. **Zaključak.** Svetloćelijski i endometrioidni podtip karcinoma jajnika imaju dobru prognozu ako se otkriju i leče u ranom stadijumu bolesti. Kod prikazane bolesnice karcinom je otkriven u prvom stadijumu i uspešno je lečen kombinovanom terapijom tj. hiruški i hemioterapijom.

Ključne reči:
adenokarcinom svetlih ćelija; dijagnoza; endometrioza; jajnik, neoplazme; lečenje, ishod.

Introduction

Endometriosis is a benign gynecological condition characterised by specific histological, molecular and clinical findings. Prevalence of endometriosis among the women of reproductive age is 10%–15%, increasing to 30% in the infertile women [1]. Endometriosis is considered as a considerable risk factor for development of several subtypes of epithelial ovarian carcinoma (clear cell and endometrioid carcinoma) known as endometriosis-associated ovarian carcinoma (EAOC) [2, 3]. The incidence of ovarian cancer in general population ranges between 5 and 9 new cases per 100,000 women per year, and ovarian cancer is known to develop in 0.3%–1.6% of women with endometriosis [4]. We presented a rare case of simultaneous clear cell/endometrioid ovarian carcinoma and endometriosis of the ipsilateral ovary.

Correspondence to: Ivana Rudić Biljić-Erski, Mihaila, Avramovića 22, 11 000 Belgrade, Serbia. E-mail: rudic.biljic@gmail.com

Case report

A 47-year-old patient was admitted to our clinic for surgery due to presence of a right ovarian endometriotic cyst and pelvic pain. The onset of pelvic pain was one month prior to hospital admission. Menstrual cycles were regular, 25 days in length. The patient was a nulligravida. The patient appeared generally well, with a normal nutritional status and blood pressure. The right ovarian endometriotic cyst was diagnosed by ultrasound 4 years before. Furthermore, the patient had history of laparoscopic surgery 13 years ago for a benign left ovarian cyst. The patient did not see her doctor for regular gynecologic exams. Family history was negative for malignancies. The gynecologic bimanual exam revealed a palpable and tender right adnexal cystic mass, measuring 50–60 mm. Two-dimensional transvaginal ultrasound revealed the anteverted uterus with a normal external uterine contour, measuring 70 × 51 × 51 mm. Endometrial lining had normal contours and its thickness measured 6 mm. A multiloculated cystic tumour of the right ovary measured 70 × 60 mm and contained hyperechoic and viscous material on ultrasound. A solid hyperechoic formation, measuring 25 × 25 mm, was seen in the lower half of the right ovarian cystic mass. The capsule of the cyst measured 3.5 mm. The left ovary measured 28 × 22 mm and was normal on ultrasound. Abdominal ultrasound was normal. Paraaortic and pelvic lymph nodes were not enlarged. Preoperative ultrasound findings of internal genitalia are demonstrated on Figures 1, 2 and 3.

Colour flow Doppler of pericystic vessels and the blood vessels of solid portions of the cyst were performed and the resistance indices (RI) of 0.50 and 0.42 were measured respectively. Increased tumour marker levels of the cancer antigen 125 (CA-125) were noted at 594 U/mL (normal range is less than 46 U/mL). Human epididymis protein 4 (HE4) levels were within a normal reference range (HE4 = 42.8 pmol/L). The risk of ovarian malignancy algorithm (ROMA index) value was calculated to be 18%, which was considered a high-risk in a premenopausal woman. Complete blood count, urea, creatinine, electrolytes, liver function tests, urinalysis and urine culture were all within normal limits. Colposcopic exam and Pap smear were normal. Internal medicine and anaesthesiology consults were sought and the examinations were found to be normal. The patient underwent a total abdominal hysterectomy with bilateral salpingo-oophorectomy. Wide adhesions covering the fundus and anterior uterus were noticed intraoperatively and adhered to the anterior pelvic wall and bladder peritoneum. A cystic formation measuring 60 × 70 mm was seen on the right ovary, which adhered to the uterus, right Fallopian tube and the lateral pelvic wall. The left ovary and Fallopian tube had a normal gross appearance, with adhesions to the uterus and peritoneum of the lateral pelvic wall. Multiple endometriotic implants were seen on the uterosacral ligaments and the pouch of the Douglas peritoneum. During the resection of right ovarian adhesions, the ovarian cyst ruptured. Gross pathological changes were not seen on the liver, stomach, large and small intestines, and the omentum. The histopathology results revealed the following: ovarian adenocarcinoma I, endometrioid/clear cell type, HG1 NG2, which was also found on the surface of the cyst. Further histopathology revealed ovarian endometriosis. Histopathology of the Fallopian tubes was normal. Uterine histopathology revealed an intramural fibroid and adenomyosis. Cervical histopathology revealed chronic cervicitis. The histopathology of removed right ovary diagnosed both endometriosis and ovarian carcinoma (Figure 4).

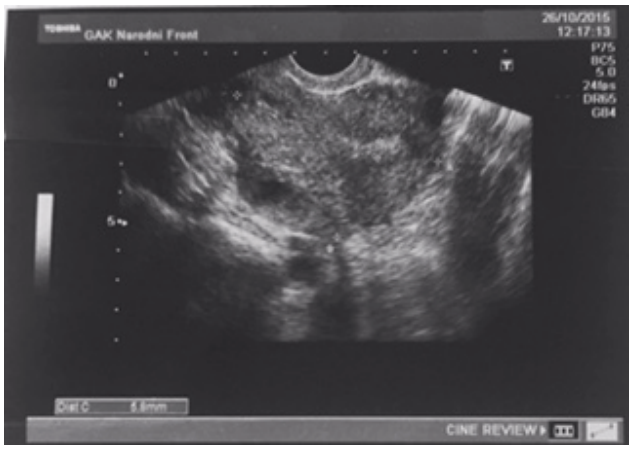

Fig. 1 – A normal sized uterus with a homogeneous echotexture.

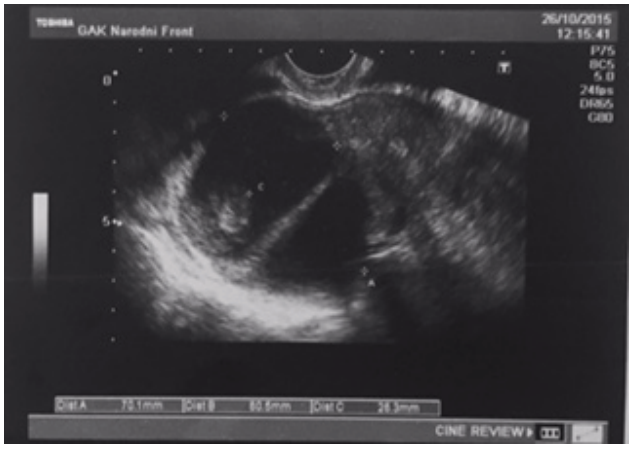

Fig. 2 – Right ovarian bilocular cystic tumour with viscous content. A regular and thin septum is present within the cyst. A hyperechoic solid tissue element is visible in the inferior half of the cyst.

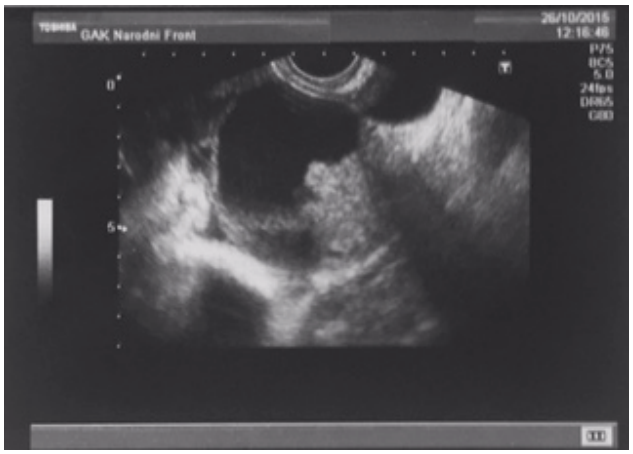

Fig. 3 – Hyperechoic solid tissue element at the inferior pole of the right ovarian cyst.

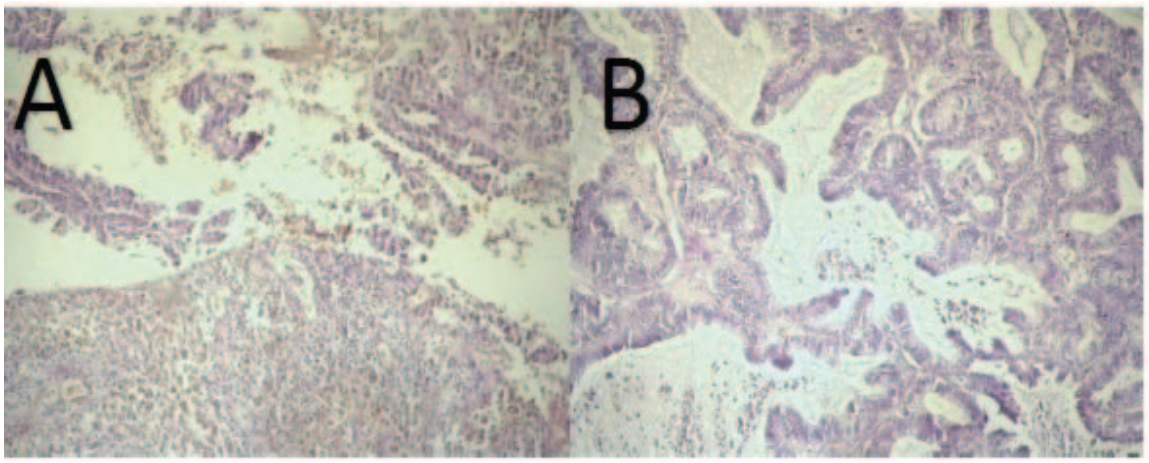

Fig. 4 – Histopathological types of ovarian carcinoma of the right ovary: A) Clear cell carcinoma and endometriosis (hematoxylin and eosin, ×10); B) Endometrioid carcinoma (hematoxylin and eosin, ×20).

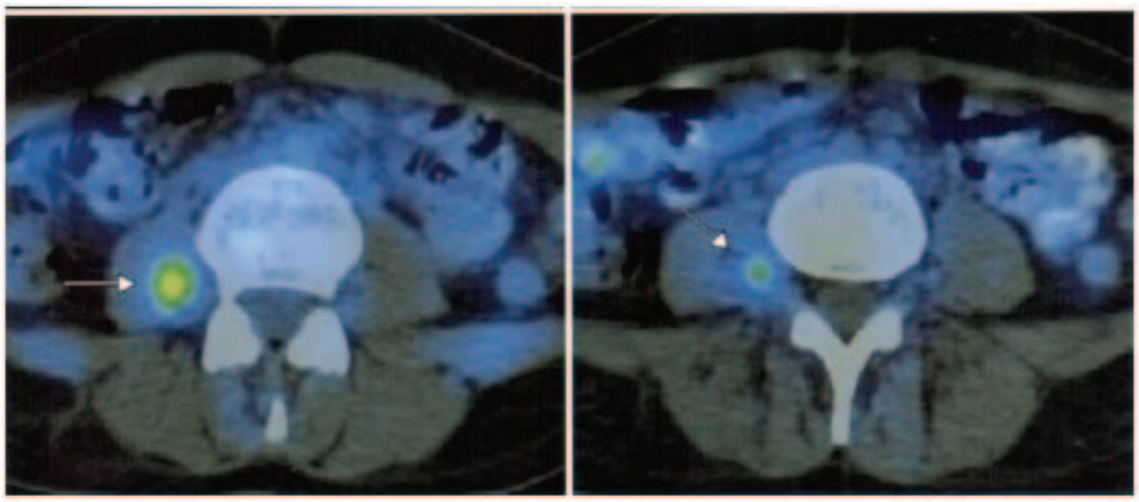

Fig. 5 – Positron emission tomography-computed tomography (PET-CT) scan: an enlarged lymph node, suspicious of metastases, is visible between the right psoas muscle and the spinal column.

The disease was staged using the Tumor-Node-Metastasis (TNM) and International Federation of Gynecology and Obstetrics (FIGO) classifications and was classified as follows: pT1c-N0-M0 (FIGO IC). The patient's case was presented to the Council for Malignant Gynecologic Diseases and the Council decided to perform positron emission tomography (PET) and computed tomography (CT) of the abdomen and pelvics. PET/CT of the abdomen and pelvis did not find any pathological lesions; pelvic and paraaortic lymph nodes were not enlarged. An enlarged lymph node, suspicious of metastasis, measuring 15 × 10 mm, was noted in-between the right psoas muscle and the spine. Postoperative findings of the PET/CT scan are shown in Figure 5.

The PET/CT findings were presented and the Council decided that the patient should undergo radical surgery according to the protocol for ovarian cancer. The patient underwent the second surgery with lymphadenectomy in the right psoas muscle region, omentectomy and multiple peritoneal biopsies. Swabs from the peritoneum of the pouch of Douglas, bilateral paracolic gutters, and subdiaphragmatic areas were obtained. Cytologic washings of the peritoneal cavity were obtained. The histopathology results were as follows: Reactive follicular hyperplasia and sinus histiocytosis lymphadenopathy; fragments of peritoneal connective vascular tissue without pathological significance. The cytological finding was negative for malignancy. The histopathological findings of the removed lymph node are shown in Figure 6.

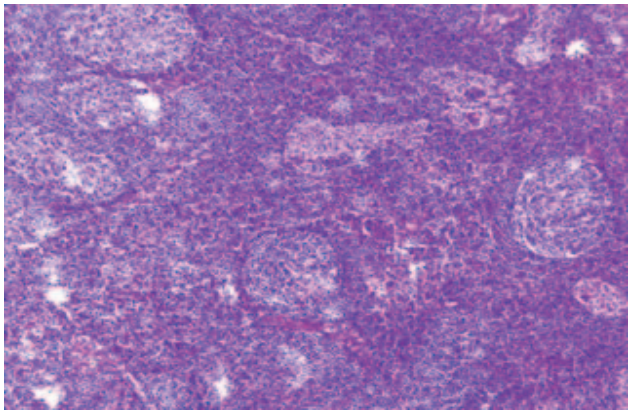

Fig. 6 – Sinus histiocytosis of the lymph node with reactive follicular hyperplasia.

These findings were presented to the Council for Malignant Gynecologic Diseases, and a decision to commence chemotherapy was made, using six cycles of the Taxol (125 mg/m^2) and carboplatin CBCDA (250 mg/m^2) protocol. Tumour markers (CA-125 and HE4) or CT of the pelvis and abdomen were to be repeated before commencing and after the completion of chemotherapy regimen. Prior to commencing chemotherapy, the CA-125 value was reported to be 70 U/L, and the abdominal/pelvic CT did not show any pathological changes. The patient was treated with six cycles of chemotherapy. The follow-up CT of the abdomen and pelvis was normal; CA-125 levels were also within a normal reference range. Six months after treatment, the patient felt generally well, without signs of metastatic disease. The follow-up CT findings of the pelvis and abdomen are shown in Figures 7 and 8.

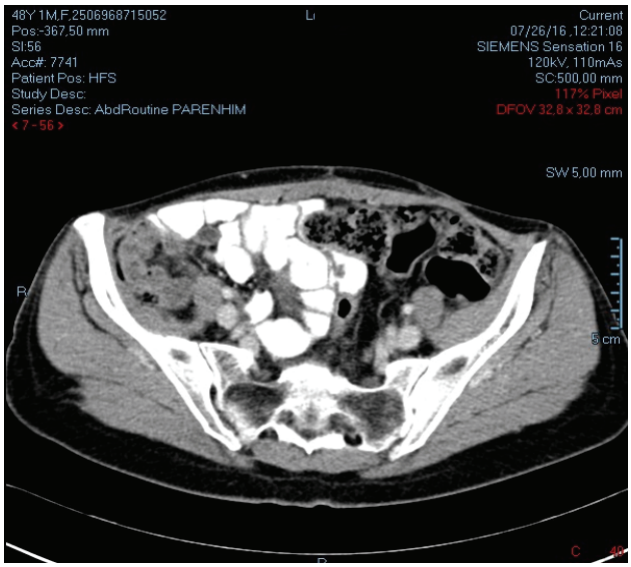

Fig. 7 – Pelvic computed tomography (CT) demonstrates normal bladder and intestines.

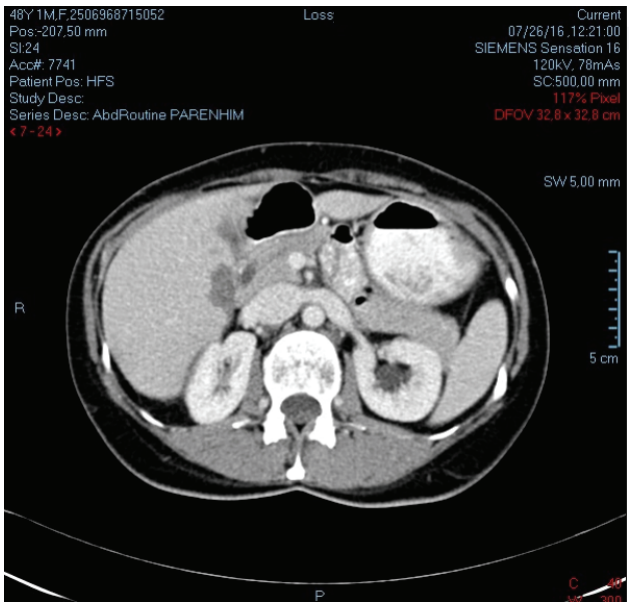

Fig. 8 – Normal computed tomography (CT) of abdominal organs.

Discussion

Endometriosis has been found to be associated with some histological subtypes of epithelial ovarian carcinoma, such as clear cell, endometrioid and low malignant potential serous carcinoma. These are known as EAOCs [5, 6]. EAOCs are usually diagnosed at an early stage in the patients with endometriosis, and these are usually low malignant potential carcinomas. Endometriosis is diagnosed in 4.2% of patients with ovarian carcinoma [6]. Endometriosis and epithelial carcinoma of the ipsilateral ovary have been associated in 2.5% of patients. The women with endometriosis have a 1.7 times higher risk of ovarian cancer than the women without endometriosis. The nulliparous women with endometriosis have a three times increased risk of ovarian cancer than the women who have given birth [2]. Our patient had a history of infertility which was assessed and had been treated. Endometrioid tumours constitute 15%–25% of epithelial ovarian carcinomas. Clear cell subtype constitutes 5%–25% of epithelial ovarian carcinomas. The mixed clear cell/endometrioid subtype constitutes 1.3% of all ovarian carcinomas. There are 30% to 40% of women who have an endometrioid carcinoma associated with endometriosis, while this frequency is 30%–55% in the women with clear cell carcinoma [5, 7]. The mechanism by which endometriosis influence the development of ovarian carcinoma is unknown. The molecular level research has identified oxidative stress, inflammation and hyperestrogenism as important mechanisms by which endometriosis may lead to ovarian carcinoma. Due to repeated hemorrhage, heme and free iron accumulate in the endometriotic lesion, leading to the production of oxydative stress, which creates a hypoxic environment that promotes the DNA damage and mutation accumulation. These events play a role in pathophysiology of ovarian carcinoma [2]. Endometriosis is characterized by genetic instability: like neoplasms endometriosis seems to be monoclonal in origin, Advances in genetic have led to the discovery of new mutations and a better understanding of the function of genes and pathways associated with EAOCs [8]. Tumor suppressor genes that were identified as contributors to the development of EAOCs include TP53, PTEN, and ARID1A as well as a proto-oncogene KRAS. ARID1A mutation (AT rich interactive domain 1A) was seen in 46% of ovarian clear-cell carcinomas and in 30% endometrioid carcinomas and was described as a possible early evant in the malignant transformation of endometriosis into carcinoma [9, 10]. The TP53 mutations were seen in 30% of endometriosis associated with clear-cell carcinomas. Hence, the TP53 abnormalities may be involved in malignant transformation of ovarian endometriosis. Some studies suggest that mutation of the tumor suppressor gene PTEN play a part in the malignant transformation of endometriosis [11]. Furthermore, inflammation also has a role in the development of EAOCs. Some studies showed that the peritoneal fluid of women with endometriosis had the increased levels of proinflammatory cytokines and growth factors such as TNF-α, IL-1, IL-6 and IL-8, but these women also had the serum inflammatory markers comparable to those found in the women with ovarian carcinoma [12]. IL-1 may upregulate the

COX2 gene expression leading to the increased secretion of PGE_2; PGE_2 stimulates processes that are characteristic of tumor growth such as angiogenesis, cell proliferation and inhibition of apoptosis. The women with a positive family history for colon cancer or endometrial cancer (Lynch syndrome 2) or hereditary nonpolyposis colorectal carcinoma, have an increased risk of endometrioid ovarian cancer [13]. The women who have mutations in BRCA1 or BRCA2 genes on chromosome 17 and 13 have an increased risk of breast and ovarian carcinomas [14]. The prognosis of EAOC is good at the early stage of the disease. The treatment options include surgical management and chemotherapy, either as separate modalities or in combination [7]. Our patient was treated both surgically and with chemotherapy. Six months after the treatment completion, the patient felt well without the disease recurrence.

Conclusion

Clear cell and endometrioid subtypes of ovarian carcinoma have good prognosis if they are diagnosed and treated at an early stage of the disease. In our patient, the carcinoma was detected in the first stage and successfully treated with combination therapy, i.e., surgical and chemotherapy.

R E F E R E N C E S

1. *Lyttle B, Bernardi L, Pavone ME*. Ovarian cancer in endometriosis: Clinical and molecular aspects. Minerva Ginekol 2014; 66(2): 155–64.
2. *Forte A, Cipollaro M, Galderisi U*. Genetic, epigenetic and stem cell alterations in endometriosis: New insights and potential therapeutic perspectives. Clin Sci 2014; 126(2): 123–38.
3. *Pavone ME, Lyttle BM*. Endometriosis and ovarian cancer: Links, risks, and challenges faced. Int J Womens Health 2015; 7: 663–72.
4. *Jemal A, Bray F, Center MM, Ferlay J, Ward E, Forman D*. Global cancer statistics. CA Cancer J Clin 2011; 61(2): 69–90.
5. *Wang S, Qiu L, Lang JH, Shen K, Yang JK, Huang MF*, et al. Clinical analysis of ovarian epithelial carcinoma with coexisting pelvic endometriosis. Am J Obstet Gynecol 2013; 208: 413.e1–413.e5.
6. *Burghaus S, Häberle L, Schrauder M, Heusinger K, Thiel F, Hein A*, et al. Endometriosis as a risk factor for ovarian or endometrial cancer-results of a hospital-based case control study. BMC Cancer 2015; 15: 751.
7. *Noli S, Cipriani S, Scarfone G, Villa A, Grossi E, Monti E,* et al. Long term survival of ovarian endometriosis associated clear cell and endometrioid ovarian cancers. International journal of gynecological cancer 2013; 23(2): 244–8.
8. *Ma X, Hui Y, Lin L, Wu Y, Zhang X, Qin X*. Possible relevance of tumor-related genes mutation to malignant transformation of endometriosis. Eur J Gynaecol Oncol 2016; 37(1): 89–94.
9. *Suryawanshi S, Huang X, Elishaev E, Budiu RA, Zhang L, Kim S*, et al. Complement pathway is frequently altered in endometriosis and endometriosis-associated ovarian cancer. Clin Cancer Res 2014; 20(23): 6163–74.
10. *Borrelli GM, Abrão MS, Taube ET, Darb-Esfahani S, Köhler C, Chiantera V,* et al. (Partial) Loss of BAF250a (ARID1A) in rectovaginal deep-infiltrating endometriosis, endometriomas and involved pelvic sentinel lymph nodes. Mol Hum Reprod 2016; 22(5): 329–37.
11. *Rechsteiner M, Zimmermann A, Wild PJ, Caduff R, Teichman A, Fink D*, et al. TP53 mutations are common in all subtypes of epithelial ovarian cancer and occur concomitantly with KRAS mutations in the mucinous type. Exp Mol Pathol 2013; 95(2): 235–41.
12. *Worley MJ, Liu S, Hua Y, Kwok JS, Samuel A, Hou* L, et al. Molecular changes in endometriosis-associated ovarian clear cell carcinoma. Eur J Cancer 2015; 51(13): 1831–42.
13. *Helder-Woolderink JM, Blok EA, Vasen HFA, Hollema H, Mourits MJ, De De Bock GH*. Ovarian cancer in Lynch syndrome: as systematic review. Eur J Cancer 2016; 55: 65-73.
14. *Teixeira N, Mourits MJ, Vos JR, Kolk DM, Jansen L, Oosterwijk JC,* et al. Ovarian cancer in BRCA1/2 mutation carriers: The impact of mutation position and family history on the cancer risk. Maturitas 2015; 82(2): 197–202.

Received on December 15, 2016.
Revised on March 02, 2017.
Accepted on March 03, 2017.
Online First March, 2017.

CASE REPORT

UDC: 616.126.3-089
https://doi.org/10.2298/VSP170312117S

Reconstructive surgery of an extremely calcified mitral valve in a Barlow disease patient – a case report

Rekonstruktivna hirurgija ekstremno kalcifikovane mitralne valvule kod bolesnika sa Barlovljevom bolesti

Ivan Stojanović*, Marko Kaitović*, Aleksandra Novaković†, Petar Vuković*

***Cardiovascular Institute „Dedinje“, Belgrade, Serbia; University of Belgrade, †Faculty of Pharmacy, Belgrade, Serbia**

Abstract

Introduction. Mitral valve calcifications are frequent finding in Barlow disease. This is making mitral repair surgery even more demanding in already complex valve pathology. **Case report.** A fifty–five-year-old Barlow disease patient underwent a mitral repair surgery due to posterior leaflet prolapse at P2 level and extensive posterior leaflet and annular calcifications as well. The prolapsed scallop was resected, while P1 and P3 scallops were detached from the annulus. After complete posterior annulus decalcification, so formed the large atrio-ventricular defect was reconstructed with the autologous pericardial patch and double suture line technique. The P1 and P3 segments were reattached there by the sliding technique and sutured with no strain. Annuloplasty was performed with a saddle rigid ring No 36. The patient was discharged nine days after the surgery with just a trace of mitral regurgitation. **Conclusion.** Annular decalcification and reconstruction in the patients with calcified Barlow mitral disease is neccessary for safe and durable mitral valve surgical repair.

Key words:
barlow syndrome; mitral valve stenosis; mitral valve annuloplasty; reconstructive surgical procedures.

Apstrakt

Uvod. Kalcifikacije mitralne valvule su čest nalaz kod bolesnika sa Barlovljevom bolesti što čini rekonstruktivnu hirurgiju zalistka kod ovih bolesnika znatno složenijom. **Prikaz bolesnika.** Bolesniku starom 55 godina je urađena rekonstrukcija mitralnog zalistka zbog prolapsa posteriornog listića i značajnih kalcifikacija na P2 segmentu i posteriornom anulusu. Nakon resekcije P2 segmenta i odvajanja P1 i P3 segmenta od anulusa, urađena je kompletna resekcija velikog kalcifikata sa skoro polovine obima posteriornog anulusa. Nastali atrioventrikularnog defekt rekonstruisan je autolognim perikardom elipsoidnog oblika sašivenim u dva sloja. P1 i P3 segment su potom reinplantirani na rekonstruisani anulus i međusobno spojeni. Rekonstruktivna procedura je kompletirana anuloplastikom pomoću sedlastog rigidnog prstena veličine 36. Bolesnik je otpušten devetog postoperativnog dana sa neznatnom mitralnom regurgitacijom. **Zaključak.** Dekalcifikacija posteriornog anulusa uz preciznu rekonstrukciju nastalog atrioventikularnog defekta je neophodna procedura za bezbednu i funkcionalno trajnu rekonstrukciju mitralnog zalistka.

Ključne reči:
sindrom barlow; zalistak, mitralni, stenoza; zalistak, mitralni, anuloplastika; hirurgija, rekonstruktivne procedure.

Introduction

Extremely enlarged and thick mixomatous leaflets along with significant annular dilatation are the main features of the Barlow mitral valve disease. Excessive leaflet mobility in these patients results in micro traumas at the leaflet base. The healing process stimulates fibrous scar formation thereafter and annular calcifications in some patients. The adjecent leaflet and myocardial tissue could be affected by the calcification process as well [1, 2]. Therefore, the calcified posterior annulus is not a rare finding in the Barlow patients [3] and makes already complex reconstructive surgery more demanding. This is a case report of a patient who underwent a succesful mitral repair surgery in spite of excessive posterior leaflet and annular calcifications.

Case report

Fifty-five-year-old patient was admitted to hospital for the chronic severe mitral insufficiency. He was in the New

Correspondence to: Ivan Stojanović, Cardiovascular Institute „Dedinje“, Avalska 3/12, 11000 Belgrade, Serbia.
E-mail: ivan0stojanovic@gmail.com

York Heart Association (NYHA) functional class III. The echocardiography exam revealed grade 4 mitral regurgitation due to the posterior leaflet prolapse at the P2 level. The prolapsed segment was at the same time immobile due to severe calcifications that were extending down into the posterior annulus. The heart chambers were moderately enlarged. Left atrium was 44 mm, while left ventricle end-systolic and end-dyastolic diameters were 43 mm and 59 mm, respectively. Left ventricle ejection fraction was 60%. The patient had no history of rheumatsim or bacterial endocarditis.

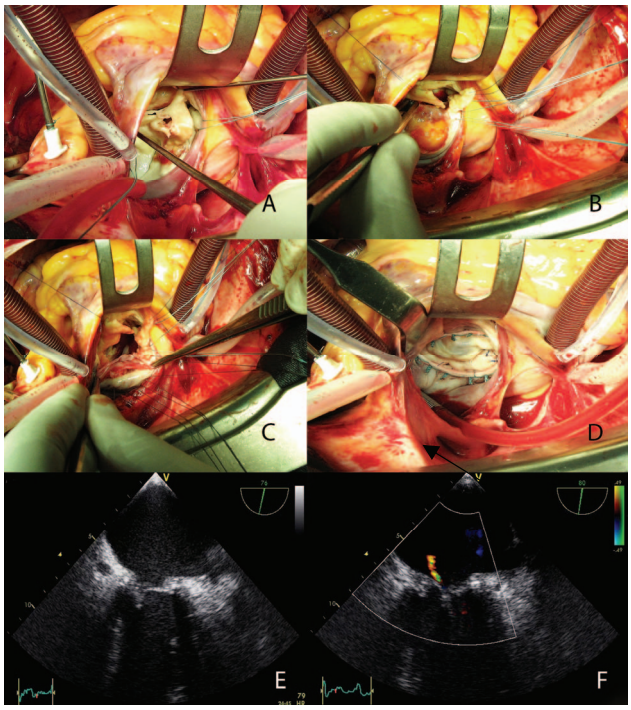

Fig. 1 – Intraoperative images.

a) Massive leaflet calcification that extends down into the posterior annulus; b) Annulus decalcification resulted in a huge atrioventricular defect (arrow); c) Atrioventricular defect was reconstructed with autologous pericardial patch (arrow); d) Preserved anatomy and fully competent mitral valve as well after the reconstruction; e) Postoperative echocardiography exam confirms long coaptation line with f) just a trace of residual mitral regurgitation.

The surgery was performed through the median sternotomy. The valve anatomy and leaflet thickness confirmed the diagnosis of Barlow disease. The posterior leaflet P2 scallop was prolapsing due to elongated and ruptured chordae and was at same time rigid and immobile due to severe calcifications. Posterior annulus was severely calcified as well (Figure 1a). The prolapsed segment was excised while the P1 and P3 scallops were detached from the annulus. Posterior annulus calcification was completely removed, leaving a large gap between the left ventricle and atrium (Figure 1b). The most demanding part of the procedure was a reconstruction of such an important atrioventricular discontinuity. The posterior annulus therefore, was repaired with 4 × 2 cm oval shape autologous pericardium (Figure 1c). Six separate pledgeted 4/0 „U“ stitches, were placed trough the lower rim of the pericardal patch, left ventricle myocardium, and thereafter pulled through the left atrial wall and tied on the left atrial side (Figure 2a). The upper rim of the pericardial patch was then sutured to the left atrial wall with 4/0 runnung polypropylene suture, making quite a strong posterior annulus reconstruction (Figure 2b). After that, the P1 and P3 scallops were reattached to the reconstructed posterior annulus by the leaflet sliding technique and sutured with no strain. Annuloplasty was performed with the N^{o} 36 SJM Saddle ring, Saint Jude Medical, SAD (Figure 1d). The postoperative course was uneventful, and the patient was dicharged nine days after the surgery with almost fully competent mitral valve just a trace of mitral regurgitation was noticed (Figures 1e and 1f).

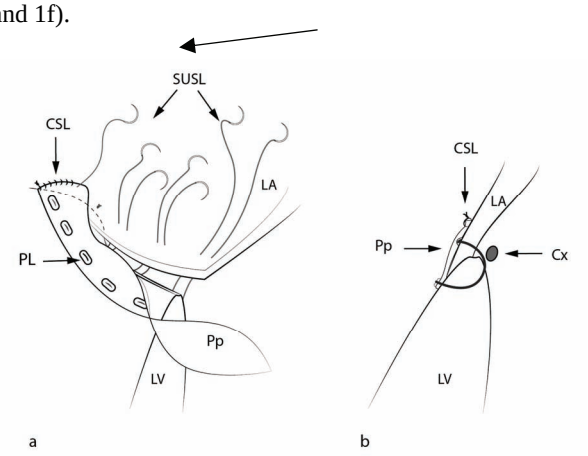

Fig. 2 – Posterior atrioventricular defect reconstruction with autologous pericardium.

a) First suture line is performed with single pledgetet „U“ stitches passed through the patch, myocardium and pulled out high on the atrial side. In that way, the atrial tissue is slided down to close atrioventricular defect, and prevent circumflex artery entrapment - atrial sliding technique (b). Second running suture line reinforces the repair and covers the first lineknotes.

CSL – continious suture line; SUSL – single „U“ stitch line; Pp – pericardial patch; LV – left ventricle myocardium; LA – left atrial wall; Cx – circumplex artery; PL – pledget on a single „U“ stitch.

Discussion

Barlow disease is one of the most complex pathologies in the mitral repair surgery. When present, annular calcifications makes mitral reconstructive surgery even more demanding. Although there is a quite enough leaflet tissue for the repair in these patients, leaflet mobility, pliability and overal repair durability as well, could not be fully achieved without the posterior annulus decalcification [4]. This is a complex and risky procedure for two reasons. Firstly, we must take care to protect circumflex artery in the atrioventicular (AV) groove (Figure 2b). Secondly, we have to keep in mind that decalcification at this level creates an AV defect [5, 6], which, if not repaired properly, results in catastrophic bleedeng afterwards. We reduced a possibility to entrap the circumflex artery by placing every single „U“ stitch under direct vision.

An additional support for such a large AV defect repair was achived by the additional runing suture. Therefore, we found that the double stitch line pericardial patch technique we decribed, is effective in preventing both adverse events (Figure 2). Furthermore, pliability of the new posterior annulus we created, provides elastic and solid base for the leaflet sliding suture as well as annuloplasty ring stitches. Such a solid, but elastic annular reconstruction allows a surgeon to acheive full leaflet mobility after the sliding plasty and to reduce the stress on a leaflet base.

Conclusion

Annulus calcifications in Barlow mitral valve disease has to be removed in order to obtain the pliable and durable valve repair. Atrioventricular defect upon decalcification could be safely reconstructed with autologous pericardium reinforeced by the double suture line technique.

REFERENCES

1. *Carpentier AF, Pellerin M, Fuzellier JF, Relland JY*. Extensive calcification of the mitral valve anulus: pathology and surgical management. J Thorac Cardiovasc Surg 1996; 111(4): 718–29; discussion 729–30.
2. *Chan V, Ruel M, Hynes M, Chaudry S, Mesana TG*. Impact of mitral annular calcification on early and late outcomes following mitral valve repair of myxomatous degeneration. Interact Cardiovasc Thorac Surg 2013; 17(1): 120–5.
3. *Fusini L, Ghulam Ali S, Tamborini G, Muratori M, Gripari P, Maffessanti F,* et al. Prevalence of calcification of the mitral valve annulus in patients undergoing surgical repair of mitral valve prolapse. Am J Cardiol 2014; 113(11): 1867–73.
4. *Ng CK, Punzengruber C, Pachinger O, Nesser J, Auer H, Franke H,* et al. Valve repair in mitral regurgitation complicated by severe annulus calcification. Ann Thorac Surg 2000; 70(1): 53–8.
5. *Fasol R, Mahdjoobian K, Joubert-Hubner E*. Mitral repair in patients with severely calcified annulus: feasibility, surgery and results. J Heart Valve Dis 2002; 11(2): 153–9.
6. *Uchimuro T, Fukui T, Shimizu A, Takanashi S*. Mitral Valve Surgery in Patients With Severe Mitral Annular Calcification. Ann Thorac Surg 2016; 101(3): 889–95.

Received on March 12, 2017.
Revised on May 23, 2017.
Accepted on August 14, 2017.
Online First September, 2017.

CASE REPORT

UDC: 616.8-089:[617.547:617.53
https://doi.org/10.2298/VSP160622143I

C1-C2 screw fixation in the patient with anomalous course of vertebral artery – a case report

C1-C2 fiksacija šrafom kod bolesnika sa anomalijom toka vertebralne arterije

Dražen Ivetić, Goran Pavličević, Branislav Antić

Military Medical Academy, Department of Neurosurgery, Belgrade, Serbia; University Defence, Faculty of Medicine of the Military Medical Academy, Belgrade, Serbia

Abstract

Introduction. The atlantoaxial complex is a very complicated structure and open reduction of C1-C2 subluxation is very demanding. Atlantoaxial instability may result from the traumatic, inflammatory, neoplastic, congenital or degenerative disorders. Anatomy of the vertebral artery is essential for surgical approach and sometimes the placement of C2 pedicle screw is not possible. In these instances, the translaminar screw placement in C2 can provide an alternative fixation point in C2, without threatening injury to the vertebral artery. **Case report.** We presented 54- year-old patient with cervical myelopathy according to traumatic atlantoaxial subluxation. Computed tomography angiography showed a bilateral vertebral artery anomaly of "high-riding" type. The patient was operated and the posterior C1-C2 screws fixation was used. Due to the vertebral artery anomaly C2 screws were translaminary inserted. Complete reduction of C1-C2 subluxation and excellent neurological improvement were achieved. **Conclusion.** Surgical treatment of C1-C2 subluxation is very challenging. Many techniques of atlantoaxial fixation have been developed. The use of C2 translaminar screw is an alternative method of fixation in the treatment of atlantoaxial instability, especially in cases with the vertebral artery anomaly.

Key words:
cervical vertebrae; joint dislocation; vertebral artery; congenital abnormalities; bone screws; neurosurgery.

Apstrakt

Uvod. Atlantoaksijalni kompleks je veoma kompleksna anatomska struktura, a otvorena redukcija C1-C2 luksacije veoma je zahtevna procedura. Nestabilnost atlantoaksijalnog kompleksa može nastati kao posledica traumatskih, inflamatornih, neoplastičnih, kongenitalnih ili degenerativnih oboljenja. Poznavanje anatomije vertebralne arterije ključno je za obavljanje hirurgije u ovoj regiji, a transpedikularno plasiranje C2 šrafa ponekad nije moguće. U ovim situacijama, translaminarno plasiranje šrafova u C2 pršljen obezbeđuje alternativan način fiksacije, bez opasnosti od povrede vertebralne arterije. **Prikaz bolesnika.** Prikazan je bolesnik, star 54 godine, sa cervikalnom mijelopatijom kao posledicom traumatske atlantoaksijalne subluksacije. Kompjuterizovana tomografska angiografija pokazala je obostranu anomaliju vertebralne arterije "high-riding" tipa. Bolesnik je operisan, učinjena je C1-C2 zadnja stabilizacija šrafovima. Zbog anomalne pozicije vertebralne arterije šrafovi su plasirani u lamine C2 pršljena. Postignuta je odlična repozicija subluksacije kao i odličan neurološki oporavak bolesnika. **Zaključak.** Hirurški tretman C1-C2 luksacije predstavlja veliki izazov. Opisane su brojne hirurške tehnike u tretmanu atlantoaksijalne fiksacije. C2 translaminarno plasiranje šrafova je alternativna metoda stabilizacije u tretmanu atlantoaksijalne nestabilnosti, posebno u slučajevima anomalije vertebralne arterije.

Ključne reči:
pršljenovi, vratni; iščašenje; a.vertebralis; anomalije; zavrtnji za kost; neurohirurgija.

Introduction

The atlantoaxial complex is very complicated structure and surgery in that region is very demanding. Reduction of the C1-C2 subluxations results in the increased space for the spinal cord and is a decompressive strategy for spinal cord compression secondary to the C1-C2 instability [1]. Atlantoaxial subluxation may result from the traumatic, inflammatory, neoplastic, congenital or degenerative disorders. Several techniques have been described to treat atlantoaxial instability, ranging from wiring techniques, transarticular screw technique, C1 lateral mass with C2 pedicle screw and C1 lateral mass screw with C2 translaminar screw. The wiring techniques are limited in their ability to achieve and maintain adequate reduction intraoperatively [1, 2]. The transarticular screw technique is excellent for maintaining alignment, but it does

Correspondence to: Dražen Ivetić, Military Medical Academy, Department of Neurosurgery, Crnotravska 17, 11 000 Belgrade, Serbia. E-mail: iveticd@yahoo.com

not enable reduction [1, 3, 4]. This technique confers immediate stability to atlantoaxial complex and is usually performed in a combination with a wiring technique to provide a substrate for bony fusion, however, this type of screw fixation is technically demanding and associated with the risk of the vertebral artery injury [5, 6]. The presence of a high-riding vertebral artery precludes the safe placement of C2 pedicle screws in C1 lateral mass screw with the C2 pedicle screw technique. The translaminar screw placement in C2 can provide an alternative fixation point in C2 in the patients with anomalous course of the vertebral artery.

Case report

A 54-year-old man was referred to our hospital for cervical myelopathy according to atlantoaxial instability. Three months before admission to our department, he suffered a trauma of cervical spine during physical activity. After few days, he started with myelopathy. On admission, he had severe myelopathy with the Nurick score 4, and 11 according to the modified Japanese Orthopaedic Association (mJOA) scale. He had a severe neck pain and his left arm was almost plaegic. The imaging studies revealed C1-C2 instability, with atlantodental interval of 5 mm (Figures 1 and 2). Preoperative multisliced computed tomography (MSCT) angiography showed that there was a bilaterally anomalous course of vertebral artery, the high-riding type (Figure 3). The operation was performed in general anesthesia, with the patient in the prone position and his head secured in a Mayfield head holder. The final positioning was performed using the real-time fluoroscopy. A standard posterior approach was performed via a medial skin incision. The C1 arch was dissected and followed laterally to the lateral mass of C1 with the use of a subperiostal dissection as described by Goel and Laheri [7]. The C1-C2 articulation was exposed and decorticated, C2 nerve root was retracted inferiorly, exposing the entry point in the midportion of the C1 lateral mass. A pilot hole was made by a diamond burr, and under fluoroscopy control, a bicortical hole was tapped. Trajectory of the hole was parallel to the base of the C1 lateral mass with 10 degrees of medial angulation. A polyaxial screw was inserted bicorticaly, and few millimeters unthreaded portion of the C1 screw stayed above the lateral mass. With the diamond burr, a small cortical windows were made in the base of the spinous process of C2, one on either side. A screw tap was made inside the lamina without any cortical breakthrough one rostral to the other, and the polyaxial screw was carefully inserted along the same trajectory. The C1 lateral mass screws and bilateral laminar C2 screws were connected with the posterior rods, the locking screws were placed and the reduction technique was performed by distraction. The C1 and C2 posterior elements were then decorticated and the autologous occipital bone graft was placed over the C1-C2 posterior elements. The patient, postoperatively, had neurological improvement and he started with physical therapy. The postoperative images showed a good position of the implants and complete reduction of C1-C2 subluxation (Figures 4, 5 and 6). Postoperatively, the patient wore a cervical orthosis for 6 weeks.

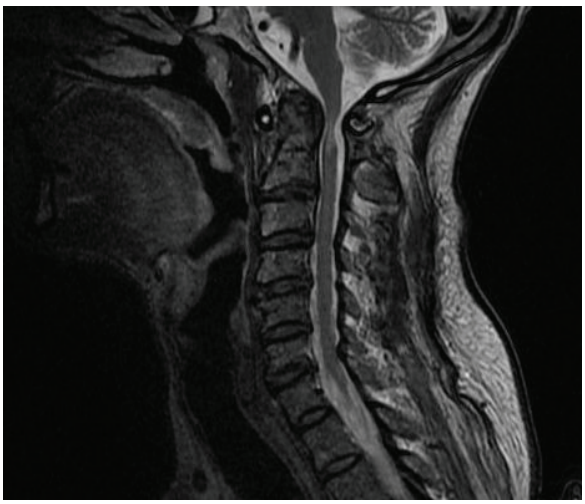

Fig. 1 – Preoperative sagittal cervical spine magnetic resonance image in a 54-year-old man with cervical myelopathy and atlantoaxial instability.

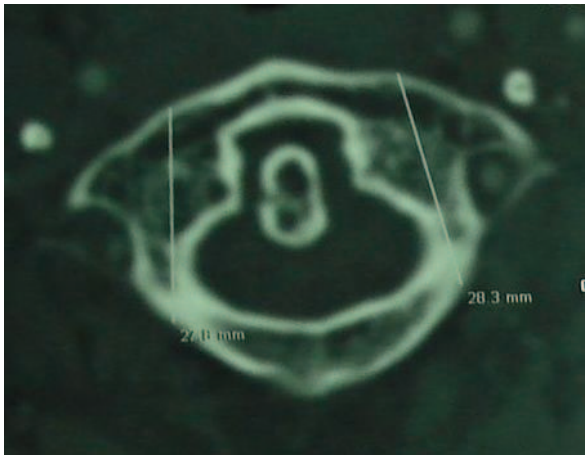

Fig. 2 – Preoperative axial computed tomography image revealing atlantoaxial instability with atlantoaxial distance of 5 mm.

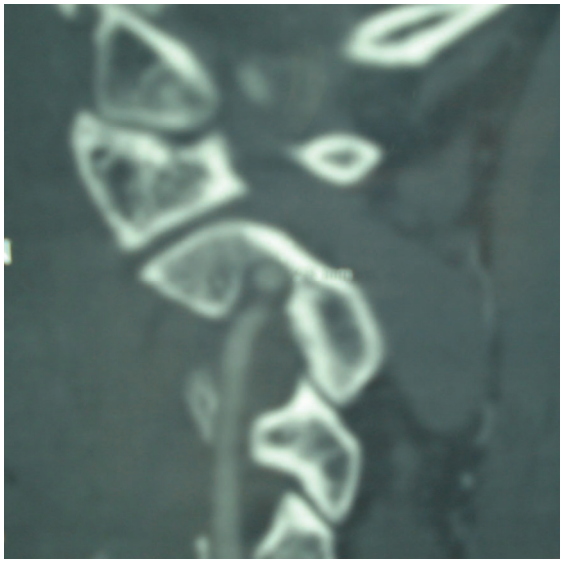

Fig. 3 – Preoperative computed tomography angiography showing the high-riding vertebral artery at the C2 level with a very narrow pedicle.

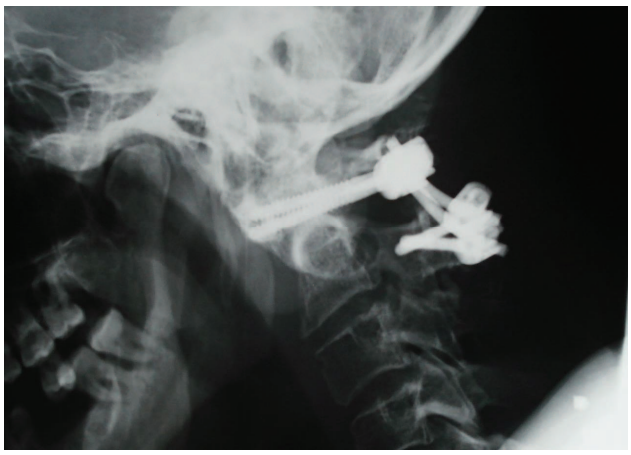

Fig. 4 – Postoperative lateral radiography showing good position of screws.

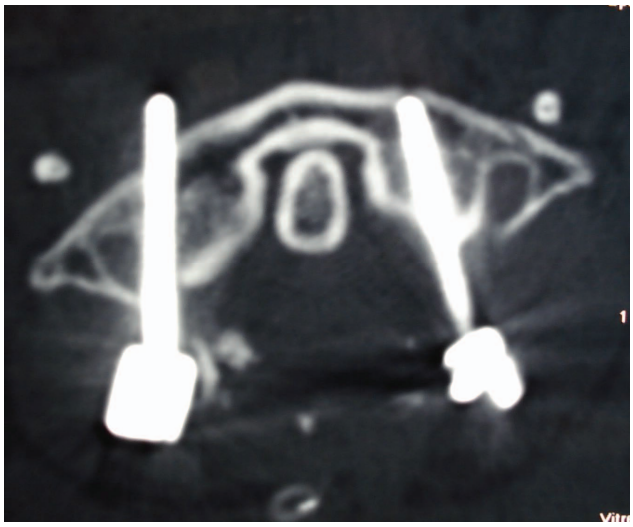

Fig. 5 – Postoperative axial computed tomography image demonstrating a good position of screws in the C1 lateral masses and complete reduction of the C1-C2 subluxation.

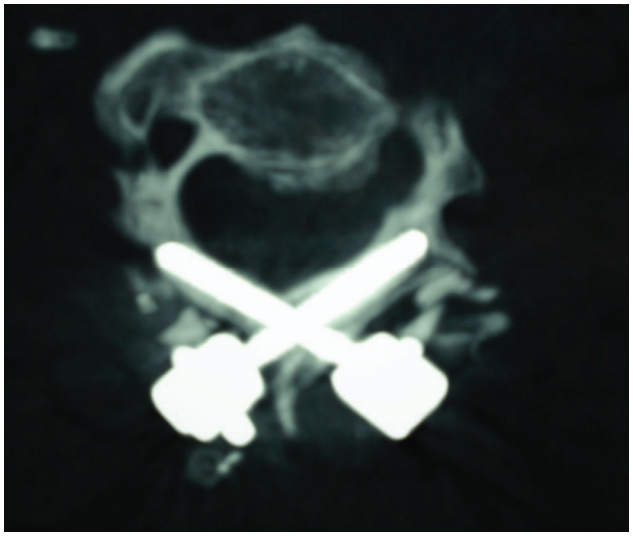

Fig. 6 – Postoperative axial computed tomography image showing a proper position of the C2 translaminar screws.

Discussion

In 1910, Mixter and Osgood [8] provided the first description of surgical treatment for atlantoaxial instability using heavy silk to tie the spinous process of C1 and C2 together. Since then, many other surgical techniques have been developed [9]. These posterior surgical techniques can be strongly divided into the wiring and screw techniques. The wiring techniques of dorsal atlantoaxial fusion are technically simple and do not require fluoroscopy. However, maintaining the reduction can be difficult, and it requires a rigid postoperative immobilization for a successful fusion [2]. Because of these disadvantages of the wiring techniques, newer screw techniques have been developed. Magerl and Seemann [10] described a transarticular screw method, and that instrumentation had superior stability in comparison to the wiring techniques [11]. This technique requires a reduction of C1-C2 luxation before fixation and an overall complication rate was high, especially in case of the vertebral artery injury [12–14]. According to these limitations of transarticular technique, Goel and Laheri described four screw C1-C2 fixation technique while other auhors [15, 16] and Harms and Melcher [17] popularized this technique. If the C2 pedicle screw cannot be placed due to the vertebral artery anomaly, an alternative techniques like C2 translaminar screw can be implemented. The vertebral artery was considered high riding if the isthmus thickness was less than 5 mm or the isthmus internal height was less than 2 mm [18]. Wright [19] and Leonard and Wright [20] described new technique which involved the insertion of polyaxial screws into the laminae of C2 in a bilateral, crossing fashion, which were then connected to the C1 lateral mass screws [9]. The intralaminar screw technique would be the safest technique in regard to the vertebral artery injury, and also, there was no need for an acute angle for the placement of screws and the C2 intralaminar screws can be placed with visual and tactile feedback without the fluoroscopy or image guidance [4, 19]. The only drawback of this technique is its requirement for an intact and adequately sized lamina. The C1 lateral mass-C2 translaminar screw constructs are biomechanicaly similar to the transarticular and C1 lateral mass-C2 pedicle screws in flexion-extension and axial rotation, although the C2 translaminar screws were significantly less resistant to lateral bending [4, 21]. Similar technique of fixation, which involves screw insertion into the base of the spinous process of the axis, was described by Goel and Kulkarni [22], also. Thorough assessment of the vascular anatomy is recommended before an operative intervention in the upper cervical spine to minimize the risk of complications. Surgical possibilities to treat the atlantoaxial instability are numerous, and according to surgical anatomy, a surgeon's skills and type of injury, surgeon can choose the best one.

Conclusion

Surgical treatment of the C1-C2 subluxation is very challenging. Many techniques of atlantoaxial fixation have been developed. The use of the C2 translaminar screw is an alternative method of fixation in the treatment of atlantoaxial instability, especially in cases with vertebral artery anomaly.

R E F E R E N C E S

1. *O'Brien JR, Gokaslan ZL, Riley LH, Suk I, Wolinsky JP.* Open reduction of C1-C2 subluxation with the use of C1 lateral mass and C2 translaminar screws. Neurosurgery 2008; 63(1 Suppl 1): ONS95–8; discussion ONS98–9.
2. *Papagelopoulos PJ, Currier BL, Hokari Y, Neale PG, Zhao C, Berglund LJ,* et al. Biomechanical comparison of C1-C2 posterior arthrodesis techniques. Spine (Phila Pa 1976) 2007; 32(13): E363–70.
3. *Claybrooks R, Kayanja M, Milks R, Benzel EC.* Atlantoaxial fusion: a biomechanical analysis of two C1-C2 fusion techniques. Spine J 2007; 7(6): 682–8.
4. *Lapsiwala SB, Anderson PA, Oza A, Resnik DK.* Biomechanical comparison of four C1 to C2 rigid fixative techniques: anterior transarticular, posterior transarticular, C1 to C2 pedicle, and C1 to C2 intralaminar screws. Neurosurgery 2006; 58(3): 516–21; discussion 516–21.
5. *Resnik DK, Benzel EC.* C1-C2 pedicle screw fixation with rigid Cantilever beam construct: case report and technical note. Neurosurgery 2002; 50(2): 426–8.
6. *Mandel IM, Kambach BJ, Petersilge CA, Johnstone B, Yoo JU.* Morphologic considerations of C2 isthmus dimensions for the placement of transarticular screws. Spine (Phila Pa 1976) 2000; 25(12): 1542–77.
7. *Goel A, Laheri V.* Plate and screw fixation for atlanto-axial subluxation. Acta Neurochir (Wien) 1994; 129(1–2): 47–53.
8. *Mixter SJ, Osgood RB.* IV. Traumatic Lesions of the Atlas and Axis. Ann Surg 1910; 51(2): 193–207.
9. *Menendez JA, Wright NM.* Techniques of posterior C1-C2 stabilization. Neurosurgery 2007; 60(1 Suppl 1): S103–11.
10. *Magerl F, Seemann PS.* Stable posterior fusion of the atlas and axis by transarticular screw fixation. In: *Kehr P, Wiedner A*, editors. Cervical Spine. New York: Springer; 1986. p. 322–7.
11. *Henriques T, Cunningham BW, Olerud C, Shimamoto N, Lee GA, Larsson S,* et al. Biomechanical comparison of five different atlantoaxial posterior fixation techniques. Spine (Phila Pa 1976) 2000; 25(22): 2877–83.
12. *Vegara P, Bal JS, Hickman Casey AT, Crockard HA, Choi D.* C1-C2 fixation: are 4 screws better than 2? Neurosurgery 2012; 71(1 Suppl Operative): 86–95.
13. *Finn MA, Apfelbaum RI.* Atlantoaxial transarticular screw fixation: update on technique and outcomes in 269 patients. Neurosurgery 2010; 66(3 Suppl): 184–92.
14. *Neo M, Fujibayashi S, Miyata M, Takemoto M, Nakamura T.* Vertebral artery injury during cervical spine surgery: a survey of more than 5600 operations. Spine 2008; 33(7): 779–85.
15. *Goel A, Desai KI, Muzumdar DP.* Atlantoaxial fixation using plate and screw method: a report of 160 treated patients. 2002; 51(6): 1351–6; discussion 1356–7.
16. *Goel A.* Treatment of basilar invagination by atlantoaxial joint distraction and direct lateral mass fixation. J Neurosurg Spine 2004; 1(3): 281–6.
17. *Harms J, Melcher RP.* Posterior C1-C2 fusion with polyaxial screw and rod fixation. Spine (Phila Pa 1976) 2001; 26(22): 2467–71.
18. *Elgafy H, Pompo F, Vela R, Elsamaloty HM.* Ipsilateral arcuate foramen and high-riding vertebral artery: implication on C1-C2 instrumentation. Spine J 2014; 14(7): 1351–5.
19. *Wright NM.* Posterior C2 fixation using bilateral, crossing C2 laminar screws: case series and technical note. J Spinal Disord Tech 2004; 17(2): 158–62.
20. *Leonard JR, Wright NM.* Pediatric atlantoaxial fixation with bilateral, crossing C-2 translaminar screws. Technical note. J Neurosurg 2006; 104(1 Suppl): 59–63.
21. *Dorward IG, Wright NM.* Seven years of experience with C2 translaminar screw fixation: clinical series and review of the literature. Neurosurgery 2011; 68(6): 1491–9; discussion 1499.
22. *Goel A, Kulkarni AG.* Screw implantation in spinous process for occipitoaxial fixation. J Clin Neurosci 2004; 11(7): 735–7.

Received on June 22, 2016.
Accepted on July 26, 2017.
Online First October, 2017.

LETTER TO THE EDITOR
(RESEARCH LETTER)

UDC: 615.38:616.15-08
https://doi.org/10.2298/VSP190219042B

Improved cytoreductive potential of plateletapheresis in the treatment of thrombocythemia: a single center study

Poboljšani citoreduktivni potencijal trombocitafereze u lečenju trombocitemije

To the Editor:

Extreme thrombocytosis (ETC; cell-count ≥ 1500 × 10^9/L) in the essential thrombocythemia (ET) patients – with altered platelet (Plt) morphology/aggregability (Plt-dysfunction) and immature reticulated Plts – increases the risk of both thromboembolic and/or hemorrhagic events (up to 50%). The evidence-based clinical guideline for therapy of asymptomatic-ET (e.g., exact cytapheresis-threshold, target Plt-count, etc.) is not yet established. In the treatment of symptomatic-ET (when low-dose aspirin or other anti-Plt and the highest doses of chemotherapy are without rapid response or contraindicated, as in pregnancy), cytoreduction by plateletapheresis is useful or essential [1–4]. The first cytapheresis in our Apheresis Center was performed in 1971 for treatment of pregnant women with hyperleukocyte-leukostasis [1, 2].

The aim of this study was to evaluate cytoreductive potential of the Spectra-Optia/IDL-System, based upon the *ex vivo* Plt-removal and the *in vivo* Plt-depletion (Plt-removal/depletion) efficacy (using our modifications of manufacturer's original protocol). The Plt-removal/depletion efficacy of this study was compared to our earlier results (historical database) and the latest literature data for different devices. To the best of our knowledge, this is the second published clinical evaluation of the efficacy and safety of therapeutic plateletapheresis using the Spectra-Optia.

In the treatment of a 68-year-old female patient suffering from symptomatic-ET (with headaches, vertigo, visual-disturbances and paresthesia) the Plt-removal/depletion procedure was performed by the Spectra-Optia/IDL-System (Terumo BCT; USA). Our modifications of apheresis protocol included the collection-preference and inlet flow corrections (altered collection speed) as well as an increase of the target cell suspension volume to improve the Plt-removal/depletion efficacy. As previously described, the Plt morphology (shape-ratio) and ultrastructural properties by the phase-contrast microscope (Polyvar, Austria) and electron-microscope (Philips-201-C; The Netherlands) were examined, respectively [5, 6]. The Plt-function by the Multiplate Analyzer (Dynabyte GmbH, Germany) was evaluated. Statistical analysis was performed by the Student's *t*–test, using the "Origin-PC-Program". The results were considered to be significant at $p < 0.05$. The apheresis therapy was approved by the Military Medical Academy (MMA) Ethics Committee.

In the treatment of this patient with ETC associated clinical emergency, using an intensive "single-plateletapheresis" (by Spectra-Optia/IDL-System) 7.5 × 10^{12} Plts were removed from circulation (cell suspension = 1150 mL). A significant Plt-depletion (from 2330 × 10^9/L to 633 × 10^9/L; $p < 0.05$) and *in vivo* Plt-fall = 72.8% (the circulating Plt ratio before and after plateletapheresis expressed in percentage; $p < 0.05$) was realized and followed by the clinical advances and prevention of thromboembolic (e.g., stroke) and/or hemorrhagic events. As replacement fluid, albumin in saline was used. There were no side effects due to intensive plateletapheresis.

The baseline aggregability of Plts in the patient′s venous blood sample was 918 aggregation units (AU)*min (normal = 923–1509 AU*min) by the Thrombin Receptor Activating Peptide (TRAP)-test [10 AU*min is equal to one Area Under the Curve (AUC) value]. The ultrastructural features of various Plt-shapes are visualized in Figure 1.

As shown, the discoid Plt-shapes had the typical ultrastructural properties without the membrane integrity destructions, intact microtubules and open canalicular system. There were also several dendritic Plt-shapes with the extensive cell membrane damages and pseudopods, reduced electron density, peripheral dislocation of granules and/or cytoplasm organelles with the resultant Plt-dysfunction.

Correspondence to: Bela Balint, Serbian Academy of Sciences and Arts, Knez Mihajlova 35, 11 000 Belgrade, Serbia.
E-mail: balintbela52@yahoo.com

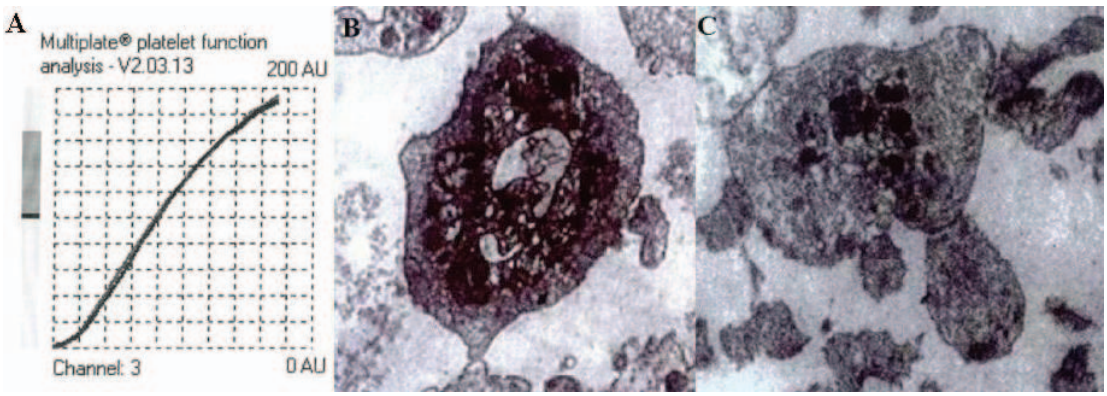

Fig. 1 – Platelet (Plt) functional and ultrastructural analysis: (A) Reduced Plt-aggregability – TRAP-test = 918 AU*min); (B) Discoid Plt-shape (prevalent incidence); (C) Dendritic Plt-shape (sporadic occurence).

As previously described [2], in the treatment of our comparable ET-patients (n = 20; procedures = 126; historical database), using the Cobe-Spectra by "single-plateletapheresis" 2.8±2.1 × 10^{12}/L, Plts (cell suspension = 800–1300 mL; $p < 0.05$) were removed. The *in vivo* Plt-depletion was approximately threefold smaller/lower. Only the use of whole "plateletapheresis-cure" (typically 5 "single-plateletapheresis"; range = 3–11) resulted with a comparable *in vivo* Plt-fall (68 ± 14%) [2].

The Plt-removal/depletion efficacy in our current study was significantly ($p < 0.05$) superior when compared to the most recent literature data [4, 7]. Precisely, after a "single-plateletapheresis" by the CS-3000-Plus (Baxter, USA) or Cobe-Spectra (Terumo BCT, USA) in the therapy of six hemato-oncological patients [4] and the treatment of one ET-patient by the Spectra-Optia/Apheresis-System (Terumo BCT, USA; version 11.3; manufacturer's protocol used), [7] the levels of *in vivo* Plt-depletions were only 38% and 56%, respectively.

In conclusion, intensive therapeutic plateletapheresis by the Spectra Optia/IDL-System is a safe and effective treatment for the patients with life-threatening ETC. The use of a "single-plateletapheresis" – with some protocol modifications – resulted in the undoubtedly superior Plt-removal/depletion efficacy (for both normal and altered cells) when compared to our earlier study (Cobe-Spectra) and literature data for the CS-3000-Plus or Cobe-Spectra, even for the Spectra-Optia setting (using original protocol).

Bela Balint*[†‡], Mirjana Pavlović[§], Gordana Ostojić[‖¶], Dušan Vučetić[‖¶], Milena Todorović[††]**

Serbian Academy of Sciences and Arts, *Department of Medical Sciences, Belgrade, Serbia; Institute of Cardiovascular Diseases "Dedinje", [†]Department of Transfusion Medicine, Belgrade, Serbia; University of Belgrade, [‡]Institute for Medical Research, **Faculty of Medicine, Belgrade, Serbia; Florida Atlantic University, [§]Department of Computer and Electrical Engineering and Computer Science, Florida, USA; Military Medical Academy, [‖]Institute for Transfusiology and Hemobiology, Belgrade, Serbia; University of Defence, [¶]Faculty of Medicine of the Military Medical Academy, Belgrade, Serbia; Clinical Center of Serbia, [††]Clinic for Hematology, Belgrade, Serbia

REFERENCES

1. *Radovic M, Balint B, Milenkovic Lj, Tiska–Rudman Lj, Taseski J.* Therapeutic leukapheresis. Transf Sci 1991; 12(3): 193–6.
2. *Balint B, Ostojic G, Pavlovic M, Hrvacevic R, Pavlovic M, Tukic Lj,* et al. Cytapheresis in the treatment of cell-affected blood disorders and abnormalities. Transf Apher Sci 2006; 35(1): 25–31.
3. *Koren-Michowitz M, Lavi N, Ellis MH, Vannucchi AM, Mesa R, Harrison CN.* Management of extreme thrombocytosis in myeloproliferative neoplasms: an international physician survey. Ann Hematol 2017; 96(1): 87–92.
4. *Prakash S, Hans R, Sharma RR, Malhotra P, Marwaha N.* Therapeutic thrombocytapheresis for symptomatic thrombocytosis in hemato-oncology patients. Ther Apher Dial 2018; 22(1): 93–5.
5. *Balint B, Vucetic V, Trajkovic–Lakic Z, Petakov M, Bugarski M, Brajuskovic G,* et al. Quantitative, functional, morphological and ultrastructural recovery of platelets as predictor for cryopreservation efficacy. Haematologia 2002; 32(4): 363–76.
6. *Balint B, Paunovic D, Vucetic D, Vojvodic D, Petakov M, Trkuljic M,* et al. Controlled–rate vs. uncontrolled–rate freezing as predictors for platelet cryopreservation efficacy. Transfusion 2006; 46(2): 230–5.
7. *Almeida-Dias R, Garrote M, Cid J, Mustieles MJ, Alba C, Lozano M.* Therapeutic thrombocytapheresis for extreme thrombocytosis after chemotherapy in essential thrombocytosis. J Clin Apher. 2019; doi: 10.1002/jca.21683. (In Press)

Received on February 19, 2019.
Accepted on March 18, 2019.
Online First March, 2019.

BOOK REVIEW/PRIKAZ KNJIGE

Diagnostic of heart diseases with computerized tomography method

Original title (in Serbian): Dijagnostika bolesti srca metodom kompjuterizovane tomografije
Author/Autor: Dragana S. Ilić, MD, PhD
Publisher/Izdavač: Zadužbina Andrejević, Beograd
Year/Godina izdanja: 2018.
ISBN: 978-86-525-0340-7

The book "Diagnostic of heart diseases with computerized tomography method" is a new monograph which provides up-to-date and in-depth discussion about cardiac multislice computerized tomography (MSCT) method. It gives the comprehensive information and review about diagnostics of cardiovascular diseases on this advanced imaging procedure. This monograph is a result of a significant and years-long scientific research of Dr. Dragana Ilić in the field of cardioradiology. The book is based on her doctoral thesis, defended on July 8, 2016, at the Faculty of Medicine, University of Niš. The book has 135 pages and represents a bilingual monograph, written in the Serbian and English language. There are no previous books in this field in the Serbian language. The book has masterfully edited following chapters: Abstract, Introduction, Clinical anatomy of the heart, Cardiac MSCT in clinical practice, Review of pathological changes of heart structures on MSCT, Importance of cardiac MSCT based on studies and meta-analyses, Conclusion, References, Index and Summary.

The book represents a great resource for those who are new to this field and a trustworthy reference for those needing answers to specific questions or looking to update their knowledge. In this monograph, some basic information about the cardiac MSCT examination is provided as well as the pathway of heart examination procedures through history up to the contemporary methods of examination. This book gives major technological advances in cardiac MSCT. A special attention is given to the anatomical presentation of coronary circulation and modified clinical approach, which enables a precise determination of the localization of pathological changes. All anatomical structures are observed, discussed and illustrated the way they are visualized on MSCT from the anatomical and pathological point of view. Some of the most important information, as well as indications and contraindications for the cardiac MSCT examination, are precisely defined and listed with the special focus on technical performance methods for some particular conditions and diseases according to the clinical indication.

The special chapter in this monograph is dedicated to some basic principles of CT physics and procedures and characteristics of the technical examination itself. A special attention is devoted to patient preparation and pretreatment before this procedure. Advantages and disadvantages as well as perspectives of cardiac MSCT are discussed in one of the chapters. Author of this book gives the comparative overview of multiple heart examination procedures which indicates the practical importance that this book can have in everyday clinical practice in decision-making, depending on the clinical condition of the patient.

The book is very easy to read and well- illustrated with over 300 tables, figures, illustrations and original pictures of outstanding and long work of Dr. Dragana Ilić. The illustrations are of a high quality and the clinical information is brought up-to-date in this rapidly evolving field. The 215 references have been carefully selected to blend both historically essential references and recent journal publications making the monograph seamless.

It would be an invaluable aid to both radiologists and cardiologists with an interest in non-invasive imaging as well as for other specialty doctors, researchers, radiology residents, trainees, students, radiology technicians and everyone who has an interest in this field. I would recommend this monograph as it will help other researchers in future to upgrade current technical achievements and possibilities of more precise diagnostics of pathological changes of the cardiovascular system.

Dr. Sonja Janković
Clinical Center Niš, Center for Radiology, Niš, Serbia
E-mail: sonjasgirl@gmail.com

DOI: 10.2298/VSP190515051E

E R R A T U M

In the article by Nemanja V. Majstorović, Srdjan P. Živković, Branislav R. Glišić.

Dental arch monitoring by splines fitting error during orthodontic treatment using 3D digital models. Vojnosanit Pregle 2019; 76(3):233-240 (https://doi.org/10.2298/VSP161212067M), the two first authors (Nemanja V. Majstorović and Srdjan P. Živković) **have equal value**.

The list of the authors should have read:

[1]Nemanja V. Majstorović, [1]Srdjan P. Živković, Branislav R. Glišić.

[1] equal value

INSTRUCTIONS TO THE AUTHORS

The VSP publishes only papers not published before, nor submitted to any other journals, in the order determined by the Editorial Board. Any attempted plagiarism or self-plagiarism will be punished. When submitting a paper to the VSP electronic editing system **(http://aseestant.ceon.rs/index.php)**, the following should be enclosed: a statement on meeting any technical requirements, a statement signed by all the authors that the paper on the whole and/or partly has not been submitted nor accepted for publication elsewhere, a statement specifying the actual contribution of each author, no conflict of interest statement that make them responsible for meeting any requirements set. What follows subsequently is the acceptance of a paper for further editing procedure. The manuscripts submitted to the VSP pass in-house and external peer review. All authors pay "Article Processing Charge" for coverage all editing and publishing expenses. Domestic authors pay 5,000 RSD, and those from aboard 150 euros. The editing and publishing fee is required for substantive editing, facts and references validations, copy editing, and publishing online and in print by editorial staff of the Journal. No additional fees, other than stated above, are required even if an author who already paid the fee would have more articles accepted for publishing in the year when fee was paid. All authors who pay this fee may, if want, receive printed version of the Journal in year when fee is payed. Please note that the payment of this charge does not guarantee acceptance of the manuscript for publication and does not influence the outcome of the review procedure. The requirement about paying "Article Processing Charge" does not apply to reviewers, members of the Editorial Board and the Publisher's Council of the Journal, young researchers and students, as well as any of the subscribers of the Journal.

The VSP publishes: **editorials, original articles**, **short communications**, **reviews**/**meta-analyses, case reports**, **medical history** (general or military), personal views, invited comments, letters to the editor, reports from scientific meetings, book reviews, and other. Original articles, short communications, meta-analyses and case reports are published with abstracts in both English and Serbian.

General review papers will be accepted by the Editorial Board only if the authors prove themselves as the experts in the fields they write on by citing not less than 5 self-citations.

Papers should be written on IBM-compatible PC, using 12 pt font, and double spacing, with at least 4 cm left margin. **Bold** and *italic* letters should be avoided as reserved for subtitles. Original articles, reviews, meta-analyses and articles from medical history should not exceed 16 pages; current topics 10; case reports 6; short communications 5; letters to the editor and comments 3, and reports on scientific meetings and book reviews 2.

All measurements should be reported in the metric system of the International System of Units (SI), and the standard internationally accepted terms (except for mmHg and °C).

MS Word for Windows (97, 2000, XP, 2003) is recommended for word processing; other programs are to be used only exceptionally. Illustrations should be made using standard **Windows** programs, **Microsoft Office** (**Excel**, **Word Graph**)**.** The use of colors and shading in graphs should be avoided.

Papers should be prepared in accordance with the **Vancouver Convention**.

Papers are reviewed anonymously by at least two editors and/or invited reviewers. Remarks and suggestions are sent to the author for final composition. Galley proofs are sent to the corresponding author for final agreement.

Preparation of manuscript

Parts of the manuscript are: **Title page; Abstract with Key words; Text; Acknowledgements** (to the authors' desire), **References**, **Enclosures**.

1. ***Title page***

a) The title should be concise but informative, while subheadings should be avoided;

b) Full names of the authors signed as follows: ***, †, ‡, §, ||, ¶, **, ††, ...** .

c) Exact names and places of department(s) and institution(s) of affiliation where the studies were performed, city and the state for any authors, clearly marked by standard footnote signs;

d) Conclusion could be a separate chapter or the last paragraph of the discussion;

e) Data on the corresponding author.

2. ***Abstract and key words***

The second page should carry a structured abstract (250-300 words for original articles and meta-analyses) with the title of the article. In short, clear sentences the authors should write the **Background**/**Aim**, major procedures – **Methods** (choice of subjects or laboratory animals; methods for observation and analysis), the obtained findings – **Results** (concrete data and their statistical significance), and the **Conclusion**. It should emphasize new and important aspects of the study or observations. A structured abstract for case reports (up to 250 words) should contain subtitles **Introduction, Case report, Conclusion**). Below the abstract **Key words** should provide 3–10 key words or short phrases that indicate the topic of the article.

3. ***Text***

The text of the articles includes: **Introduction**, **Methods**, **Results**, and **Discussion**. Long articles may need subheadings within some sections to clarify their content.

Introduction. After the introductory notes, the aim of the article should be stated in brief (the reasons for the study or observation), only significant data from the literature, but not extensive, detailed consideratuion of the subject, nor data or conclusions from the work being reported.

Methods. The selection of study or experimental subjects (patients or experimental animals, including controls) should be clearly described. The methods, apparatus (manufacturer's name and address in parentheses), and procedures should be identified in sufficient detail to allow other workers to reproduce the results. Also, give references to established methods, including statistical methods. Identify precisely all drugs and chemicals used, with generic name(s), dose(s), and route(s) of administration. State the approval of the Ethnics Committee for the tests in humans and animals.

Results should be presented in logical sequence in the text, tables and illustrations. Emphasize or summarize only important observations.

Discussion is to emphasize the new and significant aspects of the study and the conclusions that result from them. Relate the observations to other relevant studies. Link the conclusions with the goals of the study, but avoid unqualified statements and conclusions not completely supported by your data.

References

References should be superscripted and numerated consecutively in the order of their first mentioning within the text. All the authors should be listed, but if there are more than 6 authors, give the first 6 followed by *et al*. Do not use abstracts, secondary publications, oral communications, unpublished papers, official and classified documents. References to papers accepted but not yet published should be cited as "in press". Information from manuscripts not yet accepted should be cited as "unpublished data". Data from the Internet are cited with the date of citation.

Examples of references:

Jurhar-Pavlova M, Petlichkovski A, TrajkovD, Efinska-Mladenovska O, Arsov T, Strezova A, et al. Influence of the elevated ambient temperature on immunoglobulin G and immunoglobulin G subclasses in sera of Wistar rats. Vojnosanit Pregl 2003; 60(6): 657–612.

DiMaio VJ. Forensic Pathology. 2nd ed. Boca Raton: CRC Press; 2001.

Blinder MA. Anemia and Transfusion Therapy. In: Ahya NS, Flood K, Paranjothi S, editors. The Washington Manual of Medical Therapeutics, 30th edition. Boston: Lippincot, Williams and Wilkins; 2001. p. 413-28.

Christensen S, Oppacher F. An analysis of Koza's computational effort statistic for genetic programming. In: *Foster JA, Lutton E, Miller J, Ryan C, Tettamanzi AG,* editors. Genetic programming. EuroGP 2002: Proceedings of the 5th European Conference on Genetic Programming; 2002 Apr 3-5; Kinsdale, Ireland. Berlin: Springer; 2002. p. 182-91.

Abood S. Quality improvement initiative in nursing homes: the ANA acts in an advisory role. Am J Nurs [serial on the Internet]. 2002 Jun [cited 2002 Aug 12]; 102(6): [about 3 p.]. Available from: http://www.nursingworld.org/AJN/2002/june/Wawatch.htm

Tables

Each table should be typed double-spaced 1,5 on a separate sheet, numbered in the order of their first citation in the text in the upper right corner and supplied with a brief title each. Explanatory notes are printed under a table. Each table should be mentioned in the text. If data from another source are used, acknowledge fully.

Illustrations

Any forms of graphic enclosures are considered to bi figures and should be submitted as additional databases in the System of Assistent. Letters, numbers, and symbols should be clear and uniform, of sufficient size that when reduced for publication, each item will still be legible. Each figure should have a label on its back indicating the number of the figure, author's name, and top of the figure (**Figure 1**, **Figure 2** and so on). If a figure has been published, state the original source.

Legends for illustrations are typed on a separate page, with Arabic numbers corresponding to the illustrations. If used to identify parts of the illustrations, the symbols, arrows, numbers, or letters should be identified and explained clearly in the legend. Explain the method of staining in photomicrographs.

Abbreviations and acronyms

Authors are encouraged to use abbreviations and acronyms in the manuscript in the following manner: abbreviations and acronyms must be defined the first time they are used in the text consistently throughout the whole manuscript, tables, and graphics; abbreviations should be used only for terms that appear more than three times in text; abbreviations should be sparingly used.

An alphabetical list of all abbreviations used in the paper, followed by their full definitions, should be provided on submission.

Detailed Instructions are available at the web site:

www.vma.mod.gov.rs/vsp

UPUTSTVO AUTORIMA

VSP objavljuje radove koji nisu ranije nigde objavljivani, niti predati za objavljivanje redosledom koji određuje uređivački odbor. Svaki pokušaj plagijarizma ili autoplagijarizma kažnjava se. Prilikom prijave rada u sistem elektronskog uređivanja „Vojnosanitetskog pregleda“**(http://aseestant.ceon.rs/index.php)** neophodno je priložiti izjavu da su ispunjeni svi postavljeni tehnički zahtevi uključujući i izjavu koju potpisuju svi autori da rad nije ranije ni u celini, niti delimično objavljen niti prihvaćen za štampanje u drugom časopisu. Izjavu o pojedinačnom doprinosu svakog od autora rada potpisanu od svih autora, treba skenirati i poslati uz rad kao dopunsku datoteku. Takođe, autori su obavezni da dostave i potpisanu izjavu o nepostojanju sukoba interesa čime postaju odgovorni za ispunjavanje svih postavljenih uslova. Ovome sledi odluka o prihvatanju za dalji uređivački postupak. Rukopisi pristigli u Redakciju časopisa podležu internoj i eksternoj recenziji. Svi autori dužni su da plate “Article Processing Charge” za pokriće troškova jezičke, stručne i tehničke obrade rukopisa, kao i njegovog objavljivanja. Domaći autori plaćaju iznos od 5 000 dinara, a inostrani 150 eura. Dodatna plaćanja nisu predviđena čak i u slučaju da autor koji je već prethodno platio traženi iznos, ima više prihvaćenih radova za objavljivanje u godini u kojoj je izvršio uplatu. Svi autori koji su platili “Article Processing Charge” mogu, ukoliko žele, dobijati štampanu verziju časopisa tokom godine u kojoj je izvršena uplata. Plaćanje ovog iznosa ne garantuje prihvatanje rukopisa za objavljivanje i ne utiče na ishod recenzije.
Od obaveze plaćanja pokrića navedenih troškova oslobođeni su recenzenti, članovi Uređivačkog odbora i Izdavačkog saveta VSP, studenti i mladi istraživači, kao i pretplatnici časopisa.

U VSP-u se objavljuju **uvodnici**, **originalni članci, prethodna** ili **kratka saopštenja**, revijski radovi tipa **opšteg pregleda** (uz uslov da autori navođenjem najmanje 5 autocitata potvrde da su eksperti u oblasti o kojoj pišu), **aktuelne teme, metaanalize**, **kazuistika, seminar praktičnog lekara,** članci iz **istorije medicine**, lični stavovi, naručeni komentari, pisma uredništvu, izveštaji sa naučnih i stručnih skupova, prikazi knjiga i drugi prilozi. Radovi tipa originalnih članaka, prethodnih ili kratkih saopštenja, metaanalize i kazuistike **objavljuju se uz apstrakte na srpskom i engleskom jeziku**.

Rukopis se piše sa proredom 1,5 sa levom marginom od **4 cm**. Koristiti font veličine 12, a načelno izbegavati upotrebu **bold** i *italic* slova, koja su rezervisana za podnaslove. Originalni članci, opšti pregledi i metaanalize i članci iz istorije medicine ne smeju prelaziti 16 stranica (bez priloga); aktuelne teme – deset, seminar praktičnog lekara – osam, kazuistika – šest, prethodna saopštenja – pet, a komentari i pisma uredniku – tri, izveštaji sa skupova i prikazi knjiga – dve stranice.

U celom radu obavezno je korišćenje međunarodnog sistema mera (SI) i standardnih međunarodno prihvaćenih termina (sem mm Hg i °C).

Za obradu teksta koristiti program **Word for Windows** verzije 97, 2000, XP ili 2003. Za izradu grafičkih priloga koristiti standardne grafičke programe za **Windows**, poželjno iz programskog paketa **Microsoft Office** (**Excel, Word Graph**). Kod kompjuterske izrade grafika izbegavati upotrebu boja i senčenja pozadine.

Radovi se pripremaju u skladu sa **Vankuverskim dogovorom**.

Prispeli radovi kao anonimni podležu uređivačkoj obradi i recenziji najmanje dva urednika/recenzenta. Primedbe i sugestije urednika/recenzenata dostavljaju se autoru radi konačnog oblikovanja. Pre objave, rad se upućuje autoru određenom za korespodenciju na konačnu saglasnost.

Priprema rada

Delovi rada su: **naslovna strana, apstrakt sa ključnim rečima, tekst** rada, zahvalnost (po želji), literatura, prilozi.

1. ***Naslovna strana***

a) Poželjno je da naslov bude kratak, jasan i informativan i da odgovara sadržaju, podnaslove izbegavati.

b) Ispisuju se puna imena i prezimena autora sa oznakama redom: *, †, ‡, §, ‖, ¶, **, ††, ...

c) Navode se puni nazivi ustanove i organizacijske jedinice u kojima je rad obavljen mesta i države za svakog autora, koristeći standardne znake za fusnote.

d) Zaključak može da bude posebno poglavlje ili se iznosi u poslednjem pasusu diskusije.

e) Podaci o autoru za korespodenciju.

2. ***Apstrakt i ključne reči***

Na drugoj stranici nalazi se strukturisani apstrakt (250-300 reči za originalne članke i meta-analize) sa naslovom rada. Kratkim rečenicama na srpskom i engleskom jeziku iznosi se **Uvod/Cilj** rada, osnovne procedure – **Metode** (izbor ispitanika ili laboratorijskih životinja; metode posmatranja i analize), glavni nalazi – **Rezultati** (konkretni podaci i njihova statistička značajnost) i glavni **Zaključak**. Naglasiti nove i značajne aspekte studije ili zapažanja. Strukturisani apstrakt za kazuistiku (do 250 reči), sadrži podnaslove **Uvod, Prikaz bolesnika** i **Zaključak**). Ispod apstrakta, „Ključne reči“ sadrže 3–10 ključnih reči ili kratkih izraza koje ukazuju na sadržinu članka.

3. ***Tekst članka***

Tekst sadrži sledeća poglavlja: **uvod**, **metode**, **rezultate** i **diskusiju**. **Uvod.** Posle uvodnih napomena, navesti cilj rada. Ukratko izneti razloge za studiju ili posmatranje. Navesti samo važne podatke iz literature a ne opširna razmatranja o predmetu rada, kao ni podatke ili zaključke iz rada o kome se izveštava.

Metode. Jasno opisati izbor metoda posmatranja ili eksperimentnih metoda (ispitanici ili eksperimentne životinje, uključujući kontrolne). Identifikovati metode, aparaturu (ime i adresa proizvođača u zagradi) i proceduru, dovoljno detaljno da se drugim autorima omogući reprodukcija rezultata. Navesti podatke iz literature za uhođane metode, uključujući i statističke. Tačno identifikovati sve primenjene lekove i hemikalije, uključujući generičko ime, doze i načine davanja. Za ispitivanja na ljudima i životinjama navesti saglasnost nadležnog etičkog komiteta.

Rezultate prikazati logičkim redosledom u tekstu, tabelama i ilustracijama. U tekstu naglasiti ili sumirati samo značajna zapažanja.

U **diskusiji** naglasiti nove i značajne aspekte studije i izvedene zaključke. Posmatranja dovesti u vezu sa drugim relevantnim studijama, u načelu iz poslednje tri godine, a samo izuzetno i starijim. Povezati zaključke sa ciljevima rada, ali izbegavati nesumnjive tvrdnje i one zaključke koje podaci iz rada ne podržavaju u potpunosti.

Literatura

U radu literatura se citira kao superskript, a popisuje rednim brojevima pod kojima se citat pojavljuje u tekstu. Navode se svi autori, ali ako broj prelazi šest, navodi se prvih šest i *et al*. Svi podaci o citiranoj literaturi moraju biti tačni. Literatura se u celini citira na engleskom jeziku, a iza naslova se navodi jezik članka u zagradi. Ne prihvata se citiranje apstrakata, sekundarnih publikacija, usmenih saopštenja, neobjavljenih radova, službenih i poverljivih dokumenata. Radovi koji su prihvaćeni za štampu, ali još nisu objavljeni, navode se uz dodatak „u štampi“. Rukopisi koji su predati, ali još nisu prihvaćeni za štampu, u tekstu se citiraju kao „neobjavljeni podaci“ (u zagradi). Podaci sa *Interneta* citiraju se uz navođenje datuma pristupa tim podacima.

Primeri referenci:

Đurović BM. Endothelial trauma in the surgery of cataract. Vojnosanit Pregl 2004; 61(5): 491–7. (Serbian)

Balint B. From the haemotherapy to the haemomodulation. Beograd: Zavod za udžbenike i nastavna sredstva; 2001. (Serbian)

Mladenović T, Kandolf L, Mijušković ŽP. Lasers in dermatology. In: *Karadaglić Đ*, editor. Dermatology. Beograd: Vojnoizdavački zavod & Verzal Press; 2000. p. 1437–49. (Serbian)

Christensen S, Oppacher F. An analysis of Koza's computational effort statistic for genetic programming. In: *Foster JA, Lutton E, Miller J, Ryan C, Tettamanzi AG*, editors. Genetic programming. EuroGP 2002: Proceedings of the 5th European Conference on Genetic Programming; 2002 Apr 3-5; Kinsdale, Ireland. Berlin: Springer; 2002. p. 182-91.

Abood S. Quality improvement initiative in nursing homes: the ANA acts in an advisory role. Am J Nurs [serial on the Internet]. 2002 Jun [cited 2002 Aug 12]; 102(6): [about 3 p.]. Available from: http://www.nursingworld.org/AJN/2002/june/Wawatch.htm

Tabele

Sve tabele pripremaju se sa proredom 1,5 na posebnom listu. Obeležavaju se arapskim brojevima, redosledom pojavljivanja, u desnom uglu (**Tabela 1**), a svakoj se daje kratak naslov. Objašnjenja se daju u fus-noti, ne u zaglavlju. Svaka tabela mora da se pomene u tekstu. Ako se koriste tuđi podaci, obavezno ih navesti kao i svaki drugi podatak iz literature.

Ilustracije

Slikama se zovu svi oblici grafičkih priloga i predaju se kao dopunske datoteke u sistemu **aseestant**. Slova, brojevi i simboli treba da su jasni i ujednačeni, a dovoljne veličine da prilikom umanjivanja budu čitljivi. Slike treba da budu jasne i obeležene brojevima, onim redom kojim se navode u tekstu (**Sl. 1; Sl. 2** itd.). Ukoliko je slika već negde objavljena, obavezno citirati izvor.

Legende za ilustracije pisati na posebnom listu, koristeći arapske brojeve. Ukoliko se koriste simboli, strelice, brojevi ili slova za objašnjavanje pojedinog dela ilustracije, svaki pojedinačno treba objasniti u legendi. Za fotomikrografije navesti metod bojenja i podatak o uvećanju.

Skraćenice i akronimi

Skraćenice i akronimi u rukopisu treba da budu korišćeni na sledeći način: definisati skraćenice i akronime pri njihovom prvom pojavljivanju u tekstu i koristiti ih konzistentno kroz čitav tekst, tabele i slike; koristiti ih samo za termine koji se pominju više od tri puta u tekstu; da bi se olakšalo čitaocu, skraćenice i aktinome treba štedljivo koristiti.

Abecedni popis svih skraćenica i akronima sa objašnjenjima treba dostaviti pri predaji rukopisa.

Detaljno uputstvo može se dobiti u redakciji ili na sajtu: www.vma.mod.gov.rs/vsp